U. S. DEPARTMENT OF THE INTERIOR
U. S. GEOLOGICAL SURVEY

PROCEEDINGS OF THE WORKSHOP ON PALEOSEISMOLOGY

18-22 September 1994
Marshall, California

Sponsored by

U.S. Geological Survey National Earthquake Hazards Reduction Program
and Task Group II-3, Paleoseismicity of the Late Holocene,
Inter-Union Commission on the Lithosphere

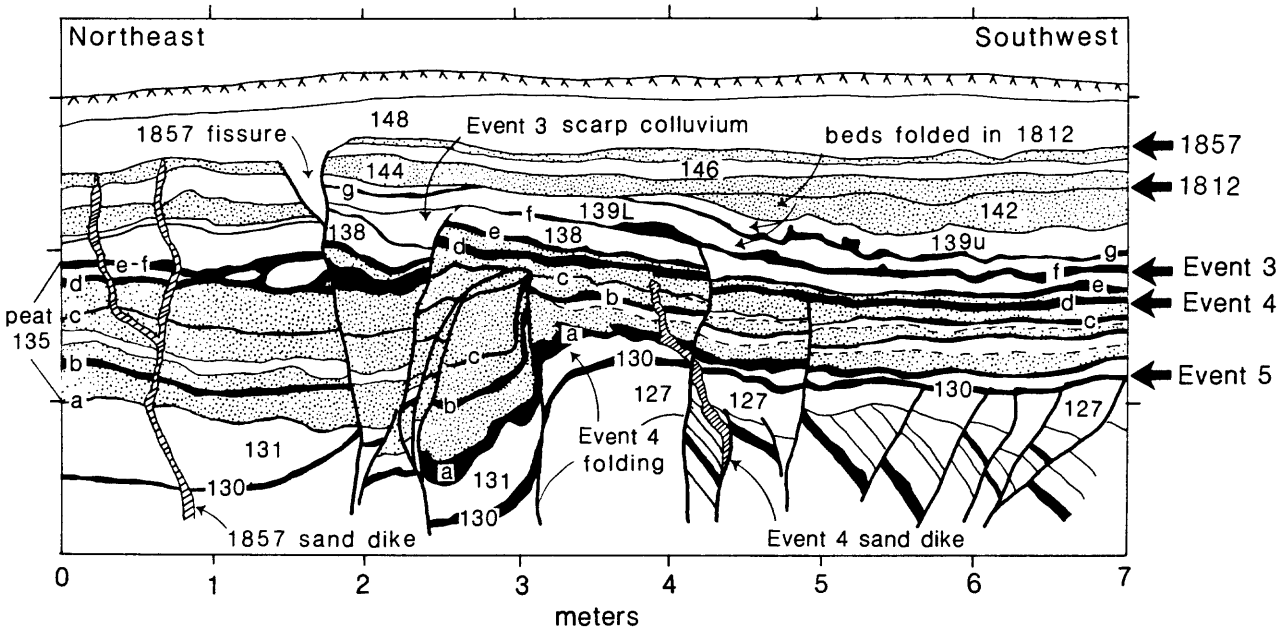

OPEN-FILE REPORT 94-568

Menlo Park, California
1994

U. S. DEPARTMENT OF THE INTERIOR
U. S. GEOLOGICAL SURVEY

PROCEEDINGS OF THE WORKSHOP ON PALEOSEISMOLOGY

18-22 September 1994
Marshall, California

Sponsored by

U.S. Geological Survey National Earthquake Hazards Reduction Program
and Task Group II-3, Paleoseismicity of the Late Holocene,
Inter-Union Commission on the Lithosphere

Conference Convenors:
Carol S. Prentice, David P. Schwartz
U. S. Geological Survey
Menlo Park, California 94025
and
Robert S. Yeats
Oregon State University
Corvallis, Oregon

OPEN-FILE REPORT 94-568

Menlo Park, California

1994

On the cover: Composite log of exposures of the San Andreas fault in Swarthout Creek, near Wrightwood, California, showing evidence for the five most recent earthquakes. Black horizons are peat layers, stippled horizons are alluvial deposits, other units are debris flows. Earthquake horizons are shown by broad arrows. From: Fumal, Pezzopane, Weldon, and Schwartz, 1993, Science, v. 259, pp. 199-203.

CONTENTS

Participants

John Adams
Geophysics Division
Geological Survey of Canada,
1 Observatory Crescent,
Ottawa K1A OY3 Canada

Rivka Amit
Geological Survey of Israel
30 Malkhe Israel Street
Jerusalem 95501 Israel

Ramon Arrowsmith
Department of Geological and
Environmental Sciences
Stanford University
Stanford CA 94305-2115

Manuel Berberian
Najarian Associates Inc.
One Industrial Way West
Eatontown NJ 07724

Kelvin Berryman
Institute of Geological and Nuclear
Science
P.O. Box 30368
Lower Hutt New Zealand

Glenn Biasi
Department of Geological Sciences
University of Oregon
Eugene OR 97403-1272

William Bryant
Division of Mines and Geology
State of California
801 K Street MS 12-31
Sacramento CA 95814-3531

William Bull
Geosciences Department
University of Arizona
Tucson AZ 85721

Roland Burgmann
Department of Geophysics
Stanford University
Stanford CA 94305-2115

George S. Burr
Physics Department
University of Arizona
Tucson AZ 85721

John Caskey
Center for Neotectonic Studies
University of Nevada MS 169
Reno NV 89557-0138

Alexandros Chatzipetros
Department of Geology
and Physical Geography
Aristotle University of Thessaloniki
GR 540 06 Thessaloniki Macedonia
Greece

Francesca Cinti
Instituto Nazionale di Geofisica
Via di Vigna Murata, 605
1-00143 Roma Italy

Carlos Costa
Universidad Nacional de San Luis
Ej. de los Andes 950 1o Piso
5700 San Luis Argentina

Anthony J. Crone
US Geological Survey
Branch of Geologic Risk Assessment
PO Box 25046 MS 966
Denver CO 80225-0046

Jessie Daligdig
Department of Geophysics
Applied Geophysics Laboratory
Sakyo-Ku
Kyoto 606 Japan

Deng Quidong
Institute of Geology
State Seismological Bureau
Beijing 100029 PR China

Craig M. De Polo
Nevada Bureau of Mines and Geology
University of Nevada, Reno MS 178
Reno NV 89557-0088

Participants

Ding Guoyu
State Seismological Bureau
No. 63 Fuxing Avenue
Beijing 100036 PR China

James Dolan
Division of Geological and
Planetary Science
California Institute of Technology
Pasadena CA 91125

R.L. Edwards
Department of Geology and
Geophysics
University of Minesota
Minneapolis MN 55455

Clark Fenton
Geophysics Division
Geological Survey of Canada
1 Observatory Crescent
Ottawa KIA OY3 Canada

Steven Forman
Department of Geology
Ohio State University
Columbus OH 43210

Lou Gilpin
Department of Earth Sciences
University of California, Santa Cruz
Santa Cruz CA 95063

Lisa Grant
Woodward-Clyde
14 Alcott Court
Irvine CA 92715

Kathryn Hanson
Geomatrix Consultants
100 Pine Street, 10th Floor
San Francisco CA 94111

He Qunlu
Institute of Crustal Dynamics
State Seismological Bureau
PO Box 2855
Beijing 100085 PR China

Suzanne Hecker
US Geological Survey
345 Middlefield Road MS 977
Menlo Park CA 94025

Mark Hemphill-Haley
Department of Geological Sciences
University of Oregon
Eugene OR 97403-1272

Christian Hibsch
Institut Français d'Études Andines
Casilla 17-11-06596
Quito Ecuador

Gordon Jacoby
Lamont-Doherty Geological Observatory
Columbia University
Palisades NY 10964

Iaakov Karcz
Geological Survey of Israel
30 Malkei Israel Street
Jerusalem 95501 Israel

Robert Karlin
Department of Geological Sciences MS 172
University of Nevada, Reno
Reno NV 89557-0138

Keith I. Kelson
William Lettis & Associates
1000 Broadway #612
Oakland CA 94607-4041

Yoshihiro Kinugasa
Seismotectonic Research Section
Geological Survey of Japan
1-1-3 Higashi Tsukuba
Ibaraki 305 Japan

Peter Knuepfer
Department of Gelogical Sciences
Binghamton University
Binghamton NY 13902-6000

Ismail Kuscu
Maden Tatkik ve Arama Genel Müdürlügü
06520

Participants

Ankara Turkey

Robert Lagerback
Geological Survey of Sweden
PO Box 670
S-75128 Uppsala Sweden

Mark R. Legg
5952 Brassie Circle
Huntington Beach CA 92649-2748

William R. Lettis
William Lettis & Associates
865 Solana Drive
Lafayette CA 94549

James Lienkaemper
US Geological Survey
345 Middlefield Road MS 977
Menlo Park CA 94025

Michael Machette
US Geological Survey
Box 25046 MS 966
Denver CO 80225

Shmulik Marco
Department of Geology
Hebrew University
Jerusalem 91904
Israel

James P. McCalpin
Geo-Haz Consulting, Inc.
P.O. Box 1377
Estes Park CO 80517

Sally McGill
Department of Geological Sciences
California State University
at San Bernardino
5500 University Parkway
San Bernardino CA 92407-2397

Richard McMullen
US-NCR
MS T10L1
Washington DC 20555

Dorothy Merritts
Department of Geosciences
Franklin & Marshall College
PO Box 3003
Lancaster PA 17604-3003

Alessandro M. Michetti
Agenzia Nazionale per la Protezione
dell-Ambiente - ENEA-DISP
Via Vitaliano Brancati 48
00144 Roma Italy

Juan Moya
Department of Geological Sciences
University of Colorado, Boulder
1300 30th Street #A1-24
Boulder CO 80303

Karl Mueller
Department of Geological
and Geophysical Sciences
Princeton University
Princeton NJ 08544

Takashi Nakata
Department of Geography
Hiroshima University
Higashi-Hiroshima 724 Japan

Alan Nelson
US Geological Survey
Box 25046 MS 966
Denver CO 80225

Andrei Nikonov
Institute of Physics of the Earth,
Bolshaya Gruzinskaya 10
Moscow D242
123810 Russia

Jay Noller
William Lettis & Associates
1000 Broadway #612
Oakland CA 94607-4041

Steve Obermeier
U.S. Geological Survey MS 905
Reston, VA 22092

Participants

Koji Okumura
Seismotectonic Research Section
Geological Survey of Japan
1-1-3 Higashi, Tsukuba
Ibaraki 305 Japan

Susan Olig
Woodward-Clyde Federal Services
500 - 12th Street #100
Oakland CA 94607

Yoko Ota
Department of Geography
Senshu University
2-1-1, Higashi-mita, Tama-ku
Kawasaki-shi 214, Japan

Silvio Pezzopane
Science Applications International Corp
US Geological Survey
Box 25046 MS 425
Denver CO 80225

P. A. Pirazzoli
CNRS-Laboratoire de Geographie Physique
1, Place Aristide-Briand,
92190 Meudon-Bellevue France

George Plafker
Branch of Alaskan Geology
US Geological Survey
345 Middlefield Road ,MS 904
Menlo Park CA 94025-3591

Carol Prentice
US Geological Survey
345 Middlefield Road MS 977
Menlo Park, CA 94025

Tom Rockwell
Department of Geological Sciences
San Diego State University
San Diego CA 92182

Robert Rothman
US-NCR
MS T10L1
Washington DC 20555

Kenji Satake
Department of Geological Sciences
University of Michigan
1006 C C Little Building
Ann Arbor MI 48109

David Schwartz
U.S. Geological Survey
345 Middlefield Road MS 977
Menlo Park CA 94025

Gordon Seitz
Department of Geological Sciences
University of Oregon
Eugene OR 97403-1272

Niko Shimazaki
Earthquake Research Institute
University of Tokyo
1-1-1 Yayoi, Bunkyo-ku
Tokyo 113 Japan

Kerry Sieh
Geological & Planetary Sciences 170-25
California Institute of Technology
Pasadena CA 91125

John Sims
US Geological Survey MS 905
Reston VA 22092

D Burton Slemmons
University Of Nevada
2905 Autumn Haze Lane
Las Vegas NV 89117

Stathis Stiros
Institute of Geology
and Mineral Exploration
70 Messoghian Street
Athens 11527 Greece

Pradeep Talwani
Department of Geological Sciences

Participants

University of South Carolina
Columbia SC 29208

Jerome Treiman
Dept of Conservation
Division of Mines & Geology
107 South Broadway, Rm 1065
Los Angeles CA 90012

Hiroyuki Tsutsumi
Department of Geosciences
Wilkinson 104
Oregon State University
Corvallis OR 97331-5506

Martitia P. Tuttle
University of Maryland
Geology Department
Bldg 237 Room 1117
College Park MD 20742

Gianluca Vlaensise
Instituto Nazionale di Geofisica
Via di Vigna Murata, 605
1-00143 Roma Italy

R.J. Van Dissen
Institute of Geological
and Nuclear Sciences
P.O. Box 30-368
Lower Hutt New Zealand

Robert Wallace
US Geological Survey
345 Middlefield Road MS 977
Menlo Park CA 94025

Weimin Wu
Institute of Crustal Dynamics
State Seismological Bureau
PO Box 2855
Beijing 100085 PR China

Patrick L. Williams
Lawrence Berkeley Laboratory
MS 50 E
University of California
Berkeley CA 94720

Christopher Wills
California Division of Mines and Geology
Bay Area Regional Office
185 Berry Street #3600
San Francisco CA 94107

Xu Xiwei
Department of Geography
University of Tokyo
Hongo, Bunkyo-Ky
Toyko 113 Japan

Haruo Yamazaki
Department of Geography
Tokyo Metropolitian University
Minami-Ohsawa 1-1 Hachioji
Tokyo 192-03 Japan

Robert Yeats
Department of Geosciences
Oregon State University
Corvallis OR 97331-5506

Hugo Yepes
Instituto Geofisico
Escuela Politecnica Nacional
Casilla 17-01-2759
Quito, Ecuador

Introduction to the USGS /ICL International Workshop on Paleoseismology, September 18-22, 1994, Marshall, California

Carol S. Prentice and David P. Schwartz

Of all the natural hazards, earthquakes are among the most frightening and disturbing, and are a major cause of damage, injury and loss of life in both industrialized and developing nations. The scientific study of earthquake phenomena, initiated in the last century, has provided a base understanding of the causes of these devastating events, but not the ability to accurately predict their future occurrence. However, we now know a great deal about which areas of the world are most prone to earthquake occurrence, and in many of these active regions we now know the likely sources of future earthquakes in some detail. This understanding is the result of scientific study of modern, historical and, in recent decades, prehistoric earthquakes. Because the repeat times of large, destructive earthquakes are typically long compared to the lengths of historical records, the study of prehistoric earthquakes has become increasingly important for defining the earthquake potential of a specific fault or region.

Paleoseismology, the use of geologic and geomorphic techniques to determine fault slip rates and the age, frequency and magnitude of prehistoric earthquakes, has made tremendous contributions in recent decades to both understanding the earthquake process and characterizing earthquake sources for seismic hazard analysis. The USGS/ICL-sponsored Workshop on Paleoseismology, September 18-22, 1994, in Marshall, California, is intended to bring together practitioners of the science and art of paleoseismology worldwide to exchange information, promote discussion, and facilitate the advance of the geological study of active fault zones. In 1987, the first conference on paleoseismology was held in Albuquerque, New Mexico (Crone, 1987). In the seven years since that landmark event, much headway has been made in the science of paleoseismology. The 1994, USGS/ICL workshop , consisting of five plenary sessions and a day-long field trip to paleoseismic sites along the San Andreas and Rodgers Creek faults, focuses on advances in paleoseismic techniques, synthesis of new paleoseismic data from around the world, Quaternary dating methods, and models of earthquake recurrence.

Paleoseismic studies of active faults are now being undertaken in a wide variety of tectonic settings worldwide; areas represented at the conference include: Australia, Canada, China, Dominican Republic, Ecuador, Fennoscandia, Greece, Iran, Israel, Italy, Japan, New Guinea, New Zealand, Puerto Rico, Philippines, Turkey, and the western, central and eastern parts of the United States. Critical questions and concerns of this workshop include defining the criteria for the recognition of the occurrence and size of an individual earthquake in the geologic record, and the appropriate use of Quaternary dating techniques to determine the age of the event. In addition, we now have sufficient data to begin to test existing and new models of earthquake recurrence and fault behavior. Is earthquake occurrence regular or clustered? How valid is the concept of a characteristic earthquake? How well can fault segmentation be used

to determine in advance the likely limits of earthquake ruptures? These questions have critical implications for using paleoseismological data to evaluate earthquake hazards. The abstracts in this volume reflect the tremendous growth and maturation of the field of paleoseismology in recent years, and provide the promise of future contributions that will greatly enhance our understanding of earthquake occurrence worldwide.

ILP workshop Sept 1994: Paleoseismology studies in Canada - a dozen years of progress

John Adams
Geological Survey of Canada
1 Observatory Cres. Ottawa K1A 0Y3
(adams@seismo.emr.ca)

Paleoseismic studies in Canada break into three groups: fault related studies, of which there are rather few; studies related to the Cascadia subduction zone; and studies investigating evidence of earthquake shaking without identifying the active fault. This abstract reviews the research of many Canadians into paleoseismology. Key workers are indicated thus: [Name].

No studies of Canadian faults have yet demonstrated convincing evidence for prehistoric, Holocene coseismic offset, though an active fault in the Yukon [Clague] suggests that onshore faults worthy of study exist. A recent bibliography of eastern postglacial faulting [Fenton] presents some likely target features, such as the pre-Holocene Aspy Fault of Nova Scotia [Grant], but investigations have been inadequate. In large part, the failure to document paleoearthquakes on surface faults stems from the lack of historical faulting in Canada. Only the 1989 M6.3 Ungava earthquake is known to have produced a surface scarp [Adams], and it showed no evidence of prior Holocene (or likely Phanerozoic) movement. Other recent earthquakes have been offshore (Queen Charlotte Fault 1949 M8.1), or in rugged terrain (Vancouver Island earthquake 1946 M7.3; Nahanni, 1985 M6.9), or too small (Miramichi, New Brunswick, M5.7 at 6 km), or too deep (Saguenay, Quebec, 1988 M5.9 at 27 km).

On Vancouver Island and the adjacent mainland there has been a recent surge of evidence for sudden coastal subsidence of marsh deposits capped by tsunami sands [Clague]. These complement similar deposits interpreted as coseismic subsidence on the Washington and Oregon coasts and extend the record of the last, c. 1700 A.D. event, northwards. Complementary work in the offshore [Adams] suggests that turbidites in the deepsea channels have a consistent earthquake trigger, establishes the existence of strong ground shaking, and establishes a chronology of the last 13 events. Other onshore studies point to a few liquefaction episodes on the Fraser Delta [Clague], but since there do not appear to be enough episodes to match the last 3-6000 years of Cascadia subduction zone earthquakes, these may well have a local cause, i.e. shallow nearby earthquakes like the one in 1872, or the one that caused surface faulting at Seattle about 1100 years ago. The search for other underwater evidence of possible earthquake shaking has had mixed results; on the one hand an excellent record of turbidite events has come from Saanich Inlet [Bobrowsky]; on the other hand some lake bottom profiling showed few prehistoric earthquake triggered submarine landslides [Shilts].

In the Cordillera, a recent study of the Hell Creek Fault, B.C. [Clague], first described by Slemmons and others, suggests that it is a sackung (slope-collapse) feature, and so one of many such features in the region rather than being coseismic. There are numerous large landslides or rockfalls in the Cordillera [Evans, Eisbacher], and while some are undoubtedly earthquake-caused (e.g., by the 1985 Nahanni earthquake) there has been no synthesis as yet. Some of the landslides dam small lakes, so their precise dating by dendrochronology may become important.

The 1946 earthquake caused regional landslides near the epicentre [Mathews], but no prehistoric analog is known.

In eastern Canada, the lack of active faults has concentrated effort on sedimentary evidence of historical and prehistorical earthquakes. The 1935 Timiskaming earthquake (Ontario-Quebec border, M6.2) turned Lac Tee white for a month after the earthquake; sonar profiles [Shilts] show this was due to collapse of gyttja on the lake's steep flanks, and cores [Doig] show the disturbed sediment on the lake floor, undisturbed sediment beneath, and disturbed sediment below that, indicating a c.1500 year-old earthquake of similar shaking intensity.

Sonar profiling in other small lakes [Shilts] has revealed some with distinctive lake-bottom disturbance - likely earthquake-caused - but many others are undisturbed. Coring in small lakes near the Charlevoix seismic zone [Doig] suggests that white silt layers in the gyttja deposits form through the resuspension of the topmost sediment and the more rapid settlement of its inorganic component: thus the silt layers are thought to record the time of an earthquake and (in a crude way) the relative shaking of the lake. Similar layers have been seen near Sept Iles [Oulette].

Many of these studies are geographically isolated, and even in adjacent lakes it is difficult to tie observations together convincingly. One study with good time control used the varve stratigraphy in (now-drained) Glacial Lake Barlow-Ojibway to demonstrate that sediment disturbances varying from 4 m to a few mm in thickness were synchronous in the 190 km long lake, so indicating the approximate epicentre of this c. 8500 yr old earthquake [Adams].

Sand expulsion occurred near the epicentre of the Saguenay earthquake and two prior generations of dykes [Tuttle] indicates a historical (?Charlevoix) and a paleo-shaking (epicentre undefined) event. Enigmatic sand mounds and clay dykes are known from the historically-active Charlevoix area [Chagnon], as is a possible sudden shoreline level change in the Late Holocene [Dionne]. In northern New Brunswick, an archaeological site is disturbed by sand dykes, interpreted to represent a post-1700 AD earthquake [Broster].

Controversy has arisen in southeastern Canada over some submarine features in Lake Ontario - "plumose structures", "linear backscatter anomalies" on side-scan records, and linear ridges - interpreted by some as paleoearthquake indicators [Wallach]. The first two now appear to be anthropogenic, and the latter to be pop-ups and so merely indicating the near-surface high horizontal stresses already well-known from onshore. Nearby, in the Rouge Valley of Toronto [Mohajer], neotectonism was inferred from faults offsetting both bedrock and Quaternary deposits; this is, however, in dispute because glaciotectonism ("ice-push"), the effects of which are observed nearby, provides an adequate explanation [Adams].

Thus in most of Canada we are still searching for the Holy Grail of paleoseismology - a Holocene fault scarp like the Meers Fault with an associated soft sediment record to provide adequate dating. Holocene surface faulting has certainly occurred, but the combination of rugged, unpopulated terrain, a large landmass 20% larger than the coterminous U. S., and with perhaps 1/100th the number of geologists actively seeking evidence, has militated against finding much evidence.

ILP Paleoseismology Workshop Sept 1994

Near-term Probability of the future Cascadia megaquake

John Adams, Geological Survey of Canada, 1 Observatory Cres. Ottawa K1A 0Y3
(adams@seismo.emr.ca)
Dieter Weichert, Pacific Geoscience Centre, Geological Survey of Canada, Sidney V8L 4B2
(weichert@pgc.emr.ca)

Adams in 1990 (Tectonics, v. 9, p. 569-583) used turbidites in deep-sea channels off the Oregon and Washington coasts as an alias for great earthquakes ("megaquakes") on the Cascadia subduction zone. He deduced a mean interval of 590 +/- 50 years and average variability of 170 years from the PELAGIC layers between them, and, using a normal distribution model, a 5% (estimated range = 2-10%) likelihood of a megaquake happening in the next 50 years. We reanalyse those data as follows:

MEAN RETURN PERIOD. The uncertainty in the mean return period can now be halved because the uncertainty on the assumed time since the last earthquake (1/2 +/- 1/2 interval on p. 576) was too conservative. The last event is now dated to about 300 years ago, which makes the denominator 12.49 +/- 0.02 intervals and the mean interval 590 +/- 32 years. Most of the remaining error comes from the unknown period between the eruption and the first ash-bearing turbidite, less from the choice of the Bacon rather than the Brown et al. (1989) date, and the uncertainty in the Bacon (1983) radiocarbon age for the Mazama eruption.

VARIABILITY. Variability of 170 years was estimated by Adams based on the average variability of pelagic intervals in the three lowest-variability cores (arguing that for repetitive common events the increased variability in some other cores must be due to location-specific factors, perhaps chiefly local erosion of the pelagic sediments by the subsequent turbidity current). We argue here that the true variability may be even lower. Instead of analysing the pelagic intervals, we analyse the turbidite thicknesses directly. For the nine turbidites in core 6509-26 that have complete thicknesses, the mean turbidite thickness is 660 mm and the coefficient of variation is 18%, or for the 590 year return period, 105 years. Why do we think this lower variability might be justified? Firstly, the estimation of the individual turbidite thicknesses are at least a factor of ten more reliable than for pelagic intervals, because the turbidites are on average 15x thicker, and so millimetre or half-centimetre errors in estimating the tops or bottoms of the interval become insignificant. Secondly, core 6509-26 was taken from a region at the far end of the Cascadia Seachannel where the turbidity currents were ponded against the Blanco Fracture zone (only 4 of the 13 post-Mazama currents overflowed this barrier). Hence the thicknesses should be a good estimate of the total sediment volume that was moved. The core 6509-26 location contrasts with cores in the upper channel where the deposition records only the waning of the current and so very indirectly the total volume of the flow.

A MEGAQUAKE ORIGIN IS PROBABLE. A regular volume of turbidite deposit suggests that: 1. a similar sized area of channel catchment contributed each time, 2. the flow conditions were similar in each successive turbidity current, 3. a similar period of time elapsed between each

event (assuming constant sediment accumulation rate in the catchment) and 4. only the sediment newly-accumulated since the last earthquake slumps during the next earthquake. Taken together, the regularity suggests great earthquakes, and it would be surprising if a combination of other phenomena could be responsible.

DATES FOR THE LAST EVENTS. From the turbidite thicknesses in core 6509-26, assuming: 1. 300 years since the last event; 2. turbidite volume represents the sediment accumulation time since the prior event; 3. 660 mm of turbidite deposit per 590-year event; and 4. no erosion or compaction, then the ages of the last 10 turbidites are: 300, 720, 1285, 1840, 2410, 3060, 3520, 4160, 4960, and 5615 calendar years before 1995 (note that the unstated errors may compound, so the final dates are rather uncertain). A comparable, and perhaps more reliable, series can be deduced by computing and then averaging ages for each of the correlated turbidites (correlated by Griggs et al., 1969 on the basis of stratigraphic position and degree of bioturbation) in cores 6509-26, 6609-24, and 6509-27. Although the coefficient of variation for the 3-core average (16%) might be expected to be lower than the individuals, if some of the variance in turbidite thickness is due to random factors, it is in fact only slightly lower (perhaps because of the non-optimum location of core 6509-27, which has a high standard deviation and a linear increase in turbidite thickness). Nevertheless, we infer that the same events are indeed responsible.

FUTURE PROBABILITY and CONFIDENCE INTERVALS. The empirical cumulative distribution of return periods based on pelagic thicknesses is shown in Figure 1. Also shown are (distribution-free) Kolmogoroff-Smirnov 90% two-sided confidence intervals, and Weibull and log-normal distributions fitted to the data. Although the Weibull is theoretically preferable, because its hazard function increases as a simple power of time, 1.4 for our data, both analytical distributions fit the data well. At present we are 300 years since the last earthquake and the empirical probability for the event to have happened already is 5%, but the distribution-free 90% confidence interval ranges from 0 to 40%. These probabilities and confidnece intervals are likely to be upper bounds because the distributions are based on the turbidites show lower variability.

CONCLUSIONS. The most significant new conclusions from analyzing both the pelagic and the turbidite thickness data are: (i) both sedimentary components point towards repetitive megaquakes; (ii) the inter-earthquake variability is low; (iii) the interval between the last two events was quite short, 430 yrs, and is different from the mean at the 95% level; (iv) the chance of a megaquake occurring in our lifetimes is below, perhaps considerably below, 10%.

*** Figure 1 here

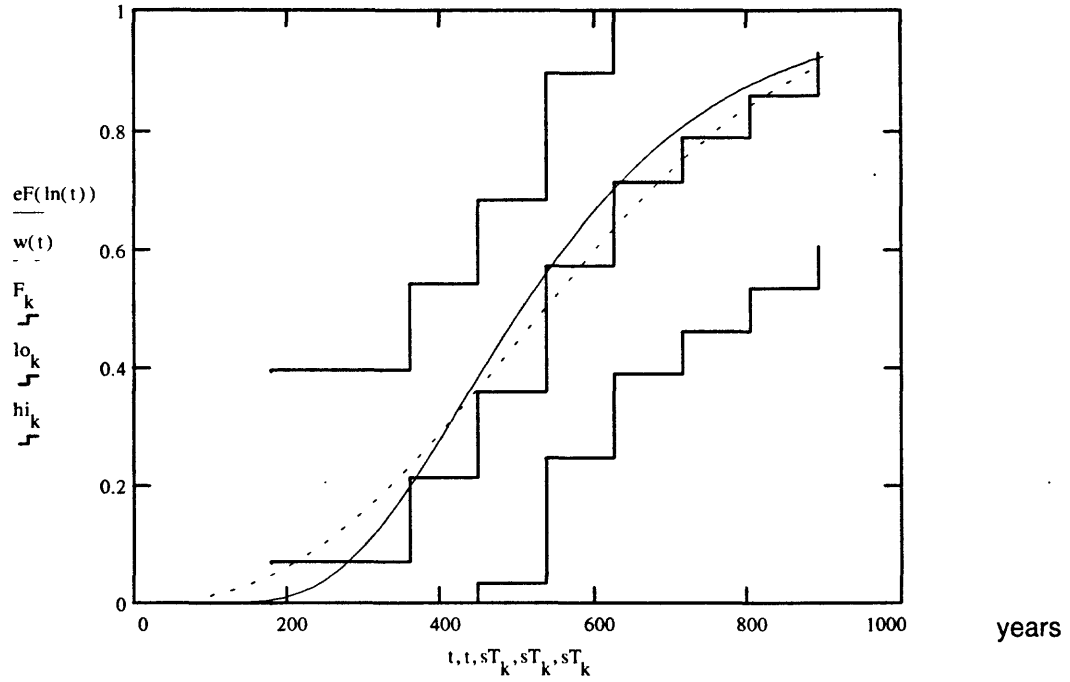

Fig. 1 Empirical distribution of interevent periods and distribution-free Kolmogoroff-Smirnov two-sided 90% confidence bounds. Also shown are lognormal (solid) and Weibull (dashed) fitted curves.

Paleosismicity in the Southern Arava Rift, Israel.

R. Amit, Inst. of Earth Sciences, Hebrew University, Jerusalem, Israel, 91904
J. B. J. Harrison, Geoscience, New Mexico Tec., Socorro, NM 87801, USA.
Y. Enzel, Inst. of Earth Sciences, Hebrew University, Jerusalem, Israel, 91904
N. Porat, Geological Survey of Israel, 30 Malkhe Yisrael Street, Jerusalem, Israel, 95501.

The southern Arava Valley and the Gulf of Elat are internal structures along the Dead Sea transform. The western and the eastern margins of the Arava Valley are bordered by large alluvial fans formed dominantly during the Pleistocene with one active channel. The surfaces of these alluvial fans are displaced by Pleistocene and Holocene normal faults which are semi-parallel to the strike slip main lineament.

The alluvial fan of Nahal Shehoret was selected as a study site as it showed the most prominent and well-preserved fault scarps which displaced early Pleistocene to Holocene stable alluvial fan surfaces and recent active channels. The surficial features were formed under various climatic conditions. The climate at present is extremely arid. During most of the Quaternary the region underwent mildly arid to extremely arid climates. The alluvial fan surfaces and the colluvial units are characterized by desert Reg soils which reach various degrees of development. They were classified as Torrifluvents, Typic Haplogypsid and Gypsic Haplosalid. Twelve trenches were excavated across fault scarps, in the active channel, and across Holocene and middle to late Pleistocene surfaces. All the faults are normal and are predominantly of multiple event type.

In determining the tectonic hazard of this area it is essential to identify the paleoseismicity associated with these faults. However, in non-consolidated sedimentary material, under extremely arid climatic conditions there is no suitable material for radiometric dating methods. As a result, several methods were developed and adapted to analyze and to recognize individual faulting events and to evaluate periods of quiescence: 1) Analyzing colluvial units along fault scarps and terrace risers; 2) Using pedogenic features (shattered gravel, gypsic and salic horizons in recent, cumulic and buried soils) as a relative dating tool; 3) Using catenary relationship along fault scarps to identifying recent tectonic activity; and 4) Using soil type (cumulic or buried) and the degree of soil development, as stratigraphic markers in separating episodes of tectonic activity on a fault scarp.

In using soils for relative age dating and colluvial wedges and buried soils for separating phases of tectonic activity we have to distinguish between colluvial units which are tectonically induced from those which are not. We trenched and compared a fault scarp and terrace risers all on the same alluvial fan surface. One of the trenched fault scarps (trench 6 - a multiple-event fault) and a trenched terrace riser of the same faulted alluvial surface were compared and analyzed. Soils and colluvial stratigraphy along fault scarps differ from those on terrace risers. Several colluvial units were identified on the fault scarp by pedogenic features as there is little variation in the stratigraphy of the entire colluvium. On the terrace riser it is possible to separate the colluvium into two units which differ stratigraphically and sedimentologically. The lower unit is composed of coarse material while the upper is composed of fine material. The colluvial units on the fault scarp are triangular in shape while those on the terrace riser are bowl-shaped. Cumulic soils indicating continuous deposition

formed on the terrace riser whereas the fault scarp colluvium is characterized by episodic deposition which is related to surface rupture that resulted in buried soils. The soils and the sedimentary composition of the colluvium at the fault scarp indicate rapid and episodic colluviation processes resulting from several tectonic events, whereas those on the terrace scarp suggest low erosion and deposition rates.

In addition, internal consistency exist between the ages determined by OSL dating, scarp degradation modelling, and the ages evaluated by using the degree of soil development of both the alluvial surfaces and the colluvial wedges. The degree of soil development on alluvial fan surfaces in this area were correlated with the Holocene Nahal Zeelim chronosequence which was dated by ^{14}C, and with soils on older alluvial surfaces dated by prehistoric artifacts in the Zin Valley. All of these methods were independently applied. Thus, this study emphasizes that in extremely arid regions soils can be used to give an estimate age of a faulted surface, a maximum estimate of the scarp age, and reliable evaluation of the recurrence intervals of faulting events.

The trenches excavated across faults of various stages and ages in the study area have demonstrated that faulting events are generally temporally clustered. Close to the present day rift center, younger alluvial surfaces were displaced by several stages of faulting. Usually the intervals between single events displacing alluvial fan surfaces on a given fault plane are not longer than 50,000 years. In one of the trenches (trench 6) with a maximum number of faulting events along the same fault plane (nine faulting events from 50,000 years till Holocene) the recurrence interval is estimated to be 1000-3000 years. The estimated recurrence intervals were determined by using soil and geomorphic methods. In addition, in trench 6 the recurrence interval was calculated independentley by using OSL dates. Close to the mountain front the situation is different where only older surfaces (latest Pliocene to early Pleistocene) are faulted. This trend fits the concept that during earlier stages of faulting there was much slower migration of faulting toward the center of the rift than during later stages.

It is possible that there is a branching of faults propagating toward the surface, especially through friable material such as coarse alluvium. This process causes faults of the same event and same stage to rupture the surface at the same time. The result is that there is a zone of surficial faults related to the same stage and there is a migration of the entire zone of faulting activity rather than of discrete faults.

Trench 6, which was dated by OSL dating method, allowed us to calculate some displacement average rates (although the soil analyses indicate an episodic and non-continuous tectonic process). In this trench we identify two sets of events within the tectonic sequence. The first set is characterized by large vertical displacements in which 4 events offsetting 1.5-1.6 m each. This set began at 38 ka and ended at 17 ka yielding an average annual slip rate of 0.3 mm. It was followed by second set, lasting until historic times, which consists of 5-7 smaller events each displacing 0.3-0.5m, resulting in an average slip rate of 0.1 mm/yr. The information we have about displacements of Holocene surfaces in the vicinity also indicates that no more than several tens of cm of vertical displacement has occurred during the last several thousand years. The resulting average slip rates on these surfaces are 0.05-0.1 mm/yr.

Based on this well-dated multiple event fault (trench 6), at least nine surface faulting events have occurred during the last 17,000 - 50,000 years in the region with a 1000-3000 year recurrence interval. A relatively low faulting activity is determined for the late Pleistocene and the Holocene periods. This conclusion is also supported by seismological data

which show that the region under investigation is characterized by low seismicity and scattered epicenters.

Assuming that the displacement amount and earthquake magnitude are correlated, the magnitude associated with the studied faults are all smaller than 7.5 and appear to change from higher magnitudes (about 7) during the latest Pleistocene, to lower magnitudes (about 6) during the Holocene.

Trench 6

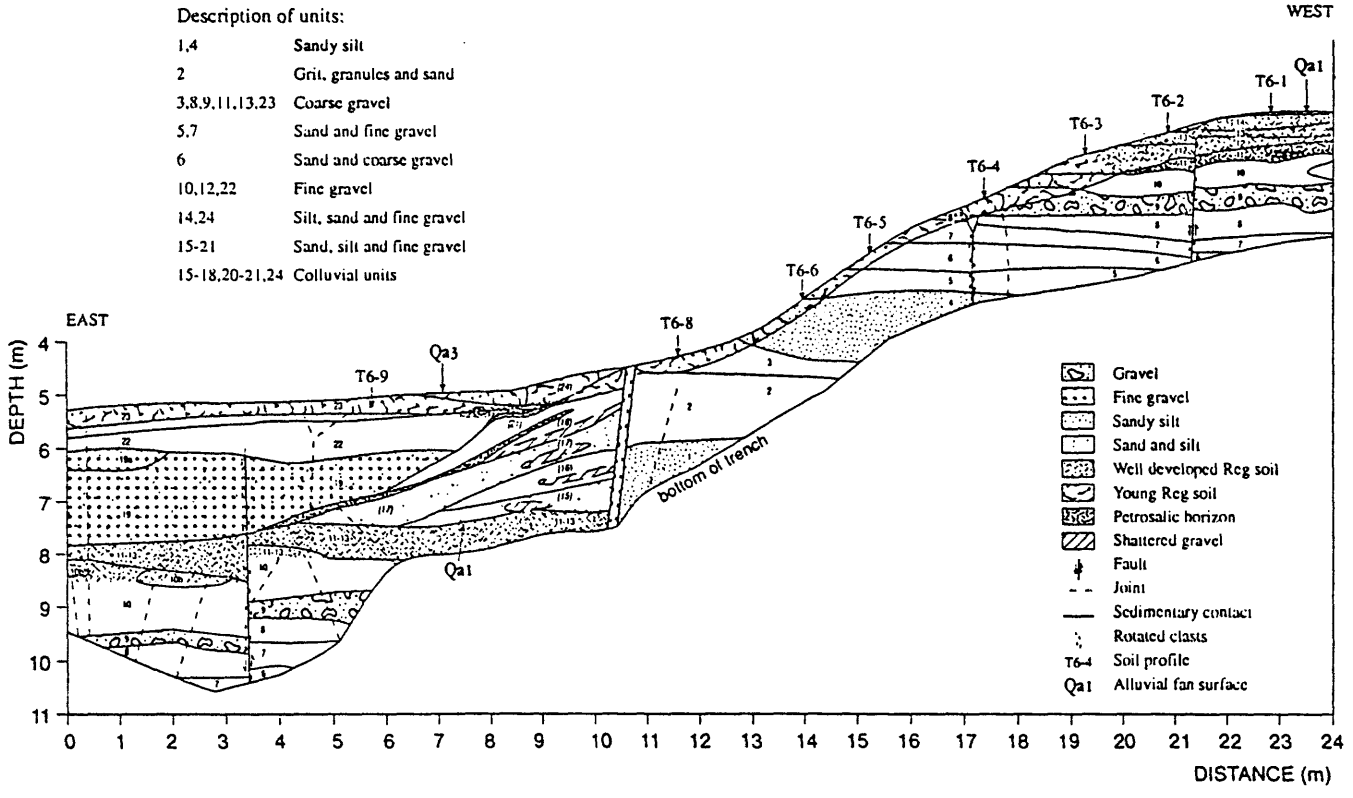

A model for geomorphic displacements applied to hillslope development in areas of active tectonics

J Ramón Arrowsmith, Department of Geological and Environmental Sciences, Leland Stanford Junior University, Stanford, CA 94305-2115; ramon@pangea.stanford.edu

The elevation of the topographic surface results from the combined effects of geomorphic processes such as erosion, transportation, and deposition and tectonic processes such as isostacy, folding, and faulting (Figure 1). The resulting landforms hold a richness of information concerning both the tectonic and geomorphic history of a region. For example, landforms can develop over time scales that are similar to, or a few times greater than, the typical great earthquake cycles of the San Andreas fault system (100s of yrs; e.g., [*Sieh,* 1978]) or that of faults of the Basin and Range (1000s of yrs; e.g., [*Schwartz and Coppersmith,* 1984]). Analysis of these landforms provides the opportunity to bridge the gaps between geodetic and geologic timescales and between the spatial scales of trenching and regional mapping. Therefore, the study of landforms may aid our understanding of how coseismic and longer term deformation are related, and enhance our knowledge of how the structures near a fault develop temporally and spatially. The model presented here provides a means of investigating the relative importance of different geomorphic processes on the resultant landforms. Temporal and spatial distributions of tectonic displacements more sophisticated than these initially faulted profiles will be added after the geomorphic portion of the model is evaluated.

Tectonic and geomorphic processes produce *displacements* of the earth's surface: tectonic processes displace it by raising the earth's crust above its surroundings or sinking it below, while the geomorphic processes displace it by transporting solid material along the earth's surface [*Penck,* 1953]. Penck's suggestion may be expressed as:

$$H(x,y,t) = H_0(x,y) + v(x,y,t) + g(x,y,t). \quad (1)$$

In which the elevation of the topographic surface, H, is a function of horizontal coordinates, x, y and time, t (Figure 1). H is equivalent to the initial shape at $t = 0$, $H_0(x, y)$, plus the vertical component of tectonic displacement, $v(x, y, t)$, and the vertical component of geomorphic displacement, $g(x, y, t)$. We differentiate (1) with respect to time:

$$\frac{\partial H}{\partial t} = \frac{\partial v}{\partial t} + \frac{\partial g}{\partial t}. \quad (2)$$

The change in elevation with time at a point is equal to the change in elevation due to tectonics plus that due to geomorphic redistribution of material. For this analysis of representative landform profiles, the horizontal dimension, x, is the distance along the profile, and the elevation along the it is H (Figure 1). We assume that all material flows along the plane of the profile. We also explicitly treat the ends of the profile with different boundary conditions (constant elevation or constant flux of material).

Determination of the vertical component of geomorphic displacement is based upon the assumption of continuity of debris along the profile [*Kirkby,* 1971; *Carson and Kirkby,* 1972]. The geomorphic displacement rate ($\partial g/\partial t$) is determined by the change in material transport rate per unit width (Q) over the slope length. We approximate the slope length by the horizontal length, and consider no volume changes during weathering:

$$\frac{\partial g}{\partial t} = -\frac{\partial Q}{\partial x} \quad \text{(continuity equation for material transport).} \quad (3)$$

If more material is available for transport than can be eroded, the situation is called "transport-limited;" whereas if more could be eroded than is available, the situation is called "weathering-limited" [*Carson and Kirkby,* 1972]. Q is equal to T, the capacity of material transport per unit width, only for completely transport limited cases. Paleoseismic investigations in areas with variable weathering rates (i. e., different climates and bedrock types) may be considered using this model.

The material that is eroded or deposited is soil; therefore, supply is dependent upon soil profile development. A second continuity equation describes the change in soil thickness:

$$\frac{\partial C}{\partial t} = \frac{\partial H}{\partial t} - \frac{\partial B}{\partial t} \quad \text{(continuity equation for soil thickness);} \quad (4)$$

such that the soil thickness ($C(x,t)$) changes with time as the soil/bedrock interface elevation ($B(x,t)$) and height (H) change with time (Figure 1, [*Ahnert,* 1970]). The soil is produced according to the following rule for mechanical weathering due to thermal and other depth-dependent processes [*Anderson and Humphrey,* 1989]:

$$\frac{\partial B}{\partial t} = -B_a e^{\{-B_b C(x)\}} \quad \text{(weathering rate equation);} \quad (5)$$

where B_a is the weathering rate of bare bedrock, and B_b scales the depth of weathering. If erosion does not remove material, the soil production rate will decrease as the soil thickens. With increased erosion, however, the overlying soil thins, and the soil production rate increases. This is a positive feedback between erosion and soil production.

The continuity approach allows us to vary the specific processes controlling the material transport rate without altering our entire analysis. Determination of T will depend upon the specific processes modeled. In this

analysis, we assert that the landforms are not as sensitive to early modification by threshold dependent processes (like slumping) as they are to the processes acting over them for the long term [*Kirkby,* 1971]. Determination of the type and rates of these processes is crucial to this model and in any paleoseismologic inferences.

The transport capacity (T) for many threshold independent processes is proportional to power functions of the flow depth of the water providing the traction for transport and the local slope. Along a profile, flow depth scales with distance from the divide. The transport capacity can be expressed with the form:

$$T = kx^m \cdot \left(\frac{\partial H}{\partial x}\right)^n \quad \text{(constitutive equation).} \tag{6}$$

That is a function of the distance from the divide (x) multiplied by a power function of the slope and scaled by rate constant k. This constitutive equation may adequately describe processes that involve overland flow (e.g., wash, rilling, gullying, and even river flow--$m > 0$, $n > 0$) as well as those processes that are slope dependent only, (e.g., creep, rainsplash, frost-heave, and animal induced disturbances--$m = 0$, $n > 0$). Variations in the values of m and n control the type of process modeled (Figure 2; [*Kirkby,* 1971; *Carson and Kirkby,* 1972; *Colman,* 1987]).

Geomorphic displacements of material along profiles of arbitrary initial shape, variable processes and specified boundary conditions are simulated numerically. First, we examine transport versus weathering limited conditions. Figure 3A shows the simulation of hillslope development with variable soil production rates (B_a and B_b) over an initially faulted profile. All other parameters are constant, including constant elevation boundary conditions and no other tectonic displacements. The left plot shows the basic case of transport limited, diffusive geomorphic displacement. The right plot shows the case of weathering limited geomorphic displacements, and the resulting bare bedrock surface is exposed over the steep portions of the profile. These results extend analyses of tectonic landforms to the full range of transport to weathering limited conditions.

If an plain is faulted to form a scarp, flux over the scarp face may be sufficient to cause gully formation and scarp incision. The transition from diffusive processes ($m = 0$, $n = 1$) to those that include overland flow ($m > 0$) is simulated by incorporating a threshold flux at a channel head. At a point along a profile over which only slope dependent processes act, if the flux exceeds a critical value (Q_{crit}), the point is a channel head, and at all nodes below it, the processes include the discharge component. Figure 3B shows a simulation of this example; in the upper left, Q_{crit} is too great, and transport capacity is only slope dependent and little change in form is observed. In the other two plots, Q_{crit} is sufficiently low to allow incision. Typical morphologic dating of fault scarps has not considered gullies, but these results indicate that their development may be simulated and tectonic displacements inferred.

Conclusions

We model idealized geometries, conditions, and histories of tectonic landforms while systematically changing various parameters. The simulations serve to develop intuition, and to indicate which parameters or processes are important and should be the focus of detailed field observations. Field investigations (particularly trenching) generally provide the greatest precision in paleoseismologic investigations; however, they are expensive and localized. Calibration of these parameters and processes may provide quantitative means of simulating landform development over a broad area, and when combined with realistic tectonic displacement patterns (i.e., those determined using dislocation methods, and corroborated by structural geologic analyses or geodetic observations), evaluation of deformation rates and inference of seismic hazard.

Acknowledgments

I am grateful to David D. Pollard for supervision of this research and to Dallas D. Rhodes for encouragement. Discussions with Robert S. Anderson, Roland Bürgmann, and Thomas C. Hanks have contributed to the development of this model. This research has been supported by the USGS-Stanford Fellowship and by USGS NEHRP grant 1434-94-G-2464.

References

Ahnert, F., Brief description of a comprehensive three-dimensional process-response model of landform development, *Zeitschrift fur Geomorph., Supplementband, 24,* 11-22, 1970.

Anderson, R. S. and N. F. Humphrey, Interaction of weathering and transport processes in the evolution of arid landscapes, in *Quantitative dynamic stratigraphy*, edited by T. A. Cross, pp. 349-361, Prentice-Hall, Englewood Cliffs, New Jersey,, 1989.

Carson, M. A. and M. J. Kirkby, *Hillslope form and process*, 475 p., Cambridge University Press, Cambridge, 1972.

Colman, S. M., Limits and constraints of the diffusion equation in modeling geological processes of scarp degradation, in *Directions in paleoseismology*, edited by A. J. Crone and E. M. Omdahl, pp. 311-316, U. S. Geological Survey Open File Report, 1987.

Kirkby, M. J., Hillslope process-response models based upon the continuity equation, in *Slopes: form and process*, edited by D. Brunsden, pp. Inst. Br. Geog. Spec. Pub., 1971.

Penck, W., *Morphological analysis of land forms*, 429 p., MacMillan, London, United Kingdom, 1953.

Schwartz, D. P. and K. J. Coppersmith, Fault behavior and characteristic earthquakes; examples from the Wasatch and San Andreas fault zones, *Journal of Geophysical Research, 89,* 5681-5698, 1984.

Sieh, K. E., Prehistoric large earthquakes produced by slip on the San Andreas fault at Pallet Creek, California, *Journal of Geophysical Research, 83,* 3907-3939, 1978.

Figure 1. A) Schematic view of the interaction between tectonic and geomorphic processes and the resulting landscape. B) Schematic hillslope profile and significant components (modified from Carson and Kirkby, 1972).

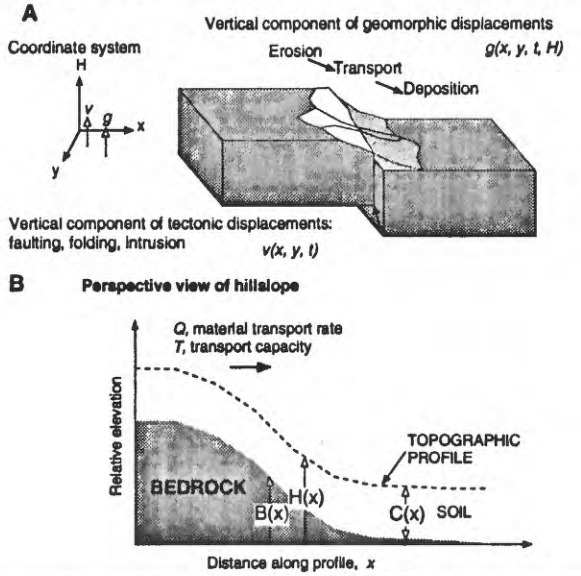

Figure 2. Approximate "characteristic forms" to which hillslope profiles tend with transport limited conditions, no differential tectonic displacements and constant elevation boundary conditions. The resultant form depends upon the process: convex for slope dependent processes such as creep, rainsplash and animal induced disturbances ($m = 0$), straight for sheetwash ($m = 1$, all n), and concave for gullying and rivers ($m > 1$, $n > 0$). After Carson & Kirkby, 1972.

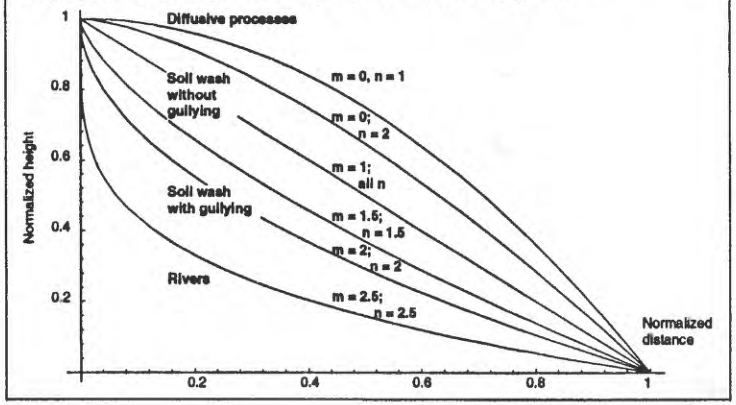

Figure 3. A) Simulations of hillslope development with variable soil production rates showing the transition from transport-limited to weathering-limited conditions. All parameters and initial and boundary conditions are the same except for B_a and B_b which vary from 1 and 1 to 0.01 and 100 respectively. B) Simulations of the formation and growth of channels along the profile. The channel head forms when the material transport rate exceeds a critical value (Q_{crit}) at a point. Downstream, the material transport capacity is defined by a non-zero m. The line with small dashes is the faulted initial topographic profile, the longer dashes signify the initial soil/bedrock interface, the solid line is the final degraded topographic profile, and the the upper edge of the grey polygon is the final soil/bedrock interface.

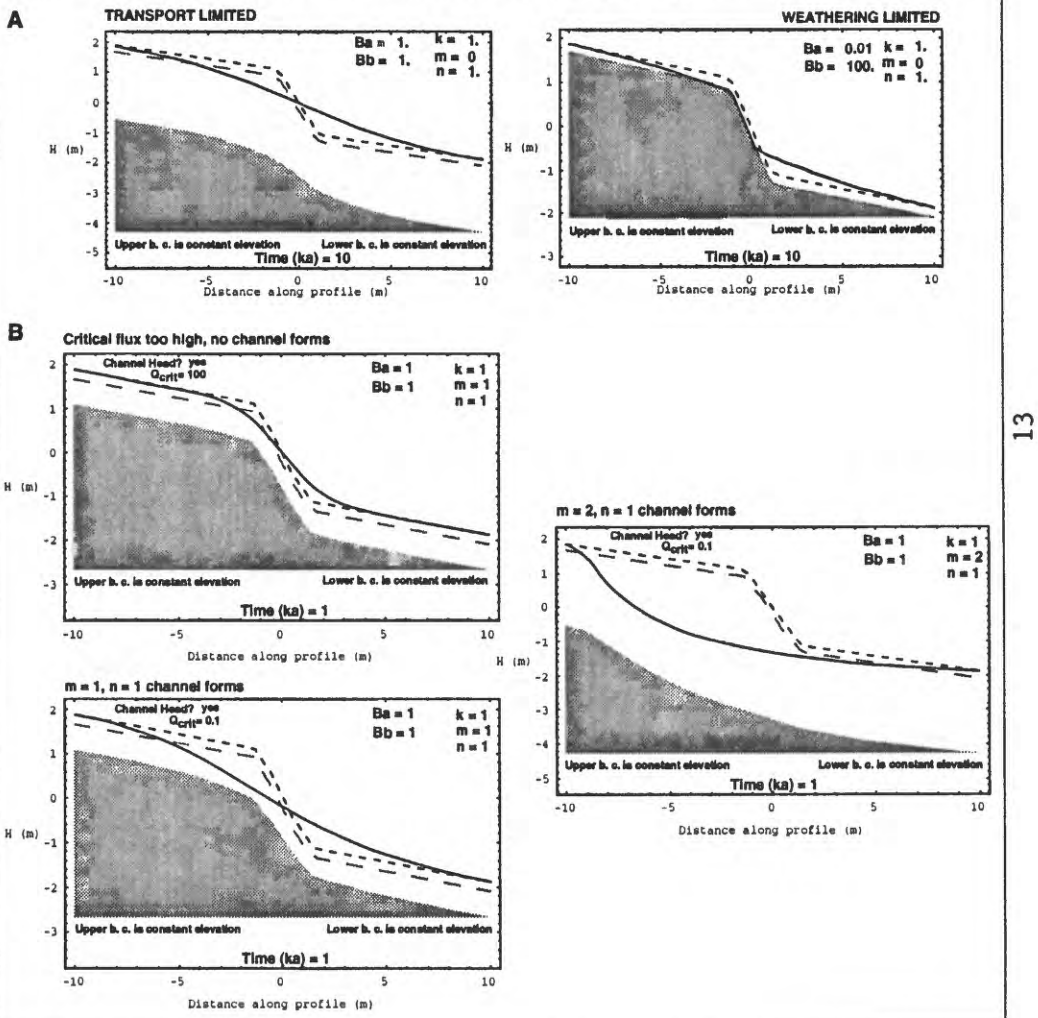

Potential of a Large Earthquake in the Erzincan Region Following the 1992 Erzincan Earthquake, M=6.9: Preliminary Trench Study Results.

Aykut A. Barka
ITU, Maden Fakultesi
Jeoloji Bolumu
Ayazaga, Istanbul 80206 Turkey
and
Steven G. Wesnousky
Center for N eotectonic Studies
University of Nevada, Reno
Reno, NV 89557

With the exception of a 75 km stretch of the fault located east of Erzincan, large earthquakes have produced surface ruptures along virtually the entire length of the North Anatolian Fault between Karliova and Lake Sapanca since 1939. Based upon historical accounts, it is possible that the 75 km segment produced the large earthquake in 1784 that caused the death of about 5000 people in the Erzincan region. The recent March 13, 1992 Ercincan earthquake, although in the vicinity of the North Anatolian fault, did not rupture along the main strand of the North Anatolian fault.

We excavated a set of exploratory trenches across and parallel to the North Anatolian fault near the junction of Ali and Gortel creeks about 30 km east of Ercincan (Figure 1). The fault trace at this point is linear, cuts through fluvial terraces of the two creeks, and shows opposite facing scarps ranging to about 40 cm height. The fault apparently controls the location of spring and marsh deposits which abut the fault. Trenches 1 and 2 were located in a lower and younger terrace inset to the terrace on which trenches 3 and 4 were excavated. Trench #4 revealed of a massive clay on the north side of the fault juxtaposed against a sequence of clays and sandy silt layers (Figure 2). The main fault extends into the active soil layer and a subsidiary strand to the south is depositionally truncated by a clay bed. A piece of wood in a layer broken by both fault strands was dated at 3810±60 radiocarbon years BP. The relationships are the basis to interpret at least 2 events have ruptured the site in approximately the last 3810 years. A pair of fault-parallel trenches crossing Trench #2 also exposed a buried channel deposit offset right-laterally 3-6 meters (Figure 3). The age of a piece of wood beneath the channel was determined to be about 1000±60 radiocarbon years BP. Division of the offset by the age yields and estimated slip rate of about 3 to 6 mm/yr. Geological and GPS data have previously been the basis to estimate the slip rate for this section of the fault is about 11±3 mm/yr. The discrepancy between the geologic and geodetic rates may simply reflect that the geologic estimate of slip rate is a minimum. For example, the radiocarbon sample in Trench #2 provides only a maximum bound on the age of the displaced channel. As well, particularly if the 3-6 m offset represents only 1 event, the radiocarbon age of 1000±60 years may bracket a period much greater than a single interevent time.

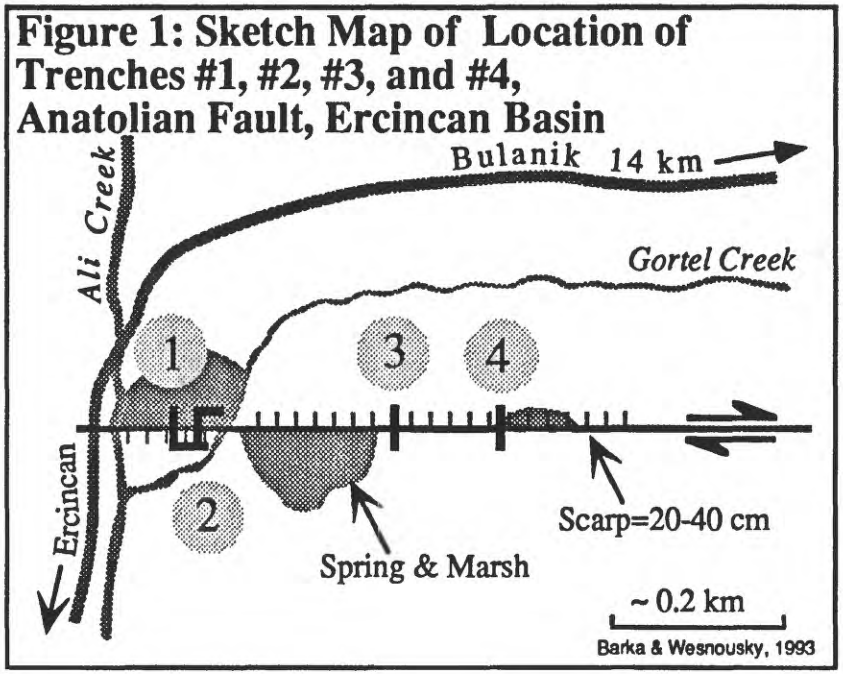
Figure 1: Sketch Map of Location of Trenches #1, #2, #3, and #4, Anatolian Fault, Ercincan Basin
Bulanik 14 km
Ali Creek
Gortel Creek
1
2
3
4
Ercincan
Scarp=20-40 cm
Spring & Marsh
~ 0.2 km
Barka & Wesnousky, 1993

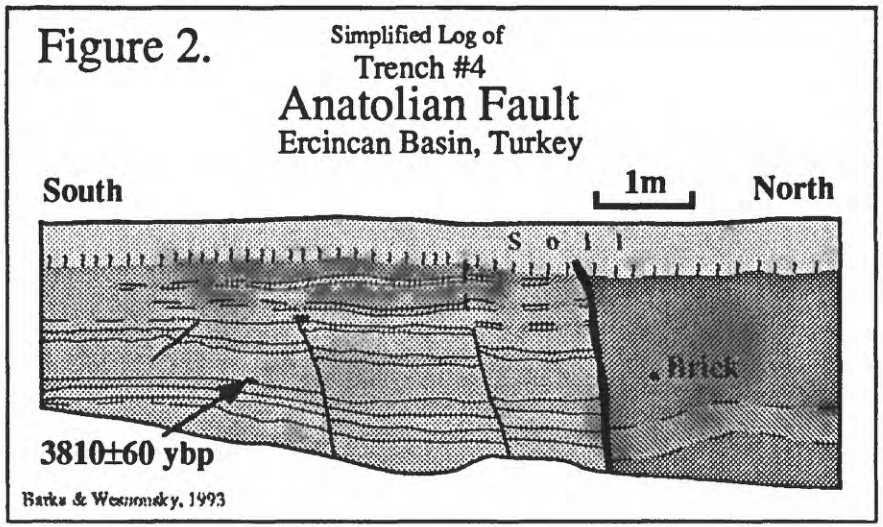
Figure 2.
Simplified Log of
Trench #4
Anatolian Fault
Ercincan Basin, Turkey
South
1m
North
S o i l
Brick
3810±60 ybp
Barka & Wesnousky, 1993

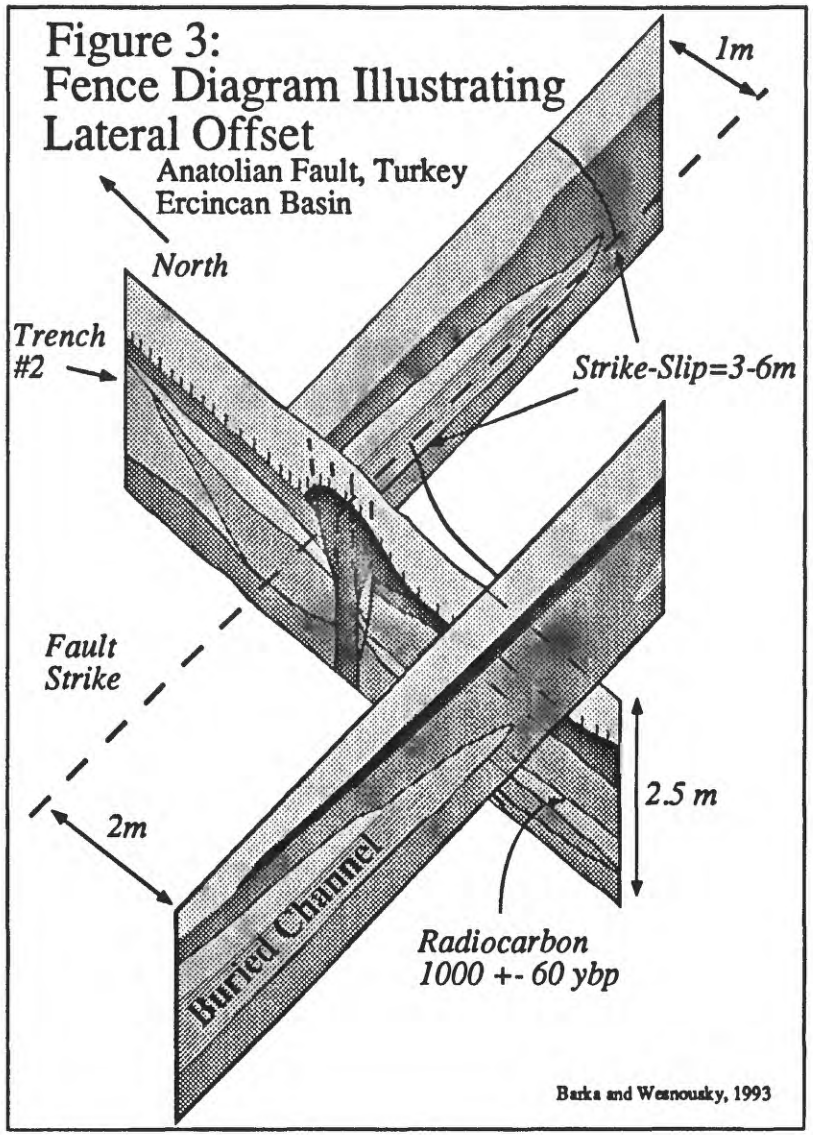
Figure 3:
Fence Diagram Illustrating
Lateral Offset
Anatolian Fault, Turkey
Ercincan Basin
North
1m
Trench
#2
Strike-Slip=3-6m
Fault
Strike
2m
2.5 m
Buried Channel
Radiocarbon
1000 +- 60 ybp
Barka and Wesnousky, 1993

New Data from Mahia Peninsula, New Zealand Pertaining to a Model of Coseismic Coastal Uplift

Kelvin Berryman, Institute of Geological and Nuclear Sciences, Lower Hutt, New Zealand
Alan Beu, Institute of Geological and Nuclear Sciences, Lower Hutt, New Zealand
Sarah Irwin, Geology Department, Victoria University of Wellington, New Zealand

Sequences of uplifted Holocene marine terraces are conspicuous features of the coastal landscape of many parts of New Zealand. Extensive sequences along the east coast of the North Island are located on the leading edge of the Australian plate, 50-150 km west of the Hikurangi Trench, where the Pacific plate is being subducted beneath the Australian plate. Reconnaissance-level studies of the Holocene terrace sequences along the east coast (eg. Berryman et al., 1989; Ota et al., 1991; Ota et al., 1992) have presented interpretations of co-seismic coastal uplift using radiocarbon dates of organic (mostly molluscs) deposits from marine sediment overlying the uplifted shore platforms as the basis for the chronology of the uplift events.

A model of terrace formation and uplift has developed (Hull, 1987; Berryman et al., 1992) which involves abrasion and chemical weathering of shore platforms, and deposition of shallow marine and beach sediments within the spring tide range during periods of tectonic stability, separated by essentially instantaneous, earthquake-related uplift. In this model the timing of uplift events has been accepted as the youngest date obtained from marine or beach sediments from the deposits overlying each shore platform of a terrace sequence. The shortcomings of this model are the paucity of radiocarbon ages that are available from any one terrace, and uncertainty in the depositional history of sedimentation on shore platforms.

One of the most complete and well-dated sequences of Holocene marine terraces in New Zealand (and worldwide) is at Mahia Peninsula (Berryman et al., 1989; Berryman, 1993), on the east coast about 50 km south of Gisborne. The Holocene coastal plain at Mahia Peninsula is subdivided into five distinct levels, each of which is interpreted to represent a co-seismic uplift event. At Table Cape in the northeast corner of the peninsula studies to date indicate that all but the oldest of the Holocene terraces is preserved. Material for radiocarbon dating (mostly intertidal molluscs) has been collected from within cover deposits of each of the terraces at Table Cape, and these samples appear to cluster in time for each of the terraces. However, samples have been collected in a fairly random fashion from the terraces, and only one sample has been obtained from the highest terrace and only two samples have been obtained from the second to highest terrace.

In March 1994 two trenches, each about 200 m long, were excavated across the Holocene coastal plain at Table Cape. These trenches provided continuous exposure of the cover deposits overlying the sequence of four uplifted shore platforms, and a unique opportunity to study the spatial and temporal distribution of sediments on uplifted shore platforms. Material for carbon dating occurred extensively throughout the deposits, and in conjunction with lithofacies description of the sediments in the uplifted terraces and on the modern shore platform, and faunal ecology, we anticipate that a more complete model of coseismic terrace uplift will be possible. More than 40 samples have been submitted for dating (June 1994) which will elucidate the age structure and depositional history of sediment accumulation.

Preliminary interpretation indicates the shore platforms are rapidly cut; that shore platform deposits are usually overlain by a high-tide, swash-zone, lithofacies, and this in turn is overlain by storm beach deposits. The high-tide deposits commonly occur in seaward off-lapping sequences indicating the marine and near-marine deposits on uplifted shore platforms were deposited in a prograding fashion. This might be interpreted as relative sea-level rise after uplift. Insufficient dating results are available at present to comment on the age structure

of the deposits, but when a full suite of dating results are available further insight into the following questions are anticipated:

- Does the sediment on the shore platforms get younger in a systematic fashion either vertically, or in distance from the fossil shoreline angle.
- Does the sediment on the shore platform span the whole time interval between uplift events.
- Do shell species from intertidal versus subtidal environments give significantly different ages in the same stratigraphic unit.
- Does the lithofacies and age distribution of sediments on individual platforms provide evidence for inter-seismic subsidence.
- How good is the model that the youngest age from each terrace closely approximates the time of co-seismic uplift.

References

Berryman, K.R. 1993: Age, height and deformation of Holocene marine terraces at Mahia Peninsula, Hikurangi subduction margin, New Zealand. *Tectonics 12:* 1347-1364.

Berryman, K.R.; Ota, Y.; Hull, A.G. 1989: Holocene paleoseismicity in the fold and thrust belt of the Hikurangi subduction zone, eastern North Island, New Zealand. *Tectonophysics 163:* 185-195.

Berryman, K.R.; Ota, Y.; Hull, A.G. 1992: Holocene coastal evolution under the influence of episodic tectonic uplift: Examples from New Zealand and Japan. *Quaternary International 15/16:* 31-46.

Hull, A.G. 1987: A late Holocene marine terrace on the Kidnappers coast, North Island, New Zealand: some implications for shore platform development processes and uplift mechanism. *Quaternary Research 28:* 183-195.

Ota, Y.; Hull, A.G.; Berryman, K.R. 1991: Coseismic uplift of Holocene marine terraces, Pakarae River area, eastern North Island, New Zealand. *Quaternary Research 35:* 331-346.

Ota, Y.; Hull, A.G.; Iso, N.; Ikeda, Y.; Moriya, I.; Yoshikawa, T. 1992: Holocene marine terraces on the northeast coast of North Island, New Zealand, and their tectonic significance. *New Zealand Journal of Geology and Geophysics 35:* 273-288.

Quantitative Approaches to Event Dating and Constraint

Glenn P. Biasi* and Ray J. Weldon, II, Dept. of Geological Sciences, Univ. of Oregon.
* now at Mackay School of Mines, Reno, NV, 89557.

We present here a quantitative method for constructing event date distributions from the calendric date distributions of event-bounding samples. Our approach avoids the loss of information that occurs when calendric date distributions are summarized to "2-sigma" ranges or "confidence intervals". In the simplest case the resulting events are characterized by the least committal distributions consistent with the ^{14}C data. Additional constraints from both the event horizon and from other stratigraphically related samples can be applied to gain greater resolution, and their consequences may be assessed graphically. Formally the methods presented here follow from simple results of inverse (Bayesian) probability, but practically they amount to counting cases favorable to an event occurring in a certain interval as a fraction of the total number of possible cases.

The principle of event dating is illustrated in Figure 1. The case (Fig. 1a) of perfect bounding dates (e.g., two historical records) illustrates the role of prior information about the event. One might know only that the paleoseismic event occurred in the past. This information can be expressed by a uniform prior event distribution. The resulting event distribution shows that given the data, the (posterior) event distribution is equally likely only between the samples. One might alternatively have a prior notion (Fig 1b) that events are more likely at some times than at others (e.g., more likely for a time after an adjoining segment fails; Sanders, 1993). Given perfect bounding date information, the portion of the prior distribution between the two samples becomes the event posterior distribution. Prior event distributions are used, implicitly or explicitly, in all paleoseismic event dating. The least committal event prior, the uniform distribution, is usually considered the most objective, and will be used in subsequent discussions.

The more typical case of an event bounded by uncertain non-overlapping distributions is shown in Figure 1c. The data require time for the bounding samples to form, but the event could have occurred within the distributions of the samples (with lesser probability) as well as between them. The probability that event year x postdates sample 1 is equal to the area under sample 1 for time less than (i.e., to the left of) x, which is just its cumulative distribution. Similarly, the probability that it predates sample 2 is the complimentary cumulative distribution of sample 2. In between the event is equally likely anywhere. If the sample calendric distributions overlap (Fig. 1d), there is no flat central range in the event distribution, but the calculation itself is identical. Note that no summarization of the underlying data is required, and that the event distributions quantitatively reflect the sample distributions themselves.

Two sources of additional constraint are commonly available to refine paleoseismic event date estimates. One source derives from additional ^{14}C samples that are away from the event horizon but constrain event-bounding sample date distributions by stratigraphic inference. Quantitative calendric date refinement (Biasi and Weldon, 1994) applied to data from the Pallett Creek and Wrightwood paleoseismic sites on the southern San Andreas fault yielded 59% average variance reduction for sample distributions using stratigraphic ordering alone, and 85% by adding sedimentation rate derived constraints to ordering (Fig. 2). Event date distributions from the narrower bounding distributions are themselves narrower and better defined (Fig. 3, dot-dash; Biasi and Weldon, in review). The other source of additional constraint is from field relations at the event horizon itself. For example, peat accumulated above the subjacent sample and below the event horizon took some time to grow, so at least that time must separate the two (Figure 1e). Prehistoric dated events at the Wrightwood site using this constraint (Biasi and Weldon, in review; Fumal et al., 1993; Weldon, 1991) are shown in Figure 3.

Types of event horizon constraint we have considered are shown in Table 1. The mathematics and a more complete motivation for these cases will be described elsewhere

Figure 1. Quantitative event constraint. Fine dashed lines are event prior distributions. Uniform priors not shown in c, d, and e. Heavy dashed lines are event distributions given the present data. Fine solid lines represent calendric date distributions for bounding samples.

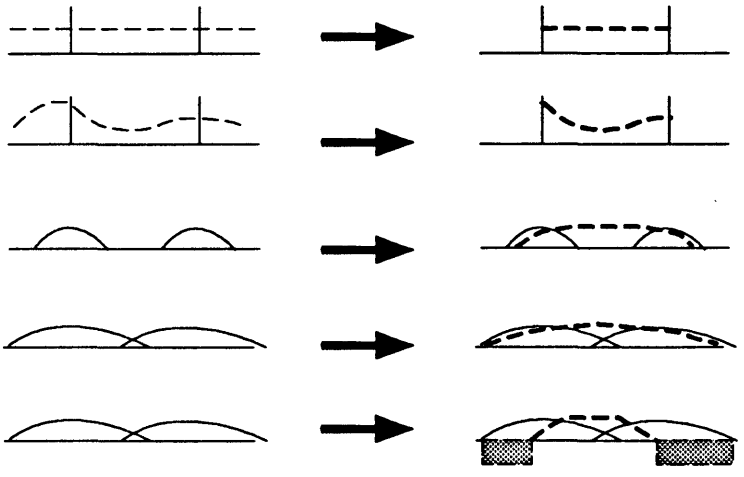

a. Perfect dates, uniform event prior

b. Perfect dates, non-uniform event prior.

c. Imperfect dates, non-overlapping

d. Imperfect dates, overlapping

e. Imperfect dates, event horizon separated from samples by some known time.

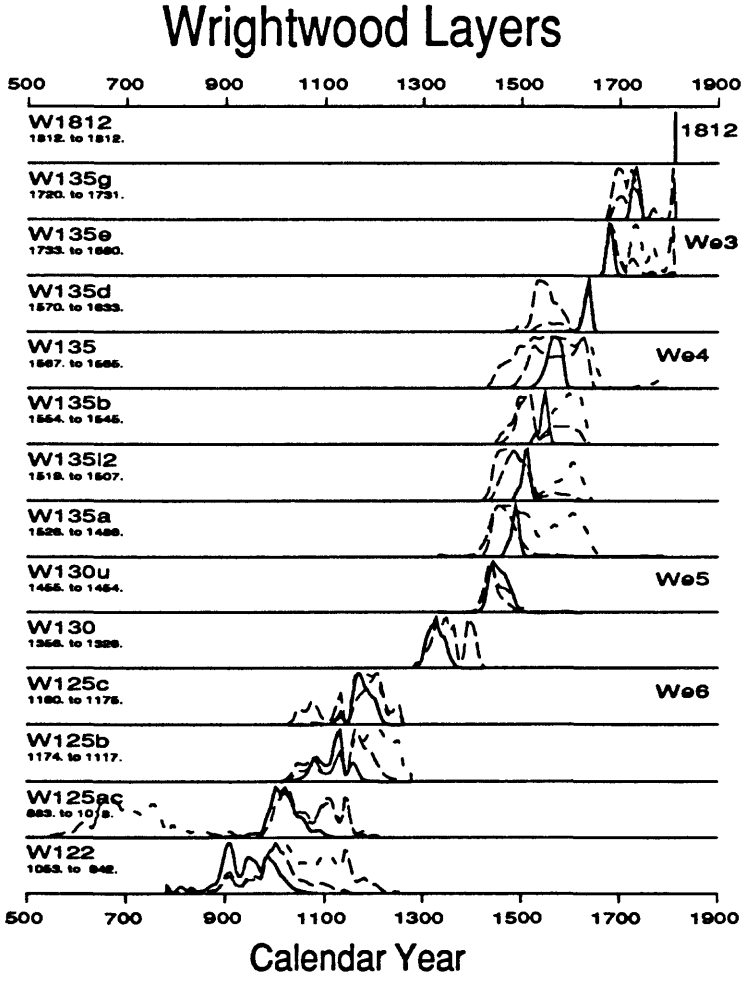

Figure 2. Layer dates at Wrightwood. Dashed: calibrated distributions. Short dash: ordering applied quantitatively (Biasi and Weldon, 1994). Solid: Peat thickness used to constrain time between sampled layers. Means of calibrated (prior) and fully constrained distributions are shown beneath the layer names. Wrightwood events are shown in their stratigraphic position on the right.

(Biasi, in prep). Atwater et al. (1991) qualitatively applied the exact separation constraint to estimate the death year of coseismically killed trees in coastal Pacific Northwest. Annual rings counted between an inner sample and the outermost provided the numerical constraint. Bayesian methods support this type of application, and do not require summarization of the underlying data to achieve resolution.

Table 1. Types of Separation Constraints

Separation	Example
At least Δx years	Time for at least organics to grow
Not more than Δx	Sample would decay or appear differently after Δx
$\Delta x \pm \delta x$	Variable sedimentation rate
Exactly Δx years	Δx annual rings separate samples

The methods sketched here provide a quantitative means of identifying constraints required by paleoseismic data. Stratigraphic ordering and quantitative relational constraints are often able to provide useful precision in event dates without the frequently subjective selection of calendric intercepts or individual ranges within a calendric distribution. Even where data are sparse Bayesian paradigms offer an improved strategy for identifying what is resolved in the data and where additional data would be most profitable.

References

Atwater, B., Stuiver, M., and Yamaguchi, D.K., 1991, Radiocarbon test of earthquake magnitude at the Cascadia subduction zone, *Nature, 353*, 156-158.

Biasi, G. and Weldon, R.J., II, 1994, Quantitative refinement of calibrated ^{14}C distributions, *Quaternary Research, 41*, 1-18.

Fumal, T.E., Pezzopane, S.K., Weldon, R.J. II, and Schwartz, D.P., 1993, A 100-year average recurrence interval for the San Andreas fault at Wrightwood, California, *Science, 259*, 199-203.

Sanders, C.O., 1993, Interactions of the San Jacinto and San Andreas fault zones, southern California: Triggered earthquake migration and coupled recurrence intervals, *Science, 260*, 973-976.

Weldon, Ray J. II, 1991, Active tectonic studies in the United States, 1987-1990, *Rev. Geophys. Supplement*, 890-906.

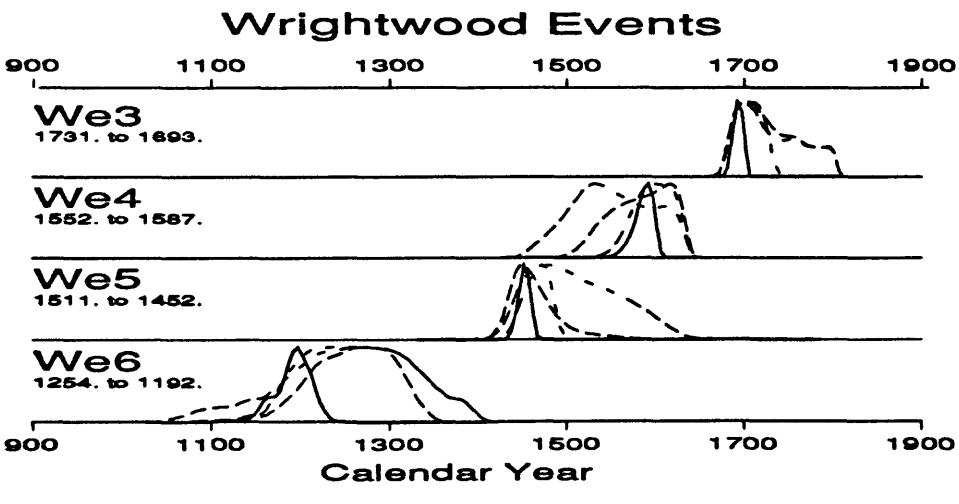

Figure 3. Dashed uses bounding calendric distributions; short dash: ordering constraint; long-short: peat constrained layer dates; solid: peat used at event horizon as well. Successive constraints yield increasing resolution, and unreasonable results lead to focused questions about the data and constraints.

Palaeoseismicity of the Souli Fault, Epirus, western Greece

M. Boccaletti, R. Caputo, Department of Earth Sciences, University of Florence, 50121, Florence, Italy
D. Mountrakis, S. Pavlides, N. Zouros, Department of Geology and Physical Geography, Aristotle University of Thessaloniki, 54006, Thessaloniki, Greece

A search to distinguish individual coseismic events in the geological record of the past several thousands years, was applied on the known Alpidic Souli strike-slip fault, Epirus, north-western Greece (greater Aegean region).

The E-W trending left-lateral Souli Fault, a relatively old structure of the area, affects Lias-Eocene carbonate and siliceous rocks and Oligocene-Burdigalian flysch (fig. 1). Along some segments of the fault, or in associated structures, young geomorphic features have been recognised emphasising an unknown recent tectonic activity.

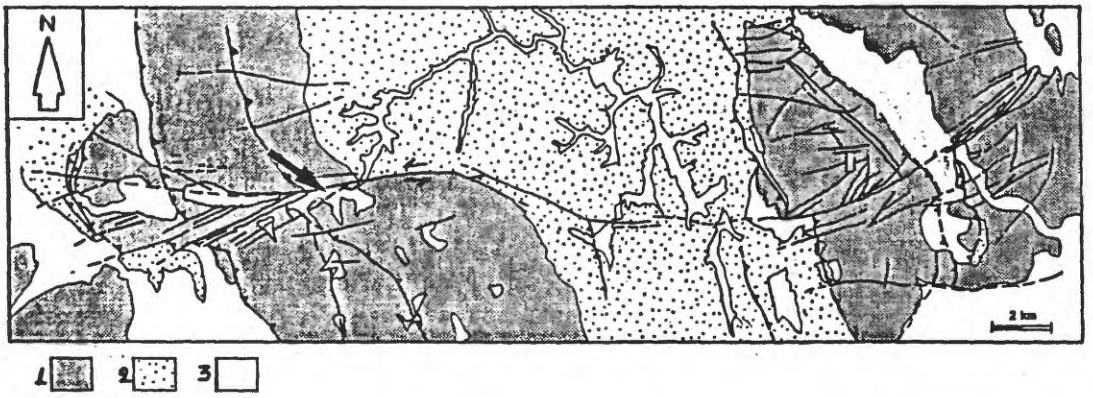

Fig. 1. Simplified geological and tectonic sketch of the Souli Fault (NW Greece), where the geometry of the fault is shown. 1. Carbonate cover (Lias-Eocene); 2. Flysch (Upper Eocene-Bourdigalian); 3. Quaternary sediments (alluvial and scree deposits mainly). Black arrow shows the site of the palaeoseismological section (log).

Such features mapped in scale of 1:20,000 are: a) Morphological scarps in alluvial deposits. The scarps are 1-1.5 m high straight features characterized by steep slope angle, while they lay in between two branches of the horsetail structure of the western edge of the fault. b) Sag pond type structures. c) Mesofaults affecting unidentified Quaternary sediments (synsedimentary tectonic activity).

The main attempt of this work was to provide a first-order approximation of the recent activity of the studied fault and the identification of prehistoric earthquakes on the basis of modern ideas and methodologies of palaeoseismology across

a natural palaeoseismological section and a lagoon - sag pond type carbon-rich layer (fig. 2).

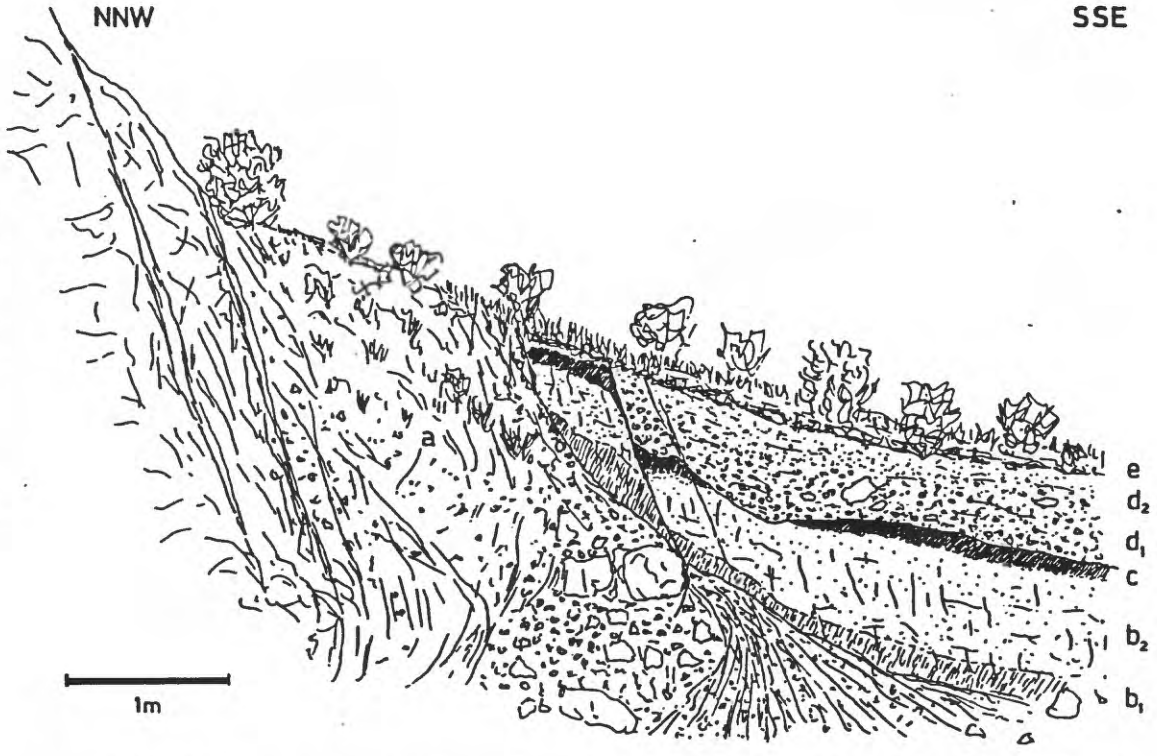

Fig. 2. The natural palaeoseismological trench as drawn in the field and from photographs. Solid dark stratum is the carbon rich lignite type layer. Letters refer to the microstartigraphic succession.

The latter gave the opportunity to date the very recent activity of the fault at about 20,000 to 26,000 years BP (^{14}C). Faulting of scarp derived colluvium and sag pond deposits along the Souli strike-slip fault has been considered as *de facto* evidence of more than one palaeoearthquakes. The definition of active fault based mainly on the time of the most recent displacement, such as ones in 33,000 or more than one in 500,000 yrs, according to the commonly used to designate the activity of fault the U.S. Nuclear Regulatory Commission and the International Atomic Energy Commission. Several distinct palaeoseismic events investigated, one of them (E_1) predates the Holocene times (about 26,000 yrs) and another one (E_2) or possibly two (E_2, E_3) post-date it. Probable older event(s) (E_0) could be considered those producing the fault mirror related with scarp deposits (fig. 3).

The relative chronology of the tecto-sedimentary events is as follows:

- deposition of layers b_1 and b_2;
- faulting along F_1;
- deposition of layer c;
- erosion of layer c and subsequent deposition of layer d_1;
- deposition of layer d_2;
- faulting along F_2, F_3 and F_4;
- pedogenesis and creation of layer e;
- actual erosion.

More precise microstratigraphic and dating analysis in this trench of the fault will help to establish the timing of the palaeoevents, while similar research along some neighbouring segments of the same fault system, showing analogous young geomorphic features, is needed.

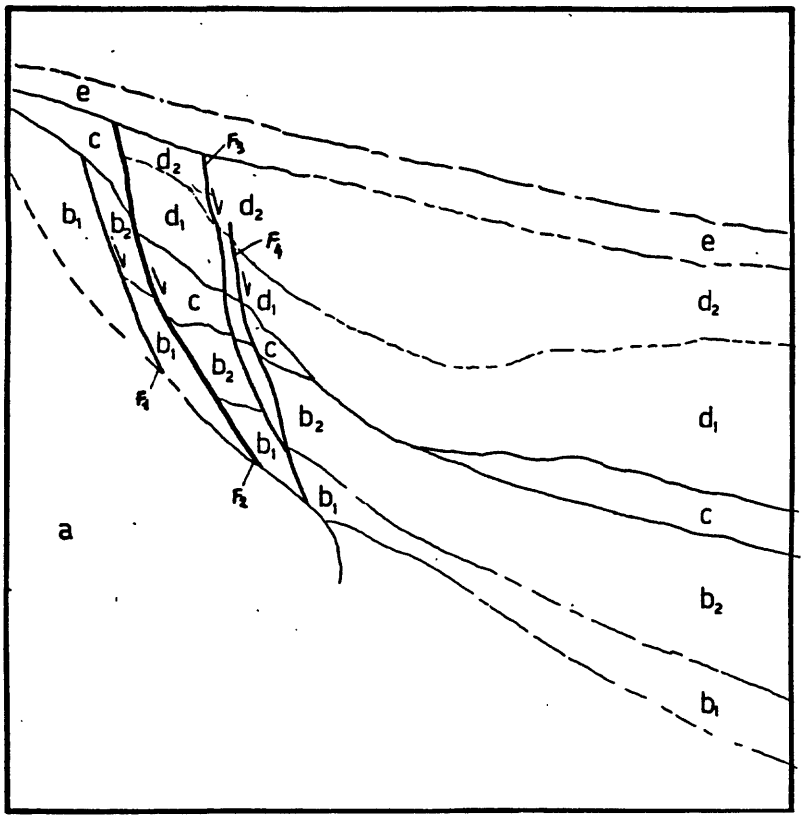

Fig. 3. Microstratigraphy at the studied section. Letters refer to the microstratigraphic succession. Several palaeoseismic events are present in the exposure. Event E_1 associated with F_1 faulting and affecting layer b predates deposits c (20,000 to 26,000 yrs), while event E_2 connected with F_2 faulting and b_1, b_2, c, d_1, d_2 layers post-dates layer c. A possible E_3 tectonic event could be associated with F_3 and F_4 faults, while older event(s) could be considered with the creation of wedge debris and boulder (layer a). The main displacement (coseismic) is 20 cm corresponding to a moderate size earthquake.

The Sangamon Strandline in Northern San Francisco Bay and its Significance for Paleoseismic Studies

Glenn Borchardt, Soil Tectonics, P.O. Box 5335, Berkeley, CA

Evidence is accumulating that northern San Francisco Bay is surrounded by a Sangamon strandline that exists 6-8 m above present sea level. Correlated to the last worldwide highstand of the sea (during oxygen isotope stage 5e at 122 ka), this datum provides an extremely useful marker for neotectonic studies. Although the strandline is buried deep within the sediments of southern San Francisco Bay due to subsidence (Atwater and others, 1977), it remains near the surface in northern San Francisco Bay due to the relative vertical crustal stability there (Borchardt, 1991). Remnants of the strandline are visible at:

1. Pinole Point, Richmond

An ancient beach is exposed in a north-facing cliff. An eastward dipping wave-cut platform has been cut into the Garrity Member of the Tertiary Contra Costa Group at elevations between 6 and 8 m. This is overlain by rounded beach cobble, marine sand, and locally derived alluvium.

2. Commodore Jones Point, Benicia

Tertiary Martinez sandstone at present sea level is overlain by 4 m of over-consolidated older bay mud, a 35-cm thick coquina, and estuarine silty clay (134 cm) and sand (23 cm) that reach an elevation of 5.9 m. The coquina contains Ostrea lurida shells dated at 80 to 130 ka via amino acid racemization (Atwater and others, 1981) and at 112±5 ka via U/Th series dating (Helley and others, 1993).

3. Lone Tree Point, Rodeo

Estuarine sand is overlain by a 100-cm thick coquina that reaches a maximum elevation of 5.1 m. It contains Ostrea lurida shells dated at 80 to 130 ka via amino acid racemization (Atwater and others, 1981). Three samples gave U/Th series dates of: 114±9, 142±13, and 132±6 ka (Helley and others, 1993).

4. Wilson Point, Pinole

An Illinoian paleosol is overlain here by a coquina with a maximum elevation of about 5 m above current sea level.

5. Rat Rock, China Camp State Park, San Rafael

Rat Rock is a tiny, flat-topped island on the west side of San Pablo Bay. Its surface, planated to the 6-m elevation, probably was formed as the lower part of the wave-cut platform that exists along the nearby shore. No doubt, other islands and resistant units in the San Pablo Bay area will yield further evidence for the Sangamon highstand.

The effects of the Sangamon highstand would have penetrated far inland. Streams draining into San Pablo Bay would have been flooded at least to the 20' topographic contour. Tidal marshes would have formed well inland of their present positions. Indeed, the Sangamon bay mud surface recently has been found at an elevation of about 6 m just north of Interstate 80 at Cordelia (Bob Wright, personal communication, 1994). Wright's preliminary calculations show piercing points on this surface to have been right laterally offset about 11 m, yielding a slip rate of at least 0.09 mm/yr for the Cordelia fault.

Another example of the use of the Sangamon strandline in paleoseismic work involves an on-going study at Point Pinole Regional Shoreline. Here the Sangamon sea crossed the Hayward fault, forming an embayment in which the ground above the fault was planated along its length for a distance of 1.5 km. All surficial deposits and geomorphological features within this partially buried embayment thus are younger than 122 ka. Soil stratigraphy in trench exposures and bore holes reveals the degree to which movement along the fault has offset the embayment. For instance, a high-elevation part of the embayment was moved northwest along the fault, crossing in front of the lowest part of the embayment. This formed a back-facing scarp which acted as a water barrier and formed a catchment for colluvium. Although the colluvium eventually buried the scarp, the shallow subsurface investigations so far reveal that the length of the scarp is between 740 and 1000 m. Thus, the slip rate calculated from these preliminary measurements is between 6.1 and 8.2 mm/yr.

References

Atwater, B.F., Hedel, C.W., and Helley, E.J., 1977, Late Quaternary depositional history, Holocene sea-level changes, and vertical crustal movement, southern San Francisco Bay, California: U. S. Geological Survey Professional Paper 1014, 15 p.

Atwater, B.F., Ross, B.E., and Wehmiller, J.F., 1981, Stratigraphy of Late Quaternary estuarine deposits and amino acid stereochemistry of oyster shells beneath San Francisco Bay, California: Quaternary Research, v. 16, p. 181-200.

Borchardt, Glenn, 1991, Vertical crustal stability between Point Pinole and Carquinez Strait during the Late Quaternary [abs.]: EOS, Transactions of the American Geophysical Union, v. 72, no. 44, p. 446.

Helley, E.J., Fitzpatrick, J.A., and Bischoff, J.L., 1993, Uranium-series dates on oyster shells from marine terraces of San Pablo Bay, California: U.S. Geological Survey Open-File Report 93-286, 6 p.

Paleoseismic Data and Probabilistic Seismic Hazard Maps, Los Angeles, Orange, and Ventura Counties, California

W.A. Bryant, M.D. Petersen, and C.H. Cramer
California Division of Mines and Geology, Sacramento, California

The California Department of Conservation, Division of Mines and Geology (DMG) is preparing provisional Probabilistic Seismic Hazard (PSH) Maps of peak ground acceleration and spectral acceleration at 0.3s and 1.0s, with exceedance probabilities of 10% in 50 years, 50% in 50 years, and 10% in 100 years for the region incorporating Los Angeles, Orange, and Ventura counties. This study was initiated following the damaging January 17, 1994 M_W 6.7 Northridge, California earthquake in order to better understand how the geology and neotectonics of the affected area contributed to losses from this earthquake. The model we use integrates geologic, geodetic, and seismic data to obtain recurrence rates of $M>6$ earthquakes.

Data from paleoseismology investigations are critical parameters for constructing PSH maps and include: 1) fault geometry and style of displacement; 2) age of latest displacement; 3) late Quaternary/Holocene slip rate; 4) fault segmentation; 5) amount of last displacement or maximum displacement per event; 6) recurrence intervals; and 7) characteristic earthquakes. We have produced a catalog of approximately 150 recognized (mapped) late Quaternary, Holocene, and historically active faults in California south of latitude 36°N and north of the California - Mexico border in order to assess the quality of seismic source models. About 40% of these faults have slip-rates reported in compilations such as Clark and others (1984), Wesnousky (1986), Thenhaus and Algermissen (p.c. 1994), and Petersen and Wesnousky, (in press). The quality of the reported slip rates is highly variable, ranging from well-constrained paleoseismology investigations (about 10%) to a best-guess estimate based on long term geologic offsets (about 40%). Often both the amount and timing of displacement are poorly constrained and reports for many strike-slip faults only contain the apparent vertical separation; the horizontal component is unknown and is either inferred or ignored. For example, the reported slip rate for the Raymond fault is 0.13mm/yr. However, this rate only reflects the vertical component of slip. Both geomorphic and seismologic evidence indicate that the fault is dominantly left-lateral strike-slip, suggesting that the seismic hazard from this source is underestimated. This inventory underscores the need for further study of the slip histories of faults in the southern California region in order to better understand their contribution to the seismic hazard of the area.

There are several sensitivity studies we will undertake in order to understand their effect on PSH Maps. For example, what effect does fault segmentation have on seismic hazards: does the hazard increase or decrease if faults rupture across segment boundaries? What are the constraints that need to be considered in deciding whether or not segment boundaries are barriers to rupture propagation? Major fault zones such as the San Andreas, San Jacinto, and Elsinore present a significant hazard to the tri-

county region and are relatively well-studied. However, geodetic data and distributed seismicity indicate that a sizeable hazard exits away from principal active faults in the study area. For example, several damaging earthquakes in the greater Los Angeles area within the past several years have occurred on either previously unrecognized faults with relatively low slip rates or concealed structures (blind thrust faults). These types of seismic sources probably have significant local contributions to seismic hazards, but the hazard can only be inferred because of a lack of currently available data. Paleoseismology studies need to be developed and/or refined to better understand the identification, extent, geometry, and rates of activity along these poorly understood seismic sources.

Earthquake Recurrence Intervals for the Alpine Fault, New Zealand

William B. Bull, Geosciences Department, University of Arizona, Tucson, AZ, 85721

New tools are needed to date and locate prehistorical earthquakes. Large earthquakes may occur offshore or without surface rupture, so earth scientists seek better ways to study prehistorical earthquakes than by trenching fault scarps or modeling scarp degradation. Studies of geomorphic processes that are sensitive to seismic shaking may 1) estimate earthquake recurrence intervals and elapsed times for specific faults, 2) locate the fault responsible for a prehistorical earthquake, 3) describe regional abundance of earthquakes, and 4) evaluate regional patterns of seismic shaking.

I use lichens to date rockfalls caused by prehistorical earthquakes in the Southern Alps of New Zealand. Coseismic rockfall events are regional in extent and can be dated by measuring sizes of lichens that colonize freshly exposed substrates. Each large earthquake adds more blocks to hillsides and stream terraces that serve as repositories for the cumulative rockfall record.

Skewed polymodal frequency distributions of sizes of lichens growing on incremental accumulations of rockfall blocks depict seismic and nonseismic rockfall events (Fig. 1). Abundance of rockfall blocks for a given event reflects intensity and duration of seismic shaking. The 43, 84, and 125 mm lichen-size modes are noted as three possibilities for recording great earthquakes. Testing of this premise included documentation of regional extent (prominent modes at many sites), and distribution relative to the adjacent Cook and Brunner segments of the Alpine fault. The 43 mm mode is conspicuous in a southern subarea and weak or absent in a northern subarea where a 40 mm mode is prominent.

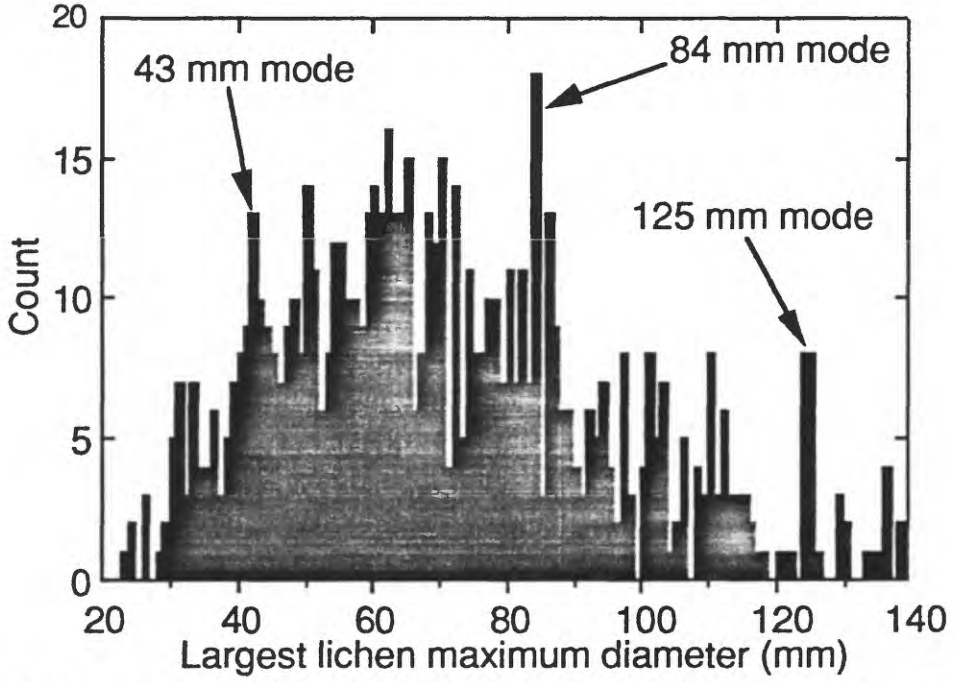

Figure 1. Frequency distribution of largest lichen maximum diameters on surficial blocks of glacial moraines near Mt. Cook. Isolated moraines are not sites of snow avalanches, and their deposits of well sorted boulders are not likely to be affected by storm events. Moraines are susceptible to seismic shaking. 1 mm class interval, n = 708.

Which of the two modes is dominant; the 43 mm mode? or the 40 mm mode? Sites where the 43 mm mode is dominant occur opposite the Cook segment (Fig. 2). Sites where the 40 mm mode is dominant occur in the northern subarea with minor overlap into the southern subarea. One or more earthquakes, on the Brunner segment of the Alpine fault, or on one of several other faults, seems responsible for the 40 mm mode.

Older events repeat the same patterns. A second pair of regional rockfall events is represented by the 84 and 80 mm lichen-size peaks (Fig. 2). Large lichens are not common, so only 28 of the 50 sites have lichens in the 125 mm and 121 mm modes; once again in the southern and northern subareas. Separation of class marks of modes for postulated Cook segment earthquakes is uniform (84.5 mm - 43.5 mm = 41 mm; 125.5 mm - 84.5 mm = 41 mm).

Four pairs of events allow calculation of earthquake recurrence intervals for the Cook segment with a lichen-growth equation. The provisional dates have 95% confidence levels of ± 3.0 to ±13.1 years. Approximate mean earthquake recurrence interval is 251.6 years, but the best data suggests 253 years. Elapsed time since the most recent earthquake is about 240 years.

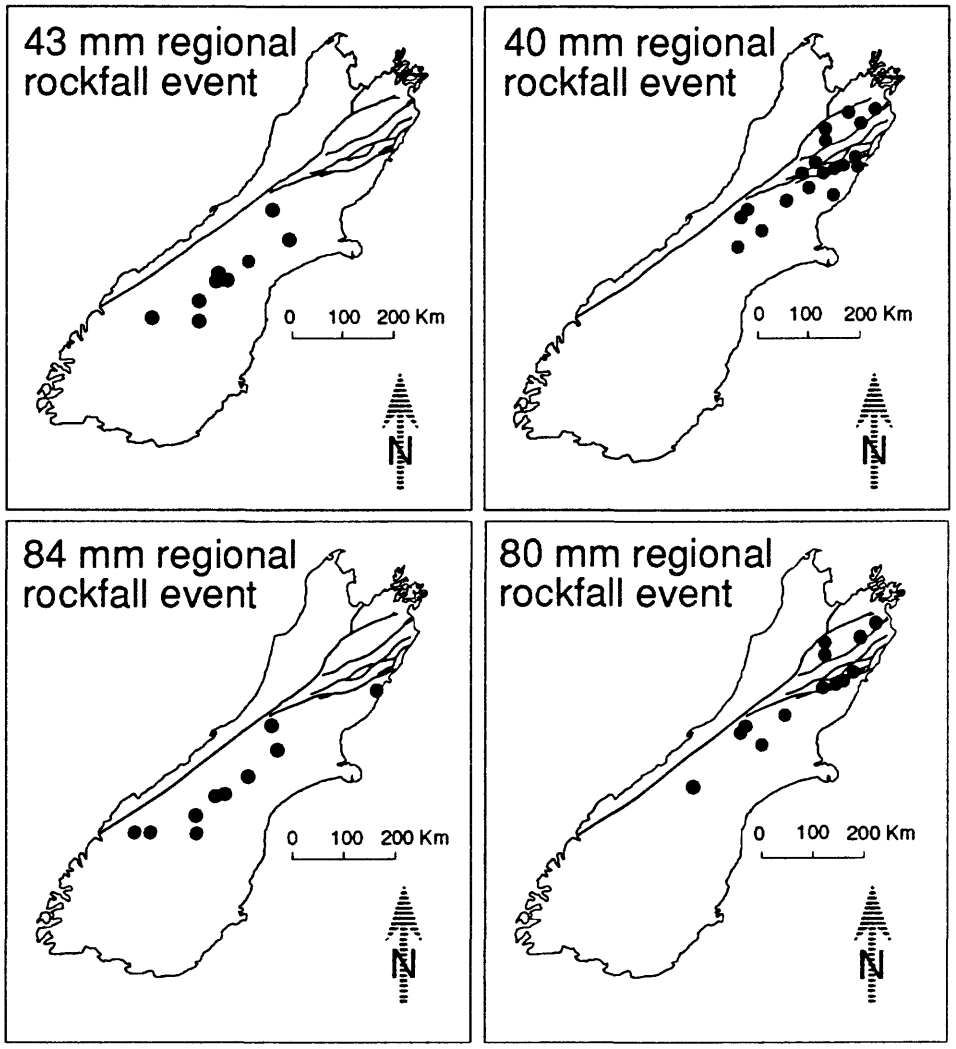

Figure 2. Locations of sites where either the 43 mm or 40 mm, and the 84 or 80 mm lichen-size mode is dominant. Distinct regional rockfall events have occurred repeatedly in the southern and northern subareas; the second earthquake of a pair occurring shortly after the first (1mm = 6 yr).

Alpine fault earthquakes seem to occur with clock-like regularity (Fig. 3). The Cook segment ruptured in 999 A. D. and 22 years later the Brunner segment is presumed to have ruptured. After 227 years of quiescence the Cook segment ruptured again followed by a Brunner segment earthquake. The next pair of earthquakes occurred after 228 years of quiescence, and the most recent pair after another 228 years. The coseismic rockfall lichenometry model easily and consistently identifies four pairs of earthquakes separated by only 18 to 25 yr.

The 40 mm mode (Fig. 2) encompasses two closely spaced regional rockfall events. Sites with 40.25 mm modes are widespread but are most common near the Brunner segment. Sites with 39.25 mm modes are most common in the eastern part of the northern subarea. The data presently available suggest that a Brunner segment earthquake occurred in about 1772 and was followed by a second northern subarea earthquake in about 1778.

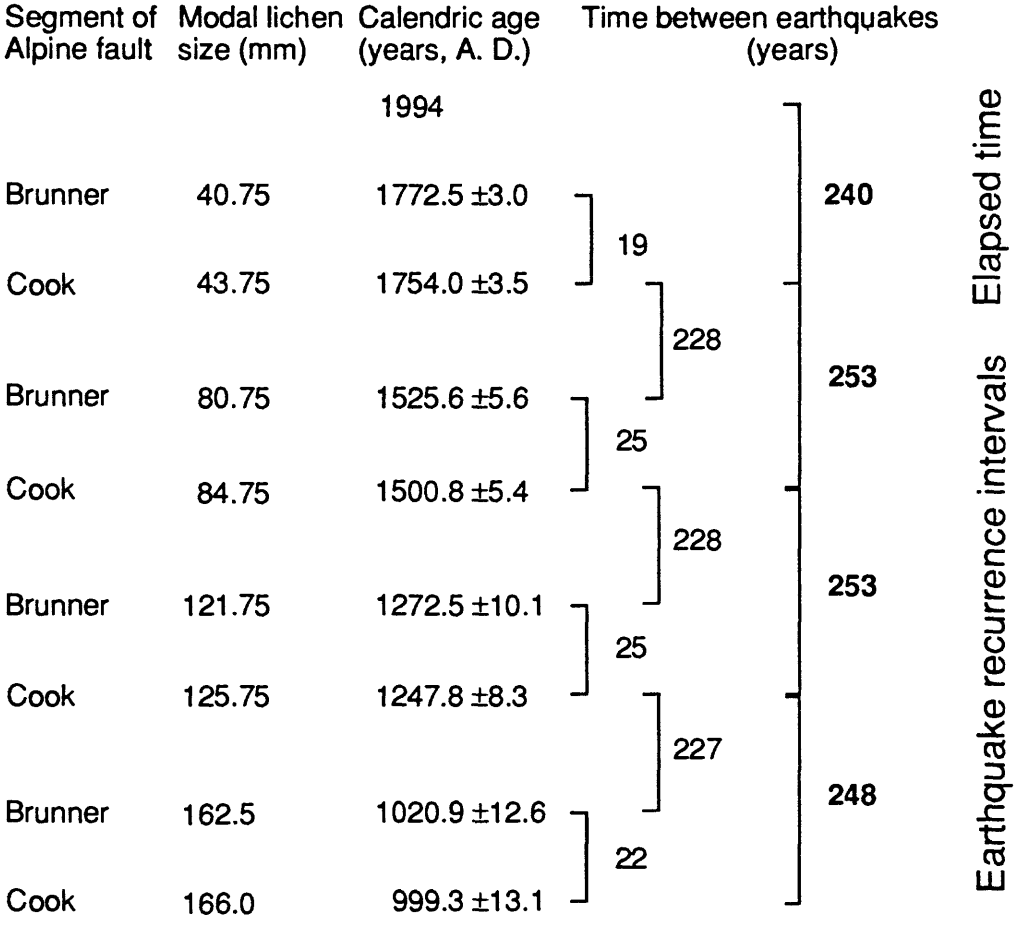

Figure 3.—Timing of four sequences of earthquakes along the Alpine Fault, New Zealand. The four pairs of lichen-size modes record exceptionally large, widespread regional rockfall events that are closely spaced in time and occur repeatedly. Lichenometric ages are estimated for the uniform growth phase of yellow rhizocarpons described by 10 historical coseismic rockfall events. The equation is $y = -0.162X + 327.893$, where y is modal lichen size and x is calendric age. Uncertainties are sums of measurement and regression errors; two standard deviations of measurement errors plus the 95% confidence limits for the regression.

In conclusion, it appears that Cook segment earthquakes occur about every 250 years, Brunner segment earthquakes about 20 years later; followed about 10 years later by another north subarea earthquake. The systematic behavior of the Alpine shear system supports the fault segmentation and characteristic earthquake models.

Slip Rates and Earthquake Hazard Along the Foothills Thrust Belt in the Southern San Francisco Bay Area

Roland Bürgmann, Department of Geophysics, Stanford University, Stanford, California
roland@pangea.stanford.edu

Ramón Arrowsmith, and Trevor Dumitru, Dept. of Geol. and Environ. Sciences, Stanford University

The large proportion of historic earthquakes in California with significant thrust slip has focused attention on active thrust faults in the San Francisco Bay area. During the 1989 Loma Prieta earthquake, Loma Prieta, the highest peak in the southern Santa Cruz Mountains (SCM), subsided about 10 cm. The southern SCM on the east side of the San Andreas fault are characterized by fault-bounded blocks that rise along active, deeply rooted, reverse and oblique-slip faults of the Foothills thrust belt (Fig. 1). Contraction is associated with a left bend along the San Andreas. The southwest dipping Foothills thrust system is composed of the Monte Vista, Shannon, and Berrocal fault zones (Fig. 2). Active faulting along the thrust belt must take place to explain the high uplift rates inferred from the youthful geomorphology and high topography. Here we estimate long-term slip rates, potential earthquake magnitudes, and average repeat times for events to evaluate the seismic hazard along the ~60 km long thrust belt.

In order to better understand the tectonic evolution and seismic risk in the area, we examine the deformation associated with the thrust belt using Late Cenozoic uplift rates, the Quaternary geomorphic expression, and historic displacements and seismicity. The assessment of long-term, as well as short-term, manifestations of deformation along the Foothills thrust belt allows us to evaluate the importance and potential earthquake risk posed by structures related to the uplifting southern SCM.

Apatite Fission Track Dating - Late Cenozoic Uplift. Fission tracks form in minerals such as apatite from the natural nuclear fission of dispersed trace amounts of ^{238}U. Decay occurs at a well-defined rate, so numbers of tracks and ^{238}U concentrations can be used to calculate fission track ages. Use of apatite fission track data for reconstructing cooling, uplift, and unroofing histories of rocks relies on the fact that tracks are erased by thermally-induced recrystallization at elevated subsurface temperatures >105-115 °C. With local geothermal gradients of about 30-35 °C/km, fission track ages thus date uplift through about the 3.5 km depth level.

Six samples from a transect across Loma Prieta yield concordant apatite fission track ages averaging 4.6 ± 0.5 Ma (Fig. 2). These ages date the time of cooling below ~110°C and suggest that about 3.5 km of unroofing has occurred over the last 4.6 m.y. Allowing for current elevations of about 1 km, this suggests an average uplift rate of the order of 1 mm/yr [*Bürgmann et al.*, 1994]. This rate represents the cumulative uplift associated with slip along all of the reverse faults in the Foothills thrust belt, since the sampling area is structurally high in the uppermost hanging wall. Further sampling across the thrust belt and to the northwest and southeast of the Loma Prieta area should reveal jumps in ages as shallower structural levels are sampled. Reverse faults of the Foothills thrust system accommodate most of the shortening across the range.

Morphometric Analysis - Quaternary Deformation. Detailed evaluation of topography, drainage patterns, and other geomorphic features can define the extent and distribution of areas of rapid Quaternary uplift. The principal effect of uplift on the geomorphic expression of an area is to increase the slope of streams, to increase channel erosion rates, and thus to increase the relief of drainage basins relative to the surrounding ridge crests. Locally, the interaction of streams with fault surface ruptures or actively deforming folds may lead to the development of offsets, knickpoints, and stream-gradient modifications.

Steep drainage slopes and high local relief indicate that the area east of the San Andreas from about Black Mountain to south of Loma Prieta forms a well-defined zone of high uplift. The highest elevations and steepest gradients are aligned with the Foothills thrust belt. The eastern flank of the range is significantly steeper than the west facing slopes. High local relief occurs along a ~30-km-long elongate zone aligned with the Berrocal fault zone north of Loma Prieta. Additional detailed geomorphic analyses suggest Quaternary slip along several faults at the northeastern margin of the SCM [*Hitchcock et al.*, 1994].

Geodetic Analyses - Historic Deformation. We utilize geodetic measurements of displacements in the San Francisco Bay area to constrain boundary element models of the historic uplift distribution due to fault slip and interseismic strain accumulation. Geodetic data (1906 San Francisco earthquake and subsequent strain transients, 20 years of interseismic deformation, 1989 Loma Prieta earthquake, and 4 years of post-Loma Prieta earthquake strain) show that the southern SCM repeatedly rise and subside through a complex sequence of Bay area deformation events. The average historic uplift rates associated with earthquakes, fault creep, and interseismic strain accumulation during the last ~150 yrs. are generally less than 1 mm/yr (Fig. 3). The southern SCM are *not* predicted to be a localized zone of high uplift rates. To achieve uplift rates of ~1 mm/yr in the Loma Prieta area in our model, slip rates along the underlying reverse fault zone must be about 2-3 mm/yr.

Following the Loma Prieta earthquake, northeast-southwest shortening of curbs and sidewalks was observed along the Foothills thrust belt [*Haugerud and Ellen,* 1990]. Parts of these fault zones have been seismically active in recent years [Kovach and Beroza, 1993] and experienced increased seismicity [*Reasenberg and Simpson,* 1992], and possibly accelerated aseismic creep at depth [*Bürgmann et al.,* 1994], in the aftermath of the Loma Prieta earthquake. Repeated GPS measurements show accelerated San-Andreas-parallel motion and contraction perpendicular to the fault that differ distinctly from the pre-earthquake fault parallel shear pattern. This may be caused, in part, by slip on one or more faults of the Berrocal and Shannon fault zones. Rapid slip along a fault of the Foothills thrust belt since the Loma Prieta event emphasizes the potential earthquake threat associated with these faults.

Seismic Risk Assessment. The long-term record revealed by geologic data indicates relatively high uplift rates in the southern SCM. Recent uplift patterns, based on models of historic deformation events, do not show significant uplift of the mountain range. Therefore, some intermittent mechanism, not yet expressed in the historic record, must be important. If the Foothills thrust system accommodates part of the geologic uplift, the Monte Vista, Shannon, and Berrocal fault zones will slip again, contributing to the uplift field. Average slip rates of 2-3 mm/yr are required on the underlying thrust system to achieve the ~1 mm/yr uplift rates suggested by the geologic data. Offset Quaternary deposits constrain the slip rate on the Monte Vista fault alone to ~0.4 mm/yr [*Hitchcock et al.*, 1994].

Evaluation of seismic risk is complicated by the recognition of triggered slip during the 1989 and 1906 earthquakes and the possibility of creep accommodating some of the fault slip as indicated by aseismic thrusting along the Berrocal fault zone following the 1989 Loma Prieta earthquake [*Bürgmann et al.*, 1994]. No paleoseismic evidence for an earthquake along the Foothills thrust belt exists to date, but offset Holocene deposits have been mapped along some faults. Records of historic seismicity in the area reach only as far back as the early 19th century. In 1865, a M 6.5 earthquake may have ruptured a thrust fault east of the San Andreas [*Tuttle and Sykes*, 1992].

The complex structure of the Foothills thrust belt makes it difficult to evaluate the potential magnitude and repeat times of earthquakes. Rupture of the ~25 km long Monte Vista fault zone could result in a M_w ~6.6 event [*Kovach and Beroza*, 1993]. An earthquake rupturing the whole length of the thrust belt from ~10 km depth to the surface could be larger than the M_w 7.1 Loma Prieta event, but would occur much closer to the densely populated Silicon Valley. Average occurrence intervals of $M > 6$ events may range from 300 to 1000 years depending on the length of the fault segment and slip magnitude. An earthquake comparable to the 1865 event in the southern SCM constitutes a significant hazard to the south San Francisco Bay region.

References

Bürgmann, R., P. Segall, M. Lisowski, and J. P. Svarc, Post-seismic strain following the 1989 Loma Prieta earthquake from repeated GPS measurements, *U.S. Geol. Surv. Prof. Pap., 1550*, in press, 1994.

Bürgmann, R., R. Arrowsmith, T. Dumitru, and R. McLaughlin, Rise and fall of the southern Santa Cruz Mountains, California, from fission tracks, geomorphology, and geodesy, *J. Geophys. Res.*, in press, 1994.

Haugerud, R. A., and S. D. Ellen, Coseismic ground deformation along the northeast margin of the Santa Cruz Mountains, *U.S. Geol. Surv. Open File Rep., 90-274*, 32-37, 1990.

Hitchcock, C. S., Kelson, K. I., and Thompson, S. C., Geomorphic investigations of deformation along the northeastern margin of the Santa Cruz Mountains, unpubl. Final Technical Report to N.E.H.R.P.

Kovach, R. L. and G. C. Beroza, Seismic potential from reverse faulting on the San Francisco Peninsula, *Bull. Seism. Soc. Am., 83*, 597-602, 1993.

Reasenberg, P. A., and R. W. Simpson, Response of regional seismicity to the static stress change produced by the Loma Prieta earthquake, *Science, 255*, 1687-1690, 1992.

Tuttle, M.P., and Sykes, L.R., 1992, Re-evaluation of several large historic earthquakes in the vicinity of the Loma Prieta and Peninsular segments of the San Andreas fault, California, *Bull. Seismol. Soc. Am., 82*, 1802-1820.

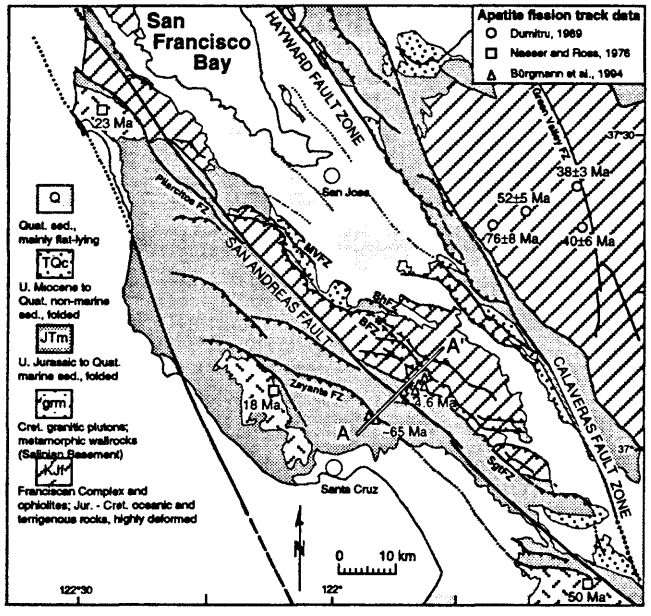

Figure 1. Geologic and fault map of the San Francisco Bay area with existing and new fission track ages. Fault abbreviations: MVFZ, Monte Vista fault zone; ShFZ, Shannon fault zone; BFZ, Berrocal fault zone; SgtFZ, Sargent fault zone; the Foothills thrust belt consists of the MVFZ, the BFZ, and the ShFZ. Modified from Aydin and Page [1984].

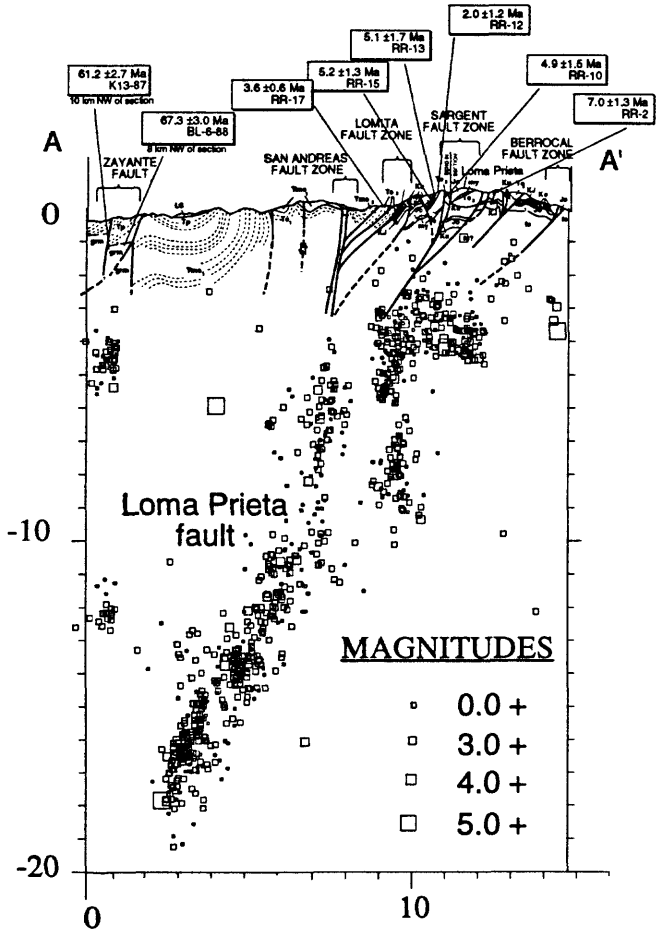

Figure 2. Cross-section showing the fault geometry inferred from geologic mapping [*McLaughlin*, 1989] and apatite fission track ages together with the aftershocks over 3 years following the Loma Prieta earthquake. Seismicity near the Foothills thrust system has been at a heightened level since the earthquake and may define a rapidly deforming region.

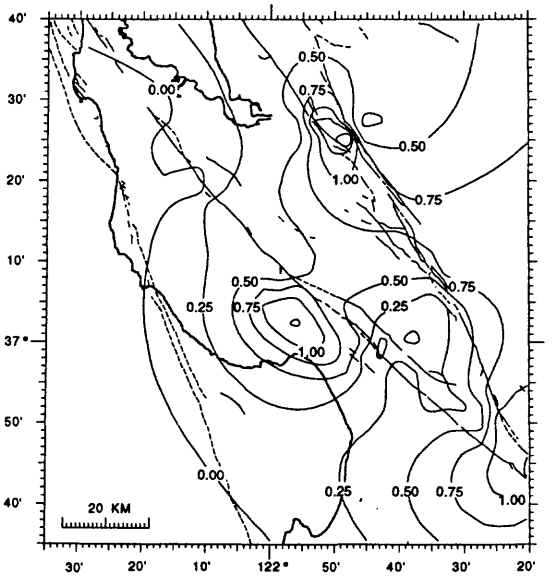

Figure 3. Vertical displacement rates in millimeters per year computed from a model of the known components of the Bay area deformation sequence. The combined effects on uplift rates of (1) slip on the San Andreas, Hayward, and Calaveras fault zones including creep and earthquake faulting, (2) full relaxation (deep slip) below the bay area faults, and (3) 1989 Loma Prieta type events assuming a repeat time of 1000 years. Two uplift zones southwest of the San Andreas fault are related to end effects of the rapidly slipping creeping section and the obliquely slipping Loma Prieta fault. Rapid uplift between the Hayward and Calaveras faults is caused by the transfer of ~8 mm of slip across a left-stepping discontinuity between the faults. Note that several topographic features, including the high-uplift zone east of the San Andreas, are not predicted by this model. Slip on the reverse faults of the Foothills thrust belt at 2-3 mm/yr could produce the geologic uplift rates.

Surface Rupture Characteristics and Slip Distribution for the 16 December 1954 Fairview Peak (M=7.2) and Dixie Valley (M=6.9) Earthquakes and Preliminary Results of Paleoseismic Investigations along the Fairview Peak Fault, Central Nevada

S.J. Caskey and S.G. Wesnousky, Center for Neotectonic Studies,
University of Nevada, Reno, NV
P. Zhang, Institute of Geology, State Seismological Bureau,
Beijing, China

With the use of 1:12k scale low-sun angle photography, we have traversed and mapped details of the surface trace and slip distribution of the 1954 Fairview Peak (FP) and Dixie Valley (DV) earthquake ruptures. The FP earthquake produced a complex pattern of surface faulting along a 63 km long, 6 km wide, north striking belt and was followed 4 minutes and 20 seconds later by the DV event. Surface ruptures of the DV event extend northward for about 45 km along the west side of DV. Fault offsets have been measured at about 600 sites. Prior investigations of these events (Slemmons, 1957) include few measurements of fault offsets and mapping at a relatively small scale. Our documentation of the sense, amount, and distribution of surface offsets along both fault systems will ultimately form the basis to construct a 3-D model of the fault systems and to examine the static failure stress changes on the DV fault induced by the FP earthquake.

FP earthquake ruptures are distributed among 5 different faults. Three of the five faults exhibit right-oblique motion, the exceptions being the Gold King fault (dip slip only) and the Phillips Wash fault (PWF) in northern Gabbs Valley which is left-oblique. The distribution of coseismic slip along the FP ruptures is complex and this is reflected in along strike variations in the amount, style, and direction of slip. New observations in the northern part of Gabbs Valley suggest that 1954 surface ruptures may overlap with surface ruptures from the 1932 Cedar Mountain earthquake by about 14 km.

DV earthquake ruptures were mainly dip slip and occurred along the Stillwater Range frontal fault and the distributed piedmont fault zone (collectively the Dixie Valley fault (DVF). The DVF exhibits along strike changes in the sense of lateral shear (Slemmons, 1957), but these changes are directly related to changes in fault strike and are all consistent with a single extension direction of about N80W. The largest vertical offsets occur along the range front ruptures (1.0-3.0 m) south of The Bend and north of Coyote Canyon. The distribution of vertical separation along this portion of the DVF is characterized by distinct bimodal pattern with a vertical slip low centered at Little Box Canyon. Map relations indicate that the piedmont fault zone merges with the range front fault at depth. Profiles across grabens showing greater heave than vertical offset and 3-pt constructions from detailed scarp line surveys indicate a moderately shallow fault dip (<45°) along much of the range front fault, particularly at Little Box Canyon area where fault dip appears to be as low 30°. The southern extent of the east-dipping DV rupture trace overlaps with and is separated from the northern-most west-dipping rupture trace of the FP event by about 6 km, indicating that fault ruptures from the two events intersect at a shallow level beneath DV.

An exploratory trench excavated across the Fairview Peak fault in the vicinity of Bell Canyon reveals evidence for a minimum of five earthquakes including the 1954 event. However, currently the timing of the paleoseismic events is poorly constrained and thus estimates of average recurrance intervals and slip rates for the Fairview Peak fault are pending.

Late Quaternary fault scarps and paleoseismology of the active basin of Mygdonia, Thessaloniki seismogenic area, northern Greece

A. Chatzipetros and S. Pavlides, Department of Geology and Physical Geography, Aristotle University of Thessaloniki, GR-54006, Thessaloniki, Greece

Mygdonia basin is located NE of the city of Thessaloniki (Central Macedonia, North Aegean region, Greece). Geologically it belongs to the Serbomacedonian geological zone, an old massif, which consists mainly of metamorphosed crystalline rocks (gneisses, amphibolites, mica schists and marbles) and post-orogenic magmatic intrusions of Mesozoic to Oligocene age. The active faults that bound the basin have mainly strike of either NW - SE, E - W and ENE - WSW direction. There are indications that the NW - SE faults have a sinistral component of movement, while the ENE - WSW faults a dextral one (oblique-slip faults). The E - W trending faults are mainly dip-slip ones. These observations and especially the cross-fault structure suggest that the tectonics of the area is perhaps more complicated than previously thought, especially if one takes into consideration the proximity of the area to the North Aegean Trough, which is considered to be the continuation of the dextral North Anatolian fault into the North Aegean Sea. There has been an effort for distinguishing independent segments along some "linear" faults of the basin according to known criteria. But in the Aegean region, the moderate to large magnitude earthquakes (M_S = 6.0) commonly involve the failure of a number of multiple fault structures. This has as result that various segments belonging to the same fault zone (antithetic, cross-faults etc.) are in motion simultaneously during an earthquake event. As fault zones we mean belts of multiple - multimode intersecting faults that lead to an often diverse pattern of fault movement. So, one can conclude that the general picture of the tectonic pattern in such seismogenic areas, and especially the Mygdonia-Thessaloniki one, is of multi-fractured type. The greatest instrumental recorded shocks of the basin were the 1902 Ms = 6.6 and the 1978 Ms = 6.5 earthquakes. There have been also many shocks with magnitude greater than 5. The 1978 earthquake in particular had a great impact in many ways, since it was the first earthquake in Greece that affected directly a big city (Thessaloniki) during modern times. From the six known historical earthquakes of the area (620 to 1759 A.C.) the observed seismic intensity (MM) was VII to IX corresponding to magnitudes of M = 6.5 - 6.6, while the same results arise from the instrumental seismicity. The application of different formulas for the estimation of the maximum expected earthquake magnitude according to the fault rupture length, which, for the 1978 shock, was 32 km, has been made. For these data, the different formulas used give magnitudes rating from 7.34 to 6.58. Generally, it seems that the maximum earthquake magnitudes of the basin should be no more than 6.6 - 6.7.

The study of the fault scarps was done by using detailed morphological cross-sections constructed by near-field topographic methods (theodolite measurements, step of x-axis measurements always ≤2m) as well as 1:5,000 scale topographic maps (4m contour interval, Greek Military Geographical Service). The method applied each time depended mainly on the scarp height. So the higher scarps were measured directly from the maps, while the smaller ones (meso- and small scale structures) from near-field data. In total, 111 cross-sections were made, from which we used 79. The main faults of the basin along much of their length define the contact between different materials. This has in result that the scarps have different behaviour concerning the relationship between their height and the corresponding slope angle.

A classification of the scarps was made, with the main criterion being the type of the scarp according to its formation procedure. The scarps were divided into three groups: **Group A:** scarps that were formed in the bedrock. They are steep scarps with a relatively big amount of displacement. These are considered to be the older generation of faults that formed the Pre-Mygdonian basin, as is shown by the corresponding sedimentation. Despite being older, their slope angle is greater than the scarps of the other groups. This of course is a result of the different physical properties of the cohesive bedrock material, in contrast to the incohesive basin sediments. **Group B:** scarps that affect the Neogene deposits. Those scarps have a big displacement and consist the faults of the post-middle Pleistocene tectonism, the one that created the main Mygdonian basin. The scarps of this group are generally the less steep of all. This happens because of the age of their formation, and the material that they deform. **Group C:** scarps that affect Neogene-Quaternary deposits. Those scarps are small and much steeper than the ones of Group B, although the material they are located into has approximately the same properties. The explanation in this case is that they are the youngest due to the active stress field, representing Holocene, if not historical, tectonic events. Their height suggests that they were probably created during recent earthquake events, probably no more than three or four events.

The equations that describe the relationship between the maximum scarp height (H) and the scarp angle (a) are: $\mathbf{a = 17.7 \log H + 4.54}$ for the scarps in the bedrock (group A), and $\mathbf{a = 11.7 \log H - 2.22}$ for the scarps in the basin sediments (groups B and C). As it can be clearly seen from the regression equations, the scarps of group A have generally a much greater slope angle than the scarps of the other groups, as has already been described above. Apart from the rock properties that have as a result this phenomenon, there is also the problem of age control. The scarps of group A represent the faults of the first generation. That means that the origin of these faults is quite old, but there is evidence, mainly from the 1978 earthquake faulting, that they are still active. Because of that, one would expect that the profiles of those scarps would be similar to those of a composite scarp. Instead, they look much more like a simple fault scarp. This assumption of course is wrong, because there is no way that scarps tens of meters high could have been formed during a few earthquake events only. So for the scarps of this type the degradation procedures are slow, and therefore the recent reactivations do not reflect a significant visible change in the scarp profiles. In contrary, the morphology of the scarps of groups B and C that are formed in similar loose materials, depends greatly on the age of their latest reactivation. This is shown clearly on their profiles, where many morphologic phenomena that can be interpreted as earthquake-induced can be found. Such are abrupt changes in the slope angle of composite scarps, different slope angles of the strands of multiple scarps, etc. The scarps of group B show in places a much steeper angle at about the middle of their height. This angle is similar to the observable angle of scarps of group C with the same height, thus indicating a chronological identification of the corresponding activity of these different faults. So apart from the well documented two major tectonic phases, a subsequent extension that could be connected with the present stress field created small-scale faults and minor reactivations of the older ones. Unfortunately this later event cannot be dated exactly by using only morphological dating techniques, due to the lack of adequate information concerning past earthquakes. The only available data concern the 1978 shock sequence. A maximum throw of 35 cm of the northern part in respect to the southern was observed, but the usual value was about 10 cm. If we assume that displacements of this order are the typical ones, then the latest reactivations of the faults, in order to create fault scarps as

high as those of group C, had to produce a number of great earthquakes of magnitude of greater than 6.

As has been discussed, the active erosion, and consequently the fault activity, is great. The recurrence interval for earthquakes of M_S = 6.5 has been determined from seismological data at 35-40 years for the whole Serbomacedonian seismic zone. In the Mygdonia basin itself, only two great shocks (1902, M = 6.6 and 1978, M = 6.5) took place during the present century, with a time interval of 76 years. In addition, surface faulting has been observed only during those earthquakes. With this assumption, and taking into consideration the fault scarp height, one could suggest, with a great degree of uncertainty, that the latest phase with great earthquakes (M_S = 6.5) started at c. 2500 yrs B.P. or even later, if creeping has played an important role in scarp formation. Because not every fault is reactivated during one earthquake though, this age should be earlier than that. It is not possible to be exact on the timing of the forming of the scarps with the presently available geological data. However, this phase should be directly connected with the present active tectonic stress regime that dominates the broader North Aegean region. A paleoseismological investigation study that is currently under way in this area in collaboration with geoscientists from the Institute of Geology of the State Seismological Bureau of Beijing, China (Cheng S., Fang Z., Pavlides S. and Chatzipetros A. [1994]. Preliminary study of paleoseismicity of the southern Langada-Volvi basin margin fault zone, Thessaloniki, Greece, *7th Congress of the Geological Society of Greece, Thessaloniki, 25-27 May 1994*), has shown that three paleoearthquakes had occurred in a specific segment at the southern border of the basin with a regular recurrence interval of about 7,000 years during the last 21,000 years. The apparent disagreement of the paleoseismological and morphotectonic dating results is due to the lack of morphological expression (scarps) of the specific fault branch studied by trenching, as well as the previously discussed complicated cross-faulting structure of the basin. Anyway, the maximum expected earthquake magnitude in the basin is about 6.5, regardless of the method used for its extrapolation.

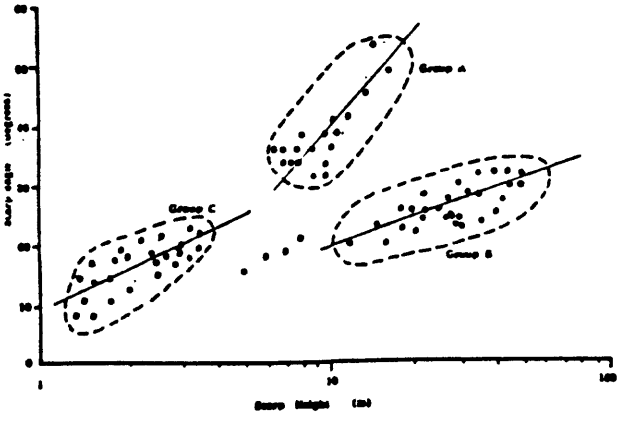

Fault scarp height-angle relationship for the scarps of Mygdonia basin. The group classification (A, B and C) is explained in the text.

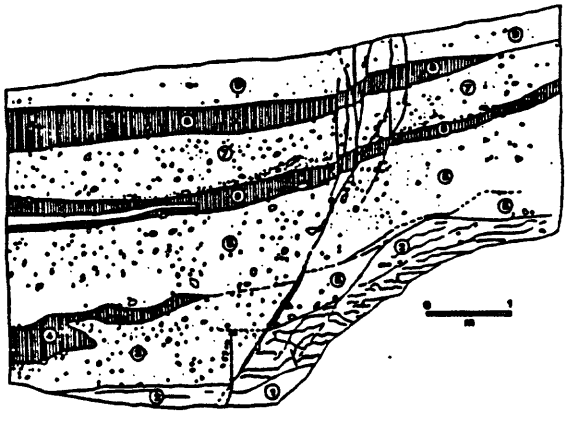

Simplified sketch of the paleoseismological trench along a fault branch of the southern margin of the basin. Dating of the paleosoils revealed a uniform earthquake recurrence interval of c. 7,000 yrs.

Investigations of Active Faulting in Italy: Observations of Surface Breaking Faults

Francesca R. Cinti, Daniela Pantosti, and Giuliana D'Addezio, Istituto Nazionale di Geofisica, Roma, Italy

The Apennines were built up during the Miocene and Pliocene by progressive northeastward thrusting of numerous sheets of marine sedimentary rocks. The stress field subsequently evolved and today the Apennines experience extension (NE-SW to E-W direction) associated with normal faulting parallel to their axis. The recognition and characterization of these modern faults, which are responsible for the large earthquakes of the region, have been the main purpose of our work during the past five years. The field recognition of the active faults, however, is strictly related to the interaction of distinct elements. Among these a major role is played by fault geometry, age of the fault, tectonic rate and fault setting (i.e., climate, topography, type of rocks). In the case of Italy, the interaction of these elements does not create the favorable conditions for clear geomorphic expression of surface breaking faults and the long-term coseismic deformation in some cases is locally poorly expressed. In fact, only a few fault segments are known to be surface breaking due to:

- the youthfulness of the fault activities (<1my)--the landscape still reflects the older compressional phase;
- the long average repeat time of the faults (order of thousands of years);
- The extremely high rate of depositional and erosional processes compared the slip rate (<imm/yr) of the modern faults.

Therefore, to reach our goal, which has the identification and exact location of the structure as a first step, we must combine several different approaches. Historical felt reports and modern seismicity data provide us the information to constrain the extent of the region to be searched for active normal faults and to identify significant singularities (e.g. segment boundaries). Then we perform direct field investigations such as geomorphic mapping, microtopographic mapping, and profiling in the near-fault zone. Once we identified a favorable site, as a second step we proceed in excavating trenches across the fault trace to characterize its behavior.

We present results obtained through these investigations on several normal seismogenic faults that show a very different seismological and geomorphologic expression. Among these, the cases of the Ovindoli-Pezza fault (central Apennines) and the Irpinia and Castrovillari faults (southern Apennines) are discussed. The Irpinia fault ruptured in 1980 (November 23, M=6.9) and produced a fault scarp not associated with preexisting geomorphic lineaments, whereas the Ovindoli-Pezza fault and Castrovillari fault show a clear geomorphic expression but were not known to have produced large magnitude earthquakes in historical time. We recognized and quantified both individual and cumulative effects of Pleistocene-Holocene coseismic deformation and evaluated slip rate, slip per event, and average recurrence time for the three faults. Moreover, the Val D'Agri case (southern Apennines) will be presented. The Val D'Agri area was struck by a large earthquake in 1857 (XI M.C.S.). This seismic event is documented in detail, but the causative fault is still not well recognised in the field.

Quaternary Faulting and Perspectives for Paleoseismological Studies in the Southeastern Sierras Pampeanas, Argentina

Carlos H. COSTA, Departamento de Geología, Universidad Nacional de San Luis, E. de los Andes 950, 5700 San Luis, Argentina
María V. MURILLO, Departamento de Ciencias Geológicas, Universidad de Buenos Aires, 1428 Buenos Aires, Argentina
Claudio VITA FINZI, Department of Geological Sciences, University College London, Gower St., London WC1E 6BT, U.K.
Carlos E. GARDINI, Departamento de Geología, Universidad Nacional de San Luis, E. de los Andes 950, 5700 San Luis, Argentina

The Sierras Pampeanas (Pampean Ranges) region is characterized by mountain blocks which crop out widely in central northwestern semiarid Argentina. The development of this geological province is coincident with a flat-lying subduction segment of the Nazca plate between 26° and 33°SL. The ranges are composed mainly of igneous and metamorphic rocks, with ages ranging from Upper Precambrian to Upper Paleozoic. The Sierras Pampeanas have been attributed to broken foreland deformation of the Andean orogen. Their present morphostructural features originated during the Cenozoic due to the uplift of fault-bounded blocks along east-dipping reverse faults. The listric geometry of these faults is indicated as the reason for general block tilting toward the east, giving rise to topographic asymmetry. According to this, Neogene fault activity was concentrated at the uplift front of the blocks. The structural style and tectonic setting are similar to the Rocky Mountains Laramide foreland deformation.

Historical seismicity assigned to low-moderate earthquakes has been reported and recorded in the Sierras Pampeanas. The village of Sampacho (Cordoba Province) was destroyed in 1936. Several cities, dams and a nuclear power plant are located along or very close to the main Neogene faults, but little is known about the seismogenic potential of the area.

Fieldwork carried out principally in the last 10 years indicates that several fault segments have undergone Quaternary movements. These studies have been hampered by the lack of Neogene deposits, but work is now being carried out on fault segments suspected of Quaternary activity in the southeastern Pampean Ranges (Sierras de San Luis y Cordoba, 31°-34°SL, 64°-66°WL). Morphological and geological evidence for Quaternary faulting has been found in the Sierra de San Luis (Las Cuevas, Loma Blanca and Potrero faults), Sierra Grande de Cordoba-Comechingones (Los Molinos and Nono fault) and Sierra Chica de Cordoba (Cosquin, Potrero de Garay and Calamuchita faults).

At Sierra de Comechingones, neotectonic faulting is found west of the main uplift front and has produced fault scarps which disrupt the general trend of the alluvial fans. The topographic throw amounts to 30 m in some places, although it is not clear if the displacement is entirely due to fault movement during Quaternary times. The fault scarps could be identified along 40 km parallel to the north-trending range front.

At Los Molinos (Merlo, San Luis Province) a reverse (45°E dip) fault scarp exposes sheared basement which overrides a paleosol and colluvial-alluvial sediments probably of Holocene age. The organic matter contained in the paleosol is being investigated for ^{14}C dating, in order to estimate the slip rate and the maximum age of the neotectonic episodes.

The Sierras Pampeanas are located within an intraplate region, where phenomena of active faulting are not so spectacular as in the Andean orogen. Moreover, the deformation rate and the seismic threat are lower. Nevertheless, the paleoseismological approach can provide valuable data for understanding the area's Neogene tectonic evolution and for identifying regional seismic hazard.

PALEOSEISMOLOGY OF QUATERNARY FAULTS IN THE "STABLE" INTERIOR OF AUSTRALIA AND NORTH AMERICA—INSIGHT INTO THE LONG-TERM BEHAVIOR OF SEISMOGENIC FAULTS

CRONE, Anthony J., and MACHETTE, Michael N.

U.S. Geological Survey, MS 966

P.O. Box 25046, Denver, CO 80225

Most earthquake-hazard assessments in "stable" continental regions (SCR) have relied on the spatial and temporal distribution of historical seismicity as a guide to identifying likely sources of future damaging earthquakes. Although earthquakes in such regions are rare compared to those along plate margins, they can produce substantial damage. Here we discuss only those SCR faults that have historic or Quaternary surface rupture. Worldwide, only 11 historical earthquakes have produced documented surface ruptures in stable continental regions (table 1). The limitations of using the short historical record to identify potentially hazardous faults are highlighted by the occurrence of six surface-faulting earthquakes during the past three decades in the stable interiors of North America and Australia and by the M_s 6.3 earthquake of 29 September 1993 near Killari, India, which caused an estimated 10,000 deaths. The faults that ruptured during these earthquakes had little or no precursory seismicity, and thus were not considered to be hazardous. Because these types of faults are commonly aseismic, they present a difficult and serious challenge to the development of accurate earthquake-hazard assessments.

Our paleoseismicity studies of faults in Australia and the United States show that the long-term behavior of seismogenic SCR faults is characterized by episodic activity. An episode can consist of one or more moderate- to large-magnitude earthquakes (M>5) separated by quiescent intervals of at least 10^4-10^5 years. Geologic and geomorphic evidence from the faults that ruptured during the 1968 Meckering, 1986 Marryat Creek, and 1988 Tennant Creek, Australia, earthquakes (fig. 1) indicates intervals of at least 50,000 years or, more likely, hundreds of thousands of years between successive surface-faulting earthquakes. At Tennant Creek, thermoluminescence dating of eolian sand that buried a bedrock scarp indicates that the penultimate event occurred more than 50,000 years ago. At Marryat Creek, the lack of any preexisting topography along the 1986 rupture and the well-developed soils exposed in two trenches indicate that the penultimate event occurred at least 100,000 years ago. In North America, studies of the prehistoric surface ruptures along the currently aseismic Meers fault, Oklahoma, and those formed during the 1989 Ungava, Quebec, earthquake (Adams and others, 1992) indicate that the penultimate surface-faulting events occurred more than 10^5 and 10^9 years ago, respectively. These North American and Australian faults support a model of long recurrence times between brief episodes of activity for seismic sources in stable continental interiors, as first noted by Coppersmith (1988).

Geologic and seismologic data document several important characteristics of major earthquakes in stable continental regions. The surface ruptures associated with these earthquakes can be more than 3 m high and more than 30 km long. The earthquakes typically reactivate preexisting faults, some of which originally formed in Precambrian time. Earthquakes large enough to produce surface ruptures (commonly M_s>5.7) tend to have shallow hypocenters (commonly <10 km depth), and the upper crustal stress field, which is dominated by horizontal compression in stable continental settings, results in mainly reverse or oblique-reverse faulting.

The inventory of seismogenic faults and possible seismic sources in the stable interior of many continental regions is incomplete. Australia is commonly perceived as a stable, relatively aseismic continent, yet from our our limited reconnaissance studies and discussions with Australian colleagues, we learned about at least 12 known or suspected, but unstudied, Quaternary fault scarps that are scattered across this sparsely populated continent. In North America, a continent whose geology is known much better than Australia's, suspected Quaternary surface faults have been recently recognized in Giles County, Virginia; Harlan County, Nebraska; and near Cheraw in southeastern Colorado

(fig. 1). Other presently aseismic and, thus, undetected hazardous faults may be present near populated areas in continental interiors. Developing a more complete inventory of Quaternary faults in stable continental regions is hindered by the poor surface expression of many seismogenic faults. This poor expression results from long-term fault slip rates that are very low compared to the rates at which surficial processes erode and obliterate fault scarps and other landforms. For example, large areas of North America have either been glaciated or covered by loess during the late Pleistocene, which has destroyed or concealed much of the evidence of surface faulting that occurred prior to about 15,000 years ago. To improve hazard assessments, we must systematically compile an inventory of Quaternary faults in continental interior settings and increase our understanding of the long-term behavior of SCR faults through paleoseismic investigations.

References Cited

Adams, J., Percival, J.A., Wetmiller, R.J., Drysdale, J.A., and Robertson, P.B., 1992, Geological controls on the 1989 Ungava surface rupture—A preliminary interpretation: Geological Survey of Canada Paper 92-C, p. 147-155.

Coppersmith, K.J, 1988, Temporal and spatial clustering of earthquake activity in the central and eastern United States: Seismological Research Letters, v. 59, no. 4, p. 299-304

TABLE 1. Data on historical earthquakes that produced documented surface ruptures in stable continental regions of the World

No. in Fig. 1	Location of earthquake	Date (yr, month, day)	Earthquake magnitudes	Dominant faulting style	Rupture length (km)	Max. scarp height (m)
1	Cutch, India	1819, June 16	M_S 7.25-8.25	Unknown	>90	7-9
2	Accra, Ghana	1939, June 22	*M* 6.5	Sinistral?	9-17	0.46
3	Central Sudan, Africa	1966, Oct. 9	m_b 5.1	Sinistral	6	0.0
4	Meckering, WA, Australia	1968, Oct. 14	M_S 6.8; m_b 6.0	Dextral>reverse	37	3.5
5	Calingiri, WA, Australia	1970, Mar. 11	M_S 5.7; m_b 5.7	Sinistral>reverse	3	<0.4
6	Cadoux, WA, Australia	1979, June 6	M_S 6.4; m_b 6.3	Dextral>reverse	28	<1.4
7	Guinea, Africa	1983, Dec. 22	M_S 6.2; m_b 6.4	Dextral	9.4	0.13
8	Marryat Creek, SA, Australia	1986, Mar. 30	M_S 5.8; m_b 5.7	Reverse>dextral & sinistral	13	~0.9
9	Tennant Creek, NT Australia	1988, Jan. 22	M_S 6.3, 6.4, 6.7; m_b 6.1, 6.1, 6.5	Reverse	32	1.8
10	Ungava, Quebec, Canada	1989, Dec. 25	M_S 6.3; m_b 6.2	Reverse>sinistral	10	1.8
11	Killari (Latur), India	1993, Sept. 29	M_S 6.4; m_b 6.3	Reverse	3	<0.5

Notes: <, less than; > greater than; ?, uncertain.; max., maximum. Names of earthquakes 1-10 provided by A.C. Johnston, Memphis State University. Magnitude notations: M_S, surface-wave magnitude; m_b, body-wave magnitude; *M* , moment magnitude.

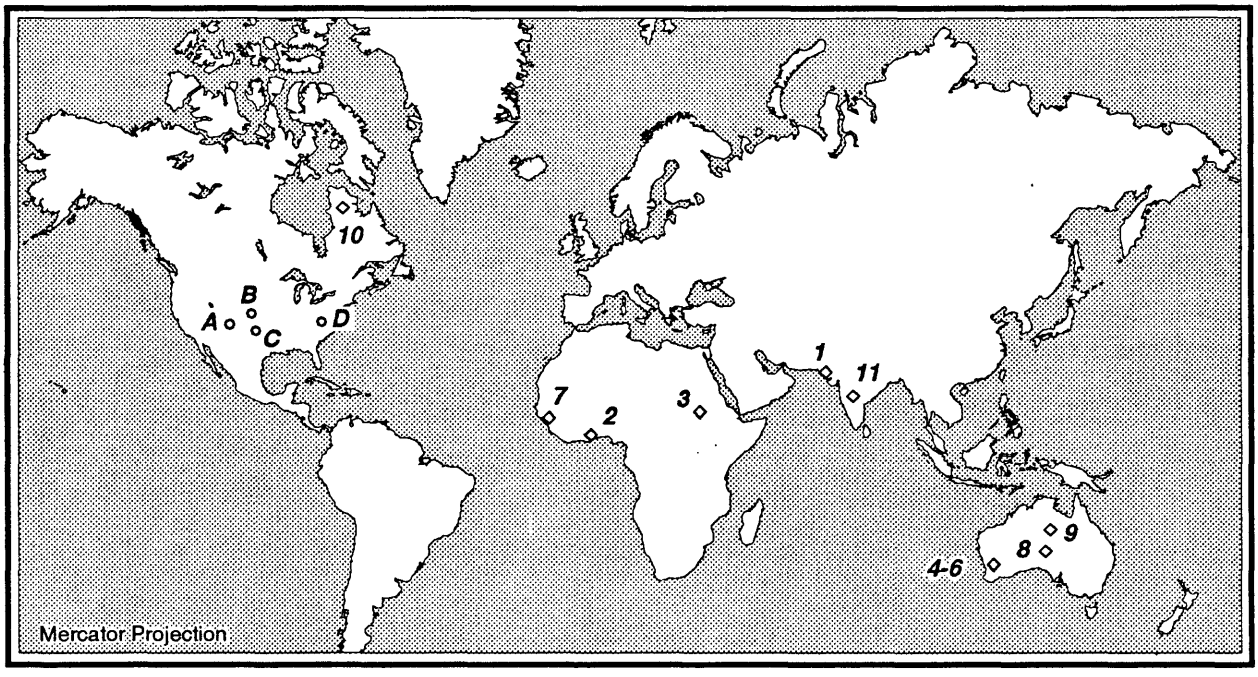

FIGURE 1. Map of worldwide historical earthquakes that have produced surface faulting in stable continental regions and selected known or suspected Quaternary faults in the stable interior of the United States. Surface-faulting earthquakes are numbered as in table 1. Faults with known or suspected Quaternary displacement are: ***A***, Cheraw fault, Colorado; ***B***, Harlan County fault, Nebraska; ***C***, Meers fault, Oklahoma; ***D***, Giles County, Virginia.

Trenching Activity Along the Digdig Fault, Central Luzon, Philippines

Jessie A. Daligdig, Philippine Institute of Volcanology (PHIVOLCS), 29 Quezon Avenue, Quezon City 1100, Philippines, presently at: Department of Geophysics, Kyoto University, Sakyo-ku, Kyoto 601-01, Japan
Hiroshi Sato, Earthquake Research Institute, University of Tokyo, Yayoi , Bunkyo-ku, Tokyo 113, Japan
Takashi Nakata, Department of Geography, Hiroshima University, Hiroshima 730, Japan
Norman M. Tungol, Philippine Institute of Volcanology and Seismology (PHIVOLCS), 29 Quezon Avenue, Quezon City 1100, Philippines
Toshio Nakamura, Dating and Material Research Center, Nagoya University, Chikusa, Nagoya 464-01, Japan

A joint trenching activity was conducted by PHIVOLCS and the Universities of Tokyo and Hiroshima in early February, 1993 along the Digdig Fault, Central Luzon, Philippines. The Digdig Fault forms the northernmost splay of the Philippine Fault Zone or PFZ (PHIVOLCS, 1986; 1991) that ruptured for at least 125 km (Punongbayan & others, 1990; Nakata & others, 1990) during the 1990 Ms 7.8 Philippine earthquake. This seismic event was the first historical rupture to be documented along the Digdig Fault although previous geomorphic studies (Allen, 1962, 1975; Nakata & others, 1977; Hirano & others, 1986) have correctly inferred that the present landforms in the study area either directly resulted from, or have been influenced by, repeated movements along this active fault. On the other hand, historical summaries of Philippine earthquakes (Saderra Maso, 1895; Repetti, 1946; SEASEE, 1985; Bautista, 1993) span only for about four centuries. This fact, coupled with the lack of dating control, has severely limited attempts to correlate specific events to activity along the PFZ and its splays (Acharya, 1980; Punongbayan & Umbal, 1990; Nakata & others, 1990; Punongbayan & others, 1990).

Detailed observation of stratigraphic and structural relationships of the trench exposures indicates that only two seismic events prior to 1990 could be identified although older events may lie deeper than the 3 m average depth of the exposures. Evidently, the southwestern block was repeatedly downthrown during these events that led to the eventual ponding of sediments on this side of the fault. Faulting was expressed as abrupt termination and/or deformation of beds, rotation and alignment of pebbles, and differences in lithology. Correlation of units was however, generally complicated by erosion and left-lateral shifting. Average horizontal shifting during the 1990 Philippine earthquake alone was about 5 m in the area. Several organic samples were obtained and are being processed by Accelerated Mass Spectrometry (AMS). The quantity of samples were conspicuously much smaller than what we anticipated, probably due to poor preservation arising from the drier conditions in tropical areas. We hope that the dating results, although quite limited, could still provide a firmer basis to put the seismic events along the Digdig Fault into proper perspective- within or even beyond the limits of the available historical data. A much clearer picture of the long term behavior of the Digdig Fault will no doubt emerge as more paleoseismic studies are conducted in the future.

Paleoseismology Along the Range-Front Fault of Helan Shan, China

Deng Qidong
Institute of Geology, State Seismological Bureau, Beijing, 100029, China

Liao Yuhua
Ningxia provincial Seismological Bureau, Yinchuan, 750001, China.

The NNE-trending range-front fault of Helan Shan along western margin of Yinchuan graben, west of Northern China, is a 130-km-long high angle right-lateral normal-strike slip fault. It cuts late Pleistocene to Holocene alluvial fans with a SE facing scarp, and offsets the Great Wall of Ming Dynasty (~400 years B.P.) right-laterally by 1.45m and vertically by 0.95m. The offset of the Great Wall is probably resulted from the M=8 Pinglou earthquake in 1739. We have surveyed large scale topographic maps along the scarps, levelled 88 profiles across the fault scarps using a plane table and a theodolite, measured kinckpoints along 31 stream channels, and excavated 14 trenches across the fault in order to study Holocene paleoearthquake and recurrence interval of large earthquakes along the fault.

On the fan Surface of the foot wall of the fault, there are four west-tilted erosinal surfaces which gradually disappear away from the fault. The elevation of these surfaces are the highest near the fault. This implies that these surfaces have been tilted and rotated by multiple activity of the faulting. The degree of erosion of older surface (T_4) is higher and that of the youngest (T_1) is the lowest. The riser between two adjacent erosional surfaces is about 1-2.5m. More than 80 topographic profiles across the scarps control the elevation difference of lower original surface between T_3, T_2 and T_1 and the scarp. It indicates that the elevation difference of T_3 is highest, which is average 7.73m and 5.57m fault scarp at Suyukou and Honguozi respectively. That of T_2 is 5.20m and 3.44m at the two sites mentioned above respectively, and T_1, 2.51m and 1.30m. The age of abandence between T_3 and T_2 is 3600-4000 years, T_2 and T_1 is 2000-2800 years.

There are indeed three bevels on the fault scarp. The first and the second slope section correspond to T_3 and T_2 erosional surface respectively. The free surface only exists on T_1 erosional surface. Slopes of the first and the second slope section are 6-21° and 15-38° respectively at Suyukou, and differ consistently 10° in the same profile. In the place where the fault scarp is high, slope of the free surface that reaches 60° may result from the M=8 earthquake of 1739. The other two slope sections represent two paleoearthquake events.

Four stream kinckpoints have been found along many stream channels that incised into alluvial fan. This appears to show multiple offsets history of the fault scarp. Eight and six trenches were excavated across the fault scarp at Suyukou and Hongguozi respectively. All of

them reveal evidences of normal fault, its multiple offsets, colluvial wedges and filling wedges along the scarp. Four earthquake events during Holocene have been consistently found along this fault. The age of each event was inferred from ^{14}C age samples.

In summary, multiple erosional surfaces and their ages, height and bevels of the fault scarp, kinckpoints of stream channel, and paleoearthquake events revealed by trenches, all indicate that there have been four large earthquake events. The ages of these events are about 8400, 4600-3600 (or 5700), 2600, and 254 years B. P.. The latest is M=8 Pinglou eathquake in 1739. The recurrence interval of these earthquakes are approximate 2300-3000 years. The magnitude of the paleoearthquakes is probably about 8 on the Richter scale because the thickness of each colluvial wedge of the paleoearthquakes is comparable with that of the M=8 earthquake in 1739.

Paleoseismology in the Northern Piedmont of Tianshan Mountain, Northwestern China

Deng Qidong, Zhang Peizhen, Xu Xiwei, Yang Xiaoping, Peng Sizhen
Institute of Geology, State Seismological Bureau, Beijing, 100029, China

Feng Xianyue
Xingjiang Provincial Seismological Bureau, Urumqi, 830011, China

Northern Tianshan mountain consists of three rows of active fold and thrust fault zones with EW striking. From south to north, the first row, Qigu fold and thrust fault zone, involves sediments as young as lower Pleistocene. The tectonic activity of this row has been low, and there is no evidence of activity since 30000 years. The second row, Manas thrust and anticline zone, is composed of Horguos, Manas and Tugulu three linear anticlines and thrust faults. The third row includes Dushanzi, Hala-ande, and Anjihai anticlines and thrust faults. Abundant fault scarps and deformation of the late Pleistocene to Holocene river terraces across the anticlines indicate recent folding and thrusting. Field investigation suggests that the 1906 M=7.7 Manas earthquake occurred along a blind thrust fault. This earthquake formed a 10-km-long fresh surface rupture and a 130-km-long recent uplift zone.

Along the Dushanzi fold and thrust fault zone and the Manas fold and thrust fault zone, we excavated 39 trenches across the fault scarps. Paleoearthquake evidence revealed by trenches mainly consists of multiple offsets, paleo-structural wedge, flexural deformation of hanging wall, multiple colluvial wedge and sag pond deposits along the thrust fault scarp. The colluvial wedge of the thrust scarp is characterized by that grain size of massive gravel increases toward the fault, that the grain size of gravel decreases away from the fault, and finally integrates to redeposited loess, and that small sized pebbles usually distributed near the bottom of the wedge. Most of sag pond deposits formed along the base of fault scarp by backward thrust on the hanging wall of reverse fault. When the fault scarp faces antithetic to topographic slope, sag ponds are formed along the foot of the fault scarp. Sediment within sag ponds is characterized by coarse grain in the low part and fine grain in the upper part. In the Tianshan region, the sequence of sag pond deposit is usually redeposited loess on top of gravels. Runoff deposit often separates sag pond deposit of different age.

The length of Dushanzi fold zone is 8[illegible] and main reverse fault along its northern limb crops out 55km in length. We have excavated 15 trenches across the fault scarps. By comparing the 11 trench logs among the 15 trenches, we can identify three paleoearthquake events along the thrust fault zone since 12000-13000B. P.. The first event occurred about 12000-13000 B. P., and

the second and the third event is 6000-8000, 3000-4000 years B. P., respectively. Considering the uncertainties of the data, recurrence interval of large earthquake is about 4000 years. Therefore, there is potential to have a major earthquake along this zone in the near future because the elapsed time of the last major earthquake is already passed 3000-4000 years.

Fourteen trenches were excavated across fault scarps within 170-km-long Manas thrust and anticline zone, and revealed four large earthquake events including M=7.7 Manas earthquake in 1906. The recurrence interval along this zone is about 5000-6000 years. Therefore, it is unlikely to have a large earthquake along this zone in the near future based on paleoseismic studies because Manas earthquake left us only 87 years ago.

Estimating Fault Slip Rates in the Great Basin, USA

Craig M. dePolo
Department of Geosciences and Nevada Bureau of Mines and Geology
Mackay School of Mines
University of Nevada, Reno

Estimating Fault Slip Rates

Fault slip rates continue to increase in importance and usage in seismotectonics, principally for gaging the activity of earthquakes along a fault and for characterizing the deformation of the upper crust. Three principal questions should be asked when determining and using fault slip rates: 1) What are the uncertainties involved with the slip-rate measurement or estimate?, 2) Is the time frame involved in the fault slip rate valid?, 3) Is the slip rate representative of the overall fault or deformational segment? Uncertainties involved in slip rate estimations include those from offset measurements, age estimations of offset units or relationships, secondary components of slip, seismic vs. aseismic slip, and the fault geometry related to the offset. The optimum time frame of a slip-rate measurement averages a cumulative offset that has occurred over several interseismic intervals; the minimum valid time frame is one interseismic interval (taken with the offset of one event to get a slip rate), and the maximum valid time frame is the time of inception of the contemporary seismotectonic regime. The minimum valid time period for slip rate estimation is dependent on the size of the earthquake along the fault (or its associated slip/event) and the general slip rate of the fault. The question of representativeness of a slip rate has spacial and temporal considerations, as well as the simple comparison and understanding of the differences between different slip rate estimations along a fault. The location of a slip rate measurement or estimate along a fault (e.g., at the end of a fault or along one of multiple parallel fault strands) needs to be noted and potentially adjusted or corrected to get a more representative slip rate for the overall system. Temporal considerations revolve around the behavior of the slip rate of a fault through time or, in other words, the nature of variations in earthquake occurrence along a fault.

In the Great Basin, faults with slip rates of 1 mm/yr or higher have minimum time frames on the order of mid to late Holocene, faults with slip rates of around 0.1 to 0.5 mm/yr have minimum time frames of latest Pleistocene to earliest Holocene, and slower slipping faults require early to mid Pleistocene time frames. The maximum time frame, in most cases, in the Great Basin is 3 to 5 Ma. Optimum time frames for faults with slip rates of $\geq$1, 0.1 to 0.5, 0.01, and 0.001 mm/yr are latest Pleistocene, ~100 to 500 ka, Quaternary, and late Pliocene-Quaternary, respectively. Several researchers have noted that in several cases in the Great Basin, earthquakes tend to cluster in time along an individual fault. Since this is probably due to variations in loading or slip rate, this behavior needs to be considered when using paleoearthquake data and/or making projections of future earthquake behavior.

Fault Slip Rate Estimation Scheme for the Great Basin

In evaluating the validity of a slip rate time frame or its representativeness for a fault, multiple slip rate determinations or estimates are desirable. To assist with this and to begin estimating slip rates for the hundreds of faults with uncharacterized activity in the Great Basin, I am developing a scheme for estimating slip rates based on: 1) constraining the amount of offset of Quaternary units, 2) characterizing range front morphology for fault activity, and 3)

characterizing the development and extent of tectonogeomorphic features. The Great Basin has a semiarid climate in general, although local variations in the amount and nature of precipitation, temperature regimes, and vegetation exist. Limiting the study mostly to the Great Basin helps limit extreme variation or biases from the geomorphic influence of different climatic regimes; in general, the semiarid climate is also condusive to the preservation of tectonogeomorphic features. The framework of this scheme is a seven part classification for faults with different slip rates in the Great Basin (see Table 1). This classification was developed considering the sensitivities involved with its use for earthquake occurrence and crustal deformation studies, and the potential ability of the estimation scheme to distinguish slip rates. Quaternary offsets differ from direct slip rate measurements in that they are less precise and may be made on offset deposits with eroded upper surfaces or buried lower surfaces, or using the height of fault facets and/or uplifted alluvium. The notion is to capture the order of magnitude of an offset over a long time frame, even though the offset is very uncertain or incomplete. Use of the nature of range-front morphology was developed by Dr. William Bull and his colleagues is being extended in this study to more directly being used to constrain fault slip rates. Use fo Bull's classification in its present form appears to help distinguish faults with normal slip rates from about 0.1 to 0.001 mm/yr. The development and extent of tectonogeomorphic expression of a fault (zone) should also relate to slip rates and is being examined. Tectonogeomorphic features obviously differ for strike-slip vs. normal-slip faults and need to be treated separately. Faults with higher slip rates tend to have a wider variety of features, larger tectonogeomorphic features, and more continuous geomorphic expression. Thresholds of existence of some features, such as fault facets, may also occur.

Multiple techniques are necessary for slip rate estimates since no single parameter seems to successfully span the range in slip rates considered (0.0001 to ~10 mm/yr), nor can any single parameter be used for all the faults. A data set is being developed from faults with known slip rates and faults with new slip rate determinations to constrain the scheme for estimating fault slip rate. Although this research is still ongoing, preliminary data suggests this scheme will be of practical usage for the Great Basin, and that this framework may potentially be used in other regions after it has been been calibrated. In reality, many slip rate measurements have large uncertainties associated with them, and consideration of "factors of uncertainty", that naturally exist, can shift, the minmimum and optimum time frames for slip rates, and can cascade through the assumptions, leading to large error estimates associated with the final values used for fault slip rate or earthquake occurrence intervals.

Table 1 Fault slip rate classification for the Great Basin

S.R. type	S.R. range (mm/yr)	Rep. S.R. (mm/yr)	Comments
AA	$\geq$2	$\geq$2	very active fault
A	0.75-1.9	1	high activity fault
B	0.25-0.74	0.5	moderately high activity fault
C	0.05-0.24	0.1	average activity fault
D	0.005-0.049	0.01	moderately low activity fault
E	0.0005-0.0049	0.001	low activity fault
F	<0.0005	$\leq$0.0001	very low activity fault or inactive

The 1932 Cedar Mountain Earthquake, Central Nevada, USA: a Major Basin and Range Province Earthquake that had a Widely Distributed Surface Faulting Pattern

Craig M. dePolo, Alan R. Ramelli, and John W. Bell
Nevada Bureau of Mines and Geology, Mackay School of Mines
University of Nevada, Reno

The 1932 Cedar Mountain earthquake (Dec. 2, 0610 UTC) was the southernmost major earthquake comprising the central Nevada seismic belt. This earthquake had a magnitude of M_s=7.2 (Abe, 1981), was predominantly right-lateral strike slip in nature, and had a widely distributed surface rupture pattern 60 to 65 km long and up to 8 to 17 km wide.

Tectonic Setting

The 1932 earthquake occurred in the west-central Basin and Range province, an active Cenozoic extensional province. This event occurred long the boundary between two large subprovinces identified by Stewart (1988), the Walker Lane belt and the central Great Basin. The Walker Lane belt, located in the westernmost part of the Basin and Range province, just east of the Sierra Nevada block, is characterized by diverse structural domains and differently oriented ranges, and appears to accommodate significant northwest-directed right-lateral deformation. The central Great Basin is more consistent with generally north- and northeast-trending ranges, commonly bounded on one or both sides by dominantly normal faults. The boundary between these two subprovinces is a northwest-trending zone known as the Walker Lane; this is a zone of discontinuous northwest-trending strike-slip faults with varying rates of Quaternary activity. The 1932 earthquake appears to have nucleated along the eastern margin of the Walker Lane or just to the east of it, and propagated into and along Walker Lane towards its southern end.

Surface Faulting

Surface ruptures from the 1932 event can be divided into three groups: from north to south, those in Gabbs Valley, those in Stewart Valley, and those in Monte Cristo Valley (fig. 1). Recent mapping of the possible northernmost end of the 1932 faulting suggests the that the 1954 Fairview Peak earthquake ruptured into and overlaps with the northern Cedar Mountain rupture zone. Surface faulting in Gabbs Valley consisted of at least eight different faults, most which are north to northeast striking. Displacements ranged from cracking to 30 cm, with normal faulting dominant. In Stewart Valley, eight surface breaks were mapped, ranging in length from 567 m to 1.4 km and in offset from 0 to 46 cm normal slip and tens of cm right-lateral slip. These occur in a very scattered, discontinuous manner; it is possible that other surface deformation in this area was not manifested as surface breaks, but rather was distributed into the relatively incompetent Miocene lacustrine sediments. The most spectacular surface faulting occurred in Monte Cristo Valley where ruptures were fairly continuous for 16 km and right-lateral offsets were up to 2 m. Ruptures in Monte Cristo Valley exhibit classic strike-slip tectonogeomorphology including offset stream channels, ramped scarps, swell and depression morphology, and sidehill benches. The overall discontinuous and distributed pattern of surface breakage from the 1932 Cedar Mountain earthquake, although dramatic, has similarities to other Basin and Range province earthquakes.

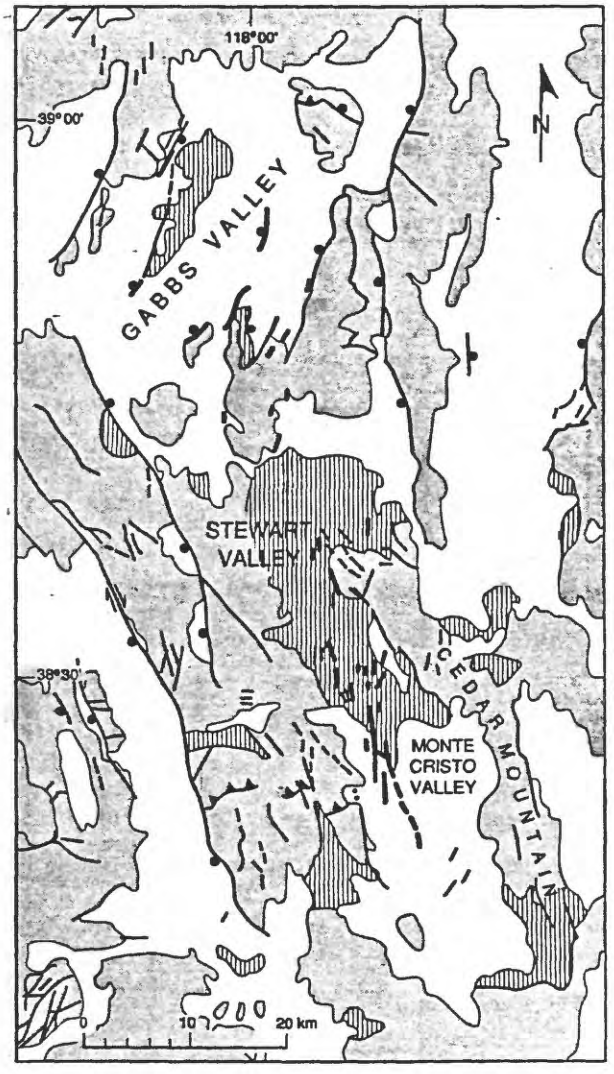

Figure 1
Surface faulting from the 1932 Cedar Mountain earthquake. Bold lines denote surface faulting, medium-weight lines denote other selected faults. Balls are on downthrown side of faults with normal components. Patterned areas are bedrock, white areas are alluvial-filled valleys and basins. Areas with vertical patterns are Tertiary sedimentary rocks.

Right-Lateral Slip Distribution in Monte Cristo Valley

Figure 2 shows measurements of right-lateral surface displacement, and approximated slip distributions for individual traces and total slip summed across traces, as projected onto a north-south line. There is significant uncertainty involved in making measurements 60 years after the event, but much of the slip distribution can be captured. Measurement uncertainties are shown by the error bars spanning the preferred values. Also shown is the location of a prominent pressure ridge within the Monte Cristo Valley fault zone.

Aside from the ends of the rupture zone, the only place that total slip falls below 1 m is in the area of the pressure ridge; this suggests as much as half of the slip went into further uplift of and shortening across the pressure ridge. Trenching studies exposed a reverse fault along the southwest side of the pressure ridge that shows slight reverse displacement of gravels within centimeters of, but not reaching, the surface. We interpret this to be faulting associated with the 1932 earthquake.

In general, right-lateral displacement along surface breaks in Monte Cristo Valley were between 0.5 and 1.5 m, with a maximum single trace displacement of 2 ± 0.5 m. The maximum surface displacement summed over two parallel traces is 2.7 (+1.2, -1) m.

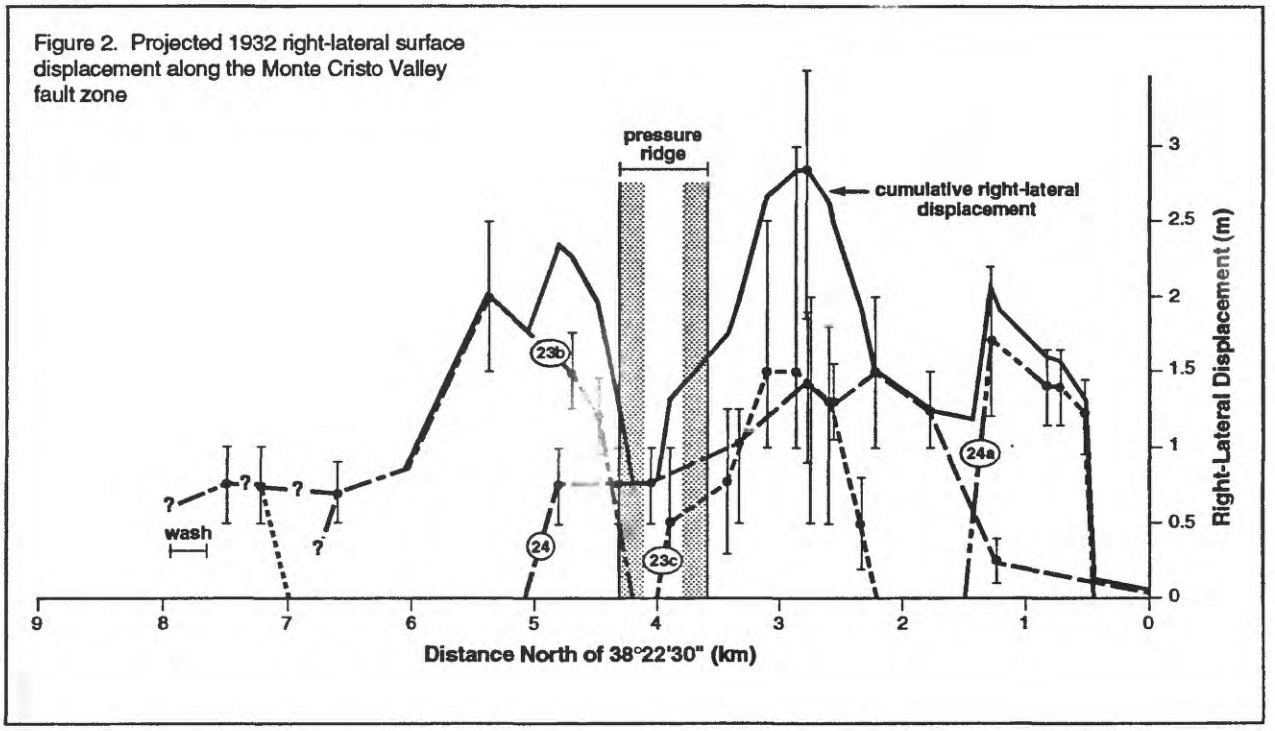

Figure 2. Projected 1932 right-lateral surface displacement along the Monte Cristo Valley fault zone

Factors that Appear to have Contributed to the Distributive Nature of Surface Faulting

Several hypotheses have been forwarded to explain the distributed nature of the Cedar Mountain earthquake; we believe that all probably contributed to different degrees, in different places. These hypotheses are:

- **multiple earthquake subevents** (Doser, 1988)
  triggered primary events on adjacent and/or proximal faults
- **upwards splaying and distribution of faulting from depth**
  (Gianella and Callaghan, 1934)
  "wrench faulting tectonics"
  ashflow detachment deflection (Molinari, 1984)
- **faulting distributed into deformation of low-competency sediments**
  distribution of faulting in low-competence Miocene sediments
  reactivation of folding in sediments (Molinari, 1984)
- **secondary or sympathetic faulting**
  faulting induced on adjacent or splay faults to the primary rupture
  triggering of shallow slip on proximal faults, probably from shaking.

References Cited

Doser, D. I., 1988, Source parameters of earthquakes in the Nevada seismic zone, 1915-1943: Journal Geophysical Research, v. 93, p. 15,001-15,015.

Gianella, V. P. and Callaghan, E., 1934, The Cedar Mountain, Nevada, earthquake of December 20, 1932: Bulletin Seismological Society America, v. 24, p. 345-377.

Molinari, M. P., 1984, Late Cenozoic geology and tectonics of Stewart and Monte Cristo Valleys, west-central Nevada: University of Nevada - Reno, Masters thesis, 122 p.

Stewart, J. H., 1988, Tectonics of the Walker Lane belt, western Great Basin: Mesozoic and Cenozoic deformation in a zone of shear, in Ernst, W.G., edt., Metamorphism and crustal evolution of the western United States: Rubey Volume VII, Prentice-Hall, publisher, p. 683-713.

Paleoearthquakes and Segmentation of the Active Altun Fault

Ding Guoyu
(State Seismological Bureau, CHINA, Beijing 100036)

The Altun fault zone is a notable huge fault zone in the Asian continent interior. It extends along the northwestern boundary of Qinghai–Xizang Plateau, cutting obliquely Kunlun Mts, passing though Kuyak, Andir River, Qargan River and Altun mountain region, and eastward stretching along the Horkor Valley, then across Danghe and Shule rivers into Yumeng Town of Gansu Province. Its large extent and strikingly linear manifestation on the surface has attracted the attention of the world geoscientists. The Altun active fault zone is composed of several faults developed along the preexisting faults or the boundaries of tectonic blocks, and shows very strong recent movement. The process of its fomation and development is closely related with the uplifting of Qinghai – Xizang Plateau.

Paleoearthquake: The Altun active fault is a strike–slip fault with large extent and manifest dislocations. Many researchers have evaluated its Quaternary slip–rate to a high grade. But, by contraries, except for the two M=7 1/4 earthquates of July 3 and July 12 of 1924 near Minfeng, there has little large earthquake recorded in history. The instrumental observations have also showed that the seismic activity of this region is low. In recent years, a great number of paleoearthquake sites were found along the Altun fault. They provided many new data to explain this contradictory phenomenon.

The newly activities of Altun active fault are mainly along a principal sliding plane. This principal sliding plane extends from west by Xolkule, passing through Kuyak, Mandalike, Qingshuiquan, Akatutagh, Horkor, Annanba, Aksay, Subai and eastward to Kuantanshan, with whole length of about 1600km. Along this principal sliding plane, a series of surface ruptures, deformations and paleoearthquake traces can be found, including many geological and geomorphological phenomena, such as offset stream, offset ridge, buried fault scarp, multiphase gliding surface of earthquake–fault, wedge–shaped fissure deposit along rupture zone, colluvial wedge, liquefaction and so on. The existence of numerous paleoearthquake traces along the fault zone proved that the Altun fault has beeb a very active fault in Holocene. The most active segments were among Kuyak–Ajiang, Tura–Huangtuquan, and Uzunyiaol–Aksay. From the interview of these exposed paleoearthquake sites, we can found that these rupture events are uneven distributed in time and space. As regards the whole fault zone, its time series consists of the quiet period and the active period, and its spatial arrangement consists of obvious fault segmentation and migration of active segments.

According to the profiles at Changcaogou, Ebotu, Uzunxiaol, etc., during the

Late Pleistocene, dated at 22000a B.P., 42000a B.P., and 70000a B.P., the obvious faulting happended in these places. But it is hard to discuss on these events before the date of 22000a B.P. because of the little data. Based on the research information of this area, 29 paleoseismic events and 12 paleoearthquake deformation zone since the date of 22000a B.P. have been discovered (Topic Research Group on Active Altun Fault 1992). Of these events, 4 active periods are divided, they are 1300–4500a B.P., 6400–9700a B.P., 12500–13500a B.P. and 16000–18000a B.P. respectively.

Because of the deficiency of trench numbers and data, to exactly determine the large event recurrence interval of the Altun fault is still difficult. But by studying the already obtained data, it is showed that the number of the paleoearthquake events and the period of its activity on different segments are different, during the Holocene 2–3 times normally and 5 times at most. The average recurrence interval of large event ($M > 7$) is 2200–5500a. In regard to the different segments, west: at Mitya, about 1900a, at Qingshuiquan, about 3200a; middle: at Horkor, about 2000a; east: at Aksay, about 6000–8000a. On the whole, they display an accreting tendency from west to east.

According to the distribution of the paleoearthquake events, the Altun Active Fault can divide into three segments: west, from Xolkule to Ajiang, its main active period is between 2000–4000a B.P.; middle, from Tura to Yulegan, its main active period is between 1500–7000a B.P.; east, from Aksay to Bagxia, its main active period is between 7000–18000a B.P.

Segmentation: As a whole, the traces of Altun active fault are quite continuous with flat wave shape. The secondary faults have an obvious en echelon character, and the right – step form is predominant. The segmentation of the Altun fault has the phenomenon of hierarchy, i.e. the rupture segment of large earthquake may be overlapped by secondary rupture segments with different levels. There are different segments along the Altun fault, belonging to three kinds of levels.

The largest segments are determined on the basis of active tectonic unit and fault activity. The altun fault, 1600 km long, is made up of three large segments, of which the west one is the Kunlun mountain segment which also consists of two sub – segments, the Alatagh and the Jusubarle segments; the middle one is the Andir mountain segment which is located to the northwest Qaidam Basin; and the east one is the Qilian mountain segment, also called the northern Altun fault. The three segments arrange in right – step, in which there exist two largest barriers: the dual Tula stepover and the Altun mountain stepover. The distribution of paleoearthquake ruptures also indicates the existence of three segments and their different active stages.

The segmentation of secondary level is based on the rupture coverage of the

largest earthquake. The Altun fault is located on the highly compressional belt between the Tibet plateau and the Tarim Basin, in which there are a lot of lensing compressional structural blocks, along the arc margin of which the new fault ruptures developed. The Altun active faults are right linked by these arc fault segments, and presents the shape of wavelike extending as a whole. Now, at least ten such arc segments can be identified. They arrange in right step with some stepovers and interruptions. These arc segments have various lengths, from 50 km to 250 km, and all the convex parts of arc segments point at NNW direction because of the northward compression of the Tibet plateau. The arc structures control the segment division of the Altun fault, and an arc structure is right a persistant rupture segment. There are many traces of paleoseismic events along these segments since 20000 a B.P.. The 12 discovered deformation zones of paleoearthquakes have certain identity with these arc segments which are regarded as persistant rupture units since then.

Each arc fault segment is often composed of several en echelon secondary faults, in which there exist a lot of stepover barriers. They present the third level segmentation. Some paleoearthquakes with very large rupture scale (> 100km), regarded as of 8± magnitude on the basis of displacement, linked up the whole arc structures. The Topic Research Group on Active Altun Fault Zone under State Seismological Bureau (1992) had already identified 13 such scale paleoseismic events along the Altun fault. Some rupture events (M 6–7) occupied only a part of an arc segment. They belong to the third level fault segments. From the view of statistics, this kind of paleoearthquake rupture segments, often located on the left wing or west wing of arc fault, are related to the direction of fault compression and the direction of regional stress.

On the whole, although there has little record of recent and history large earthquakes along the Altun fault, the series of surprising Holocene paleoseismic deformations of the fault have demonstrated that this large fault has a history of highly seismic activities in the period of Holocene (and longer). Date of the events showed that there were two periods of large events in Holocene, the 1300B.P. – 4500B.P. and the 6400B.P. – 9700B.P., which give a seismic active stage (episode) of a long time (about 3000 years). Now, it is at the quiet period since the end of the last active episode. This quiet period has lasted for more than 1500 years. There are many discussions on shorter seismic active period (earthquake grouping), but because of the deficiency of the short history earthquake record, the several hundreds to several thousands years episode of large earthquake activity was remaining knowing a little. Further studies of paleoearthquakes and active fault will help in understanding some of complexities of earthquake activities in a long period.

Paleoseismologic Analysis of the Santa Monica-Hollywood fault system: Implications for Earthquake Size and Frequency in the Northern Los Angeles Basin

James F. Dolan and Kerry Sieh, Seismological Lab 252-21, Caltech, Pasadena, CA 91125, and Thomas K. Rockwell, Department of Geological Sciences, San Diego State University, San Diego, CA 92182
All authors also at: Southern California Earthquake Center, University of Southern California, Los Angeles CA 90089

Introduction

Until recently, earthquake scenarios for the greater Los Angeles metropolitan area have focused primarily on the effects of a great earthquake (M=8; the so-called 'Big One') occurring on the San Andreas fault (SAF), which at its closest is located more than 50 km northeast of downtown Los Angeles. In recent years, however, a number of Southern California Earthquake Center (SCEC) scientists have focused their research efforts on identifying seismic hazards associated with faults directly beneath the densely populated greater Los Angeles metropolitan area, which has more than 12 million inhabitants. As part of this effort, during the past three years we have conducted a geomorphologic and paleoseismologic analysis of the Hollywood (HF) and Santa Monica (SMF) faults along the northern edge of the Los Angeles Basin. These faults traverse some of the most densely urbanized and well-known real estate in the world, including downtown Hollywood, Beverly Hills, West Los Angeles, Santa Monica, Pacific Palisades, and the Malibu coast. Because of the proximity of these faults to major population centers, moderate-to-large earthquakes (M=6.5 to 7.5) could cause as much damage as a much larger earthquake occurring on the SAF. The appropriateness of our concerns about such 'urban' faults was dramatically demonstrated by the January 17, 1994 M=6.7 Northridge earthquake, which occurred on a previously unrecognized, moderately south-dipping thrust fault beneath the densely populated San Fernando Valley. In addition to causing 61 deaths, this moderate earthquake caused more than $15 billion in property damage, making it the most expensive earthquake in U. S. history. In the discussion below we describe the results of our research on the Santa Monica and Hollywood faults and discuss the implications of these data for earthquake size and frequency in the region.

Santa Monica Fault

The onshore Santa Monica fault extends for 19 km from Century City, across West Los Angeles and Santa Monica, to Pacific Palisades, where it trends offshore. Marine data indicate that the fault continues parallel to the coast westward at least as far as Point Dume west of Malibu (Vedder and others, 1986). The onshore portion of the fault traverses a densely urbanized area, and our geomorphologic mapping of the fault revealed only one 200 m-long stretch of the fault that was not covered by either buildings or streets. Excavation of five trenches across this site in West Los Angeles revealed a complex fault zone characterized by near-surface strain partitioning. Our data indicates that the 'fault scarp' actually represents a 'fold scarp' formed by south-tilted strata that have been deformed by a shallow blind thrust fault. Evidence for recent surficial faulting in the trench is dominated by numerous near-vertical faults and fractures, many of which exhibit stratigraphic evidence of strike-slip offset. The tilted strata exposed in our trenches encompass two paleosoils whose ages are constrained by mean residence time (MRT) ages and the degree of soil development. The upper paleosoil is apparently early Holocene in age. An MRT date from the A horizon of the lower soil indicates that it was buried approximately 12,000-15,000 years ago. The tilted strata are onlapped by undeformed late Holocene alluvium from the recent Sepulveda fan to the east. We interpret three sediment packages deposited downslope from the most prominent of the

strike-slip faults as colluvial wedges formed after surface rupturing earthquakes. All three developed after burial of the lower paleosoil during latest Pleistocene time, indicating that the fault has apparently been active during Holocene time. These data also suggest that the SMF has an approximately 4,000-5,000 year recurrence interval for surface rupturing events.

Hollywood Fault

The Hollywood fault extends for approximately 14 km along the southern edge of the Santa Monica Mountains from the Los Angeles to northwestern Beverly Hills. During 1992-93 we conducted a detailed study of an 800 m stretch of the fault zone just west of downtown Hollywood using data from storm drain trenches, continuously cored borings, and a 1954 sewer tunnel (Dolan and others, 1993). These data show that the most recently active strand of the fault, which dips very steeply (65-95°N), has displaced late Pleistocene paleosoils approximately 1.5 m down-to-the-north. Although the HF exhibits a long-term pattern of north-side-up reverse motion, this unexpected recent mountain-side-down displacement, coupled with the very steep dip of the fault, indicates that recent motion along the fault has been predominantly left-lateral strike-slip. Furthermore, displacement of a 17,000 year old paleosoil, as well as the overlying paleosoil, strongly suggests that the fault is active. However, analysis of surficial and buried soils exposed in a 450 m-long trench cut across the main trace of the fault reveals that no surface rupturing earthquakes have occurred on the fault in at least 2,000-4,000 years, suggesting very long recurrence intervals for the HF.

The Santa Monica Mountains Fault System: Implications of Preliminary Paleoseismologic Data For Earthquake Size and Frequency

Our ultimate goal is to understand the frequency and size of earthquakes in this densely populated region. The Hollywood fault, by itself, is capable of producing a Mw 6.8 earthquake, whereas the Santa Monica fault could produce a Mw 7.0 earthquake. These maximum credible earthquakes, both larger than the recent Mw 6.7 Northridge earthquake, represent a significant seismic hazard to the Los Angeles region. However, these faults are also part of a much larger system, that, if it ruptured in its entirety, could produce a Mw 7.6 earthquake. This system, which we refer to as the Santa Monica Mountains system, encompasses the Hollywood, Santa Monica, and Malibu Coast faults, as well as a large blind thrust ramp responsible for uplift of the Santa Monica Mountains. The blind thrust ramp, first identified by Davis and others (1989) as part of their Elysian Park thrust system, dips gently northward and extends for more than 75 km from near downtown Los Angeles westward to Point Mugu. Although Davis and others (1989) map their Elysian Park thrust system, and the associated Santa Monica Mountains anticlinorium, as continuous structural features from Point Mugu through downtown and East Los Angeles to the southern Puente Hills, our geomorphologic analysis of the region indicates that their EPT encompasses two distinct thrust fault ramps, one beneath the Santa Monica Mountains (our Santa Monica Mountains blind thrust fault) and one extending ESE from the Elysian Park Hills through downtown Los Angeles and beneath the Puente Hills (which we continue to refer to as the Elysian Park thrust fault).

Perhaps the most important question that we can answer with paleoseismologic information from the Los Angeles region is: Do faults typically rupture individually in moderate-moderately large earthquakes (e. g., Mw 6.5-7.0), or do they rupture much less frequently as part of fault systems during larger earthquakes (e. g., Mw 7.5), with potentially devastating consequences for the metropolitan area? Although incomplete, paleoseismologic data from the Hollywood and Santa Monica faults, as well as from the adjacent Malibu Coast fault, suggest the possibility that large portions of the Santa

Monica Mountains system may rupture together in large earthquakes. These data indicate that HF, SMF, and MCF have all ruptured during Holocene time, but that the most recent surface rupturing earthquakes occurred several thousand years ago (Drumm, 1992; Dolan and Sieh, 1992; Dolan and others, 1993). Furthermore, average recurrence intervals for the Santa Monica and Malibu Coast fault (Drumm, 1992) are on the order of 3,000-5,000 years, far longer than would be expected if these faults rupture by themselves. Similarly, occurrence of the most recent surface-rupturing earthquake on Hollywood fault more than 2,000-4,000 years ago indicates a much longer period than would be expected if the Hollywood fault ruptured by itself. These data, although not definitive, suggest that the surficial faults of the Hollywood-Santa Monica-Malibu Coast system rupture either in series or in conjunction with other faults. The most obvious potential candidate fault is the Santa Monica Mountains blind thrust fault. We believe that all four faults in the system are linked mechanically at depth, with surficial HF-SMF-MCF representing predominantly strike-slip faults that accommodate the strain partitioned left-lateral component of motion on the system.

Our future research efforts on faults in the metropolitan region will focus on a more accurate determination of recurrence intervals and the dates of the most recent earthquakes in order to compare these data with expected data for different faulting scenarios. The existing data suggest, but do not prove, the possibility that large earthquakes (Mw 7.5) have occurred in the Los Angeles metropolitan region in the past, and will recur in the future.

References

Davis, T. L., Namson, J., and Yerkes, R. F., 1989, A cross section of the Los Angeles area: Seismically active fold and thrust belt, the 1987 Whittier narrows earthquake, and earthquake hazard: Journal of Geophysical research, v. 94, p. 9644-9664.

Dolan, J. F., and Sieh, K., 1992, Tectonic geomorphology of the northern Los Angeles Basin: Seismic hazards and kinematics of young fault movements: Engineering geology field trips: Orange County, Santa Monica Mountains, and Malibu Guidebook and Volume, Assoc. of Engineering Geologists 35th Annual Meeting, Long Beach, CA, Oct 1992, p. B-20-B-25.

Dolan, J. F., Sieh, K., Guptill, P., Miller, G., Rockwell, T., and Smirnoff, T., 1993, Structural geology, fault kinematics, and preliminary paleoseismologic results from the Hollywood fault: New data from continuously cored borings and geotechnical trenches, Hollywood, California: EOS, v. 74, p. 427.

Drumm, P., 1992, Holocene displacement of the central splay of the Malibu Coast fault zone, Latigo Canyon, Malibu: *in* Pipkin, B., and Proctor, R. (eds.) Engineering Geology Practice in Southern California, Star Publishing Company, Belmont, California, p. 247-254.

Vedder, J. G., Greene, H. G., Clarke, S. H., and Kennedy, M. P., 1986, Geologic map of mid-southern California continental margin (Map 2A): *in* Greene, H. G., and Kennedy, M. P., eds., California continental margin geologic map series (area 2 of 7; map sheet 1 of 4), U. S. Geological Survey, Menlo Park, CA, and California Division of Mines and geology, Sacramento, CA, 1:250,000.

Paleoseismicity and Liquefaction Potential of a Sangamon Marine Terrace Near the San Andreas Fault, Sonoma County, California

Michael J. Dwyer, Consulting Engineering Geologic Services
1185 Carr Avenue, Santa Rosa, CA 95404

Glenn Borchardt, Soil Tectonics
P.O. Box 5335, Berkeley, CA 94705

A sandy marine terrace adjacent to the San Andreas fault along the southern Sonoma County coastline has undergone secondary faulting and minor uplift during the last 122 ka. Despite this physical movement and the strong, long-duration shaking produced by hundreds of M8 earthquakes, the water-saturated, relatively clean sands in the lower part of the terrace have not liquefied. A 400-m trench along the length of the terrace revealed neither paleoliquefaction features, nor evidence of lateral spreading within the upper 4 m of the 14-m thick deposit. However, standard geotechnical engineering tests showed intervals with low blow counts, low < #200 mesh counts and saturated conditions, indicative of high liquefaction potential. Based on the testing inputs, a computer program showed that intervals up to 3 m in thickness could liquefy during a M8 earthquake on the nearby San Andreas. Drill holes showed that the wave-cut platform beneath the marine sand slopes westerly 2 to 3 degrees providing ample opportunity for lateral spreading had liquefaction occurred during past events. The key to resolving this apparent contradiction in evidence for liquefaction potential involves the study of soil development in relation to paleoseismic history.

The study site investigated is the marine terrace located opposite Bench Mark 17 (U.S. Geological Survey, Bodega Head 7½ Minute Quadrangle), and 90 m east and 18 m above the northeast edge of Bodega Harbor. The San Andreas fault is about 90 m west of the terrace edge. The terrace is part of a broad flight which extends from 5 to 160 m above sea level. The original form of the flight, consisting of a series of topographically ascending steps, has been modified by stream erosion and deposition of prograding continental sediments derived from the adjacent uplands. In contrast, the form of the study site has been largely unmodified by erosion and no continental deposits are present. The terrace surface slopes gently westward at 0.5 to 4.5 degrees. The wave-cut platform at the base of the sediments consists of graywacke sandstone of the Franciscan assemblage. As along much of coastal California, the Bodega terrace is the result of Quaternary sea level fluctuations superimposed on an emergent coastline. All the numerous Sonoma County marine terraces are within 3 km of the San Andreas fault and have experienced a history of shaking similar to the Bodega terrace.

The soils developed on the terrace deposits are clayey sands 3.0 to 3.5 m thick. Based on their development and similarity to other well-dated soils along coastal California, they are interpreted to be Sangamon in age. Bore hole samples show that the lower one-half to two-thirds of the terrace deposits is mostly sand. Bedding in the terrace deposits is well developed, generally undulating, with individual units ranging from 3 to in excess of 150 cm. The beds dip gently to the west at 3 to 4 degrees and are mostly undeformed.

Trench excavations revealed the presence of, narrow (0.25 to 10 cm), often closely spaced, vertical to nearly vertical soil tongues. In plan and profile their boundaries vary

from uniform to undulating or irregular, and they occasionally coalesce. Their general trend is northwesterly and the lateral continuity of individual features is probably a few meters or less. Initially these features were thought to be clastic dikes of liquefaction origin, but detailed observations revealed otherwise: the material infilling the tongues is consistently composed of clay or very clayey silt/sand materials finer than their surroundings; the soil tongues widen as they ascend from the trench floor; and the infill material compositionally varies in response to the differing terrace or soil units through which it passes. We conclude that these soil tongues formed from the top down, with many of them following long, narrow fractures resulting from uplift of the area since Sangamon time. We found no injection features that could have resulted from liquefaction or lateral spreading. Liquefaction was not reported at the terrace as a result of the 1906 San Francisco earthquake.

The site terrace was probably formed during oxygen isotope stage 5e, after 122 ka, when the sea level was at least 6 to 8 m higher than present. The highest point of the wave-cut platform is now 14 m above sea level, which implies an uplift rate of about 0.06 mm per year (14 minus 7 m).

The trench through the large swale in the middle of the terrace exposed minor, closely spaced faults, having displacements of 15, 23, and 81 cm. The sense of movement on the faults was vertical, normal, and reverse. The faults terminated between 1.7 and 3.6 m below ground surface in the lower horizons of the Sangamon soil. Vertical fault displacement locally back-tilted the normally west dipping terrace deposits. This formed the swale whose surface has been largely preserved due to the long-term absence of erosion or deposition on the terrace. This preservation is apparently due to a right-lateral jog in the well-incised Johnson Gulch just east of the site. The jog has intercepted runoff and slope wash from the Coast Range uplands to the east and diverted it from the study site.

Geotechnical computer programs, such as the one that indicated a high liquefaction potential of the site terrace deposits, do not establish unequivocally that liquefaction will occur. While such programs are useful, they only provide a simplified index of liquefaction potential which should be weighed against pedogenic, geologic, and paleoseismic evidence. The program inputs consist of bedrock acceleration, material densities, blow counts, and gradation values (< #200 sieve), along with depths below ground surface, and water levels. However, such programs do not include direct accommodation for other important inputs such as stress history and the amounts of fine clay films, oxides, and other cementing agents that may bridge sand grains. Also, that percentage of the < #200 sieve comprised of clay is not included.

During its early history, the beach sand comprising the terrace probably was freely drained. However, clay formed from the beach sand and gradually increased the water-holding capacity of the soil. The production of these slow-draining clays thus concurrently raised the water table during the later history of the deposit. As a result, much of the deposit was cemented before it was saturated and no liquefaction was possible at any time during its evolution.

The paleoseismicity, soil stratigraphy and geological work at the terrace all clearly show that the potential for liquefaction there is low. Additionally, there is no documentation that liquefaction of Pleistocene marine terraces has ever occurred during

historic earthquakes in California (Les Youd, personal communication, 1994). We recommend that input on stress history, and quantities of cementing agents and fine clays be integrated into future generations of these programs. Such steps should help reduce future conflicts in liquefaction potential between the results of geotechnical computer programs and paleoseismic/soil stratigraphic/geologic results.

LENGTH-DISPLACEMENT PROFILES AND RATES OF DISPLACEMENT DECAY ON SURFACE RUPTURING BASIN AND RANGE NORMAL FAULTS: EVIDENCE FOR CHARACTERISTIC EARTHQUAKES?

Clark H. Fenton, Woodward-Clyde Federal Services, 500 12th Street, Oakland, CA 94607
(email: chfento0@wcc.com)
Susan S. Olig, Woodward-Clyde Federal Services, 500 12th Street, Oakland, CA 94607
(email: ssoligx0@wcc.com)

For an "ideal" fault, displacement decreases from a maximum at the center of the rupture plane to zero at the tip-line. For normal faults, the tip-line is defined as an ellipse, with an axial ratio of between 3:1 and 2:1 with the minor axis being parallel to the slip direction. The slip gradient is low over most of the rupture plane but increases rapidly towards the tip-line. However, when a fault intersects a free surface, i.e. surface rupturing faults, or in cases where there is slip transfer to an adjacent or intersecting fault, more complex patterns of displacement are observed. Irregularities in along-strike displacement profiles for surface-rupturing normal faults, in part, reflect complexities in the rupture process and the fault plane geometry.

To determine the rate of displacement decrease towards the ends of Basin and Range normal fault segments, data from both historical surface ruptures (e.g. Lost River fault) and prehistoric fault scarps (e.g. Pajarito fault) were analyzed. To facilitate comparison between faults of varying lengths and between faults with different numbers of events, distances along the fault were normalized by total surface-rupture length and displacement values were normalized by maximum displacement on the fault. To remove the effects of differing rheological conditions for faults that may not rupture the entire seismogenic crust, only fault segments longer than 30 km (i.e., elliptical axial ratio $\geq$2:1 assuming a 15-km-thick seismogenic crust) were analyzed. Despite some irregularities, all the faults studied show reasonable agreement with the elliptical fault plane model. However, a sudden drop in displacement as a result of slip transfer to an adjacent fault segment is commonly observed. From the rates of displacement decay and knowledge of the maximum offset and the offset at any point along a fault, the normalized distance from the end of the fault can be calculated. The relationship defining rate of displacement decay can then be used to help identify the location of potential segment boundaries and may be useful in characterizing rupture scenarios along segmented fault systems, especially when detailed paleoseismic information is lacking.

PALEOSEISMOLOGY IN NORTHWESTERN EUROPE: INVESTIGATIONS OF POSTGLACIAL INTRAPLATE FAULTING

Clark H. Fenton, Woodward-Clyde Federal Services, 500 12th Street, Oakland, CA 94607
(email: chfento0@wcc.com)

Until recently intraplate regions have been considered infertile ground for the study of paleoseismology. However, the choice of such 'stable' regions by several countries in western Europe as potential sites for high-level nuclear waste repositories has initiated an increased research into understanding their Quaternary tectonic behavior for evaluating earthquake hazards. Detailed field investigations in both the United Kingdom and Northern Fennoscandia (Norway, Sweden and Finland) have revealed evidence for movement along a number of faults since the end of the last glaciation, ~10ka.

Late Quaternary surface faulting was first reported from Northern Finland by Kujansuu in 1964, but it was not until Lundqvist and Lagerbäck (1976) described the lateglacial to postglacial age movement on the Pärvie fault in Swedish Lapland that the possibility of such movements were actually more widespread was even considered. Studies carried out by the Swedish Nuclear Fuels and Waste Management Company (SKB) during the search for a hard-rock site for a high-level radioactive waste repository, the work of Nils-Axel Mörner of Stockholm University and a comprehensive aerial photographic search and subsequent field investigation by Robert Lagerbäck of the Geological Survey of Sweden were all instrumental in bringing the phenomena of postglacial faulting in a 'stable' crustal environment to light internationally. More recent work by Odleiv Olesen of the Geological Survey of Norway has increased the database of postglacial faulting in Northern Fennoscandia.

In the United Kingdom the first description of Late Quaternary fault activity was from the Forth Valley where Sissons (1972) described offset and tilting of lateglacial age shorelines. Subsequent work by Sissons and his research students demonstrated further displacements of lateglacial age raised-shorelines along the west coast of Scotland. The significance of these offset shorelines was not recognized until Sissons & Cornish (1982) discovered faulting offsetting the shorelines of a lateglacial age lake in Glen Roy and proposed the theory of differential isostatic uplift using pre-existing basement faults for stress release, giving rise to elevated levels of seismic activity during deglaciation. Elevated seismic activity in the immediate postglacial environment was also hinted at by both Holmes (1984) and Ballantyne & Eckford (1984) in their respective studies on Highland rock-slope failures. The first specific studies of postglacial fault activity in Scotland, performed by Colin Davenport and Phil Ringrose, gave insight into the degree of fault movement and seismic activity during the lateglacial and postglacial period. Adding a wealth of new data on fault movements, Ringrose (1987) showed that such fault activity was spatially associated with regions of maximum glacio-isostatic uplift. Fenton (1991) revealed a chronology of faulting events related to the decay of glacial-loading stresses.

In Scotland the pattern of faulting comprises dextral strike slip on N- to NNW-striking faults, sinistral movement on WNW- to NW-striking faults and reverse movement along NE-striking faults. Offsets are on the order of 1-10 m along faults 1-10 km in length, spaced at about 10 km intervals. All faulting has occurred within the area of the Late Weichselian (Late

Wisconsin) glaciation. The scale of faulting in Northern Fennoscandia is an order of magnitude larger than that in Scotland. There faults are predominantly NE-striking, reverse faults, 50-200 km in length with offsets of the order of tens of meters. These faults form three parallel belts about 100 km apart. Again these faults lie within the area of Late Weichselian ice cover. In both Scotland and Fennoscandia widespread soft-sediment liquefaction, slope failures and near-surface ground dilation and 'pop-ups' are associated with faulting. Based on fault dimensions and distribution of ground deformation features, maximum magnitude estimates for these earthquakes are of the order of M_W8.0 for Northern Fennoscandia and M_W7.0 for Scotland. The majority of this activity occurred as singular events during or immediately following deglaciation. However, in Scotland there is evidence for recurrent activity during the late Quaternary, as well as for surface faulting occurring as recently as 2,500 years BP. This, and the fact that much of the faulting in Scotland involves a component of strike-slip movement, shows that this period of tectonism was not entirely controlled by glacial-loading stresses, but was the product of the interaction of loading stresses with the regional stress field of a rift-dominated passive margin environment.

Paleoseismic studies in the United Kingdom, like those in other intraplate regions, are still very much in their infancy. Surface faulting has not occurred in either the United Kingdom or Fennoscandia for the duration of the historical record (the past 700 years). This lack of historical analogues has been a major problem in paleoseismic investigations. In order to understand the genesis of the faults and seismically-induced deformation features observed, researchers have had to turn to similar tectonic environments that have been subject to surface faulting and damaging seismic activity during modern times; namely Australia, Canada and India. In this respect, the surface faulting associated with 1989 M_S6.3 Ungava earthquake in eastern Canada has provided the only modern example of ground rupture in an area of formerly glaciated stable craton. Recent surface ruptures in both Australia (e.g. Tennant Creek) and India show similar geometries to the postglacial faults mapped in Europe.

The methodology and philosophy of paleoseismic studies in glaciated intraplate regions is similar to that used in more active tectonic environments. Recency of faulting is revealed by offset of late Quaternary deposits and geomorphic features. However, the general lack of late Quaternary stratigraphy in many of these areas can make the recognition of individual paleoseismic events impossible. In some areas where all surficial deposits have been removed by glacial or glacio-fluvial agents, postglacial faulting is revealed merely by offset of glaciated surfaces.

Many features produced in the severe postglacial climate have been misinterpreted as being the result of paleoseismic activity. Glacially-eroded scarps and meltwater channels have a striking resemblance to bedrock fault scarps and have been consequently misidentified. Likewise, bedrock ridges and knolls disrupted by periglacial frost heave have been misinterpreted as being the result of bedrock fault rupture. The climate of the lateglacial and postglacial environment can lead to the formation of fissuring (frost or ice wedges), involutions and other forms of soft sediment deformation that have often been mistakenly attributed to strong seismic shaking. The use of deformed sedimentary sequences alone has been shown to be inconclusive in revealing paleoseismic activity. Likewise, the use of landslides as indicators of paleoseismic activity has also proved inconclusive. A spatial and temporal relationship with surface rupturing

events needs to be demonstrated before sediment deformation and landsliding can be attributed to seismic activity with any degree of confidence.

The recognition of paleoseismic events in recently glaciated intraplate regions is problematic. However, by careful fieldwork and an integrated approach to the study of surface faulting and related ground-shaking effects, the prehistoric earthquake history of such regions can be revealed.

Luminescence Geochronology: Shedding Light on the Timing of Paleoseismic Events

Steven L. Forman, Byrd Polar Research Center and Dept. of Geological Sciences,
The Ohio State University, Columbus, Ohio 43210-1002

Significant innovations in Quaternary geochronology in the past decade have afforded increased resolution in determining the timing of paleoseismic events. Leading these advances is the development of dosimetry-based techniques such as thermoluminescence (TL) and optically stimulated luminescence (OSL) providing for the first time the ability to directly date Quaternary sediments. Luminescence geochronology is an important tool in deciphering tectonic records because it is one of the few techniques that can be applied in a variety of terrestrial stratigraphic settings, potentially dating paleoseismic events spanning the last ca. 200,000 years. Although luminescence geochronology has broad temporal and sedimentologic utility, each sample may exhibit unique luminescence and dosimetric characteristics thus, the technique must be judiciously applied. Luminescence geochronology achieves its greatest utility for paleoseismology with an understanding IN THE FIELD of the linkages between tectonics, sedimentology, pedology, luminescence properties and environmental radiation.

The basic principles of luminescence geochronology for Quaternary sediments are similar to those used in dating archaeological materials. In contrast, for pottery the exposure to heat during firing removes any luminescence signal that has accumulated in the minerals, whereas in sediments the inherited luminescence signal in quartz and feldspar grains is reduced to some low definable level by light exposure. The geological luminescence signal accumulates from this level after burial. The extent of solar resetting of the luminescence signal is controlled primarily by the mode of sedimentation which dictates the spectral characteristics, the duration of light exposure, and the light intensity that the sediment is subjected. In addition, the residual level attained is influenced by the susceptibility of minerals to light bleaching.

The geological luminescence signal emitted by mineral grains is acquired by exposure to ionizing radiation mostly from the radioactive decay of U, Th, and ^{40}K. Radiation causes electrons to be displaced from orbitals, which are subsequently trapped within lattice-charged disequilibrium sites, called electron traps. Heating or light exposure of sediments causes vibration of the mineral lattice and eviction of electrons from traps. Some of these electrons may be conducted to luminescence centers and be emitted as light. This light signal is actually three dimensional, defined by temperature, and the light intensity and wavelength of light emission. In most TL dating procedures the ultraviolet or blue regions are selected for analysis.

Sediment grains are long-term radiation dosimeters, with the luminescence signal a measure of radiation exposure during the burial period. The radiation level responsible for producing the luminescence signal is termed the equivalent dose (ED; measured in grays (100 rads = 1 gray) and determining this value solves half of the luminescence age-equation (Equation 1).

$$A = \frac{ED}{D_a + D_b + D_g + D_c} \quad \text{(Equation 1)}$$

where: D_a = Annual alpha dose compensated for reduced efficiency of Alpha radiation
D_b = Annual beta dose; D_g = Annual gamma dose; D_c = Annual cosmic ray dose

The lower half of this equation is the dose rate, which is an estimate of the environmental radioactivity of the sediment for the time of burial. This is usually assessed by measuring the U, Th and K content of the sediment. This oversimplified equation encompasses the assumptions and analyses that are used to calculate a luminescence age estimate

There are many different types of sediments that can be or have the potential to be dated by luminescence. The selection and sampling of sediment is the first crucial step in the luminescence analysis. A luminescence age is a measure of the time since the last sunlight-exposure (or heating) event of the sediment. For a luminescence age to be meaningful the reduction in the luminescence signal, usually by sunlight, must be related to a significant tectonic event (i.e. emplacement of a sandblow, colluviation post-faulting). The luminescence dating of sediment that was exposed to little or no light during a specific event will yield a spurious age.

In general, the preferred sediment for luminescence dating (particularly for TL analysis) has had prolonged (i.e. >8hrs) exposure to sunlight prior to deposition, accumulated as a relatively homogeneous stratigraphic unit, > 50 cm thick, and has not undergone significant water content variations or diagenetic changes during burial. Selection of this preferred sample for a stratigraphic setting requires a sedimentary facies analysis that considers the efficiency of sunlight bleaching with transportation and deposition.

In many sedimentary settings the fine-grained (4-11μm) polymineral fraction is preferred for dating; it is an abundant particle size, often receiving extended light exposure during transport in air or water. Also, dosimetry calculations for this particle size are relatively straightforward. However, in a number of sedimentary environments fine-grained particles are rare or may be secondary detrital contaminants, and thus the coarse grained (100-150μm) fraction is preferred. There is concern whether such large grains during transport and deposition received adequate light exposure to reset the luminescence signal. However several studies indicate that quartz grains from dune sands receive sufficient light exposure to yield luminescence age estimates in good agreement with radiocarbon control.

Eolian deposits such as loess, cover loams, and sand dunes are often ideal for luminescence dating because of their long (>8 hrs) light exposure prior to deposition. Buried soil A horizons, certain fault derived distal-colluvium and playa lake deposits receive usually sufficient light exposure to yield TL age estimates in agreement with a radiocarbon chronology.

Fluvial and lacustrine sediments often receive limited light exposure during deposition because of the light filtering effects of water and turbidity. Thus, waterlain sediments have a higher residual level than corresponding well light-exposed terrestrial sediments. Application of the total bleach and regeneration techniques (which assume full light bleaching) to waterlain sediments often yield overestimates in age. The partial bleach and other laboratory procedures have been used to compensate for the incomplete bleaching of water-lain sediments and in some situations have yielded apparently accurate TL age estimates. The advent of OSL provides a more sensitive tool for discerning inherited from time acquire luminescence, ultimately providing a better geochronometer for rapidly deposited and waterlain sediments.

Sediment that is rapidly deposited and receives little (<1 hour) or no light exposure are inappropriate for luminescence dating. Tills, debris flows, coarse-grained colluvium, liquified sediments, deltaic, fluvial, and some glacial lacustrine/marine sediments receive insufficiently sunlight exposure with deposition; the majority of the luminescence signal is inherited. These sediments yield substantial overestimates in age by the previously mentioned methods, providing dubious chronologic control.

The temporal limitation of the luminescence technique is difficult to assess because of the many different factors that control the acquisition and retention of the luminescence signal. In general, the luminescence technique is most useful for sediments spanning the last 100 ka, but

may be applicable in certain situation to ca. 500 ka or older. The precision of the technique is usually between 5 to 20% with maximum resolution on time-scales of 10^3 to 10^5 years.

A recent study of eolian quartz-grains from Australia indicates the importance of low environmental dose-rate for extending the longevity of the luminescence method. The dose rate is a measure of the level of natural radiation that induces electron charge transfer, which is eventually measured in the laboratory as luminescence. Thus, the lower the environmental radiation, the slower the buildup of displaced electrons and the resultant luminescence level. The Australian dune sands have a comparatively low environmental dose rate (0.5 grays/ka) that is one quarter the level typical for sediments. Therefore, the TL signal is acquired at a slower rate, extending the temporal usefulness of the technique well beyond 100 ka. In contrast, many sediments from the intermountain western United States have dose-rate values 8 to 12 times higher and sediments >300 ka are close to luminescence saturation, significantly reducing the accuracy and precision of the analysis. The observed temporal limitations of luminescence geochronology may be partially related to the level of environmental radioactivity. Sites with a dose rate value of <2.5 grays/ka may be more amenable for extending the luminescence technique to >200 ka, but may have limited sensitivity on the 1000 year time-scale. Conversely, sites with relatively high dose rate (>4 grays/ka) may be at or close to saturation of the TL signal after 200 to 400 ka, but may provide a sensitive geochronometer for the past 100 ka.

This assessment underscores one of the main limitations of luminescence geochronology: the natural spatial and temporal variability in environmental radioactivity, and the susceptibility of silicate minerals to growth and retention of a luminescence signal. Thus, we currently believe that it is not prudent to universally extend apparently positive results in luminescence geochronology because of the site specific and mineralogic controls on the time-dependent luminescence signal.

An exciting recent development in luminescence geochronology is the advent of optically stimulated luminescence (OSL). The OSL signal is order of magnitude more sensitive to solar resetting providing potentially a more accurate measure of the time since burial. OSL should give more precise ages of well light exposed tectonically buried soil A-horizons, with errors on ages between 5 and 10% or less with multiple determinations. The dating of poorly light-exposed colluvial and alluvial sediments in tectonic association may be possible with OSL. A limitation for the wider applicability of TL to paleoseismic studies is the volume of data required to establish a statistically significant age estimate, particularly with the partial-bleach method. The amount of data needed to determine a statistically verifiable OSL age and the level of data reduction is considerably less for OSL analysis than TL, potentially increasing the availability of the technique to the paleoseismic community. There is a need for a comparative study of TL and OSL properties of colluvium and other sediments associated with seismic events to ascertain the utility of specific luminescence methods in paleoseismology.

Paleoseismic events are often identified by burial of a land surface by tectonically generated sedimentation. Often determining the timing of past earthquakes focusses on dating a buried soil- A horizon beneath colluvium or a sand-blow emplaced during or soon after a seismic event. Luminescence geochronology has shown significant promise in dating soil burial events. However, there is a paucity of knowledge of the luminescence age structure in soils. In particular, it is unknown if incipient versus well developed A horizons are solar reset to the same level and to a similar depth. A corollary problem is the luminescence age-depth relation in soils and associated changes in dose rate. It is imperative that future studies couple luminescence analysis with a more rigorous assessment of the effect of pedogenesis on the time-dependent luminescence signal.

Seismic Potential of the Capital City of Tehran (Iran)

M. Ghorashi, Geological Survey of Iran, P. O. Box 13185- 1494
Tehran- Iran

Abstract

Tehran the largest city and capital of Iran, considered as a metropolis in the rigion is situated in an enlargement along Alborz Mountain front with alluvial materials originating from the rise of Alborz Range.

Earthquakes are one of the major geological hazards to the environment of the Tehran region where urban and industrial developments are progresing at fast rate.

In order to evaluate the seismic and faulting hazards to the Tehran region, Quaternary faulting and seismicity (historical and instrumental) of the area were carefully analysed.

The major Quaternary faults to the capital city of Tehran are mainly mountain- bordering faults which were responsible for the formation of the present physiographic features. Since most of the Iranian seismognic faults are mountain- bordering reverse faults (Berberian 1981, 1983), therefore these faults in the Tehran region, are the possible sites for the generation of future earthquakes. In addition, a large number of minor faults are widespread throughout the city. Reactivation of the major Quaternary faults with resultant earthquakes, may trigger some movements along the minor faults.

Despite the occurrence of several historical destructive earthquakes, the Tehran region is seismically quiet at least since the 19th century and has not experienced a strong earthquake. The understanding of seismic potential of the city of Tehran is complicated by the fact that seismicity during the 20th century is relatively low, and the data for earlier times are incomplete.

However, on the basis of the present state of knowledge it is concluded that the occurrence of an earthquake of magnitude Ms = 7.0 or with an intensity Io = IX would be catastrophic for the capital city of Tehran.

Paleoseismicity of the SW Extent of the 1964 Alaskan Earthquake Rupture Zone, Eastern Aleutian Arc, Kodiak Islands, Alaska.

Lou Gilpin, Department of Earth Sciences, University of California, Santa Cruz, CA
Gary Carver, Humboldt State University, Geology Department, Arcata, CA
Eileen Hemphill-Hailey, U.S. Geological Survey, Pacific Marine Branch, Menlo Park, CA

The Kodiak Islands subsided up to 1.8 meters in 1964 as a result of the M_w 9.2 "Good Friday Earthquake". Ten tsunami waves were recorded along the SE shorelines of the islands. We have completed a geologic transect of the Islands from NW to SE, perpendicular to the trench, to investigate the marsh stratigraphic sequences that record the paleoseismicity. One goal of this project is to determine the extent of rupture by comparing the Kodiak paleoseismicity with the well established paleoseismic data for the eastern extent of the 1964 earthquake rupture zone. We will present evidence for previous "1964 type" events using the peat stratigraphy in the marshes of the Kodiak Islands.

Paleoseismic events are recorded in the marsh stratigraphy as distinct buried marsh surfaces characterized by abundant in-place leaf bases of herbaceous marsh plants, and tidal debris. The Interseismic period is represented by stratigraphic intervals of predominantly plant root material. The intertidal, middle marsh Triglochin maritimum peat are characteristic of the salt marsh, brackish environment. These peats are distinguished from the overlying peats without Triglochins, by diatom analysis and other sedimentologic indicators. The events are typically separated by 0.3 to 0.75 meters of peat. The two peat types are often separated by a fine gravel or sand layer up to several cm thick, that we interpret as tsunami deposited. Up to three of these subsidence events have been identified in the marshes of Shuyak and Afognak Islands, the northern-most of the Kodiak Islands.

The regularity of the stratigraphic spacing of event horizons and distribution of sample sites across most of the Kodiak Islands supports our interpretation of abrupt, probably coseismic, subsidence events affecting a large area of the Kodiak Islands and the Eastern Aleutian forearc.Three of the events record salinity changes as determined by diatom analysis. We use this evidence to infer elevation changes. Possible, alternative causes of the salinity changes involve lateral fluctuations in the fresh water marsh. Other sections with similar abrupt changes in the peat and sediment characteristics do not show changes in the salinity, as determined by diatom analysis. The very rapid rebound of the islands probably eliminates much of the evidence of the subsidence event. One sample section shows a "contamination" of the peat immediately underlying the event horizon, however a sample from 2-5 cm below the event horizon Indicated a salinity change. This "contamination " may be caused by post-seismic reworking of the newly submerged surface, or subsequent root penetration at the new marsh surface.

Calibrated ^{14}C ages (Stuvier and Beck, 1986) of samples from the Kodiak Islands suggest generally contemporaneous submergence at numerous sites spanning the Islands. The two oldest of these events may be correlative with the 800 and 1300 year BP events recorded by coseismic uplift at the Copper River Delta and Middleton Island at the eastern extent of the 1964 rupture zone. The youngest event determined by dates clustering in the 400-500 year BP range may indicate a shorter recurrence interval for great earthquake events on the Kodiak Islands arc segment, as compared to the Prince William Sound arc segment, to the northeast.

Paleoseismicity of the San Andreas Fault in the Carrizo Plain: Implications for Characteristic Earthquakes, Segmentation Models and Seismic Hazard

Lisa B. Grant, Woodward-Clyde Consultants, 2020 E. First Street, Su. 400, Santa Ana, CA.

Models of earthquake recurrence,calculations of earthquake probability and theories about the mechanical properties and segmentation of strike-slip faults have been strongly influenced by interpretations of paleoseismic data about the earthquake history of the San Andreas fault in the Carrizo Plain (Schwartz and Coppersmith, 1984; Sieh and Jahns, 1984; Stuart, 1986; Rundle, 1988; Sieh and others, 1989; Huang and Turcotte, 1990; Scholz; 1990). Measurements of offset stream channels near Wallace Creek have been interpreted to imply that the Carrizo "segment" of the San Andreas fault is a relatively strong segment, or asperity, that ruptures every 240 to 450 years in large magnitude "characteristic" earthquakes with repeated large amounts of seismic slip (Schwartz and Coppersmith, 1984; Sieh and Jahns, 1984; Sykes and Seeber, 1985; Sieh et al., 1989). Using the characteristic earthquake model to calculate conditional probability of rupture of the Carrizo segment for a thirty year period, the Working Group on California Earthquake Probabilities (1988) concluded that the Carrizo segment has the lowest probability of imminent rupture of any of the segments south of the central creeping zone. However, the results of recent paleoseismic studies indicate that the recurrence times for Carrizo earthquakes have been highly irregular, and that the amount of slip in past events has varied both spatially and temporally (Grant and Sieh, 1993 and 1994; and Grant and Donnellan, 1994). These findings 1) cast doubt on the significance of segmentation models of the San Andreas that are based on the amount of slip in the "characteristic" 1857 earthquake and 2) imply that the likelihood of a large earthquake in the Carrizo Plain could be substantially greater than previously thought.

Exposures in trenches across the San Andreas fault near Wallace Creek show that at least five surface-rupturing earthquakes have occurred in the Carrizo Plain since approximately A.D. 1218 (Grant and Sieh, 1994). The most recent earthquake, event A, was the 1857 Fort Tejon earthquake that ruptured approximately 360 km of the San Andreas fault from approximately Parkfield to near Cajon Pass (Sieh, 1978). The penultimate surface rupture, event B, most likely occurred within the time period A.D. 1405-1510. Three previous earthquakes, events C, D and E occurred prior to event B, but after A.D. 1218. Thus, approximately 350 to 450 years separated the most recent two events (A and B), and the previous three events were closely spaced in time. Depending on how the radiocarbon dates are interpreted, the average time between events B,C,D and E was 97 to 116 years. Grant and Sieh (1994) proposed that events B,C,D and E formed a temporal cluster of earthquakes. By correlating the dates of Carrizo earthquakes with events at other paleoseismic sites along the southern San Andreas fault, they argued that although some of the earthquakes in the cluster may have been similar to the "characteristic" 1857 rupture, some of the events were either smaller or ruptured to the north (Figure 1). Thus it appears that the San Andreas fault in the Carrizo Plain has not generated repeated identical, or characteristic, earthquakes for the last five earthquake cycles. Furthermore, Grant and Sieh (1994) argued that the Carrizo "segment" is not much stronger than the Mojave "segment" because the average recurrence interval for the last five Carrizo earthquakes (160 yrs) is not much longer than the average interval at Pallett Creek ($\sim$ 120 yrs).

The maximum amount of slip associated with the 1857 earthquake was approximately 9-

10 m near Wallace Creek (Sieh and Jahns, 1984). The Carrizo segment of the San Andreas fault has been defined as the section of the fault with the greatest amount of surface slip in the 1857 earthquake. Resurveys of 1855 survey monuments, excavation of buried offset channels, and analysis of offset surface features show that the amount of slip varied by several meters along a 2.5-km-length section of the fault near Wallce Creek (Grant and Donnellan, 1994; Grant and Sieh, 1993). The 97-116 year average time intervals between events B,C,D and E imply that an *average* amount of slip associated with these events was on the order of 3 to 4 m. It is unlikely that 12m and 11 m slip accompanied events B and C, respectively, as originally hypothesized by Sieh and Jahns (1984). Thus, although the amount of slip per event is poorly constrained, it appears that it has varied both spatially and temporally over the last few earthquake cycles. Therefore, the "segments" of the San Andreas fault that have been defined based on the 1857 spatial slip distribution may not correspond to inherent differences in behavior of different sections of the fault. It may be more useful to divide the San Andreas fault into segments based on structural or mechanical properties (e.g. the central creeping zone).

I propose that temporal clusters of earthquakes and variable surface slip are caused, at least in part, by incomplete co-seismic strain release as illustrated in Figure 2. Strain accumulates at a constant rate until the strength of the fault zone is exceeded, causing failure through rupture nucleation, or via propagation of a rupture from a distant section of the fault. The rupture pulse may pass too quickly to relieve all the accumulated strain (Heaton, 1990), resulting in variable slip along the fault plane at the surface and at depth. The areas of partial strain release are then more likely to fail subsequently due to large differential stresses caused by uneven strain release. Thus, a subsequent rupture is likely to nucleate within a relatively short time period. This process repeats, causing a cluster of earthquakes, until all of the strain is released. Then the fault enters a longer quiescent period as strain accumulates at a uniform rate. Repetition of this sequence may cause seismic cycles characterized by clusters of earthquakes at the end of longer interseismic periods. It may be possible to test this theory through combining geodetic observations of strain, measurement of subsurface slip distribution by inversion of seismic waveforms, and by analyzing paleoseismic and historic measurements of surface slip. The probability of future large earthquakes may be highest after a long period of quiescence, and following an earthquake that releases accumulated strain incompletely or unevenly.

REFERENCES

Grant, L. B. and A. Donnellan, 1994. *Bull. Seism. Soc. Am.*, v. 84, no. 2, 241-246.

Grant, L. B. and K. Sieh, 1994. *J. Geophys. Res.*, v. 99, no. B4, 6819-6841.

Grant, L. B. and K. Sieh, 1993. *Bull. Seism. Soc. Am.*, v. 83, no. 3, 619-635.

Heaton, T. H., 1990. *Phys. Earth Planet. Inter.*, v. 64, 1-20.

Huang, J. and D. L. Turcotte, 1990. *Nature*, v. 348, 234-236.

Rundle, J. B., 1988. *J. Geophys. Res.*, v. 93, 6255-6274.

Schwartz, D. P. and K. J. Coppersmith, 1984. *J. Geophys. Res.*, v. 89, 5681-5698.

Scholz, C. H., 1990. *Nature*, v.348, 197-198.

Sieh, K. E., 1978. *Bull. Seism. Soc. Am.*, v. 68, 1421-1448.

Sieh, K. E. and R. H. Jahns, 1984. *Geol. Soc. Am. Bull.*, v. 95, 883-896.

Sieh, K. E., M. Stuiver and D. Brillinger, 1989. *J. Geophys. Res.*, v. 94, 603-623.

Working Group on California Earthquake Probabilities, 1988. *U.S. Geol. Surv. Open File Rep.*, 88-398.

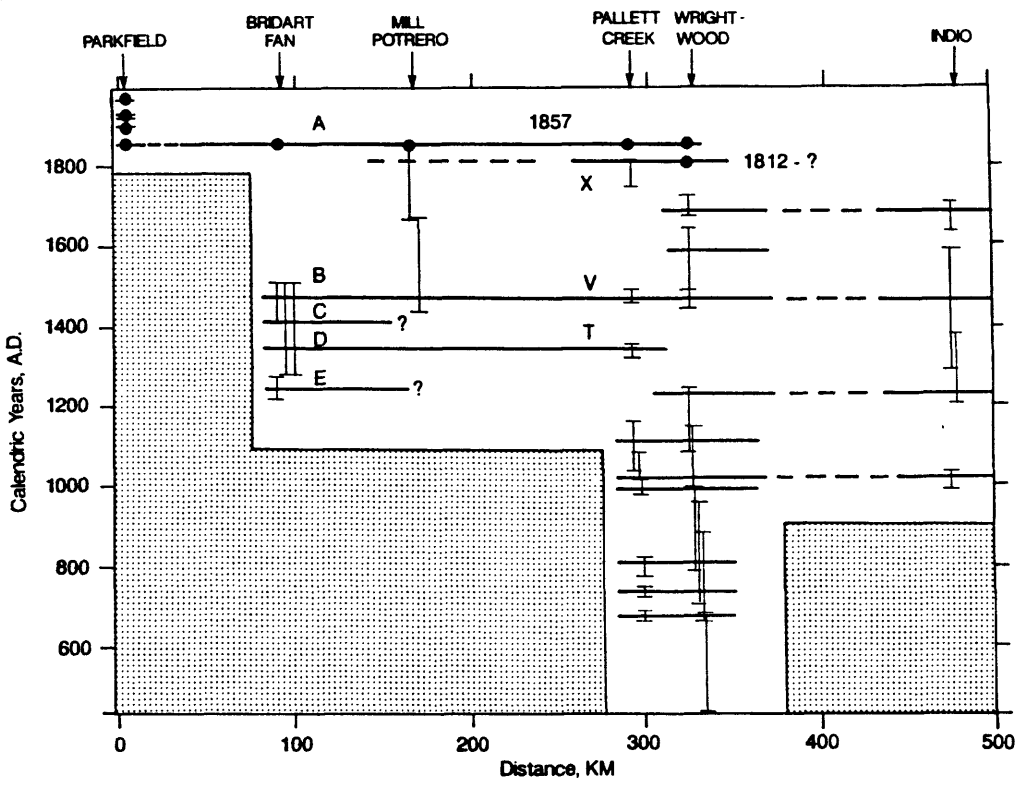

Figure 1: Correlation of ruptures (horizontal lines) between paleoseismic sites along the southern and central San Andreas Fault. Dates of events are shown by vertical bars. There is no published paleoseismic data in stippled areas.
From Grant and Sieh, 1994.

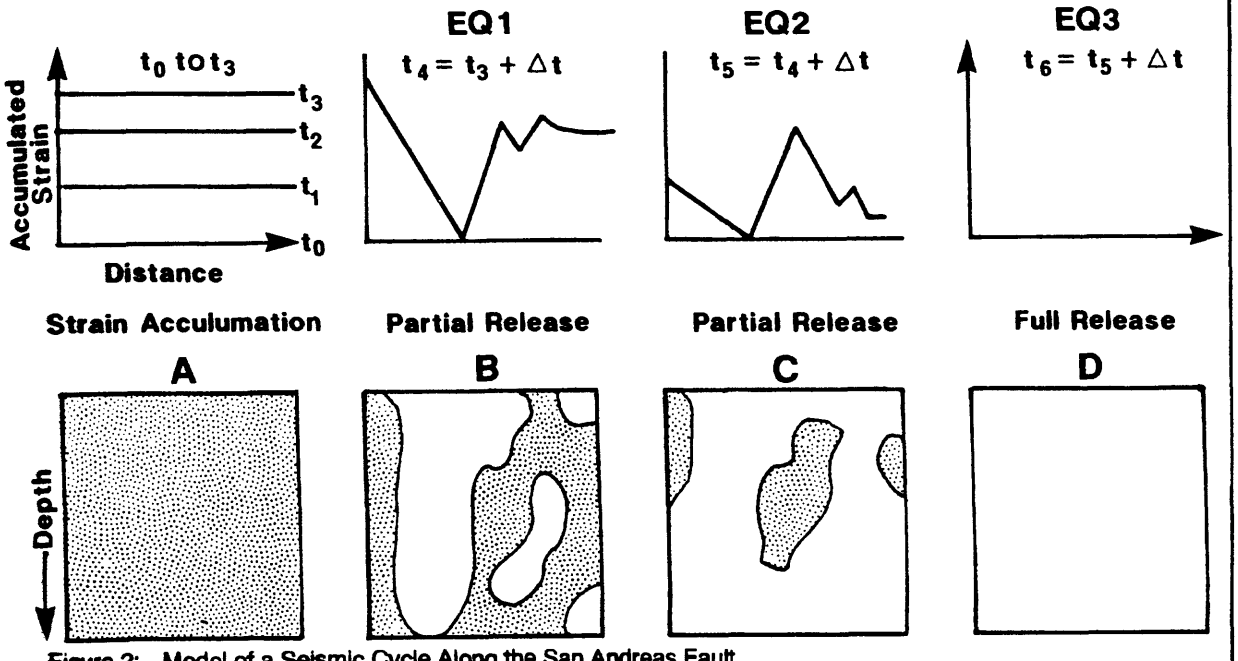

Figure 2: Model of a Seismic Cycle Along the San Andreas Fault.
A) Strain accumulates during the interseismic time period; B) A rupture releases strain unevenly along the fault at the surface and at depth; C) A second earthquake occurs within a relatively short time, Δt; D) Subsequent earthquake(s) occur until the strain is completely released.

Style and Rate of Quaternary Deformation of the San Simeon and Hosgri Fault Zones, Onshore and Offshore South-Central California

K.L. Hanson, Geomatrix Consultants, 100 Pine Street, 10th Floor, San Francisco, California
W.R. Lettis, William Lettis & Associates, 1000 Broadway, Oakland, California

The San Simeon and Hosgri fault zones are the southernmost two components of a complex system of right-slip faults in south-central coastal California that includes the San Gregorio and Sur faults (Figure 1). Different approaches were used to assess the contemporary style and rate of faulting along the San Simeon fault zone that extends partially onshore and the Hosgri fault zone that lies offshore along its entire length.

Paleoseismic investigations of the onshore San Simeon fault zone included detailed studies of offset marine terraces and drainages to estimate the late Pleistocene slip rate (Hanson and Lettis, 1994), and trenching investigations to assess the Holocene behavior and slip rate (Hall and others, 1994). A variety of dating techniques, including uranium-series dating of a bone sample, thermoluminescence dating of fine-grained sediments, radiocarbon dating, and soil geomorphologic studies were employed in conjunction with these studies.

The Hosgri fault zone lies entirely offshore where direct observations of fault geometry and conventional paleoseismic investigations cannot be used to assess style and rate of deformation. However, constraints on the rates of both vertical and horizontal slip along this fault zone were developed from an integrated analysis of a broad spectrum of data, including shallow high-resolution and deep penetration CDP seismic reflection data; geologic and geomorphic data along the Hosgri and San Simeon fault zones and the intervening Simeon/ Hosgri pull-apart basin; the distribution and nature of near-coast seismicity; regional tectonic kinematics; and comparison of the Hosgri fault zone with worldwide strike-slip, oblique-slip, and reverse-slip fault zones (Hanson and others, in review).

These geologic, seismologic, geophysical, and tectonic data clearly show that both the San Simeon and Hosgri faults are convergent right-slip (transpressional) faults having a late Quaternary slip rate of 1 to 3 mm/yr. Slip-rates estimated for both fault zones, include cumulative lateral and vertical components of slip across the entire fault zone, encompassing high- and low-angle fault strands and structural relief due to folding proximal to the fault zone. The rates are based on paleoseismic and Quaternary mapping studies conducted along the San Simeon fault zone, evaluation of the transfer of slip across the San Simeon/Hosgri pull-apart basin, and consideration of regional tectonics and geodetic rates of crustal shortening in south-central coastal California.

Evidence supporting strike-slip deformation also includes (1) long, narrow, linear zones of faulting and associated deformation; (2) the presence of asymmetric flower structures; (3) kinematically consistent localized extensional and compressional deformation at releasing and restraining bends or steps, respectively, in the fault zones; (4) changes in the sense and magnitude of vertical separation both along trend of the fault zone and vertically within the fault zone; (5) strike-slip focal mechanisms along the fault traces; (6) a distribution of seismicity that delineates a high-angle fault extending through the seismogenic crust; (7) high ratios of lateral to vertical slip along the fault zones; and (8) separation by the faults of two tectonic domains (offshore Santa Maria Basin, onshore Los Osos/Santa Maria domain) that are

undergoing contrasting styles of deformation and orientations of crustal shortening (Lettis and others, in review).

In characterizing the style of faulting along these fault zones, we assessed alternate tectonic models by evaluating complex geologic and geophysical phenomena, including (1) the cumulative effects of multiple deformational episodes that can produce complex, difficult-to-interpret fault geometries, patterns, and senses of displacement; (2) the difficult imaging of high-angle fault planes and horizontal fault separations on seismic reflection data; and (3) the effects of strain partitioning that yield coeval strike-slip faults and associated fold and thrust belts (e.g., Lettis and Hanson, 1992).

The San Simeon and Hosgri fault zones, which are part of the larger San Gregorio-San Simeon-Hosgri system of near-coastal faults, accommodate a significant amount of transpressional strain along the North-America-Pacific plate margin. The geologically determined slip rate of 1 to 3 mm/yr is consistent with geodetically modeled estimate of fault-parallel shear west of the San Andreas fault.

REFERENCES

Hall, N.T., Hunt, T.D., and Vaughan, P., 1994, Holocene behavior of the San Simeon fault zone, south-central coastal California, in Alterman, I.B., Cluff, L.S., and Slemmons, D.B. (eds.), Seismotectonics of the Central Coast Ranges: Geological Society of America, Special Paper 292, in press.

Hanson, K.L., and Lettis, W.R., 1994, Estimated Pleistocene slip rate for the San Simeon fault zone, south-central coastal California, in Alterman, I.B., Cluff, L.S., and Slemmons, D.B., (eds.), Seismotectonics of the Central Coast Ranges: Geological Society of America, Special Paper 292, in press.

Hanson, K.L., Lettis, W.R., McLaren, M.K., Savage, W.U., and Hall, N.T., in review, Style and Rate of Quaternary deformation of the Hosgri fault zone, offshore south-central California: submitted to Keller, M. (ed.), Santa Maria Province Project, U.S. Geological Survey Bulletin 1995.

Lettis, W.R., and Hanson, K.L., 1992, Crustal strain partitioning: implications for seismic hazard assessment in Western California: Geology, v. 19, p. 559-562.

Lettis, W. R., Hanson, K.L., Unruh, J.R., and Savage, W.U., in review, Quaternary tectonic setting of south-central coastal California: submitted to Keller, M. (ed.), Santa Maria Province Project, U.S. Geological Survey Bulletin 1995.

Pacific Gas and Electric Company, 1988, Final report of the Diablo Canyon Long-Term Seismic Program: U.S. Nuclear Regulatory Commission Docket 50-275 and 50-323.

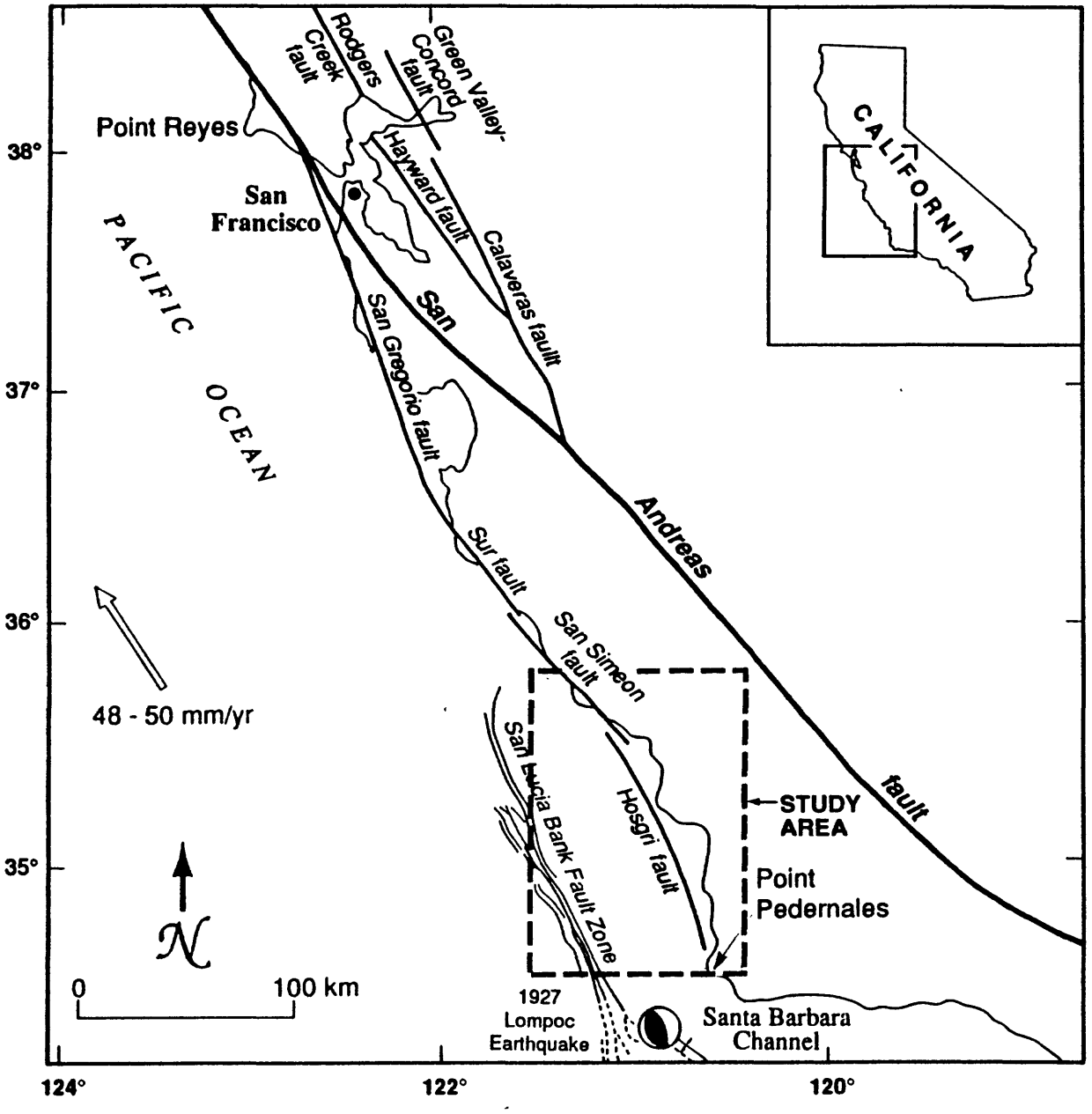

Figure 1. The San Simeon and Hosgri fault zones, which lie within the transpressional plate margin of the south-central coastal California, are the southernmost components of the San Gregorio/Hosgri fault system. This complex system of faulting, which is subparallel to the central California coast, splays off the San Andreas fault between Point Reyes and San Francisco on the north and appears to die out approximately 410 km to the southeast near Point Pedernales. An integrated analysis of onshore and offshore geologic, seismologic, geophysical, and tectonic data (Pacific Gas and Electric Company, 1988; Hanson and Lettis, 1994; Hanson and others, in review) clearly show that both the San Simeon and Hosgri faults are convergent right-slip (transpressional) faults having a late Quaternary slip rate of 1 to 3 mm/yr. These faults, therefore, are accommodating a significant amount of the relative plate motion (DeMets and others, 1990) between the Pacific and North American plates (indicated by large arrow).

Geometric Structures, Holocene Slip Rates and Paleoearthquakes Along the Xidatan–Dongdatan of Kusaihu–Maqu Active Fault in Northern Qinghai–Xizang Plateau

He Qunlu and Zhao Guoguang,Institute of Crustal Dynamics, SSB, Beijing 100085

Abstract

The Ku(saihu)–Ma(qu) left–lateral strike–slip fault of northern Qinghai–Xizang plateau, China, being an important suture belt, is one of the most active faults in The World. The Xidatan–Dongdatan (XD), located along the middle of the fault, ranges from west Jingxiangu to west Xiugou basin, about 140km in length.

Detailed field studies have revealed that the XD is a pull–apart wide valley. The dilatational nature of the stepover between Jingxiangu and Reshui is obviously demonstrated by the presence of a series of near eastwest–trending normal faults along both sides of the valley(Fig.1).

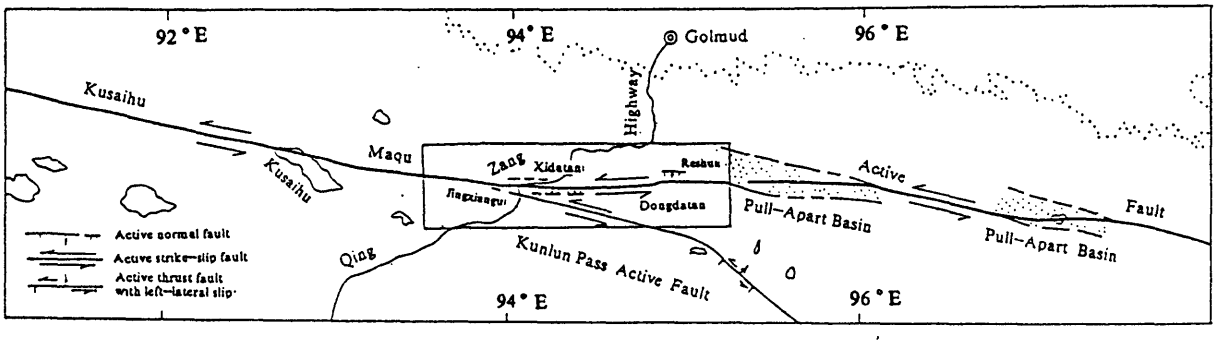

Fig.1 The geometric structures of the XD section along the Ku–Ma active fault

The major features of geometric structures along the XD section are the apparent multi–order en echelon discontinuities, which can be divided into three orders based on the comparative scales. The paleoearthquake studies verify that the first and second orders have arrested seismic rupture propagations of about M = 8 and M = 7 respectively. For example, the seismic surficial deformation zone of the great earthquake(M>8) occurred about 3750yr B.P., is distributed along the XD section, as long as 120km. It was stopped at Reshui of the western Xiuyou basin. The third order discontinuity has apparent geomorphic expressions, showing a series of small pull–apart basins or "push–up" hills.

The left–lateral slip rates of the XD section are determined by matching offset geomorphic features and more geochronologic data. Horizontal offsets were measured on terrace risers, small streams incised across the fault section, and pluvial fans, totalling about 70 displacement data. Twenty–four radiocarbon (^{14}C) and thermoluminescence(TL) dates were obtained associated with the starting offsets of the geomorphic features. Twelve independent determinations of the slip

rate along the XD yield an average slip rate of 10 ± 1.5mm / yr for the past 12,000yr. The slip rate along the Xidatan section is about 11.5mm / yr, and the slip rate along the Dongdatan is about 9.3mm / yr, whereas the slip rate is about 8.4mm / yr at the bend area between Xidatan and Dongdatan.

Based on local maximum coseismic displacements of 5m (M = 7—7½) and 10m (M > 8) with the average slip rate of 10mm / yr, the tentative recurrence intertals are 500yr and 1,000yr Separately along the whole section. The interval of the Xidatan is longer than that of the Dongdatan according their different slip rates.

The earthquake deformation zone along the XD seetion, which was modificated by several paleocarthquakes, is of larger scale and more complex on the older geomorphic surfaces than that of the younger geomorphic surfaces. Two excavations and two natural profiles across the XD section have provided for at least 7 earthquakes in the past 4,000yr on the basis of the dating and seismic deformational investigation(Fig.2).The oldest event occurred in 3750 ± 330yr B.P.. The latest event in 433 ± 127yr B.P. The evidence suggests an actual average recurrence interval of about 530yr. The interval of the Xidatan is shorter than that of the Dongdatan, which coincides generally with the interval calculated by the slip rate and maximum coseismic displacement.

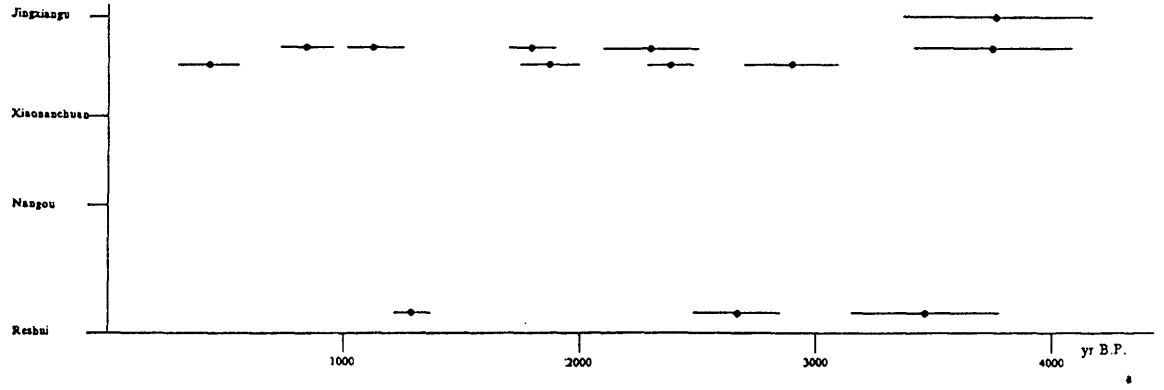

Fig.2 The distribution of the paleocarthqakes along the XD section of Ku–Ma active fault

There is no great earthquake record in this area, so the study mentioned above has an important significance in preventing and reducing seismic hazard.

The characteristic earthquake revisited: geological evidence of the size and location of successive earthquakes on large faults

S. Hecker and D. P. Schwartz, U.S. Geological Survey, Branch of Earthquake Geology and Geophysics, 345 Middlefield Road, Menlo Park, California

In the decade since the characteristic earthquake model was introduced, advances brought by earthquake research have provided new opportunities for considering the model. The characteristic earthquake model states that individual faults and fault segments tend to generate essentially the same size, or "characteristic", earthquakes at or near the maximum magnitude that can be produced by the geometry, mechanical properties, and state of stress of that fault or segment. This general observation was noted at about the same time by several workers using different data sets. Schwartz et al. (1982) and Schwartz and Coppersmith (1984) conceived the model using data on displacement per event from paleoseismic studies along the Wasatch and San Andreas faults. These data showed that at a point on a fault the amount of displacement during successive surface faulting earthquakes remains essentially constant. A major implication of this conclusion was that earthquake recurrence on an individual fault does not conform to an exponential (constant b-value) model. Wesnousky et al. (1983, 1984) compared recurrence based on geologic slip rates of Quaternary faults and the 400-year -long historical earthquake record in Japan and concluded that the data are best fit with a maximum moment model, a variation of the characteristic earthquake model in which recurrence is expressed as the recurrence of only the maximum-size event. Similarly, Bakun and McEvily (1984) concluded that the Parkfield segment of the San Andreas fault produces a "characteristic Parkfield" earthquake with essentially the same event-to-event epicenter, magnitude, foreshock pattern, rupture direction, lateral extent of aftershocks, and amount of slip.

A major misconception about the characteristic earthquake is that it implies uniform or quasi-periodic recurrence intervals. The term characteristic refers only to the successive repeat of similar displacement events and not to the amount of time between them. Indeed, dating of paleoearthquakes has defined a spectrum of recurrence behavior. Whereas high -slip-rate master segments of major plate-boundary faults tend to exhibit quasi-periodic behavior, faults off of main structures or faults in intraplate regions can have recurrence intervals that are highly variable or clustered even while the repeated size of events is the same.

Characteristic earthquakes are intimately related to fault segmentation, which is emerging as a field of earthquake research with important implications for increasing our understanding of the mechanics of faulting and for evaluating seismic hazard. The concept of fault segmentation is based on the common observation that fault zones, especially long ones, do not rupture their entire length during a single earthquake. As noted, where the amount of surface slip during successive events can be compared at the same location, it is frequently observed that this amount has remained essentially constant. It follows that the slip distribution along the fault, and by inference the rupture length, has also remained essentially constant. This argument, augmented with the results of structural and paleoseismicity studies, clearly implies that the location of rupture is not random, that there are physical controls in a fault zone that define the extent of rupture and divide a fault into segments, and that rupture segments can persist through many seismic cycles. If a particular segmentation model can be well constrained, ideally by combining both paleoseismicity data and geometric/structural data, the location and size of future ruptures can be ascertained. In fact, fault segmentation provides the framework for time-dependent probabilistic earthquake forecasts. However, the degree to which fault segments behave as independent rupture segments over time and our ability to identify these segments prior to an earthquake are complex issues and are the sources of greatest uncertainty and disagreement in segmentation modeling. This is particularly true for long multi-segmented strike-slip faults.

Although the characteristic earthquake model describes a basic type of fault behavior for large events, it is by no means inclusive. Since 1984 a significant amount of new historical and paleoseismic information on slip per event has been generated worldwide. This includes data from surface fault ruptures associated with the 1980 Irpinia, 1983 Borah Peak, 1987 Superstition Hills,

and 1992 Landers earthquakes as well as from many faults that have not produced historical events. This information is currently being reviewed to produce a worldwide slip-per-event database. To date, we have compiled information on slip per event for twenty-seven faults, representing all major fault types and a variety of tectonic settings worldwide. Two-thirds of these faults appear to demonstrate characteristic earthquake behavior. The results are preliminary, however, and we are in the process of refining our data analysis to include consideration of 1) measurement uncertainty, 2) problems with event recognition, 3) the quality and quantity of observations, and 4) the degree of study documentation. We are also addressing the issues of how much inter-event slip variability can be accomodated by the model and the degree to which factors such as tectonic environment and length of the earthquake cycle control similarities or differences in the amount of slip during successive events on a fault.

LATE QUATERNARY PALEOSEISMICITY AND SEGMENTATION ALONG THE SOUTHERN LEMHI FAULT, SOUTHEASTERN IDAHO

M.A. HEMPHILL-HALEY, Department of Geological Sciences, 1272 Department of Geological Sciences, University of Oregon, Eugene, Oregon 97403-1272 (formerly at Woodward-Clyde Federal Services, 500 12th Street, Oakland, CA 94607)
T.L. SAWYER, Wm Lettis & Associates, 1000 Broadway, Suite 612, Oakland, CA 94607
P.L.K. KNUEPFER, State University of New York, Binghamton, NY 13901
S.L. FORMAN, Byrd Polar Research Center, 103 Mendenhall Laboratory, The Ohio State University, Columbus, OH 43210
I.G. WONG, Woodward-Clyde Federal Services, 500 12th Street, Oakland, CA 94607

The 28 October 1983 M_W 6.8 (M_S 7.3) Borah Peak earthquake along the Lost River fault in southeastern Idaho focused attention on the seismogenic potential of normal faults situated north of the eastern Snake River Plain (ESRP). As part of a seismic hazards evaluation for the Idaho National Engineering Laboratory (INEL), we conducted a paleoseismic investigation of the southern Lemhi fault, which lies immediately east of the Lost River fault (Figure 1). The objectives were to evaluate: (1) the timing and displacements of the most recent event (MRE), and possibly the two or three preceding events, along two geomorphically-defined segments of the southern Lemhi fault; (2) temporal evidence for earthquake recurrence; and (3) whether existing segmentation models adequately define potential earthquake ruptures. We sought to understand whether segments were correctly recognized (i.e. whether each geomorphically defined segment rutprues independently), or whether they ruture as a single segment or in overlapping ruptures.

The 150-km-long Lemhi fault bounds the western front of the Lemhi Range (Figure 1) and exhibits predominantly normal displacement. Previous segmentation models for the Lemhi fault have been based on comparison of alluvial fault scarp morphology and identification of possible segment boundaries related to geometric and geologic changes along the fault length (Crone and Haller, 1991; Turko and Knuepfer, 1991). Two segments proposed for the southern third of the Lemhi fault are, from south to north, the Howe and Fallert Springs segments. The boundary between the Howe and Fallert Springs segments was defined as the South Creek block, a large, low-relief, rhombic salient that extends almost 8 km valleyward from the range front. The origin of the block is uncertain; it may be either a low-angle listric fault or a shallow gravity slide overlying alluvium. The character of the block is significant in that a shallow slide block may be less likely to impede coseismic rupture than a deep-seated structure. Although earlier investigators did not observe prominent scarps across the block, we identified diffuse, discontinuous scarps within the block along strike with the range front. Based on geomorphic evidence, Crone and Haller (1991) and Turko and Knuepfer (1991) interpret the most recent scarps along both segments as late Pleistocene with Fallert Springs scarps being slightly younger than those along the Howe segment.

To better understand the paleoseismic history of the southern Lemhi fault, we excavated five trenches (Figure 1) in early Wisconsin-aged (60-80 ka) to late Pinedale-aged alluvial fan surfaces (ca. 15-25 ka): two on the Howe segment (at East Creek and Black Canyon) and three on the Fallert Springs segment (at Camp Creek and Coyote Springs (two trenches)). We used thermoluminescence (TL) and ^{14}C dating methods, as well as pedogenic development, to assess the timing of events and duration of interseismic intervals. Our analyses show that the Howe and Fallert Springs segments have more complex paleoseismic histories than previously proposed, and there is evidence that the South Creek block did not consistently serve as an impediment to rupture.

Our results suggest that the entire Fallert Springs segment may have ruptured in single events during the late Pleistocene, whereas only the northern end ruptured during the Holocene. At Camp Creek, immediately north of the South Creek block, we found compelling evidence for two events and permissive evidence for a third, older, event. Reworked loess buries the youngest colluvial

wedges, thus the two youngest events occurred before 24-19 ka. A weakly developed Bw horizon exists along the upper penultimate wedge suggesting only a short interval of time between it and the MRE. A TL sample taken from a buried Av horizon formed in the top of the oldest wedge provides a date of about 75 ka for that event. At Coyote Springs, within the northern Fallert Springs segment, two trenches were excavated: one in the principal fault and a second in a graben-bounding antithetic fault. These trenches expose evidence for three surface-rupture events along the principal fault splay but only two events along the antithetic splay. Evidence for a Holocene MRE is found along the principal splay but not the antithetic splay. The penultimate event identified in the principle splay is coincident with the MRE along the antithetic splay. A maximum limiting age range of 26-16 ka for that event was derived from a polygenetic soil formed downslope, and within the upper part, of the oldest colluvial wedge. An Av horizon buried by the oldest wedge yields a maximum limiting age range of 23-14 ka for the oldest exposed event. The fairly narrow overlap in ages is consistent with minimal soil development on the older colluvial wedge suggesting that only a brief amount of time elapsed between the two events. Based on geologic and chronologic evidence collected at both the Camp Creek and Coyote Springs sites, it is permissive that the penultimate and older events at Coyote Springs are the same as the MRE and penultimate events at Camp Creek. However, there is no evidence for a Holocene event at Camp Creek. The lack of Holocene displacement along the antithetic splay at Coyote Spring and a relatively small MRE colluvial wedge (0.5 to 1 m thick) along the principal splay may be evidence for the terminus of a surface rupture event near that site.

Paleoseismic analyses of the Howe segment suggest that its northern end, and possibly its entire length, may have ruptured together with at least the southern half of the Fallert Springs segment during some faulting events. At East Creek, at least two and possibly three events are represented by colluvial wedges. The MRE wedge is interbedded with reworked loess, probably derived from the ESRP, that was deposited from about 25 to 15 ka. TL dates on the loess bracket the event between 19 and 15 ka. The penultimate event occurred before 27-25 ka and possibly substantially before that time based on development of a strongly cemented $CaCO_3$ horizon (Stage III). At Black Canyon to the north, stratigraphic relations, TL and radiocarbon dates, and soil development provide evidence for three events clustered between 24 and 17 ka. Individual colluvial wedges possess weakly developed Bw soil horizons. This suggests that a 7000 year period of relatively vigorous seismic activity has been followed by about 17,000 years of quiescence at this site. The penultimate event wedge is no more than about 0.5 m thick at its proximal end compared to the bracketing wedges which are on the order of 1 m thick. It is conceivable that this event is the result of rupture extending southward through the South Creek block into the Howe segment. Geologic and chronologic evidence, along with the resolution limitations of the dates, permit the youngest colluvial wedge identified at East Creek to be related to one of the three colluvial wedges identified at Black Canyon. However, the degree of soil development within the penultimate wedge at East Creek is not consistent with soils formed on any of wedges identified at Black Canyon. Thus it appears surface rupture was not consistent within the Howe segment and it appears that, within the resolutionof the dating, portions of both the Howe and Fallert Springs segments sometimes rupture together, at other times portions of the two previously defined segments rupture independently.

Based on our analyses we conclude that the current segmentation model for the southern Lemhi fault is inadequate to characterize past surface-rupture activity or to define potential future surface ruptures. Thererfore, we propose that the previous segmentation terminology for the southern Lemhi fault be abandoned. The proposed segment boundary at the South Creek block may have had little, if any, influence on surface rupture propagation for some events, but may have arrested others. It is not evident whether actual rupture boundaries exist within the currently defined segments, or if zones of overlapping rupture between adjacent sections of the fault better describe its southern extent. Finally, evidence for temporal clustering of events exists immediately south of the South Creek block, with the possibility that one or more of these events resulted from the overlap of surface rupture from portions of the fault to the north, which would appear to support the latter model.

REFERENCES CITED

Crone, A.J. and K.M Haller, 1991, Segmentation and the coseismic behavior of Basin and Range normal faults, examples from east-central Idaho and southwestern Montana, U.S.A., Journal of Structural Geology, v. 13, p. 151-164.

Turko, J.M. and P.L.K. Knuepfer, 1991, Late Quaternary fault segmentation from analysis of scarp morphology, Geology, v. 19, p. 718-721.

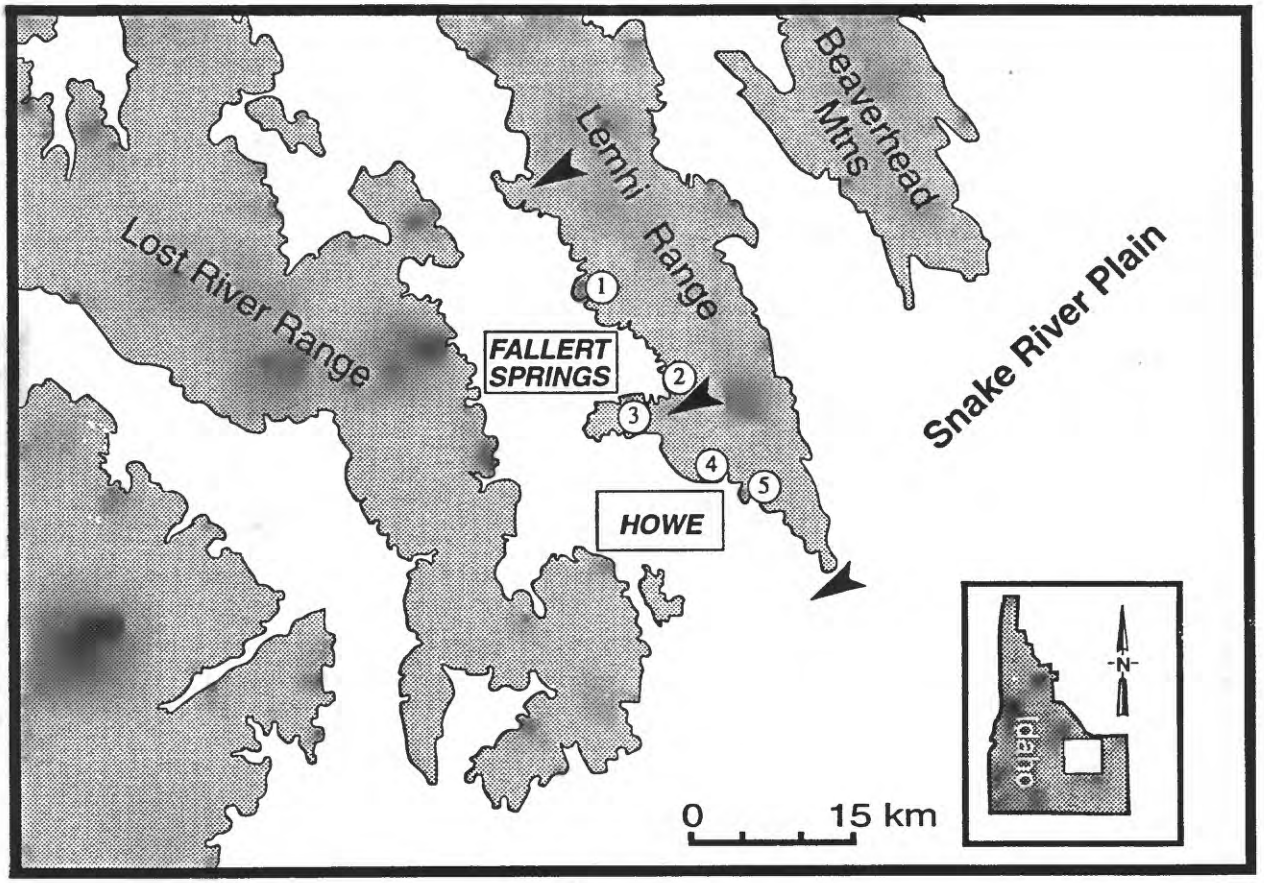

Figure 1 - Map of the southern Lemhi fault. Arrowheads indicate previously proposed segment boundaries with segment names in boxes. Numbered sites include: 1) Coyote Springs site, 2) Camp Creek site, 3) South Creek block, 4) Black Canyon site, 5) East Creek site.

HOLOCENE LIQUEFACTION IN QUITO (ECUADOR): A PALEOSEISMIC RECORD.

HIBSCH Christian, Instituto Francés de Estudios Andinos. Casilla 171106596, Quito, Ecuador.
YEPES Hugo, ALVARADO Alexandra, PEREZ Hugo †, Instituto Geofisico y Departamento de Geologia. Escuela Politécnica Nacional. Quito, Ecuador.
SEBRIER Michel, URA 1369 CNRS, L.G.D.I, Bat. 509, Université Paris XI, 91405 Orsay Cedex France.

While it is still being discussed whether paleoliquefaction data should be considered as paleoseismic evidence or not, the importance of the seismic hazard in a region like Quito, where, unfortunately, seismic networks are still poorly developed, has lead us to test the validity of the method. As is the case for the whole western hemisphere, the historic seismicity of Quito is limited to five centuries; this duration is considered inferior to the estimated recurrence time of the major expected earthquakes for each known main active fault. Since the neotectonics background of the entire country is not yet completely defined, it has been necessary to look for an approach capable of extending the historical seismicity records in order to improve the seismic hazard analysis for the city. Even with the uncertainties stemming from the difficulties in proving the tectonic origin of the paleoliquefaction levels, the highest number of earthquakes defined by this method was still below the number obtained by historic analysis.
Ecuador is situated in an active subduction zone that has produced many major earthquakes. Inland, in the continental crust, several active faults have also been recognized. Major right-lateral faulting is found along NNE-SSW to ENE-WSW striking faults, while reverse faulting is mainly encountered along N-S trends in a restraining bend system between the Chingual and Pallatanga right-lateral faults and also along the eastern Andean foothills. Quito is located on top of one of these compressional structures (the Quito reverse fault) in which two small Quaternary basins have developed. The northern basin sediments have been studied thanks to excavations for building foundations. Lacustrine and fluvio-lacustrine deposits, paleosoils, silts, volcanic ashes and tuffs have been found in different outcrops. Stratigraphic correlations and basin reconstruction are still in progress, punctuated by the rhythm of ongoing excavations. The correlation of the different paleoliquefaction levels is not yet totally completed, but the analysis of one interesting outcrop has permitted the proposal of several hypothesis discussed below.

An outcrop in the "Calle Pinzón", on the eastern side of the northern basin of Quito has shown 20 different levels of paleoliquefaction recorded in only 2.70 meters of sediments for a duration estimated to 1000 yrs (Fig. 1). The thicknesses of the deformed levels range from some millimeters to more than 30 centimeters. The seismic history of Quito (Del Pino & Yepes, 1990) indicates that earthquakes have affected the city up to intensity IX in the MSK scale (Fig. 1, A). A first estimation of the paleoseismic intensities has been made, subjectively comparing the different degrees of paleoliquefaction and assuming they corresponded to seismic intensities ranging from VI (minimum expected intensity able to produce liquefaction) to IX (maximum intensity described in the historic seismicity). This estimation has given a graph of intensity distribution (fig. 1, B) whose profile is more or less similar to the one obtained from the historic analysis, but this estimation still is not satisfactory in comparison to a historical record of half the duration. A second estimation has been made, taking into account the descriptions of Sims (1973) about the effects of quaternary earthquakes in California upon lacustrine deposits of the Van Norman lake. In this case, known seismic intensities and the associated liquefaction have been directly compared. About 1 cm of sediments were deformed for an intensity VI (MM) and about 4 to 5 cm for an intensity VIII-IX (MM). These results suggest a progression ratio of the thickness of deformation produced by liquefaction by each step of seismic intensity ranging from $\sqrt{4}$ to $\sqrt{5}$ (2 to 2.24), starting with a basic deformation of 1 cm. Such a progression ratio appears also to agree with the one in the relation defined between the horizontal ground acceleration and the seismic intensity $\log a_H = 0.014 + 0.30 I_{MM}$ (Trifunac & Brady, 1975) which give a progression ratio close to 2. This ratio was applied to Quito, starting also with 1 cm of basic deformation but the obtained results were inconsistent with the historic seismicity (many intensities above IX; fig. 1, C). A final result was obtained with the same progression ratio but with consideration of a basic deformation of 2 cm thick rather than 1 cm for a seismic intensity of VI (MM/MSK). The final graph (fig. 1, D) has proven the most satisfactory for earthquakes with intensities higher than VII.

It also points out the possible occurrence of an earthquake that has produced an intensity of X, which could be quite possible if the Quito fault were to reactivate. The deficiency of the number of earthquakes of lower intensities might be due to either physical properties of the sediment or to the erasing effects of larger earthquakes.

Even considering all the uncertainties, these results suggest the importance of developing such a method with a statistical approach of liquefaction effects for historic earthquakes and at the same time fundamental research in laboratory.

DEL PINO I., YEPES H. (1990).- Apuntes para una historia sísmica de Quito.- *Centro Histórico de Quito. Problematica y perspectivas. Dirección de Planificación. I. Municipio de Quito, Ecuador.*

SIMS J. D. (1973).- Earthquake-induced structures in sediments of Van Norman Lake, San Fernando, California.- *Science, Vol. 182, pp. 161-163.*

TRIFUNAC M. D., BRADY A. G. (1975).- On the correlation of seismic intensity scales with the peaks of recorded strong ground motion. *Bull. of Seism. Soc. of America, Vol. 65, N° 1, pp. 139-162.*

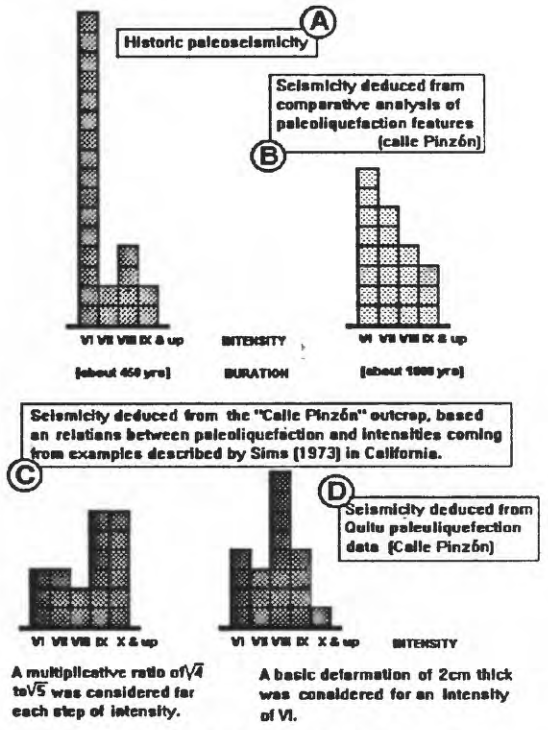

Figure 2: distribution of seismic intensities.

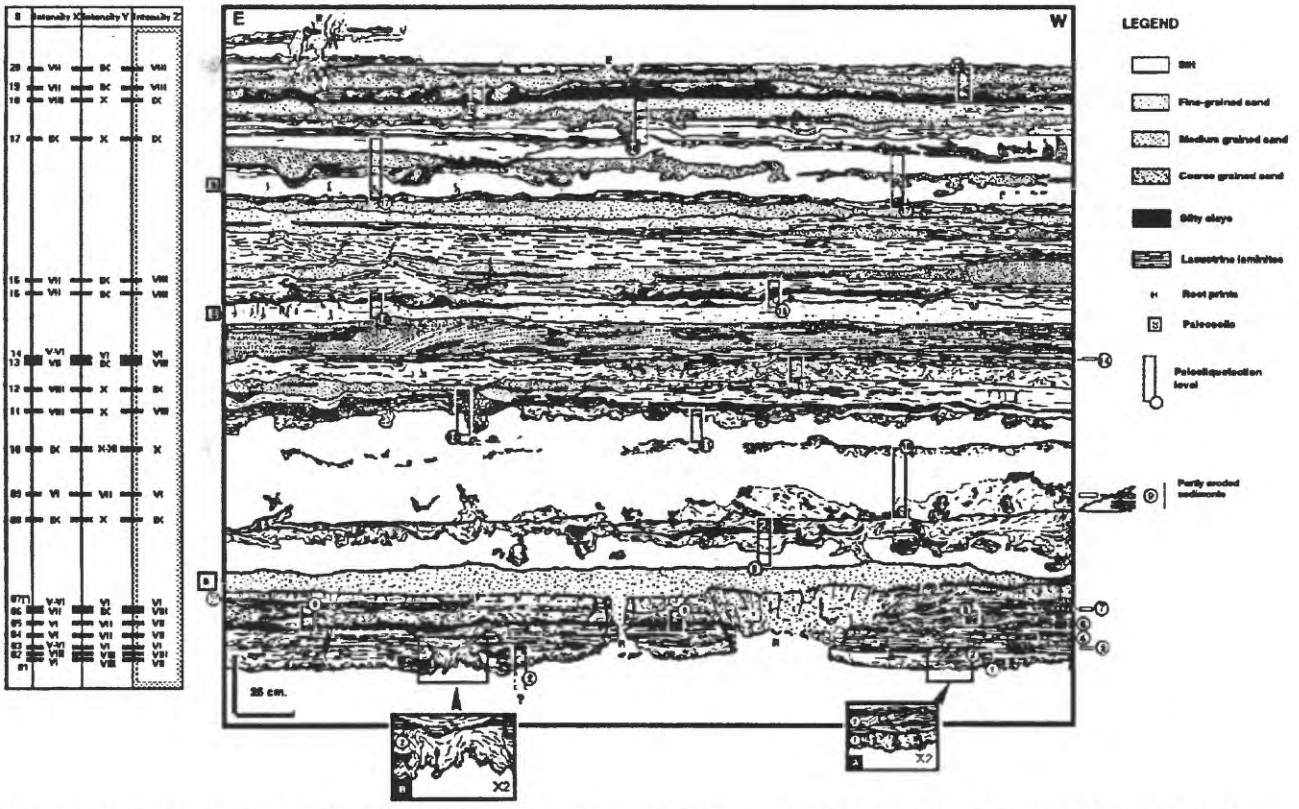

Figure 1: Paleoliquefaction levels in the "Calle Pinzón" outcrop. A & B: zooming showing different shacking figures of the lacustrine laminites in response to the seism #2. The change in size is due to the presence of an underlying level of clay and lime of about 1 meter thick. The tables (X to Z) refer to the different assumed seismic intensities (see text and Fig. 2).

Cataclastic rocks associated with extreme crustal extension, southern Basin and Range: Evidence for paleoseismicity along low-angle normal faults ?

Barbara E. John, Department of Geology and Geophysics, University of Wyoming, Laramie, Wyoming 82071

Recent interest in extensional tectonics has focused on the existence and nature of low-angle normal or detachment faults. Controversy has centered on the question of whether gently dipping normal faults were initiated and moved seismically in their present low-angle configuration, or were active with relatively high dips, and have been rotated passively to a more gentle orientation through time. The mechanism for development of low-angle normal faults exposed in Cordilleran core complexes (and elsewhere worldwide) remains controversial. The exhumed Cenozoic normal fault system exposed in the Chemehuevi Mountains area of southeastern California provides constraints on the initiation angle and geometry of an extensional fault system that has accommodated extreme crustal stretching. The mapped fault geometry, associated cataclastic fault rocks, inferred evolution of the fault system, and detailed thermochronology place tight constraints (including magnetude of slip and integrated slip rate) on the environment of crustal attenuation.

Extension involving the upper and middle crust in the Chemehuevi Mountains area was accomplished along a stacked, anastomosing sequence of brittle, northeast-dipping low-angle normal or detachment faults discordantly cutting heterogeneous quartzofeldspathic basement. The large displacement (>18km), regionally developed Chemehuevi detachment fault (CDF) separates footwall and hanging wall rocks from different structural levels in the crust, typically with gross lithologic 'mismatch'. Above the CDF, the hanging wall was distended by innumerable high-angle faults, accommodating to 100% average extension regionally. Footwall accommodation to movement on the fault system was small. The older, small displacement (≤2 km) Mohave Wash fault lies structurally below the Chemehuevi detachment. Moderately to steeply dipping (40° to 80°) NW-trending (110° to 170°) normal faults, and NE-trending (050° to 060°) strike-slip faults truncate and are truncated by the Mohave Wash fault. These faults have tens to hundreds of meters separation, but are nowhere know to cut the structurally higher CDF; throughout the area the youngest fault is demonstrably the regionally developed Chemehuevi detachment. This relationship precludes the possibility of rotations of the low-angle normal faults to their gentle orientation by younger higher angle faults

Fault rock type and the mineral deformation mechanisms associated with movement on the detachment faults suggest that they were initiated and moved within the brittle and transitional brittle-ductile seismogenic regimes. Fault rocks produced by slip include incoherent gouge, breccia, rocks of the cataclasite series, and rare protomylonite and pseudotachylite. Thickness of these fault rocks varies from less than 1 meter to more than 200 meters. Fault rocks associated with the small displacement Mohave Wash fault are characterized by microfracturing over broad regions (up to 200 meters), with evidence for repeated fracturing and fluid flow events. Those associated with the major slip Chemehuevi detachment show overprinting relations that imply an evolution from wide zones of hydrothermally altered cataclasite (as the Mohave Wash fault) at moderate levels in the crust, to a narrower zone of breccia within the upper crust, to a sharp, planar discontinuity marked by breccia and locally gouge at very shallow crustal levels. Examination of these fault rocks indicate that cataclastic flow and frictional sliding were the dominant deformation mechanisms. Elongate quartz and potassium feldspar suggests that in the structurally deepest exposures of the fault system, incipient crystal plastic behavior in quartz and pressure solution became important deformation mechanisms.

Minor cross-cutting veins of pseudotachylite with subhorizontal generating surfaces occur in, and adjacent to the detachment fault zone(s). Elsewhere the faults are characterized by a high concentration of cross-cutting mineralized veins and fractures that imply episodic fracturing and fluid flow associated with detachment faulting. The presence of pseudotachylite suggests that the fault system was seismically active during at least part of its movement history, a conclusion supported by the lack of a strong shape fabric within the cataclasites.

Application of $^{40}Ar/^{39}Ar$ and fission track thermochronology to rocks in the footwall of the Chemehuevi fault system provides further constraints on the timing, initiation angle and evolution of regional detachment faulting. Geographic patterns of cooling ages in the footwall provide a basis for interpreting the unroofing history of the domed footwall (at different mineral closure temperatures for hornblende, biotite, and potassium feldspar) as the footwall moved from under the northeast-dipping hanging wall. Contoured values of mineral age decrease northeastward in the slip direction. $^{40}Ar/^{39}Ar$ and fission track data together provide information about paleotemperatures of parts of the lower plate to the Chemehuevi detachment fault before, during, and after major crustal extension took place. These thermochronologic data indicate a moderate difference in paleotemperature across the footwall prior to faulting. At the onset of extension between 22 and 24 Ma, granitic rocks exposed in the southwestern and northeastern portions of the footwall were at ~100°C and >400°C, respectively, separated by a distance of some 23 kilometers down the known slip direction. This gradual increase in temperature with depth is attributed to the gentle warping of an originally subhorizontal isothermal surface, and constrains the exposed part of the Chemehuevi detachment fault to have had a regional dip initially of 15° to 30°.

Analysis of $^{40}Ar/^{39}Ar$ and fission-track ages also leads to estimate the integrated fault slip rate as the footwall was tectonically denuded and cooled. Northeastward-younging is seen for each mineral (hornblende, biotite, potassium feldspar, and apatite). Assuming that these ages represent cooling during extension, they can be used to interpret the slip rate at which footwall rocks moved >18 km relative to the hanging wall along the base of the northeast-dipping Chemehuevi fault system. Extensional slip calculated this way averages 7-8 mm/yr between 19 and 15 Ma, comparable to calculated rates elsewhere in the southern Cordillera.

Together the structural, isotopic, and fission track data confirm the suggestion that faults accommodating large magnetude slip can be initiated and move within the seismogenic regime at moderate- to low-angles (ie. ≤ 30°). This conclusion demands re-evaluation of current mechanical and seismologic data, as well as many models of continental extension.

INTERDISCIPLINARY EVIDENCE OF PALEOSEISMICITY ALONG THE DEAD SEA RIFT: ASSUMPTIONS AND RELIABILITY

Iaakov Karcz, Geological Survey of Israel, Jerusalem, 95501
Fax 972 238 0688; e-mail karcz@vms.gsi.gov.il

The apparent, nearly tenfold discrepancy between the estimates of total and seismic slip along the Dead Sea Rift (DSR) is attributed alternately to aseismic creep, underestimate of occurrence of large magnitude earthquakes in geological record, and to partitioning of strain along subsidiary tectonic elements. Since the gap between the time scales of instrumental seismicity (10^1-10^2y) and of tectonic models (10^5-10^6y)is wide, attempts were made to derive slip rates employing concepts, methods and techniques of Geodesy, History, Archeology, Sedimentology and Geomorphology. Reliability and resolution of thus obtained estimates are determined by the budget of assumptions made in derivation, analysis and tectonic interpretation of data from cognate fields. In some cases however, if the ultimate result appeared to fit well into the preconceived seismotectonic model for DSR, the sweeping nature of implicit assumptions was overlooked. The impact on reliability of such "interdisciplinary" estimates is illustrated below.

Geodetic studies Tectonic geodesy assumes that, when free of operational errors and of geotechnical and geophysical side effects, the changes in elevation, direction and distance determined by repeated measurements reflect movements of the crust.

Vertical component of movement is derived from repeated precise levelling along networks of benchmarks 1-2 km apart, a technique capable of a millimeter-scale accuracy. Comparison of data obtained in Israel since 1934 suggested at first that tectonically controlled movements of the order of few mm/year are taking place. The inferred pattern however appears to include artifacts of inapplicable assumptions inherent in levelling operations and analysis (e.g. statistical homogeneity of the network). Redesign of the country-wide vertical control network is therefore under way.

Horizontal component of movement is obtained from repeated electrooptic (EDM) and space technology (mainly GPS) measurements, which attain subcentimeter accuracies. In Israel, a test work monitors crustal activity along the politically accessible segment of DSR. The outer part, 20 x 45 km in area, spans the DSR margins between Lake Kinneret and Lebanese border, and is tied to close spaced network across the inferred trace of the transform. Since 1987 the area was seismically quiescent, and repeated annual surveys indicate that any steady aseismic horizontal slip could not exceed 1-2mm/y. To assess whether accumulation of strain is now taking place, a long-term GPS monitoring network is now developed to cover the area between the DSR and the Mediterranean, and attempt is made to initiate a joint monitoring program with Egypt, Cyprus and other Arab countries along the Red Sea-Dead Sea system.

Historic Seismicity Since instrumental record is very short, estimates of seismic slip and search for any past large earthquakes, require a study of historical records. Indeed, more than a dozen catalogues of historic seismicity in Israel and the Levant were published in the past hundred years. The catalogued information, converted into the probable values of magnitude, epicentral distance and intensity was used in derivation of characteristic seismicity and recurrence equations. Such equations, however, are reliable only when based on a systematic retrieval of contemporary felt-reports. In this

case however, secondary historical sources and previous catalogues were used rather than texts written shortly after any given event. Consequently, the present macroseismic data base for Israel and the Levant is neither complete nor accurate, and suffers from errors in identification, dating, location and extent of individual historic earthquakes. Analysis of primary historic materials reveals errors in evaluation of even most-widely cited major earthquakes. For example, the catastrophic M >7.2 earthquake of 749 CE, with death and destruction from Egypt to Iran, turned to be a conflation of two moderate events, several years apart and many hundreds of kilometers apart. Similarly, the 1546 CE earthquake, reputed to reflect a major rupture at the interplate boundary, had in fact a magnitude of only about 6, and affected only a part of central Israel. While the general sporadic nature of regional seismicity is evident, the time and space distribution is not and requires a systematic study of contemporary historic materials, particularly if possible occurrence of seismic gaps and seismic migration is to be considered.

Archeoseismicity Indications of past seismic damage were reported from numerous archeological sites across the Middle East. They provide a physical proof of ancient disasters, be it evidence of total destruction or abrupt abandonment of site, or be it an assemblage of features of structural damage (e.g. fractures and displacements; oriented collapse of buildings, walls and columns; tilts and distortion). Moreover, the sites show the type and quality of construction needed in assessment of historic vulnerability and site intensities. Caution is needed in identification of earthquake damage and its distinction from that caused either by man (e.g war or conflagration) or by deterioration and decay of buildings. Ongoing studies have shown that while features of damage are often misinterpreted (whether due to seismotectonic preconception or due to zest for archeological drama) and rarely document specific events, they are important in assessment of past seismic activity, and indispensable where written records are scarce.

Seismic sedimentology Some sedimentary features, particularly soft-sediment deformation and clastic dykes or blow outs are often used to document seismic events. Identical features, however, are known to form without any seismic intervention. The problem therefore is not to show that given structures may have been triggered by an earthquake, but to eliminate the other mechanisms.

In Israel, much of the search for sedimentological evidence of past seismicity has focused on lacustrine deposits of the Dead Sea and its 11,000-60,000 BP precursor, Lake Lisan. The fine aragonitic layers in the laminated sequences were attributed to massive precipitation triggered by pre-earthquake increase in carbonate rich discharge from Dead Sea springs. Excellent correlation was claimed between the frequency and magnitude of historic earthquakes in the past 2 Ky and the distribution and thickness of aragonite laminae in a 170 cm long core taken in 1940 at the sediment/water interface. An equally excellent correlation was claimed between historic seismicity in the past 2 Ky and the frequency and intensity of the spectacular features of soft sediment deformation and mass movement within the Lisan deposits. While both these correlations agree well with the seismotectonic model and at first appear entirely plausible, they not only contradict each other, but also rely on unwarraned and fallacious assumptions. Thus, even though the accumulating evidence (ongoing Ph.D. work of S.Belitzki) indicates widespread, largely vertical movements along the central segment of DSR in the past 10 Ky, quantitative correlation of sedimentary structures with seismicity remains unreliable.

A History of Past Earthquakes in the Puget Sound Area Recorded in Holocene Sediments from Lake Washington

Robert E. Karlin, Dept. of Geological Sciences, Mackay School of Mines, University of Nevada-Reno, Reno, NV
S. E. B. Abella, Dept. of Zoology, University of Washington, Seattle, WA

Large earthquakes can trigger slumping on the steep walls of lake basins and landslides in the drainage area, resulting in turbidite deposition in the lake and increased detrital flux from inlets. Holocene sediments in piston cores from Lake Washington contain a series of terrigenous layers that were episodically deposited in the lake. Sedimentological, geochemical, and paleomagnetic analyses on nine piston cores show that the detrital layers are temporally and areally correlatable, indicating basinwide disruptions. Susceptibility peaks are coincident with opaque layers on x-radiographs. The layers are relatively coarse grained and are characterized by high aluminosilicate abundances and low organic carbon and low biogenic silica contents. The thicknesses and geographic distributions of the layers suggest that they are not due to floods or delta destabilization. Sidescan swath imagery and subbottom profiling show that large slumps, subaqueous landslides, and debris flows are common along the margins of the lake.

A detailed chronology was established from 21 radiocarbon ages on 5 cores. A prominent turbidite was deposited about 1000-1100 years ago as the result of a large earthquake probably occurring on the Seattle Fault. Other events observed in the sediment record at 1500 to 1700, 2400 to 2500, and 2800 to 3200 years ago coincide with periods of landsliding previously inferred from the dating of drowned trees in the lake. The most recent event appears to have occurred ~300 to 500 years ago. More than 30 events are recorded in the last 12,000 years, and 21 disturbances have occurred since the time of deposition of the Mazama Ash about 7600 years ago. If all the events are due to earthquakes, the Puget Sound region has been subject to major shaking every 300 to 400 years. The strong intensities needed to trigger subaqueous slides could arise not just from local sources such as the Seattle Fault, but also from great subduction earthquakes occurring along the coast.

North Oso Canyon Fault - Candidate for San Andreas - Parallel Left Lateral Paleoquakes?

B. Keller, Metcalf & Eddy, Inc., 450 B Street, San Diego, California 92101

The east side of the intersection of geologic features parallel to the San Andreas fault and to the Garlock fault is characterized by faults and lineations on the southeast side of the Tehachapi Range. The eastern-most Garlock trend features are the NW - side-up Range Front fault and the SE-side-up Pinyon Hill fault, with a graben between them. The eastern-most San Andreas trend features are the North Oso Canyon fault and Dark Gully lineation, which truncates the Garlock trend faults and graben. Mapping for environmental studies by the author and Lindvall, Richter & Associates indicates that the North Oso Canyon fault is the geomorphically youngest appearing of these features. The North Oso Canyon fault intersects Oso Canyon, the southwestern-most major drainage of the Tehachapi Range, in two places. The lower intersection has an apparent left lateral offset of the stream channel of about 250 m. The channel wall is comprised of erodable Pleistocene terrace deposits, suggesting that this is a relatively young feature. Aerial photographs and surface reconnaisance allow features on the trend of the North Oso Canyon fault to be traced west to Castac Lake, on the main strand of the Garlock fault, and east to the modern desert alluvium of Antelope Valley. More detailed studies, such as trenching, have not been done.

Multiple Holocene Earthquakes Along the Reelfoot Fault, Central New Madrid Seismic Zone

K.I. Kelson, G.D. Simpson, C.C. Haraden, and W.R. Lettis,
William Lettis & Assoc., Inc., 1000 Broadway, Suite 612, Oakland, CA 94607
R.B. Van Arsdale, Dept. of Geological Sciences, Univ. of Memphis, Memphis, TN 38152
J.B. Harris, Kentucky Geological Survey, Univ. Kentucky, Lexington, KY 40506

Four shallow trenches, analysis of aerial photography, shallow-borehole transects, and a shallow seismic reflection survey across the Reelfoot scarp in northwestern Tennessee provide paleoseismologic data on the timing and style of Holocene near-surface deformation associated with the Reelfoot fault. This east-vergent reverse fault has abundant contemporary microseismicity and underlies the Lake County uplift, a low-amplitude anticline developed in Mississippi River Holocene meander-belt sediments. The Reelfoot scarp forms the eastern margin of the Lake County uplift. Recent analysis of aerial photography and field observations show that the scarp is at least 27 km long and extends from the southern end of Reelfoot Lake (which is impounded by the scarp), across the Mississippi River, and perhaps into southern Missouri west of the town of New Madrid. Surface deformation along the northern part of the fault during the m_b7.2 New Madrid earthquake of 23 Jan 1812 apparently crossed the Mississippi River and may have been responsible for historical accounts of "waterfalls" and "upstream flow" along the river immediately following the earthquake.

We conducted paleoseismologic research at two sites along the Reelfoot scarp. Trenches and shallow boreholes show that the scarp morphology mimics the style of near-surface deformation of fluvial strata. Deposits exposed in a trench across the central part of the scarp include prominent marker beds that define a 5-m-high east-facing fold. Although no major fault was encountered in this trench, the fold probably is related to movement on a buried west-dipping reverse fault. At a second site along the north-central part of the scarp, one trench exposed a low-angle shear plane at the base of the scarp. This feature dips westward beneath the scarp and coincides with the up-dip projection of a reverse fault interpreted from shallow seismic reflection data. However, vertical separation across this shear plane is minor; the majority of deformation along the scarp is accommodated via anticlinal folding rather than brittle faulting. We interpret that the scarp is a fault-propagation fold developed over the west-dipping reverse fault imaged on the shallow seismic reflection line.

Deposits exposed in several trenches provide evidence of multiple late Holocene earthquakes along the Reelfoot fault. A trench across the central part of the scarp exposed unweathered sand dikes interpreted as a product of the 1811-12 earthquakes, and colluvial deposits interpreted as a result of surficial deformation between about AD 1380 and 1450. Along the north-central part of the scarp, several trenches exposed a small linear graben present in the hanging wall above the west-dipping shear plane. In addition to down-dropped fluvial sediments, the graben is associated with fine- to medium-grained sand that was extruded onto an existing scarp during an AD 1811-12 event. Based on 19 radiocarbon age-estimates from sediments exposed in these trenches, we identify evidence of two and possibly three moderate to large earthquakes within the past 2200 years that pre-date the AD 1811-12 sequence. The time between the AD 1811-12 earthquakes and the penultimate event is about 400 years. The time between the penultimate and third-most-recent ruptures also is about 400 years, although several radiocarbon ages are equivocal. Fluvial sediments that on lap the base of the scarp probably post-date the 1812 earthquake and may record a temporary diversion of the Mississippi River to the south into Reelfoot Lake.

Based on several trench exposures at the two sites, each of the late Holocene earthquakes had a slightly different style of deformation. The third and possible fourth most-recent-events

produced a small graben a few tens of centimeters deep in the hanging wall of the reverse fault. This graben likely is related to minor extension in the crest of the fold. The penultimate event produced about 90 cm of throw in the graben, as well as folding along the up-dip projection of the reverse fault and uplift in the hanging wall. These relations suggest that graben development increased through time concomitant with growth of the anticline, or that the events are of different magnitude. Although there is abundant evidence of liquefaction in the trenches, there is no conclusive evidence that any of the pre-1811 events generated liquefaction-related deposits. Lastly, the 1811-12 events produced abundant liquefaction, prominent folding of fluvial strata along the scarp, and minor faulting in the graben. Notably, up-dip clockwise rotation of strike of faults bordering the graben illustrate a slight right-lateral component of slip during the 1811-12 deformation.

Repeated Holocene surficial deformation associated with the Lake County uplift also is shown by patterns of paleochannel migration within the Mississippi River meander belt. Soil survey data and cross-cutting relationships among abandoned channel-point bar complexes show that the Mississippi River was influenced by Holocene deformation of the Lake County uplift. During the early to middle Holocene, the river occupied a broad meander belt cut into Pleistocene fluvial and eolian deposits. During the middle to late Holocene, the river was confined along the northwestern part of the meander belt, perhaps as a result of growth of the southern part of the Lake County uplift. Progressively younger soils to the north across the central and northern part of the uplift provide evidence that deformation forced the river to the north. During the late Holocene, the river has remained at the northern edge of the meander belt where it traverses the uplift. Thus, soils-geomorphic relations support the interpretation that there have been multiple episodes of surficial deformation associated with the Lake County uplift, and that the uplift may be growing northward.

Research supported by the U.S. Geological Survey (USGS), Department of the Interior, under USGS award numbers 14-08-0001-G2116 and 1434-93-G-2293. The views and conclusions contained in this document are those of the authors and should not be interpreted as necessarily representing the official policies, either expressed or implied, of the U.S. Government.

Holocene Slip Rate and Recurrence of the Northern Calaveras Fault at Leyden Creek, Alameda County, California

Keith I. Kelson, Gary D. Simpson, William R. Lettis, Colleen C. Haraden, Chesley R. Williams, and Stephen C. Thompson

William Lettis & Associates, Inc. 1000 Broadway, Suite 612 Oakland, CA 94607

Information on geologic slip rate and earthquake recurrence is required to assess the potential for a large earthquake on the northern Calaveras fault, which traverses a heavily populated area in the eastern San Francisco Bay region. To obtain these data, we conducted paleoseismologic investigations at Leyden Creek, which crosses the fault 1.4 km north of Calaveras Reservoir. The well-defined fault trace at this site is marked by a prominent west-facing scarp and the juxtaposition of serpentine on the east against Cretaceous sandstone and siltstone on the west. At the site, five fluvial terraces are preserved on the western (upstream) side of the fault. On the eastern (downstream) side of the fault is a narrow bedrock canyon that constricts the modern valley and has constricted the latest Pleistocene and Holocene paleovalleys. Detailed field studies show that the margin of a buried bedrock valley margin trends nearly perpendicular to the fault and is offset 54 $\pm$ 5 m in a right-lateral sense. Based on radiocarbon ages for alluvial sediments pre-dating and post-dating this paleovalley margin, we estimate an age of 11 $\pm$ 1 ka for the valley margin and a Holocene slip rate of 5 $\pm$ 1 mm/yr for the fault at Leyden Creek.

Five trenches excavated across the fault provide information about the styles and timing of deformation at this site. Slickensides show that the most-recent sense of separation was predominantly lateral with a minor component of down-to-the-west separation, which is consistent with the west-facing fault scarp and the net slip vector derived from the offset valley margin. Multiple displaced scarp-derived colluvial deposits are interpreted as results of at least four, and possibly six, episodes of surface rupture within the past 2600 years. Twenty-one radiocarbon samples from scarp-derived colluvium and interfingered alluvial deposits suggest the following possible timing of surface-rupture earthquakes:

		Earthquake Timing	
Earthquake	possible range	preferred (approx.)	interval (approx., yr)
Z (or creep)	AD 1670 to 1861	AD 1861?	560?
Y	AD 1270 to 1380	AD 1300	300 to 600
X	AD 650 to 1050	AD 700 to 1000	300 to 600
W?	AD 400 to 430	AD 400	400
V	150 BC to AD 110	0 BC/AD	500 to 600
U	520 BC to 390 BC	600 to 500 BC	

These data suggest an average time interval between surface-rupture events of about 300 to 600 years, with a preferred interval of about 500 years. Of these possible events, the greatest amount of uncertainty lies in the timing of the most-recent event. The age estimate for the youngest faulted deposit (cal AD 1670 to 1950) encompasses the time of the only historical moderate to large event on northern Calaveras fault, the 1861 San Ramon Valley earthquake. Historical accounts of the 1861 earthquake document only 13 km of possible surface cracking, and intensity data suggest that the magnitude was only about M5.6 (Toppozada et al., 1981). If this event produced primary surface faulting at Leyden Creek, then rupture occurred along a 32-km-long section of the fault from near San Ramon almost to Calaveras Reservoir. There is little or

no scarp-derived colluvium at Leyden Creek directly associated with this possible event, which suggests that the amount of displacement at Leyden Creek was very small. Alternatively, the deformation observed in the trenches attributed to the 1861 earthquake may instead be a result of recent fault creep.

At Leyden Creek, scarp-derived colluvial deposits interpreted as products of individual surface ruptures consist of either large colluvial wedges 1.0 to 2.0 m thick, or small colluvial wedges and sheets less than 0.5 m thick. Because the time interval between ruptures has been fairly constant (500 $\pm$ 100 years) over the past 4 or 5 earthquake cycles, we postulate that the differences in colluvial-wedge thickness are related to amount of surface displacement, and thus to earthquake magnitude. If so, relatively large earthquakes occurred at about 0 AD/BC and about AD 700 to 1000, which yields a recurrence interval for large-magnitude earthquakes roughly twice that estimated for all of the events combined.

The Leyden Creek site lies adjacent to or within a 1.5- to 3.0-km-wide, 7-km-long releasing double bend at Calaveras Reservoir that may act as a rupture-segment boundary between the southern and northern sections of the Calaveras fault. Surface-rupture events at Leyden Creek may therefore reflect earthquakes along either the southern end of the northern Calaveras fault, or the northern end of the southern Calaveras fault. The smaller displacements observed at Leyden Creek may reflect the die-out of ruptures that occurred on sections of the fault to the north or south of Leyden Creek. The larger displacements may reflect earthquakes large enough to rupture through the double bend. These relations suggest the possibility of using trench stratigraphy to assess the relative frequency of moderate and large surface-rupture events.

The slip rate for the northern Calaveras fault and the recurrence interval between surface-rupture events interpreted from Leyden Creek are consistent with the results from a second site along the fault, located about 3 km to the north. This site, which is located where the fault crosses Welch Creek, lies north of the Calaveras Reservoir double bend. Although research at the Welch Creek site is preliminary and deposit age-control is limited, offset of a 5 to 13 ka fluvial terrace back-edge yields an estimated Holocene slip rate of between 1 and 7 mm/yr, with a preferred value of 4 to 6 mm/yr. In addition, multiple scarp-derived colluvial deposits support the interpretation that several surface ruptures occurred at Welch Creek within the past approximately 2800 years. Refinement of the slip rate and event chronology, and comparison with results from Leyden Creek, are pending further investigation.

Research supported by the U.S. Geological Survey (USGS), Department of the Interior, under USGS award numbers 14-08-0001-G1987, 1434-93-G-2338, and 1434-93-G-2339. The views and conclusions contained in this document are those of the authors and should not be interpreted as necessarily representing the official policies, either expressed or implied, of the U.S. Government.

Studies of Paleoseismology at Okushiri Island, Hokkaido, Northern Japan

Yoshihiro Kinugasa, Geological Survey of Japan
1-1-3 Tsukuba, Ibaraki, 305 Japan

A M=7.8 earthquake hit Okushiri Island, about 50km west off Hokkaido, northern Japan, on July 12, 1993, and caused massive damage to the island as well as Hokkaido.

Various kinds of post-earthquake studies have been carried out to reveal the characteristics of the earthquake and to estimate the repeatability of the similar event in the area. Difficulty is, however, the area used to be a kind of "frontier" in Japan, and almost no historical record exists on seismic activity before 19th century.

Crustal deformation associated with the July 12 event has been revealed by measuring the heights of tidal zone creatures along the coast of the island. The result shows the south of southwest ward down tilting with subsidence up to 80cm, unlikely east of southeast ward down tilting with long-term uplift of 1m/ka since the Last Inter-Glacial period.

A tremendous amount of twigs and logs blew up together with liquefied sand which has been observed at trench excavated on the western coast of the island of Hokkaido. The huge amount of these materials suggests inundation of a tsunami in the past, and C^{14} age (200 ± 80 y.B.P.) of these materials coincides well with the age of big tsunami hit this region in 1741 A.D.

The trench survey at Okushiri Island revealed one previous liquefaction episode. The age of it is sometime between 2,550 ± 90 y.B.P. and 1,970 ± 80 y.B.P.

Additional works such as detailed study on deformation of marine terraces and study on earthquake triggered turbidites on the ocean flower will be carried out soon.

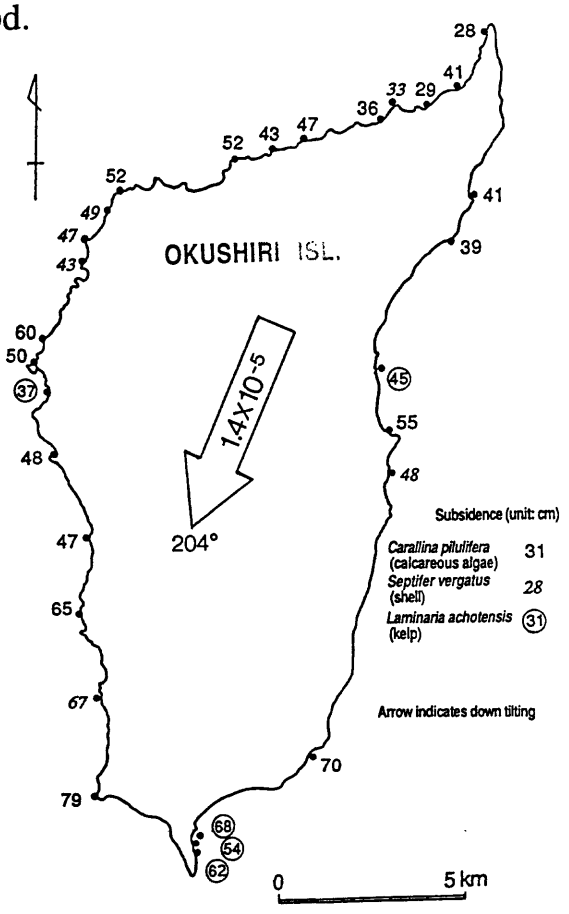

Crustal Movement by the Quake

Implications for the Nature of Rupture Segmentation from Paleoseismic Studies of Normal Faults, East-Central Idaho

Peter L.K. Knuepfer, Department of Geological Sciences, Binghamton University, Binghamton, NY 13902-6000

One of the most important reasons for paleoseismic investigations of active faults is to define the repeatability of surface-rupture patterns. In particular, we want to understand whether rupture patterns repeat in both length and displacement, and thus to what extent it is possible to infer future activity from past behavior. Furthermore, we wish to understand the relationship between *rupture segments*--sections of a long fault that rupture independently during a particular seismic cycle--and *structural segments*--the subdivisions of a fault that have distinct structural (as opposed to paleoseismic) histories. It is critical to approach these questions using all available tools--not only paleoseismic trenching, but also geomorphic studies of fault scarps to extend the trench results laterally away from the few sites available for detailed subsurface work.

The 1983 Borah Peak earthquake along the Lost River fault focused considerable attention on a group of active, normal-slip faults north of the Eastern Snake River Plain of Idaho. During the last decade, studies that have included reconnaissance and detailed mapping of fault scarps and distribution of Quaternary alluvial geomorphic surfaces, quantitative assessments of relative ages of fault scarps based on their morphology, and detailed trenching studies at several sites have attempted to assess the temporal and spatial characteristics of paleoseismicity along these faults. Thus the region has seen a wide variety of studies germane to understanding rupture segmentation. Normal faults in the Basin and Range province have properties that are advantageous in assessing paleoseismic and fault-behavior questions. Repeat times between surface ruptures are thousands of years long, thus providing enough time for accumulation of colluvial deposits at the base of fault scarps and development of soils in these deposits that facilitate recognition of individual ruptures as well as improve the likelihood of dating individual paleoseismic events (repeat times generally are longer than the resolution of dating techniques). Furthermore, the production of infrequent, relatively simple steps (fault scarps) formed in the landscape during surface rupture, in an arid area produces a clear geomorphic record of each event. I will discuss principal results from studies of the Lemhi and Lost River faults and then consider the broader implications of these studies for assessing both paleoseismic and possible future fault activity.

During the last eight years, my students and I, Woodward-Clyde Consultants, and Crone and Haller of the U.S. Geological Survey, have conducted a wide range of paleoseismic studies along the Lemhi fault (e.g., Hemphill-Haley and others report on trenching studies from the southern end of the fault elsewhere in this volume). We have modeled scarp degradation along the fault to define the extent of the youngest rupture events and assess whether they occurred on discrete sections of the fault. The scarp modeling suggests that, during the last seismic cycle, the fault broke in a series of independent ruptures, with each event occurring at a distinctly different time (within the resolution of scarp morphology) than that of adjacent rupture segments. At least six segments are defined, although scarp morphology alone did not clearly differentiate the two southernmost segments.

We next combined detailed mapping of late Quaternary alluvial-fan surfaces with fault-scarp mapping to see whether these rupture segments have persisted. For convenience, we have combined geomorphic surfaces into four broad age groups: Holocene (post-glacial), late Pinedale (mostly 15-30 ka), early Wisconsin (around 60-80 ka), and Bull Lake and older (greater than 130 ka). In some areas we are able to distinguish early (30-40 ka) from late (15-25 ka) Pinedale surfaces. Age assignments are approximate and are based on correlations of surfaces to the regional glacial chronology (following work of Pierce and Scott) and thicknesses of carbonate rinds on subsurface cobbles. The four northern segments of the Lemhi fault

(Ellis, Falls Creek, Big Gulch, and Warm Creek) have distinct histories--no rupture in post early Wisconsin time (although 12+ m on Bull Lake surfaces) on the Ellis segment; a relatively smooth increase in offset over time along the Falls Creek segment; approximately equal offsets of late Pinedale and early Wisconsin surfaces along the Big Gulch segment; and progressively increasing displacement with time along the Warm Creek segment. Scarps along the latter segment offset nearly all geomorphic surfaces, whereas the youngest surfaces offset along the Falls Creek and Big Gulch segments are of early Holocene age. The southern part of the fault is not easily subdivided based on surface offsets, although Bull Lake surfaces are offset less in the southernmost 20 km of the fault than in the 25 km immediately south of the Warm Creek segment. Overall, the geomorphic and mapping studies indicate that at least the northern two-thirds of the Lemhi fault displays persistent segmented behavior; significantly, the Big Gulch segment (and possibly the Ellis segment) displays a period of low activity followed by a period of more frequent ruptures.

We incorporated trenching along all of the segments (except the northernmost Ellis segment) to test our understanding of the segmentation history. Trenches along the Falls Creek, Big Gulch, and Warm Creek segments confirm our interpretation from geomorphic studies that each segment had distinctly different ruptures in the latest Quaternary: about 7 ka on the Falls Creek segment, in early post-glacial time on the Big Gulch segment, and in the late Holocene on the Warm Creek segment. Trenching along the southern part of the fault has been more critical in helping us better understand the complicated history of fault ruptures. A surface rupture event that occurred around 20 ka (within the limitations of thermoluminescence dating) apparently affected the entire southern third of the fault, yet other events apparently ruptured only short parts of the southern section. Furthermore, rupture events appear to be clustered at individual trench sites: two or three events occurred in the interval 17-24 ka, whereas no events are post-15 ka except at one trench site. Two of the trenches show evidence for long interseismic times prior to 25 ka, based on the degree of soil formation on faulted alluvial fan gravels and colluvial wedge deposits. Thus, surface ruptures were temporally clustered in the late Pinedale, and individual events ruptured different parts of the fault zone.

Studies along the Lost River fault have been less complete, although considerable paleoseismic information is available from this fault as well; much of the work is not yet published. Detailed mapping after the 1983 Borah Peak earthquake by Crone, Schwartz, and Vincent, among others, indicated that the rupture pattern along the Thousand Springs portion of the fault nearly duplicated that of the prior surface rupture event that occurred some 6-8 ka ago. Furthermore, Vincent has shown that the southern extent of the 1983 rupture mimicked that of the pre-1983 rupture. The 1983 rupture extended northward into a portion of what has been defined as the Warm Springs segment, although displacement was much smaller than along the Thousand Springs segment. Crone has interpreted this northern continuation as secondary faulting, but from a paleoseismic point of view it must be treated as part of the same primary rupture. The pre-1983 rupture on the Warm Springs segment produced greater displacement than the 1983 rupture (up to 10 times as much), and it may have occurred earlier than the pre-1983 rupture of the Thousand Springs segment (within the uncertainties of available dates). Thus, although the displacement pattern on the Thousand Springs segment appears to have repeated during the last two surface ruptures, as a whole the 1983 rupture pattern differs from that of the prior event(s) along the Thousand Springs and Warm Springs segments.

Schwartz reports evidence of temporal clustering of surface ruptures on the Mackay segment of the fault (next segment south of Thousand Springs). Pinedale and late Bull Lake (?) surfaces are displaced the same amount; he interprets this as evidence that the fault segment was quiescent between 140 ka and 30 ka or so, although age constraints are limited. Fault segments farther south also appear to indicate temporally clustered activity. My reinterpretation of a trench near Arco excavated by Malde is that at least two older events, closely spaced in time (due to limited soil formation within colluvial-wedge deposits) are separated from at least one younger event by a relatively long soil-forming interval within scarp-derived colluvial deposits. Recent trenching by Woodward-Clyde (Olig and others in this volume) substantiates this

interpretation, although they find that two events occurred subsequent to the buried soil. These new trench results provide strong evidence of clustered earthquake activity: two closely spaced ruptures are separated from at least two earlier ruptures (also closely spaced in time) by a much longer soil-forming interval indicating relative stability of the fault scarp and a longer interseismic time.

These groups of studies along the Lemhi and Lost River faults show that some *rupture segments* persist through repeated earthquake cycles. In some cases, rupture patterns repeat almost identically along some portions of the faults; more commonly, however, the amount of displacement may differ from one event to the next (although within a narrow range that is consistent with Schwartz and Coppersmith's notion of a characteristic earthquake). Yet, there are at least as many sections of the faults for which simple *rupture segments* cannot be defined: ruptures do not repeat over the same length for these sections, and ruptures can include two or more *structural segments*. The other very important result of these studies is a large body of evidence that large portions of these faults rupture episodically; i.e., there are clusters of ruptures on individual sections or segments of faults. Overall, I find it immensely encouraging that in some cases faults behave in a seemingly simple, straightforward, and repeatable fashion. The presence of temporal clustering, and the fact that many parts of the faults have overlapping, "non-characteristic" rupture patterns, point to the importance of thorough paleoseismic studies, especially on faults with low slip rates, before trying to use the principle of fault segmentation to assess earthquake hazards. Finally, these studies also illustrate the importance of incorporating information from the entire fault length rather than relying primarily on trenching of a few sites. Much of our insight into behavior of the Lemhi fault, especially its northern half, was gained by detailed mapping and geomorphic analysis of fault scarps. Similarly, the ability to recognize overlapping ruptures between the Thousand Springs and Mackay segments, and the pre-Pinedale behavior of the Mackay segment, on the Lost River fault is due primarily to detailed Quaternary and geomorphic mapping.

LARGE PRE-HISTORIC EARTHQUAKE(S) IN COASTAL SAN DIEGO COUNTY, CALIFORNIA

Gerry Kuhn, 2439 Sacada Circle, Carlsbad, CA
Mark R. Legg, ACTA Inc., 23430 Hawthorne Blvd. #300, Torrance, CA
Eric Frost, Department of Geological Sciences, San Diego State University, San Diego, CA

Paleoseismological investigations in California have typically focused on surface fault rupture of major, well-defined, known faults such as the San Andreas. Unknown or blind faults pose more difficult problems for paleoseismological investigation, requiring surrogate features that evidence past earthquakes. Offshore faults represent another common type of "blind" fault in that their submerged character precludes direct investigation (at least with present technology) of paleo-fault rupture. Like blind thrust faults in California and faults associated with major earthquakes, both historic and pre-historic, in the eastern U.S., offshore faults require identification of secondary ground failures, such as liquefaction-related features, in coastal or island areas as evidence of paleoearthquake occurrences.

We recently identified evidence of large-scale liquefaction near the City of Carlsbad, in north San Diego County, California. In general, the liquefaction is evident as abundant and widespread injection dikes of fine grained white sand, inferred to be ancient beach sands, into and through plastic clay-rich surficial deposits, recognized as an ancient intertidal lagoon. Review of aerial photography of the region, taken before the recent coastal development, showed areas covered by "Mima Mounds", that field inspection, both in graded railroad cuts and within an undeveloped open field in the area of the mounds, shows to be liquefaction "sand blow deposits" (terminology after Sieh, 1978). Along these exposures, subcircular to linear areas of clean white sand were identified, surrounded by brown to red-brown clay and silty-clay lagoonal deposits. At one location, tan sands have been injected both vertically and laterally through clay-rich deposits. Similar sand blow deposits have also been identified in the Camp Pendleton area near Las Pulgas Canyon.

The area covered by the sand blow features appears to correlate with the areal extent of ancient lagoons. In the Carlsbad area, these deposits cover about 10 km^2 and are now elevated more than 15 meters above sea level. At Camp Pendleton, these features cover more than 10 km^2 and are elevated in excess of 25 meters above sea level. The paleo-lagoons lie within what is inferred to be the Nestor (ca. 120 ka) or Bird Rock terrace (ca. 80 ka; Eisenberg, 1985; Lajoie and others, 1991), although fossils (*Donax gouldi* and *Mytilus sp.*) recovered from the lagoon and beach strata may show a younger age based upon excellent condition and preservation of color. (One fossil was also found in growth position). Root casts and immature soil profiles developed at the top of the lagoon deposit are likely Holocene in age, and a north to northeast-trending zone of faulting cuts this horizon in the vicinity of the liquefaction features.

Major known active faults in this area (Fig. 1) include the Newport-Inglewood-Rose Canyon fault zone (NIRC) which lies from 4-6 km offshore, west of the coastline where the liquefaction features are observed. North to northeast-trending branch and secondary fault zones extend onshore from the NIRC at several places including the Christianitos fault zone near San Onofre and an unnamed zone about 10 km north of Carlsbad (Fig. 1; Euge and others, 1973; Hannan, 1975). Abundant fracturing and faulting of the lagoon deposit, which offset the young soil horizons present in the area of the liquefaction features, is presumed to

represent a similar branch or secondary fault zone. Lineaments identified in aerial photographs and spot checks from field mapping suggest that this zone is continuous for at least 5-10 km onshore. Slickensides and geomorphic features indicate a significant component of lateral slip on these faults. At present, the fault responsible for the mainshock(s) associated with the sand blow deposits and surficial faulting, and the length of the primary fault rupture are unknown, but the large lateral extent (>25 km) and size of the sand blow deposits along the coast implies that an earthquake(s) of Magnitude 6.5 or greater was likely.

Although the age of faulting and liquefaction events remain to be precisely determined, the size of the sand blow deposits, area affected, and uplift of former intertidal deposits suggest that coastal uplift in this region may occur by infrequent, large earthquakes. Such events would be very destructive to coastal development in southern California both directly from the strong shaking and induced-ground failures, and also by the potential for major local tsunami generation. Based upon the character of faulting in the area, and especially the offshore faulting as imaged by multichannel seismic reflection profiles, we suggest that these large earthquakes occur along the deeper parts of the offshore Newport-Inglewood-Rose Canyon fault zone, which we infer to become listric, dipping more gently eastward at depth into the major regional detachment fault system. Such a fault geometry is consistent with interpretations in the Los Angeles Basin where the Compton-Los Alamitos trend is considered a major ramp structure of this detachment system (Shaw, 1993). Our postulated east-dipping fault structure is consistent with wide-angle seismic profiles obtained across the coastline in the Oceanside area (Y.G. Li, D. Okaya, and T. Henyey, personal communication, 1993). Youthful northwest-trending thrust faults, which cut the seafloor in places, have been identified near the base of the continental slope in this area (Crouch and Bachman, 1989; Fischer and others, 1991) and demonstrate the late Quaternary obliquely-convergent style of deformation in this region. This tectonic style provides a viable mechanism for the observed uplift of coastal marine terraces in this region and may represent a serious earthquake hazard.

REFERENCES

CDMG, 1992, Preliminary fault activity map of California: California Division of Mines & Geology *Open-File Report 92-03*, Scale 1:750,000.

Crouch, J.K., and S.B. Bachman, 1989, Exploration potential of the offshore Newport-Inglewood fault zone: *American Association of Petroleum Geologists Bulletin*, v. 73, p. 536.

Eisenberg, L.T., 1985, Pleistocene faults and marine terraces, northern San Diego County: *in* Abbott, P.L., ed., On the manner of deposition of the Eocene strata in northern San Diego County: San Diego Association of Geologists, p. 87-91, 3 plates.

Euge, K.M., C. Miller, and L. Palmer, 1973, Evidence for a possible onshore extension of the Rose Canyon fault in the vicinity of Oceanside, California [Abstract]: *Geological Society of America Bulletin*, v. 5, p. 39.

Fischer, P.J., and G.I. Mills, 1991, The offshore Newport-Inglewood-Rose Canyon fault zone, California: Structure, segmentation and tectonics, *in* Abbott, P.L., and W.J. Elliott, editors, Environmental perils, San Diego region: San Diego Association of Geologists guidebook, p. 17-36.

Hannan, D.L., 1975, Faulting in the Oceanside, Carlsbad and Vista areas, northern San Diego County, California: *in* Ross, A., and R.J. Dowlen, eds., Studies on the geology of Camp Pendleton and western San Diego County, California: San Diego Association of Geologists guidebook, p. 56-59.

Lajoie, K.R., D.J. Ponti, C.L. Powell, S.A. Mathieson, and A.M. Sarna-Wojcicki, 1991, Emergent marine strandlines and associated sediments, coastal California; A record of Quaternary sea-level fluctuations; vertical tectonic movements, climate changes, and coastal processes: *in* Decade of North American Geology, DNAG, Geological Society of America, v. K-2, chapter 7.

Legg, M.R., 1985, Geologic structure and tectonics of the inner continental borderland offshore northern Baja California, Mexico: Ph.D. dissertation, University of California, Santa Barbara, California, 410 p., 7 plates.

Shaw, J.H., 1993, Active blind-thrust faulting and strike-slip fault-bend folding in California: Ph.D. dissertation, Princeton University, Princeton, N.J., 216 p.

Sieh, K.E., 1978, Prehistoric large earthquakes produced by slip on the San Andreas fault at Pallett Creek, California: *Journal of Geophysical Research*, v. 83, p. 3907-3939.

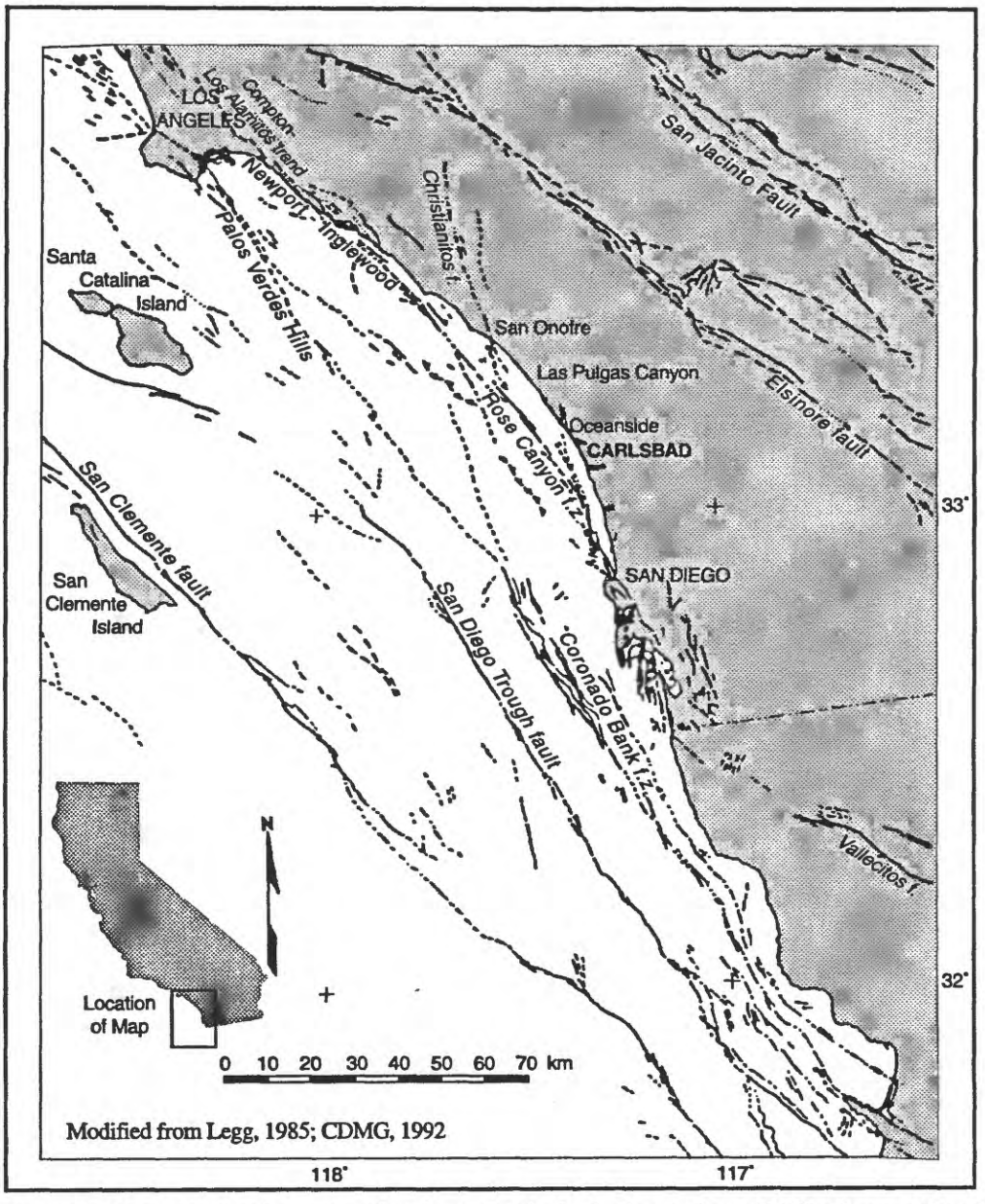

Figure 1. Map showing locations of major active faults in the southern California coastal and offshore area. Paleo-earthquake features discussed in this study are located in the vicinity of Carlsbad and Las Pulgas Canyon.

ACTIVE FAULT MAP OF TURKEY AND ITS IMPLICATION ON PALEOSEISMOLOGY

Ismail Kusçu, Fuat Saroglu and Ömer Emre
Geological Research Department, MTA, Ankara

An active fault map of Turkey (1:1,000,000) was published in late 1993 as the first step towards better understanding of the seismotectonics of Turkey and to update the seismic zonation for hazard mitigation. The authors of the map studied the entire territory of Turkey applying as even criteria as possible to attain objective recognition of active faults, through interpretation of aerial photographs and extensive field survey as well as thorough review of previous works concerning tectonics and seismicity. The map delineates all known active faults and epicenters of recent earthquakes.

In Turkey and neighboring regions in this century, 89 large earthquakes of magnitude larger than 5.9 occurred and most of them accompanied surface ruptures. There were 17 earthquakes with magnitude larger than 7.0. These earthquakes in this century claimed about 60,000 lives and destroyed some 400,000 buildings. The epicenters of the earthquakes of magnitude larger than 6 are usually coincide with active faults and often associate surface ruptures. As to the earthquakes with magnitude smaller than 6, identification of seismogenic fault is less clear, and the ones smaller than magnitude 5 usually do not show clear lineation along active faults.

Beside the well-known series of large earthquake on the North Anatolian fault, only some tens of earthquakes in this century were correlated with active faults. The number of 19 century and earlier earthquakes with known source area is not so many because of the lack of reliable documents. Through the preparation of the active fault map, the authors could suggest possible correlation of such earthquakes as 901 Erzurum (Ms=6.1), 1903 Patnos (Ms=7.0), 1905 Malatya (Ms=6.8), 1916 Tokat-Samsun(Ms=7.1), 1919 Soma (Ms=6.9), 1924 Horasan (Ms=6.8), and historical events of 1668 Anatolian-Caucasus and 1784 Erzincan to certain active faults.

Pre-1900 earthquake catalogues report historical earthquakes on the same faults and enable us to make a generalization on the recurrence interval of the earthquakes in Turkey: The earthquakes with magnitude larger than 7 occur every 300-400 years, while the earthquakes with magnitude 5 to 7 occur every 10 years.

Detailed mapping of the active faults and fault-breaks accompanied by recent earthquakes in Turkey brought better understanding of some characteristic features such as trace, geometry and the segmentation of the active faults. However, this mapping is still considered as a rather preliminary work. For instance, the classification of the faults according to activity and probability is not attained yet. This is mostly because of the poor accumulation of recent and Quaternary sediments and the limited distribution of young terrace surfaces as references for tectonic movements. In order to evaluate the activity of each fault, more detailed survey and Quaternary dates are needed.

Research on the active tectonics and the history of earthquakes in Turkey has been just initiated in late 1980s. This research is now bringing new information on recurrence intervals, slip-rate, and slip-per-event. The active fault map will give the foundation of the paleoseismology in Turkey and will take quantitative data in order to fulfill its objectives.

Evidence of early Holocene earthquakes in northern Fennoscandia

Robert Lagerbäck, Geological Survey of Sweden, Box 670, S-751 28 Uppsala, Sweden

The vanishing of the last inland ice sheet in northern Fennoscandia was accompanied by extensive faulting and violent earthquakes. Morphologically prominent fault scarps, interpreted as post- or late-glacial, are described from the northern parts of Finland (Kujansuu 1964), Sweden (Lundqvist & Lagerbäck 1976; Lagerbäck 1979, 1990) and Norway (Olesen 1984, 1988). The scarps, typically some 5-10 metres high, are forming fault lines extending up to about 150 km (Fig. 1). Attempts have been made to date fault displacement relative to the glacial and postglacial stratigraphy by trenching across some of the scarps in northern Sweden and it is shown that the faulting occurred soon after the local deglaciation some 9000 years ago.

The dimensions of the features suggest that the faulting was associated with intense seismicity and seismically induced phenomena are frequently found in the region. Numerous landslides, dating from the early postglacial period, occur in the vicinity of the faults (Kujansuu 1972; Lagerbäck 1990). The landslides occur in gentle slopes and are developed in glacial till of sandy composition, not expected to slide or flow under normal conditions.

Internal deformational structures, interpreted to be seismically induced, were also found to be very common in wide areas below the highest coastline in northern Sweden (Lagerbäck 1990, 1991). These seismites are mainly developed in sandy or silty sediments (Fig. 2) but are also recorded in glacial till (Fig. 3). Extensive deformation proved to be very common in sediments deposited, or already in existence, during the deglaciation phase or shortly after whilst almost no deformation was found in younger deposits. This agrees fully with the concept of a short-lived early Holocene co-seismic faulting. The investigations have demonstrated a wide variety of seismically induced sediment deformations which aims to serve as reference material when studying possible seismites in other areas.

With regard to field methods, it is concluded that trenching across fault scarps constitutes a useful tool for assessing the timing of fault movements in glaciated areas. An active search for seismites has proved fruitful when concentrated on deposits and environments favourable for the development of such structures.

References

Kujansuu, R. 1964. Nuorista siiroksista Lapissa. Summary: Recent faults in Lapland. *Geologi 16,* 30-36.

----1972. On landslides in Finnish Lapland. *Geological Survey of Finland. Bulletin 256.* 1-22.

Lagerbäck, R. 1979. Neotectonic structures in northern Sweden. *Geologiska Föreningens i Stockholm Förhandlingar 100,* 263-269.

----1990. Late Quaternary faulting and paleoseismicity in northern Fennoscandia, with particular reference to the Lansjärv area, northern Sweden. *Geologiska Föreningens i Stockholm Förhandlingar 112,* 333-354.

----1991. *Seismically deformed sediments in the Lansjärv area, Northern Sweden.* SKB Technical Report 91-17. Swedish Nuclear Fuel and Waste Management Co., Stockholm.

Lundqvist, J. & Lagerbäck, R. 1976. The Pärve Fault: A late-glacial fault in the Precambrian of Swedish Lapland. *Geologiska Föreningens i Stockholm Förhandlingar 98,* 45-51.

Olesen, O. 1984. *Sen-/postglaciale forkastninger ved MASI, Finnmark.* Norges Geologiske Undersökelse, Rapport 84.171.

----1988. The Stuoragurra Fault, evidence of neotectonics in the Precambrian of Finnmark, northern Norway. *Norsk Geologisk Tidskrift 68,* 107-118.

Fig. 1. Location of landslides developed in glacial till (black dots) and fault scarps interpreted as of late- or postglacial age in northern Fennoscandia. Barbs along fault lines are turned towards the lower block. Screening shows areas below the highest coastline, that is, areas covered by water shortly after deglaciation some 9000 years ago and thus favourable for development of earthquake induced sediment deformations in connection with faulting. (From Lagerbäck 1990, slightly modified. Additional information about landslides in northern Norway is obtained from L. Olsen, Geological Survey of Norway, *pers. comm.).*

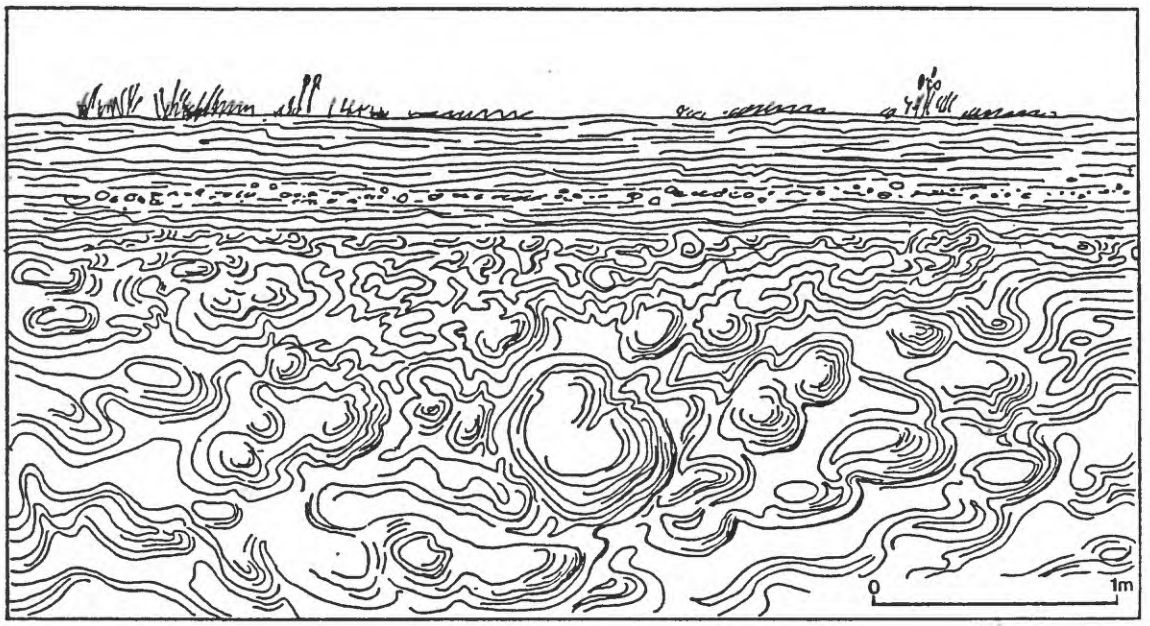

Fig 2. Strongly deformed sandy and silty sediments in the Lansjärv area, northern Sweden. The layering in the upper part of the section is undisturbed, demonstrating that the distortion took place before the locality was raised above the sea and the sedimentation ceased. The distortions are interpreted as being caused by seismically induced liquefaction, compaction and dewatering during the build-up of the sequence.

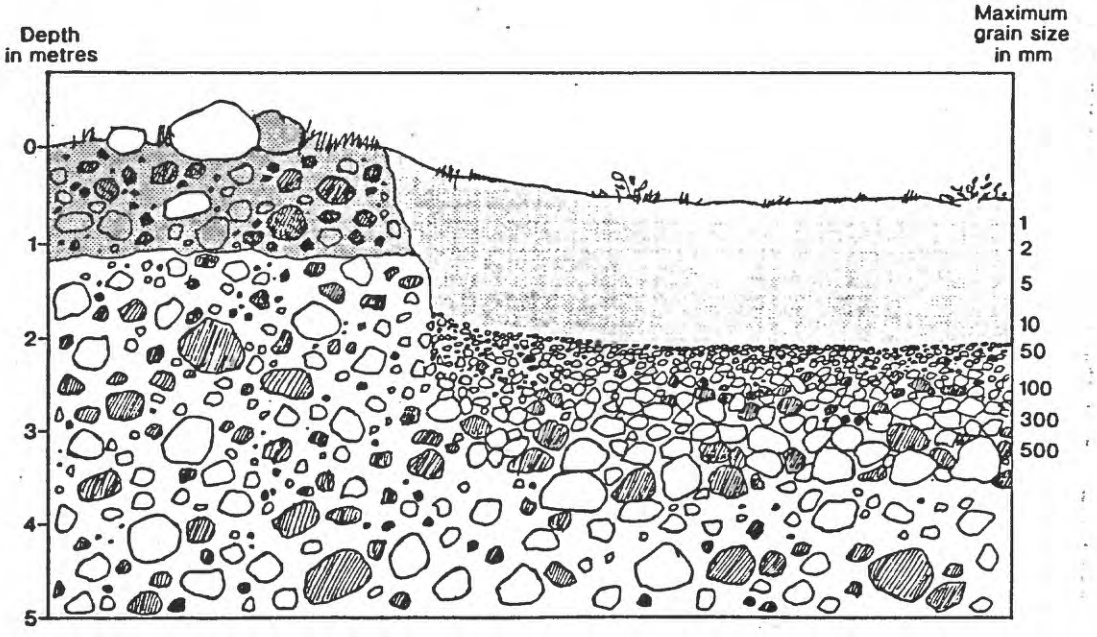

Fig. 3. Typical section through "graded till" in the Lansjärv area, northern Sweden. The undeformed stratigraphy, to the left, contains a 1.2 m thick brownish sandy till resting on a thick grey sandy till. To the right, the primary stratigraphy is completely destroyed to a depth of about 4 m. The size of clasts successively increases downwards and the biggest boulders are found at the bottom. The disturbed sequence is extremely compact and the deformations occur as subcircular patches, often tenth of metres across, and are traced by the total absence of stones and boulders in the subsided ground surface. The grading of the glacial tills is interpreted to be seismically induced and has so far been found only near to the faults.

Holocene Slip Rate of the Hayward Fault at Union City, California

James J. Lienkaemper (U.S. Geological Survey, Mailstop 977, 345 Middlefield Rd., Menlo Park, CA 94025)
Glenn Borchardt (Soil Tectonics, P.O. Box 5335, Berkeley, CA 94705)

Measured offsets of well-dated alluvial fan deposits near the Masonic Home in Union City, constrain Holocene slip rate of the Hayward fault between 7 and 9 mm/yr. Our best minimum geologic slip rate over the past 8.3 ± 0.1 ka (*i.e.*, 8300 yr) is ≥8.0 ± 0.6 mm/yr. A steep stream channel cut into bedrock flows out of the East Bay Hills, crosses the fault, and deposits its load on an alluvial fan. We cut two 5-m deep, fault-parallel trenches in 1989 and 1990, at distances of 20 and 30 m away from the main fault through the crest of the fan. These trench walls reveal a series of nested channel fills. These channels had cut into old surfaces that are indicated by paleosols developed on the flood silts. We distinguished many channel fills by their shape, clast size, elevation and relation to paleosols and can match them on the detailed logs of both trenches.

Two distinct episodes of fan development occurred during the Holocene. Reconstructing the apex positions of these units indicates that about 40 ± 6 m and 66 ± 5 m of fault slip has occurred since their inceptions at about 4.7 ± 0.3 ka, and 8.3 ± 0.1 ka, respectively. Figure 1 illustrates these reconstructions for mid-Holocene apex E (stars) and early Holocene apex G (solid circles). We lowered the age and age uncertainty of the younger unit from earlier reports based on new multiple radiocarbon dates. The 4.7 ka slip rate of 8.5 ± 1.4 mm/yr is not significantly different at 95% confidence from the 8.3 ka slip rate of 8.0 ± 0.8 mm/yr. Future work may improve the slip rate of the 4.7 ka unit. Rates from two late Pleistocene fan units at this site fall between 7 and 10 mm/yr, but need much more work to be as accurate as the two Holocene rates. Current values show no distinguishable changes in slip rate in the last 15 ka.

Because historic surface creep rate near Union City is 5 mm/yr, the larger, ≥8 mm/yr, Holocene slip rate implies that strain is now accumulating on a locked zone at depth. The ≥8 mm/yr rate seems minimal, because earlier trenching evidence implies that some unknown amount of fault deformation occurs outside of the narrow fault zone assumed in measuring slip. *Lienkaemper and Borchardt* [this volume] suggest that the fast creep rate of 9 mm/yr, measured near the southern end of the Hayward fault, may underestimate deep slip rate, because 1868 surface slip occurred there in addition to the continuing fast creep. If the historic deep slip rate equals the long-term rate, then the 9 mm/yr fast creep rate reflects the minimum seismic loading rate of the Hayward fault better than the ≥8 mm/yr Holocene rates do.

Figure 1.

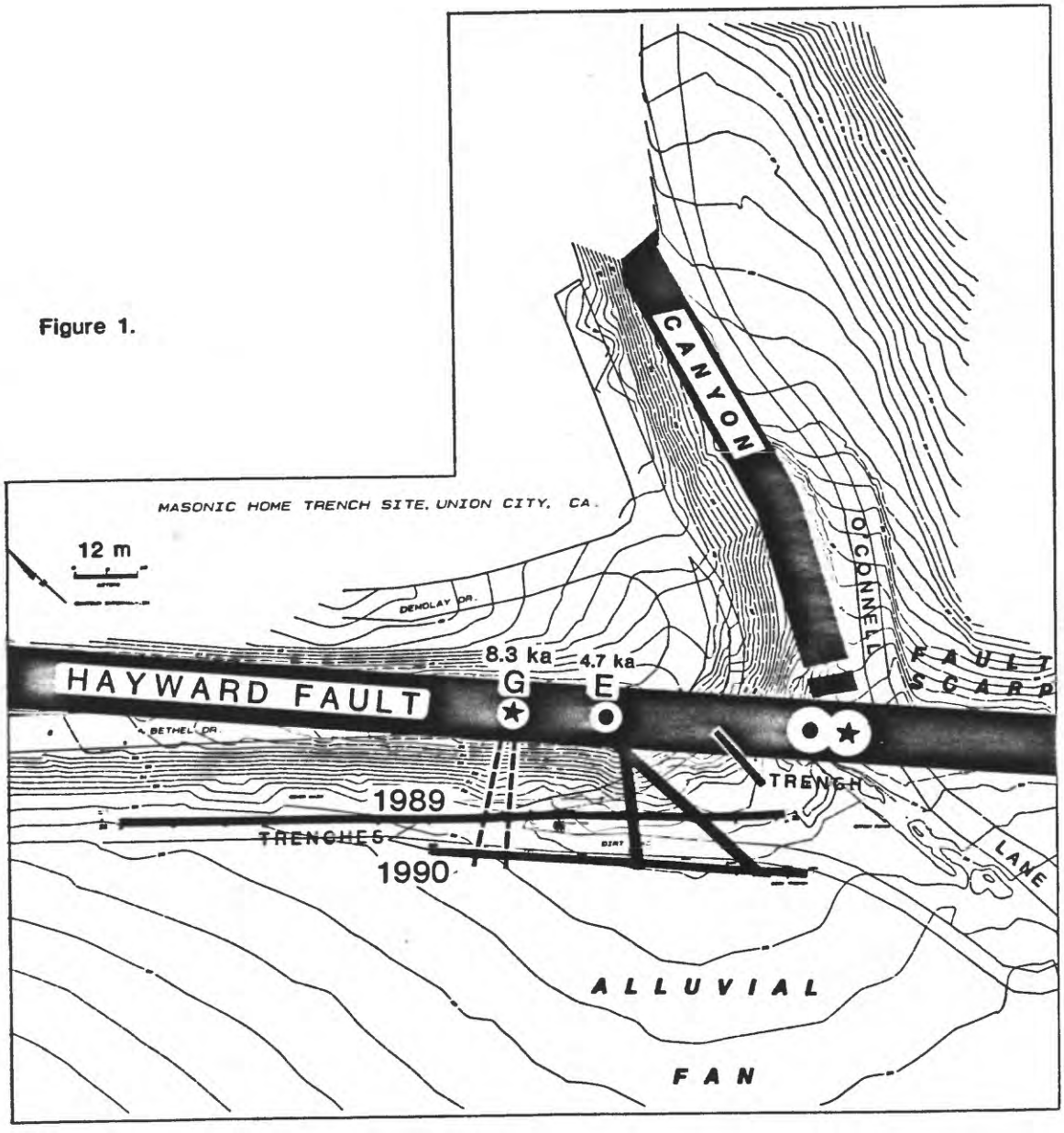
MASONIC HOME TRENCH SITE, UNION CITY, CA.
12 m
DEMOLAY DR.
CANYON
O'CONNELL
FAULT SCARP
8.3 ka
4.7 ka
G
E
HAYWARD FAULT
BETHEL DR.
TRENCH
1989
TRENCHES
1990
DIRT
LANE
ALLUVIAL
FAN

DIGITAL MAP AND COMPUTER DATABASE OF MAJOR ACTIVE FAULTS (AND FOLDS), WESTERN HEMISPHERE

M.N. Machette, K.M. Haller, and R.L. Dart
U.S. Geological Survey
Branch of Earthquake and Landslide Hazards
MS 966, P.O. Box 25046
Denver, CO 80225

As part of the International Lithosphere Program's (ILP) Project II-2 "World Map of Major Active Faults," we are compiling a series of digital maps for the Western Hemisphere that will show the location, age, and activity rate of major earthquake-related features such as faults and fault-related folds and a relational computer database that describes these features. The World Map project is a key part of the new Global Seismic Hazards Assessment Program (ILP Project II-0) for the International Decade for Natural Hazard Disaster Reduction and is closely associated with ILP Project II-3 "Paleoseismcity of the late Holocene" (R.S. Yeats, Chairman).

The project is centered around three maps that are being compiled by regional and national coordinators. The South American map was intiated at a February 1993 meeting in Quito, Ecuador, and is proceeding at a slow pace, whereas the Central American and Caribbean maps are still being organized under Paul Mann's direction. The North American map is being coordinated by Michael Machette (United States), John Adams (Canada), and Fernado Ortega (Mexico). The United States part of the project was started in 1993 and, with the cooperation of state and regional participants, should be completed by the end of 1996. As an example of ILP Project II-2, this poster session will focus on our efforts to create a digital map and computer database of active faults in the United States.

THE PROJECT

No modern digital map or catalog of active faults exists for the United States, even though understanding the extent and character of active and older Quaternary faults is a critical element of seismic-hazards analysis. Although basic fault data are available for all States, the degree of completeness of this data varies greatly. There are recent map compilations for a few States and data for California, Nevada, and Utah are now in digital form; however, a comprehensive fault database is only available for Utah. Thus, a considerable amount of compilation is required to insure that national products are up to date and provide fairly uniform coverage.

Th United States map project is being funded by the National Earthquake Hazards Reduction Program of the U.S. Geological Survey. The primary elements of the project are general supervision and interpretation of geologic and tectonic information (Michael N. Machette, Project Chief), data compilation and entry for fault catalog (all personnel), database design and management (Kathleen M. Haller), and digitization and manipulation of data in ARC/INFO† (Richard L. Dart). In addition, we are relying on help from knowledgeable local and regional experts in Quaternary faulting, neotectonics, paleoseismology, and seismology in the United States.

STRATEGY

Given the limited time to produce the map and database (three years at the most), the project must be limited to compilation of only those elements needed for ILP's Global Seismic Hazards Assessment Program. Those elements focus on characterizing earthquake source zones in terms of length of rupture, amount of displacment, recurrence intervals, slip rates, etc. We anticipate that the project will identify shortcomings of current research on Quaternary faulting, in terms of quantity, quality, scope, and regional coverage, and that it will promote new efforts to collect paleoseismological data in neglected areas.

In some cases, seismicity has been used to define some potentially active faults. Recent large-magnitude earthquakes (such as the 1959 Hebgen Lake, 1983 Borah Peak, and 1992 Landers earthquakes) have shown, however, that much of the faulting away from active plate margins occurs along faults that have no significant pre-event seismicity, and only a fraction of active faults are characterized by ongoing

seismicity (*e.g.*, the San Andreas). Thus, our 100-150 yr historic record of seismicity is probably not a reliable indicator of faults that may be potentially active. Throughout the Western United States, Quaternary faults commonly have low slip rates (<1 mm/yr) and recurrence intervals of 10^4-10^5 yr. Thus, for this project we define active faults as those having Holocene (<10 ka) and late Pleistocene (10-130 ka) movement.

THE MAP

The map of the United States will be compiled on topographic base maps at 1:250,000 scale and digitized and edited using ARC/INFO† GIS software on a Sun† workstation. This scale will allow eventual output as State maps (1:500,000-1:750,000 scale) or regional maps (1:1,000,000-1:2,500,000 scale) without serious loss of information. The base maps are widely available and have been used for many of the state compilations of Quaternary faulting in the Western United States (*e.g.*, Utah and Nevada). Most previous regional compilations have been at a scale of 1:2,500,000, which is inadequate for digital mapping and can only describe the longer (>50 km) faults in a region. In addition to fault location and style, the maps will show time of most recent movement and slip rate (a measure of fault activity). Five age categories of Quaternary faults will be shown in color on the map:

1) Historic (past 150-250 yr in U.S. and Canada and past 400-500 yr in Mexico),
2) Holocene and latest Pleistocene (<15 ka),
3) Late Quaternary (<130 ka),
4) Late and middle Quaternary (<750 ka), and
5) Quaternary (<1.6 Ma).

These age categories allow some flexibility among regions as required by differing levels of investigation and abilities to date prehistoric faulting. Sense of slip will be shown by conventional map symbols. Three ranges of slip rate, depicted by line thickness, will be used to differentiate rates of activity:

A) >5 mm/yr—Plate-boundary and associated faults and subduction zones (San Andreas fault; Cascadia; and Mexico subduction zones),
B) 1-5 mm/yr—Lesser strike-slip (Garlock fault) and major extensional faults (Wasatch fault), and
C) <1 mm/yr—Most extensional and intraplate faults.

THE DATABASE

The purpose of a computer database is to provide a large quantity of data that can be accessed quickly and efficiently using a variety of parameters. For this database, we anticipate that the user would want search-and-retrieve capabilities on a personal computer. The user may want to sort the data by such parameters as region (by 1°x 2° cell), time of most recent movement (one of five categories), slip rate (one of three categories), sense of movement, or by several of these parameters.

We intend to build our database using Microsoft Corporation's FoxPro†, a relational database program that has recently been greatly enhanced. The process starts with data acquisition and synthesis. First, the compiler must determine if the structure is (1) a simple fault, (2) a fault having sections (intermediate complexity), or (3) a segmented fault. Then using the appropriate form, the compiler tabulates information about the fault's parameters. The forms were designed in Microsoft Word† for the Macintosh†, but they also are available in WordPerfect† and other common word processors and on a variety of platforms (DOS†, Windows†, SUN†).

We import the data in tab-delimited form to FoxPro†. The basic fields are restricted to 254 characters, but the note option is available for more extensive comments. Each of the fields are potential search objects. The database allows us to custom format the reporting of data and to collapse unused fields or notes.

The database will be released in several forms. Paper-copy catalogs can be published for individual States, provinces, and regions as USGS- or State-sponsored reports. The databases will be available for Windows† and Macintosh† computers on diskette and (or) CD-ROM with a run-time version of FoxPro†, which will allow the user to browse, sort, and print the data; however, the data cannot be altered under the run-time version of the database program.

† Use of brand or trade names does not signify endorsement by the USGS or DOI.

A 50,000 Year Continuous Record of Earthquakes and Surface Ruptures in the Lisan Formation, the Dead Sea Graben

Shmuel Marco[1,2], Amotz Agnon[1], Mordechai Stein[1], Hagai Ron[2]
1. Department of Geology, the Hebrew University, Jerusalem 91904, Israel,
2. Institute for Petroleum Research and Geophysics, Holon, Israel.

A 50,000 year long paleoseismic record that includes synsedimentary faults with surface ruptures is recovered in the lacustrine Late Pleistocene Lisan Formation. The record is ten-fold longer than the archeological and historical one. The Lisan Formation stands out with excellent preservation of finely laminated varves which were deposited continuously, with extensive correlatable outcrops overlying 220 km of the Dead Sea Transform, and with unprecedented U-series dating by Thermal Ionization Mass Spectrometry (TIMS).

Lake Lisan occupied part of the Dead Sea Transform tectonic depression from 70,000 to 18,000 years ago when it shrank to form the modern Dead Sea. The paleoseismic record in the Lisan Formation includes two features: synsedimentary surface ruptures and 'mix layers'. Surface ruptures with vertical displacements up to 2 m are found in a fault zone on the Dead Sea shore, 2 km east of Massada, where archeological evidence and historical accounts indicate strong earthquake damage. The faults are normal and reflect a dominant E-W extension. Undisturbed layers unconformably overlie the faults.

The faults are associated with 'mix layers' which indicate that the ground motion was strong enough to fluidize and re-suspend the sediments at the bottom of Lake Lisan. Detailed sections across the faults show that a 'mix layer' formed at the water-sediment interface whenever a rupture occurred. The mix layers are considerably thicker on the down-thrown block.

In contrast to the common Lisan facies of alternating laminated evaporitic and detritic seasonal varves, the mix layers exhibit unusual thickness, structure, and fabric: they are locally up to one meter thick and consist of non layered mixture of fine grained matrix and tabular fragments of varves of various size (several millimeters to centimeters). In places, grain-supported texture shows a gradual upward transition to a matrix-supported texture. No imbrication or other transport indicators were found. The lower contact of the mix layers is often irregular, protruded by fragments from the underlying layers. Mushroom-shape diapirs originating in the underlying varve layers penetrate some of the mix layers. The mix layers frequently overlie folded varve layers. The folds are asymmetrical, recumbent, with up to 30 cm wavelength, and in places box-type folds, usually overlying a décollement surface. Each mix layer is restricted to a single stratigraphic horizon separated by undeformed beds and correlatable over large area. In several occurrences we found extension fissures that extend only downward from mix layers. These fissures are several centimeters wide, filled with material from the mix layer, and show no vertical displacement.

Similar mix layers have been described and used to identify paleoseismic events, [e.g. *Doig,* 1991, *Scott and Price,* 1988, *Sims,* 1973]. The association of the deformations with strong earthquakes is also backed by similar phenomena observed in recent events [*Allen,* 1986, *Sims,* 1975]. For example, re-suspension of sediments was directly observed in lakes less than 10 km from the epicenter of the 1935 Témiskaming, Canada, M6.3 earthquake. Independently, piston cores recovered a 20 cm thick chaotic layer, composed of black gyttja and tabular fragments of a previously formed silt layer [*Doig, R.,* 1991].

The mix layers in the Lisan Formation are therefore interpreted as layers of formerly regular, planar, continuous varves that ruptured and partly re-suspended by strong shaking. During an earthquake, the varves at the top of the sediment were brecciated, partly re-suspended and formed a mix layer when settled. At the same time the more cohesive varves below were folded. The décollement surface formed just above the lithified varves that did not deform. Slope failure as an alternative origin of the mix layers seems unlikely because they lie horizontally and in many cases it is possible to "restore" the fragments within the mix layers to their origin in the underlying layers, indicating vanishingly small lateral transport. Diapirs that intrude mix layers

and fissures filled with mix material formed close after the mix event. The tops of the layers correspond to the stratigraphic level of the events.

Mix layers are found throughout the Lisan Formation also away from observed faults. In three detailed columnar sections, one near Massada and two in the Peratzim Valley, we found about 30 mix layers. The average intervals between their tops are 101 cm in section M1, 130 cm in PZ1,and 109 cm in section PZ2. The thickness of the mix layers and the intervals between them follow a log linear frequency-thickness and frequency-interval relationship. The significance of the mix layer thickness is as yet poorly understood. It may reflect a combined effect of the acceleration, velocity, duration, and amplitude of the ground motion, as well as bottom sediment conditions. On the other hand, the distance between the mix layers can be readily transformed to time intervals, provided sedimentation rates are known.

Ages were determined by measuring Th and U isotopic compositions of aragonite varves by TIMS. This technique achieves analytical precision of 1-2% and improves the resolution of the U–series ages by a factor of 5 to 10 over the conventional α-counting method [*Stein et al.*, 1992]. Our measurements show an average sedimentation rate of about 0.8 mm/year. This gives an average recurrence period of 1400 years of strong earthquakes in the Dead Sea graben. For comparison, the mean recurrence period of M≈7.3 earthquakes along the segment of the Arava-Dead Sea-Jordan river during the 4000 year historic record is estimated at 1500 years [*Ben-Menahem*, 1991].

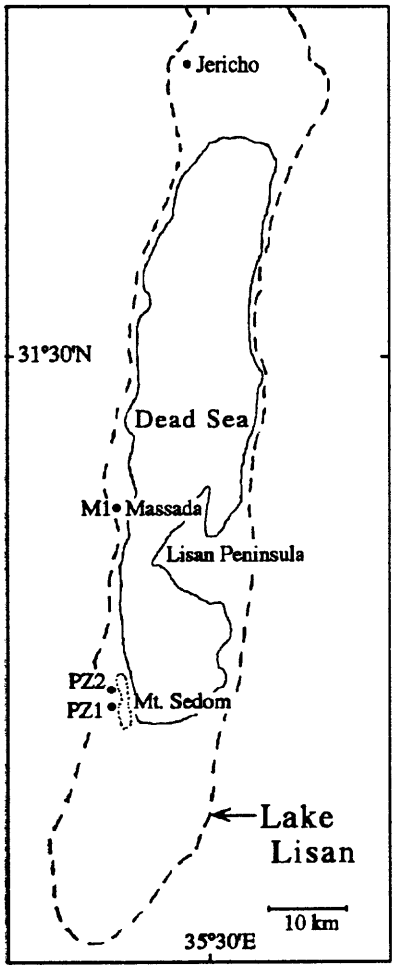

Location map.

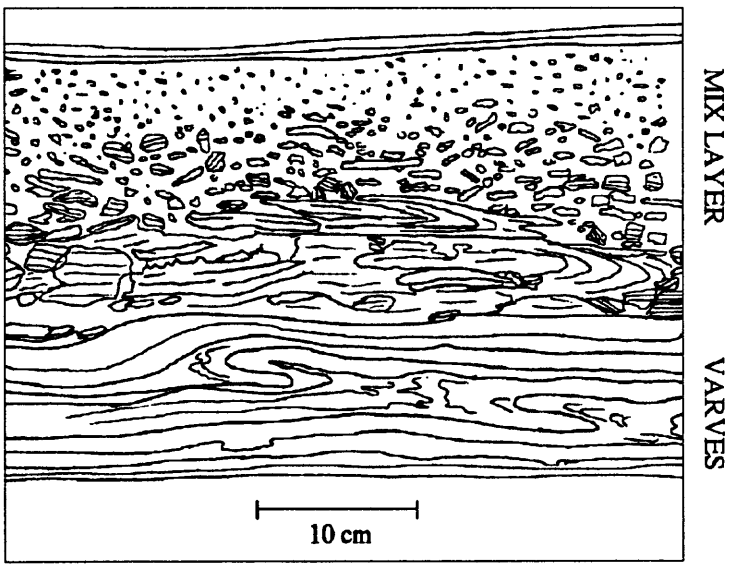

A mix layer, traced from a photograph.

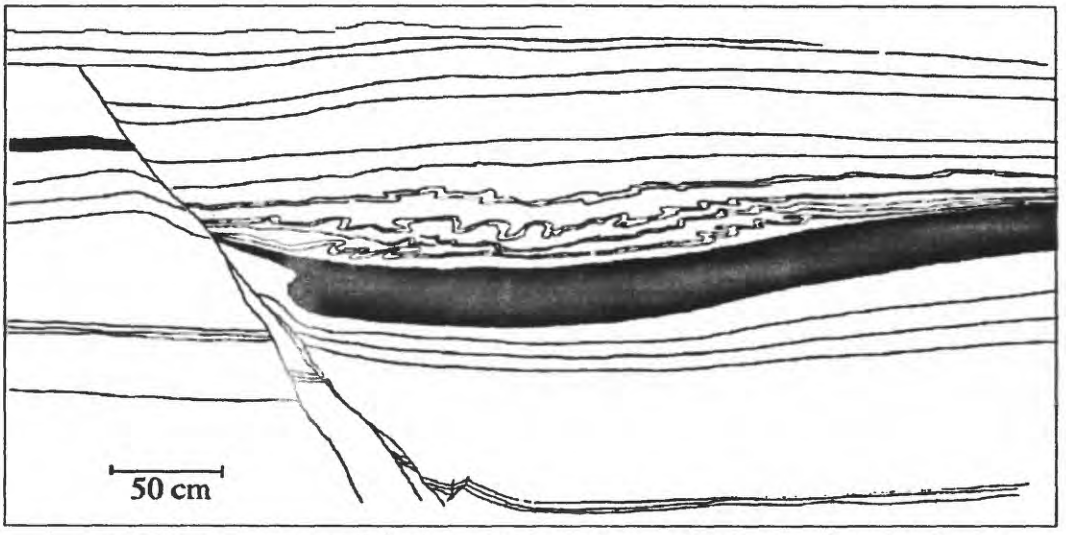

A synsedimentary normal fault near Massada overlain by undisturbed layers. A mix layer is painted black. Drawn from a photograph.

References

Allen, C. R. *Seismological and paleoseismological techniques of research in active tectonics.* In: Active Tectonics. Edited by R. E. Wallace, c., 148-154, National Academy Press, Washington, 1986.

Ben-Menahem, A., Four thousand years of seismicity along the Dead Sea rift, *J. Geophys. Res. 96 (B12),* 20,195-20,216, 1991.

Doig, R., Effects of strong seismic shaking in lake sediments, and earthquake recurrence interval, Témiscaming, Quebec, *Canadian Journal of Earth Sciences 28 (9),* 1349-1352, 1991.

Scott, B., and S. Price, Earthquake-induced structures in young sediments, *Tectonophysics 147* 165-170, 1988.

Sims, J. D., Earthquake-induced structures in sediments of the Van Norman Lake, California, *Science 1/2* 161-163, 1973.

Sims, J. D., Determining earthquake recurrence intervals from deformational structures in young lacustrine sediments, *Tectonophysics 29* 144-152, 1975.

Stein, M., S. L. Goldstein, H. Ron, and S. Marco, Precise TIMS ^{230}Th - ^{234}U ages and magnetostratigraphy of Lake Lisan sediments (paleo Dead Sea), *AGU Spring Meeting, Montreal,* 1992.

Holocene Paleoseismicity and Temporal Clustering on the Wasatch Fault Zone, Utah, USA

J.P. McCalpin, GEO-HAZ Consulting, Inc., Estes Park, Colorado
S.P. Nishenko, U.S. Geological Survey, Branch of Seismology, Denver, Colorado

Numerical age estimates for Holocene paleoearthquakes on the Wasatch fault zone (WFZ) have been made since the late 1970s, based primarily on samples collected from fault-zone trenches. Previous compilations of paleoseismicity during the past 6 ka (e.g. Machette et al, 1992) emphasized the uncertainties in numerical age estimates, and defined broad (500-1000 years) age ranges within which faulting probably occurred. For this study, however, discrete ages on paleoearthquakes were required for statistical tests of recurrence patterns. While we fully appreciate the many sources of uncertainty in the existing suite of numerical ages, we have nonetheless attempted to reduce these uncertainties to a minimum by treating sample ages in a systematic manner. Doing this required: 1) formalizing the conceptual model that relates the raw age of the sample to the date of the paleoearthquake, 2) reexamining the stratigraphic setting of all numerical ages, and 3) retrieving the original raw laboratory ages for all dated samples so uniform corrections to all ages could be applied.

In a typical fault-zone exposure on the WFZ, the unconformity between scarp-derived colluvium and the pre-faulting soil constitutes an "event horizon" that records the occurrence of a paleoearthquake. Because this unconformity is created in a time-transgressive manner as laterally-accreting colluvium buries the pre-faulting soil, the age of the unconformity is closest to the age of the earthquake nearest to the fault plane. It is therefore not surprising that ca. 50% of the radiocarbon ages cited in the compilation of Machette et al (1992, Appendix) were collected from the upper part of buried, weakly-organic soils immediately under the event horizon less than 3-5 m from the fault. The balance of the dated samples represent (in order of poorer constraints on paleoearthquake age), disseminated organics in distal colluvium; organics in alluvium, debris-flow deposits, and sag pond silts that are interbedded with scarp-derived colluvium; charcoal from the overlying debris wedge; and the lower parts of thick organic soils developed in post-faulting colluvium.

As of 1988 47 trenches and 4 natural exposures had been logged and sampled at 20 sites on 6 segments of the WFZ (Machette et al, 1992). Subsequently 14 additional trenches were excavated on the Brigham City segment (McCalpin and Forman, 1993), 2 on the Weber segment (Stafford and Forman, 1993; McCalpin et al, 1994), and 3 on the Salt Lake City segment (Lund, 1992). A total of 266 numerical ages have been obtained since 1980, which constitutes the largest geochronologic data set on an active normal fault in the world. After reexamining the trench logs, we chose 81 ages (69 maximum limiting ages and 12 minimum limiting ages) that most closely limit the timing of the 19 known Holocene paleoearthquakes on the WFZ. The maximum limiting ages (58 ^{14}C, 11 TL) provide the best constraints on paleoearthquake timing (Fig. 1).

Previous workers had remarked upon the seemingly anomalous cluster of paleoearthquakes within the past 1500 years as perhaps indicative of temporal clustering, with the further implication of contagion between segments. Temporal clustering in the space-time diagram was assessed via the moving window test and the Perkins test. In the

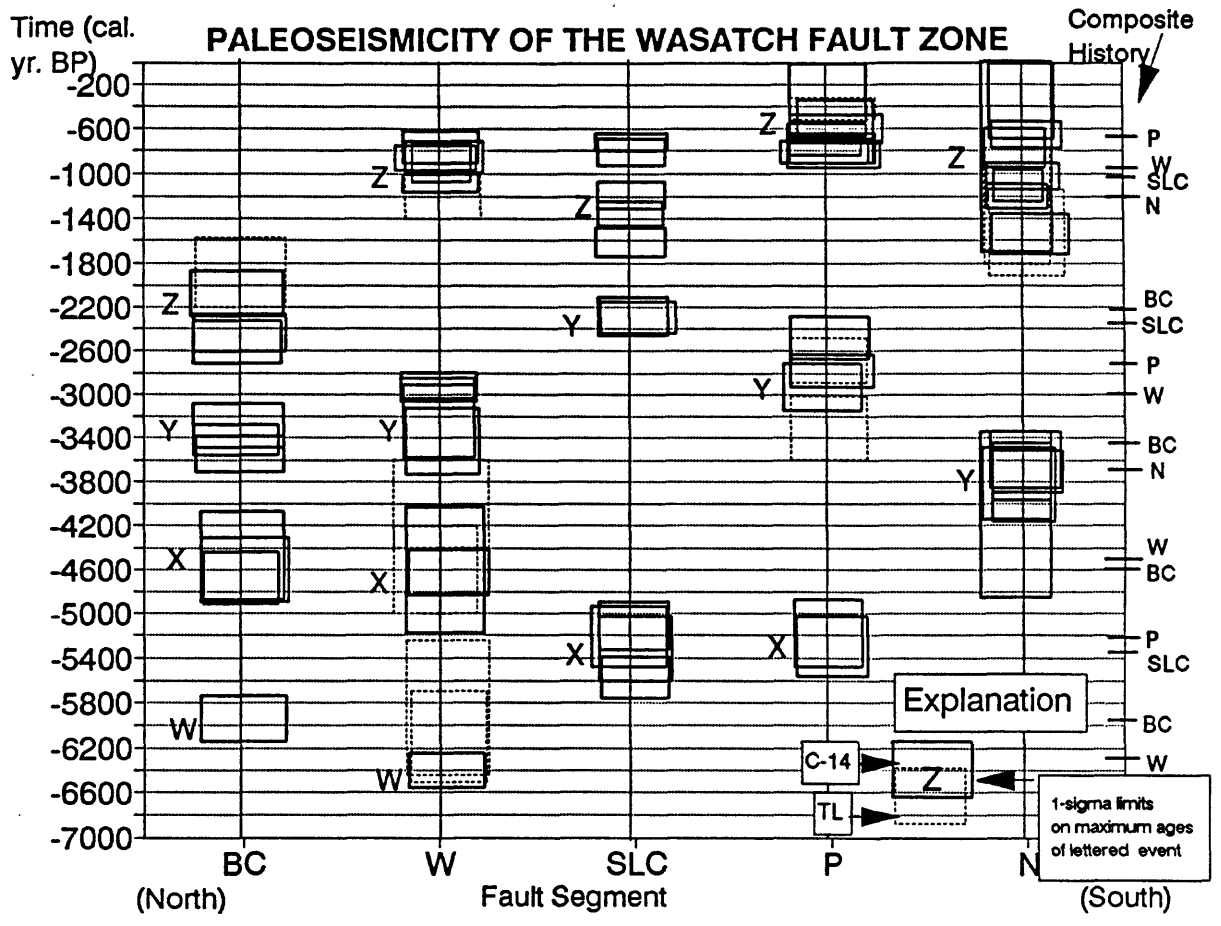

Fig. 1. Paleoseismicity space-time diagram for the past 7 ka on the five central segments of the WFZ. Boxes show 1-sigma limits of close maximum limiting ages on paleoearthquakes (solid for ^{14}C, dashed for TL). The weighted mean of the limiting ages for each lettered paleoearthquake (W-Z) on each segment (see abbreviations) are shown graphically at the far right; this time series comprises the observed composite paleoseismic history. Abbreviations: BC=Brigham City, W=Weber, SLC=Salt Lake City, P=Provo, N=Nephi.

moving window test, a synthetic time series of 100 paleoearthquakes is generated for each segment by Monte Carlo simulation, using the weighted mean recurrence intervals from the observed paleoseismic record. These values are: Brigham City, 1261±81 yrs; Weber, 1786±233 yrs; Salt Lake City, 2172±845 yrs; Provo, 2286±219 yrs, and Nephi, 2500±625 yrs. Standard deviations range from 6%-39% of the recurrence interval, with a mean value of 17%; this coefficient of variation is similar to that observed for earthquakes in plate-boundary regions. The series of synthetic paleoearthquakes for each segment are plotted as five parallel time lines, in the same format as Fig. 1, but covering a span of 200,000 yrs and containing 500 events. This long, synthetic space-time diagram is then examined to see how often temporal clusters and gaps occur that are identical to those seen in the observed paleoseismic history (Fig. 1). For example, the WFZ history displays one cluster of 4 events within 550 yrs and one gap of 0 events in 1015 yrs.

A moving window 6 kyr long is passed sequentially over the synthetic paleoseismic history at 1 kyr intervals. 51% of the ca. 200 window positions contain a cluster as defined above, while 53% of windows contain an aseismic gap of 1015 yrs long or longer. The tightest cluster in the 200 kyr synthetic record is five events (one on each segment)

within only 38 years, and two events "occurred" in an identical year on different segments, all entirely from random interactions. The longest gap was 1887 yrs long. 14% of the 200 window positions contained one cluster and one gap, such as seen in the observed paleoseismic history. In other words, the cluster and gap pattern in Fig. 1 has a 14% chance of arising from random interactions between five totally independent segments.

The Perkins test compares the frequency distribution of recurrence intervals in observed versus synthetic composite paleoseismic histories (a composite history is merely a time series that contains all events from multiple fault segment time series). In a composite history generated without contagion, recurrence intervals always display a negative exponential relationship, whereas increasing bimodality in the frequency histogram indicates increasing temporal clustering (Perkins, 1987). The observed composite history for the WFZ contains three departures from an exponential curve: 1) shortage of very short (< 100 yrs) recurrence intervals, 2) a slight deficiency of mid-range (300-600 yr) recurrence intervals, and 3) no recurrence intervals of 800-1000 yrs, but one of > 1000 yrs. The latter two anomalies constitute very weak evidence of temporal clustering. Taken together with the results of the moving window test, it is likely that the clusters and gaps in the observed WHZ paleoseismic history are the fortuitous result of random interactions between independent fault segments. The scarcity of very short recurrence intervals, compared to theoretical expectations, suggests that some physical mechanism may be preventing earthquakes from occurring until at least 100 years after the previous event.

References

Lund, W.R., 1992, New information on timing of large earthquakes on the Salt Lake City segment of the Wasatch fault zone; implications for increased earthquake hazard along the central Wasatch Front: Wasatch Front Forum, v. 8. no. 3, p. 12-13.

Machette, M.N., Personius, S.F. & Nelson, A.R., 1992, Paleoseismology of the Wasatch fault zone: a summary of recent investigations, interpretations, and conclusions, in Gori, P.L & Hays, W.W. (eds.) Assessment of Regional Earthquake Hazards and Risk Along the Wasatch Front, Utah. U.S. Geological Survey Professional Paper 1500, p. A1-A71.

McCalpin, J.P. and Forman, S.L., 1993, Assessing the paleoseismic activity of the Brigham City segment, Wasatch fault zone; probable site of the next major earthquake on the Wasatch Front?, in Jacobson, M.L. (comp.), Summaries of Technical Reports, v. XXXIV, U.S. Geological Survey Open-File Report 93-195, p. 485-489.

McCalpin, J.P., Forman, S.L. and Lowe, M., 1994, Reevaluation of Holocene faulting at the Kaysville site, Weber segment of the Wasatch fault zone, Utah: Tectonics, v. 13, no. 1, p.1-16.

Perkins, D.M., 1987, Contagious fault rupture, probabalistic hazard, and contagion observability, in Crone, A.J. and Omdahl, E.M (eds.), Directions in Paleoseismology: U.S. Geological Survey Open-File Report 87-673, p. 428-439.

Stafford, T.W. Jr. and Forman, S.L., 1993, Radiocarbon and thermoluminescence dating of Wasatch faulting events, Garner Canyon, Utah: Utah Geological Survey Contract Report 93-4, May 1993, Salt Lake City, Utah, 15 p.

Variability of Surficial Slip in the 1992 Landers Earthquake: Implications for Studies of Prehistoric Ruptures

Sally F. McGill, Department of Geological Sciences,
California State University, San Bernardino, CA 92407
Charles M. Rubin, Department of Geology, Central Washington University,
Ellensburg, WA 98926

Offset geomorphic features are commonly used to infer the amount of slip in past large earthquakes on active strike-slip faults. These slip values are then used to estimate the sizes and frequencies of prehistoric earthquakes on the fault. In studies of prehistoric ruptures, however, it is sometimes difficult to determine which geomorphic features have been offset in the most recent earthquake alone and which have been offset in more than one past earthquake. For example, along the section of the Garlock fault in Pilot Knob Valley, it is not clear whether offsets scattered between 2 and 6 meters all formed in a single slip event with a large degree of variability in the amount of slip along strike, or whether the larger offsets within this range had been displaced in the past two slip events combined, and the smaller offsets were younger and had been displaced in the most recent event alone (McGill and Sieh, 1991).

If the variability in slip along strike during an earthquake is small compared to the mean slip per event, it may be possible to determine the number of slip events associated with a given set of offset geomorphic features from a plot of offset versus distance along the fault, as Sieh (1978) did for the 1857 rupture along the San Andreas fault. In the 1992 Landers earthquake, however, the variability in slip along each fault (*i.e.*, the standard deviation of all slip measurements along that fault) was > 50% of the mean slip along that fault. If this degree of variability is common for large earthquakes then other methods of determining the amount of slip in prehistoric earthquakes must be developed.

One approach to estimating the number of slip events associated with offset features is to construct a histogram showing the number of features offset any given amount. McGill and Sieh (1991) reasoned that if the offsets scattered between 2 and 6 meters along the Garlock fault in Pilot Knob Valley all formed in the most recent slip event, then one would expect the offsets to be distributed uniformly or unimodally within this range. The offsets scattered between 2 and 6 meters in Pilot Knob Valley, however, are bimodally distributed, suggesting that features offset around 2-4 meters were displaced in the most recent earthquake alone, whereas features offset around 4-6 meters were displaced in the past two slip events combined (Figure 1A).

McGill and Sieh (1991) assumed that a histogram of offsets from a single earthquake would have a single peak, even though that peak might be very broad because of variability in the slip along the fault. Preliminary analysis of offsets that we measured along a 5-km length of the Emerson fault, however, indicates that offsets from a single earthquake can produce a bimodal histogram (Figure 1B). To see whether or not this was a common feature of the Landers earthquake, we used measurements made by many geologists along the surface rupture of the Landers earthquake to construct histograms for all of the faults that ruptured in the 1992 Landers earthquake.

Most of the histograms for faults that ruptured in the Landers earthquake are multimodal, confirming that a multimodal histogram of offsets should not necessarily be interpreted as evidence for multiple earthquakes. In some cases, however, the different peaks in the histograms correspond to particular segments of the faults, suggesting that if a short enough fault segment is considered, a single rupture event may in fact produce a single-peaked histogram. The 5-km-long segment that produced the bimodal histogram shown in Figure 1B can be broken down into 1.5- to 2-km segments that have histograms with one dominant peak, but they still have minor peaks at other offset values. The fault lengths over which nearly unimodal histograms are observed is so short, however, as to be of little use in deciphering the number of prehistoric earthquakes associated with certain offset geomorphic features. Along many prehistoric ruptures, there simply are not enough offset features within a 1.5-km-long stretch to produce a meaningful histogram. Furthermore, there are other segments of the Landers rupture that do not produce unimodal histograms at any length scale, except that which includes only 1 or 2 measurements.

If a running average of the offset is subtracted from each offset measurement before constructing the histograms, the histograms for the Emerson and Camprock faults each have a single peak. This suggests that the multiple peaks in figure 1B might be related to long-wavelength variations in slip that were filtered out by subtracting the running average. After subtracting a running average from the Pilot Knob Valley offsets along

the Garlock fault, however, the histogram still has multiple peaks. This suggests that variations in these offsets have a shorter wavelength and might represent multiple slip events. Further work is needed to determine whether or not this type of analysis might be useful in determining the number of earthquakes associated with offset geomorphic features. Similar plots for the Johnson Valley and Landers faults have multiple peaks, but this may be due to sparser measurements along these faults.

Another method employed by McGill and Sieh (1991) to distinguish features offset in a single event from those offset in multiple events was to compare the slip gradient required for a single event interpretation of prehistoric offset data to the maximum slip gradients observed in historical ruptures. For example, along the Garlock fault in eastern Pilot Knob Valley a terrace riser offset 2.7 ± 0.7 m is less than 10 m west of a terrace riser offset 5.6 ± 0.7 m. This represents a slip gradient (*i.e.*, strain) of 0.29 m-slip/m-fault length, or about 3 x 10^{-1}). A short distance away, a terrace riser offset 5.3 ± 0.3 m is located only 10 m away from a terrace riser offset 3.4 ± 0.5 m. This represents a slip gradient of 2 x 10^{-1}. Because there were no documented historical precedents for such extreme slip gradients, McGill and Sieh (1991) concluded that the features offset 2.7 and 3.4 m had been offset in the most recent event alone, whereas the features offset 5.6 and 5.3 m had been offset in the past two events combined.

Prior to the 1992 Landers earthquake, however, slip measurements less than 50 meters apart on historical strike-slip ruptures had never been reported, to our knowledge, and most measurements were hundreds of meters or more apart. Thus, the lack of a precedent for such extreme slip gradients might simply have reflected a lack of closely spaced slip measurements. The Landers earthquake provided an opportunity to make closely spaced slip measurements along a historical rupture. The maximum slip gradient observed along the Emerson fault was 2 x 10^{-1}, between two features offset 250 and 535 cm located only 12-20 m apart (distance between offset features estimated from air photos). This is almost as extreme as the maximum slip gradient in Eastern Pilot Knob Valley, making McGill and Sieh's (1991) assignment of 2 events for the 5.6 and 5.3 m offsets less convincing. The maximum slip gradients on other faults that ruptured in the Landers earthquake were on the order of 10^{-2}, as were the maximum slip gradients for the 1979 Imperial Valley and the 1987 Superstition Hills earthquakes. The median slip gradients for faults that ruptured in the Landers earthquake were 10^{-3} to 10^{-4}.

References cited:

McGill, S. F., and K. E. Sieh, Surficial offsets on the central and eastern Garlock fault associated with prehistoric earthquakes, *J. Geophys. Res., 96,* 21,597-21,621, 1991.

Sieh, K. E., Slip along the San Andreas fault associated with the great 1857 earthquake, *Bull. Seismol. Soc. Amer., 68,* 1421-1448, 1978.

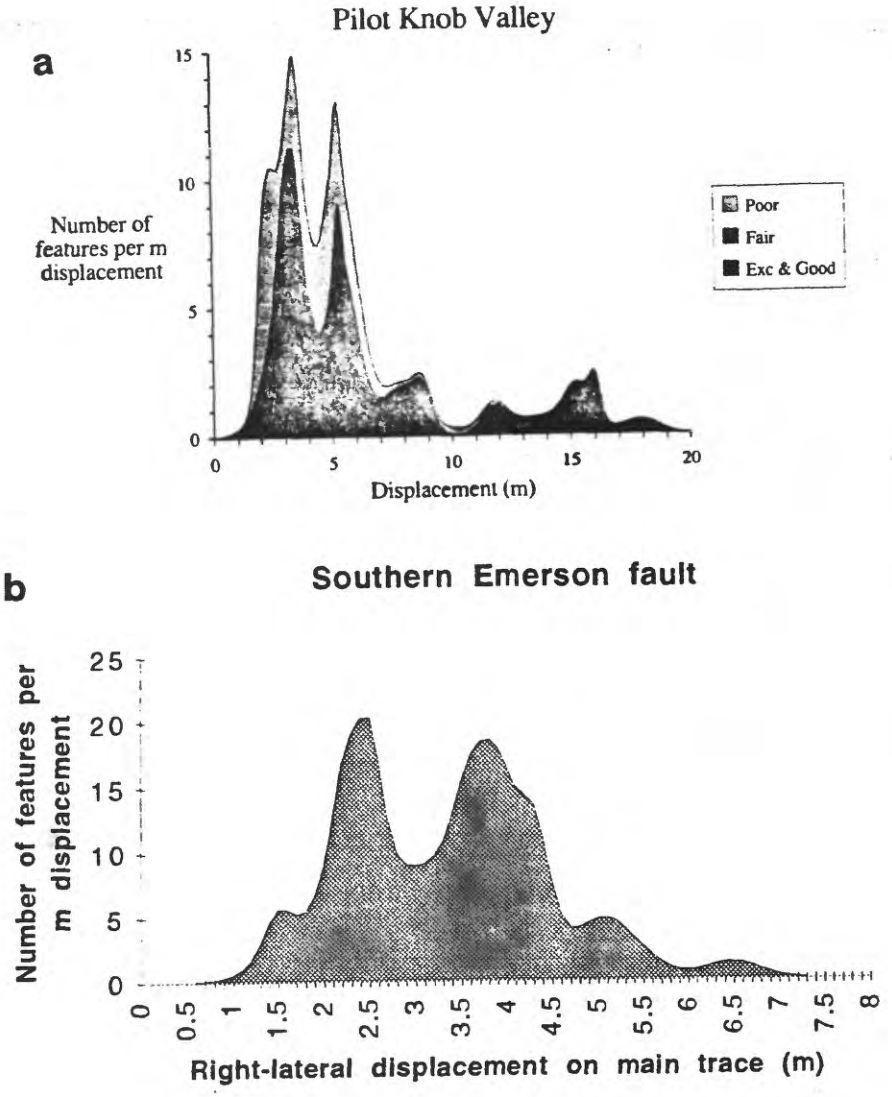

Figure 1: Histogram-like plots of laterally offset geomorphic features A) along the Garlock fault in Pilot Knob Valley and B) along a 5-km-long section of the Emerson fault that ruptured in the Landers earthquake. Each offset measurement is treated as a Gaussian probability density function, and the density functions for all the offsets are then summed to produce this figure. The area beneath each peak represents the number of features offset the amounts spanned by the width of the peak.

The Mendocino Triple Junction: Active Faults, Paleoseismicity, and Rapid Uplift

D. J. Merritts, Geosciences Department, Franklin & Marshall College, Lancaster, PA
A. E. Brustolon, Geosciences Department, Franklin & Marshall College, Lancaster, PA

Some of the highest rates of crustal deformation, surface uplift, and seismic activity in North America occur at the Mendocino triple junction (MTJ), where the northern tip of the San Andreas fault (SAF) meets the Cascadia subduction zone (CSZ) and Mendocino fault (MF) (Fig. 1). Nevertheless, the locations of the northern several hundred km of the SAF and the southern several tens of km of the CSZ are uncertain. The 1906 M_S 7.8 earthquake on the SAF is thought to have ruptured 450 km, from near San Francisco to the MTJ, but the only evidence of possible surface rupture north of Point Arena, where the fault trace goes offshore, is at the tip of Point Delgada. Two needs for understanding the tectonics and assessing the seismic risk of northern California are critical. One is delineating the active trace and geometry of the northernmost 140 km of the SAF and the southernmost few tens of km of the CSZ. The other is determining whether or not, and how often, repeated great earthquakes have occurred along these structures.

The focus of this research is the use of ages and altitudes of emergent Holocene platforms to obtain patterns of deformation and paleoseismic data along the CSZ and SAF in the MTJ region. An important aspect of this analysis is the attempt to separate a rising, post-glacial sea level record from that of episodic surface uplift. The 1992 Cape Mendocino earthquake (M_S 7.1) provides an opportunity to compare historic data with geomorphic observations in order to understand temporal and spatial patterns of crustal deformation. This earthquake occurred along a NE-dipping (12°), 22-km long thrust fault (depth 10 km), and ruptured either the southernmost tip of the CSZ, or a subsidiary fault that soles in the megathrust. About 300 km^2 of land was elevated up to 140 cm, and ~200 km^2 was lowered ~20 cm (Fig. 1). Along the same coastline, and 25 km to the south, Holocene platforms have been elevated up to 15 m above a rising sea level.

After the earthquake in 1992, we surveyed the treads and inner edges of all raised Holocene marine platforms in the region, a coastal distance of ~50 km. About 1300 points were surveyed with a Lietz total geodetic station, with high concentrations in areas of exposed platform remnants. Many remnants could be followed for several kilometers, and samples for radiocarbon age dating were collected at more than 20 sites. Coordinate survey data were plotted in map view (1:12,000) and overlain on a 100% enlargement of 1:24,000 U. S. Geological Survey topographic maps as a further check on survey accuracy. Two projection lines were established for final analysis: 1) A N10°W transect from Punta Gorda to Cape Mendocino (paralleling the inferred trace of the CSZ, line of profile used by others to plot coastal uplift based on marine organism die-off, and strike of the 1992 earthquake); and 2) A N35°W transect from Point Delgada to Punta Gorda (paralleling the commonly assumed trace of the SAF and strike of the August 1991 Honeydew earthquake). Survey points and transect locations were projected perpendicularly from their original positions to these lines and all altitudinal data were plotted to construct a coastal emergence profile (Fig. 2).

The coastline can be divided into two zones based on amount and style of surface uplift (Fig. 2). In Zone I, the pattern of deformation is similar to that of the 1992 earthquake. Holocene coastal uplift terminates abruptly at Cape Mendocino, and tapers to zero near Punta Gorda. Platform ages range from ~730 to 6890 yrs BP. A zone of reverse faulting with active folding occurs at the southern end of Zone I, at the east-west-trending Cooskie Creek shear zone. A second zone of uplift can be defined from Punta Gorda southward, where Holocene platforms are more deformed and span a greater age range (~510 to 7780 yrs BP). Holocene coastal uplift terminates abruptly 4 km north of Point Delgada, near Gitchell Creek (Fig. 1). Zone II is defined by at least four Holocene platforms warped into several tight antiforms. A region of locally very high uplift rates (5-10 m/kyr) occurs just south of Big Flat, coincident with maximum relief and the steepest stream gradients along the coast.

Radiometric dating of platforms and their overlying deposits indicates that, because of eustatic sea level rise, the number of emergent platforms is less than the number of uplift events. It is assumed here that the Barbados sea level curve, with detailed age control, is a reasonable proxy for sea-level rise in northern California, and that the oldest platform, or location of first Holocene emergence (pre-emergence platform), occurs where the uplift rate is highest. Maximum and minimum ages for a platform indicate the period of time during which the platform remained close to sea level, and represent at least two events--when it emerged above the water for the first and last times, respectively. Other emergence events might have occurred during the interim, but their timing is difficult to determine. The data in Fig. 2 are used to infer possible uplift histories in Zones I and II. Constraints for these interpretations are the present altitudes of platform inner edges; ages of platforms and overlying deposits; and altitudes of platform formation from the Barbados sea level curve. Assumptions are 1) long-term uplift rates are roughly constant at a site; and 2) ages of pholad shells taken from borings represent approximate ages of coseismic emergence.

Using these constraints and assumptions, it is possible to infer amounts of coseismic uplift and recurrence intervals between seismic events. In Zone I, five earthquakes resulting in emergence occurred at about 6.5, 4.9 (inferred), 3.5, 2.2 (estimated age), and 1.0 kyr BP, as well as in 1992 AD. Recurrence intervals range from ~1000 to 1600 years. Maximum uplift per event was 3.5-4.5 meters for prehistoric earthquakes, but only 1.4 m for the historic event. Ages of three of the five prehistoric events are based on radiometric dates for shells obtained from platforms, while that which raised platform #3 is only known to have occurred between about 2.5 and 1.0 kyr BP, and that between 6.5 and 3.5 kyr BP is inferred. A difficult feature to interpret in Zone I is the small amount of uplift during the 1992 earthquake. If all uplift in the region were the cumulative result of such events, it is not likely that four distinct platforms separated from one another by prominent risers would exist. In fact, if long-term uplift of 3.5 m/kyr is combined with an average recurrence interval of 1396 yrs, an estimated 4.9 m of uplift occurs per event. At present, three models are considered equally plausible: 1) much larger earthquakes than that of 1992 have occurred at least four times in the past 6.5 kyr; 2) frequent, moderate-sized events, like that of 1992, have been clustered in time such that distinct platforms give the appearance that larger events occurred; and 3) earthquakes of many different sizes, as well as interseismic uplift, have occurred, resulting in platforms associated with both large events and the cumulative effects of several smaller events.

For Zone II, if each platform was raised by coseismic uplift, the dates of such events are about 7.7, 6.2 (inferred), 4.6, 3.3, 2.4, and 0.6 kyr BP. Recurrence intervals range from ~1000 to 1800 years. At least one event probably occurred between 7.7 and 4.6 kyr, when sea level rose faster than the rate of landmass uplift, and is inferred to have occurred at 6.2 kyr BP from an average recurrence interval of 1400 years. Maximum uplift per event was 4-6 m, with exception of 2.5 m for the most recent event. Uplift per event and average recurrence interval are greater in Zone II than in Zone I.

Similar ages of shells obtained several km from one another on the same platform, the occurrence of historic coseismic emergence, and similarity in long-term pattern of uplift with that from the 1992 earthquake support the hypothesis that each platform in Zone I is predominantly the result of coseismic uplift along thrust faults, but similar evidence is not available for Zone II. For now, it is assumed that platforms in Zone II are also the result of coseismic uplift. It is possible, however, that in both zones some or all events interpreted as only one earthquake are actually the result of ≥two, smaller events, closely spaced in time, with each the cause of less than the net amount of uplift assumed for one large event. Finally, the interpretations presented here do not preclude additional interseismic uplift, but do assert the following: the existence of prominent risers between platforms indicates that episodic, rapid uplift is probably the dominant cause of net uplift. In both zones, the number of platforms is not equivalent to the number of prehistoric earthquakes. Rather, it is a minimum of the number of events that resulted in sudden, rapid uplift, because platform preservation is also a function of changing sea level.

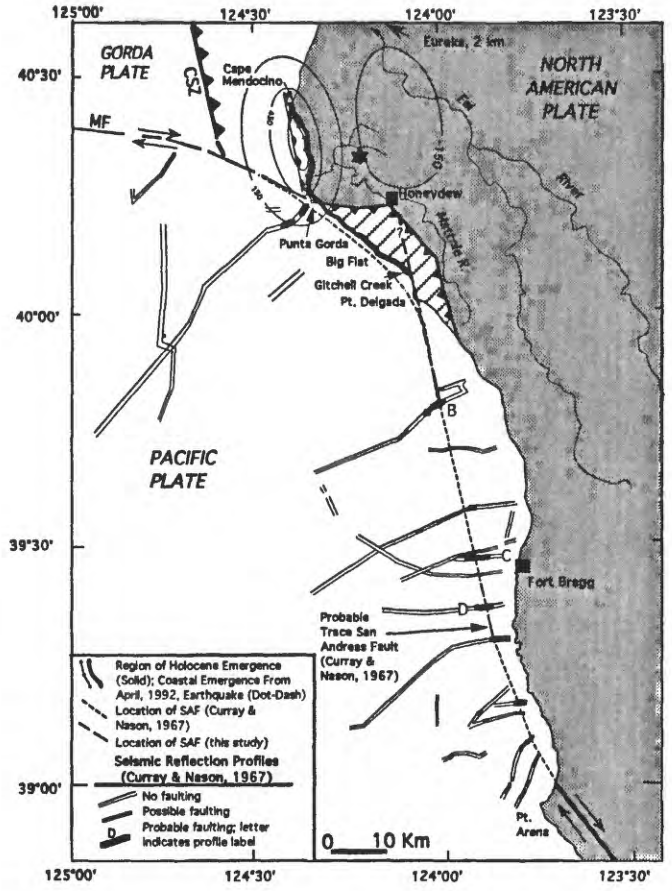

Figure 1. Location map and tectonic setting of the MTJ region. Hachured region is King Peak subterrane and dark tip is Point Delgada subterrane; together the two comprise the King Range terrane. Eastern boundary of King Range terrane is Mattole Shear zone; northern boundary is Cooskie shear zone. Both are older thrust structures with evidence of more recent, near-vertical strike-slip deformation (E. Betuner, pers. comm., 1993). Seismic lines illustrate constraints for traditional location of SAF. Star indicates location of epicenter of 1992 Cape Mendocino earthquake. Contours (mm) are deformation pattern of 1992 earthquake predicted from displacement modeling of the fault plane, assuming uniform slip; modeled uplift pattern agrees well with--but is less than--that from geodetic work and surveys of intertidal marine organism die-off (Oppenheimer et al, 1993). MF: Mendocino fracture zone; CSZ: Cascadia subduction zone.

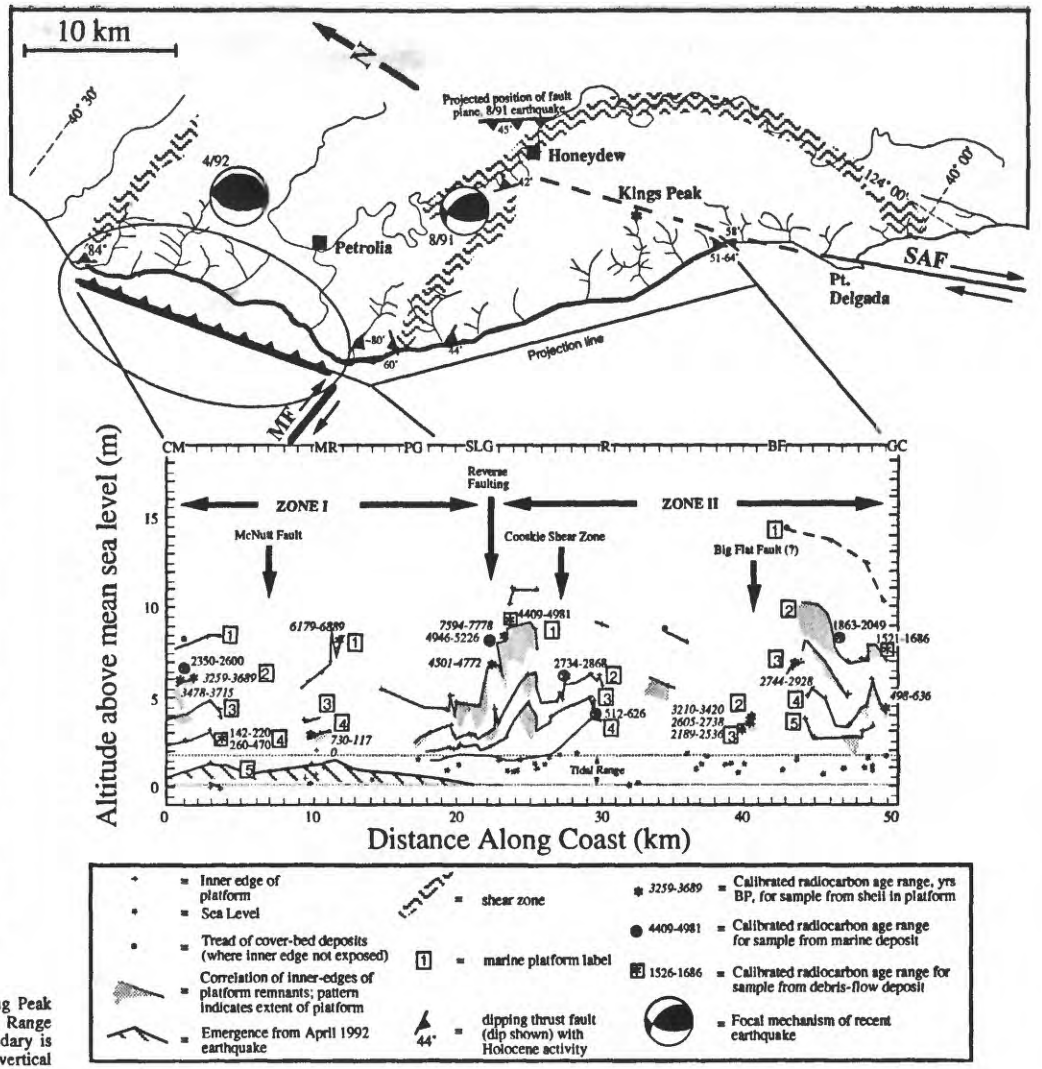

Figure 2. Holocene surface uplift along the coast from Cape Mendocino (CM) to Gitchell Creek (GC). Upper part of figure is map view showing projection lines of middle part of figure. Middle part is a vertical view displaying ages (yrs BP) and altitudes of uplifted terrace platforms and radiocarbon dating sites. Line segments correlating inner edges of uplifted platforms represent traces of originally horizontal strandlines. Based on analyses presented in the text, platforms are labelled 1-5 in Zones I and II, but are not necessarily the same age or surface between zones. Vertical differences in altitude between these lines at a given site, divided by the differences in ages of formation, provide an estimate of surface uplift rate at that location. Places where inner-edge altitudes fluctuate rapidly along shore probably are associated with shallow faulting and/or folding, as at the mapped McNutt Fault and Cooskie Creek shear zones, and the proposed Big Flat fault. MR=Mussel Rock. PG =Punta Gorda. SLG=Sea Lion Gulch. R=Randall Creek. BF=Big Flat. (Fault strikes and dips from unpubl. field notes of Beutner, 1973-1976, and Merritts, 1991-1992).

Paleoseismology and Historical Seismicity for Seismic Hazard Assessment in Italy: Examples from the Fucino and Pollino Tectonic Structures

A. M. Michetti and L. Ferreli, GNDT (National Group for Protection against Earthquakes) c/o ANPA - Disp; e-mail: michetti@edult2.disp.enea.it
L. Serva and E. Vittori, ANPA - Disp (National Environmental Protection Agency), Via Vitaliano Brancati, 48, 00144, Roma, Italy.

As in most of the regions with ancient civilization, earthquake hazard analyses in Italy are mainly based on historical seismic catalogues. However, even if the Italian catalogue spans more than 2000 years and is probably the best of the world in terms of information quality, recurrence interval of damaging events can be longer than the historical record. Moreover, the completeness of seismic catalogues progressively decreases going back in the past.

Consequently, in Italy the most efficient way to conduct paleoseismic studies for seismic hazard evaluations is to verify if the seismicity level assessed from historical data is in contrast with the geological evidence. To illustrate this point we present two recent case studies from A) the Fucino basin (Abruzzo, Central Apennines; see inset map in Fig. 2) and B) the Pollino range (Calabria, Southern Italy; Fig. 2).

A) In the Fucino basin historical researches have not discovered yet evidence of large earthquakes before the 13 Jan., 1915 event (Ms = 7.0; 33000 people killed). This suggested to previous Authors that 1915-like events have a long return period (> 1000 years). To test this hypothesis, we chose a site for trench investigation along one of the Holocene scarps rejuvenated during the 1915 event. Surface faulting occurred at least along two parallel normal faults bounding the eastern side of the basin, the Celano - Gioia Fault and the Parasano - Cerchio Fault, over a length of 13 and 10 km, respectively, with an average downthrow of 30-90 cm toward SW. At the trench site, near the village of San Benedetto de' Marsi, the coseismic scarp lays within the area formerly covered by the Fucino lake, that was the third largest in Italy before being completely drained for farming in 1875 A.D.. Therefore, we expected to explore a very young and complete stratigraphy.

Figure 1 summarizes the evidence collected in the three trenches we excavated at this site. The first 60 cm of deposits near the ground surface are completely reworked by plowing. The youngest mappable sediments are fluvio-lacustrine silty-sand beds (Unit 5) that thickens abruptly in the fault hanging wall. The attitude of these beds suggests the occurrence of a coseismic fault slip during the deposition of Unit 5 (event A, penultimate earthquake prior to the 1915 event). Underneath the Unit 5 deposits, the fluvio-lacustrine sequence in the hanging wall cannot be correlated to that in the footwall, because the overall displacement exceeds the depth of the trenches. The Unit 3 deposits exposed in the hanging wall represent a distinctive lacustrine debris wedge. This suggests the occurrence of a surface faulting event (event B) older than, but close to, the age of the Unit 2 top horizon. Unit 3 includes Roman pottery of the "Sigillata Italica" type, produced only between the I century B.C. and the I century A.D.. Hence, events A and B have a historical age anyway.

Even within the errors related to the detrital nature of the collected samples, the interpretation of radiocarbon dating provides further chronological constraints (Fig. 1). This suggests that event B took place between the VII and the IX century A.D.. Event A occurred after the X century and almost certainly before the XIV century, as since then the historical record is considered complete for large earthquakes.

The evidence for these events compared to the 1915 surface faulting indicates that M > 6.5 are associated with each displacement. Therefore, the return period for large earthquakes in the Fucino basin is shorter than that indicated by the historical seismic catalogue alone.

B) The Pollino range is located at the boundary between the Apennine Chain and the Calabrian Arc, in a region characterized by an intense Quaternary tectonics. However, unlike

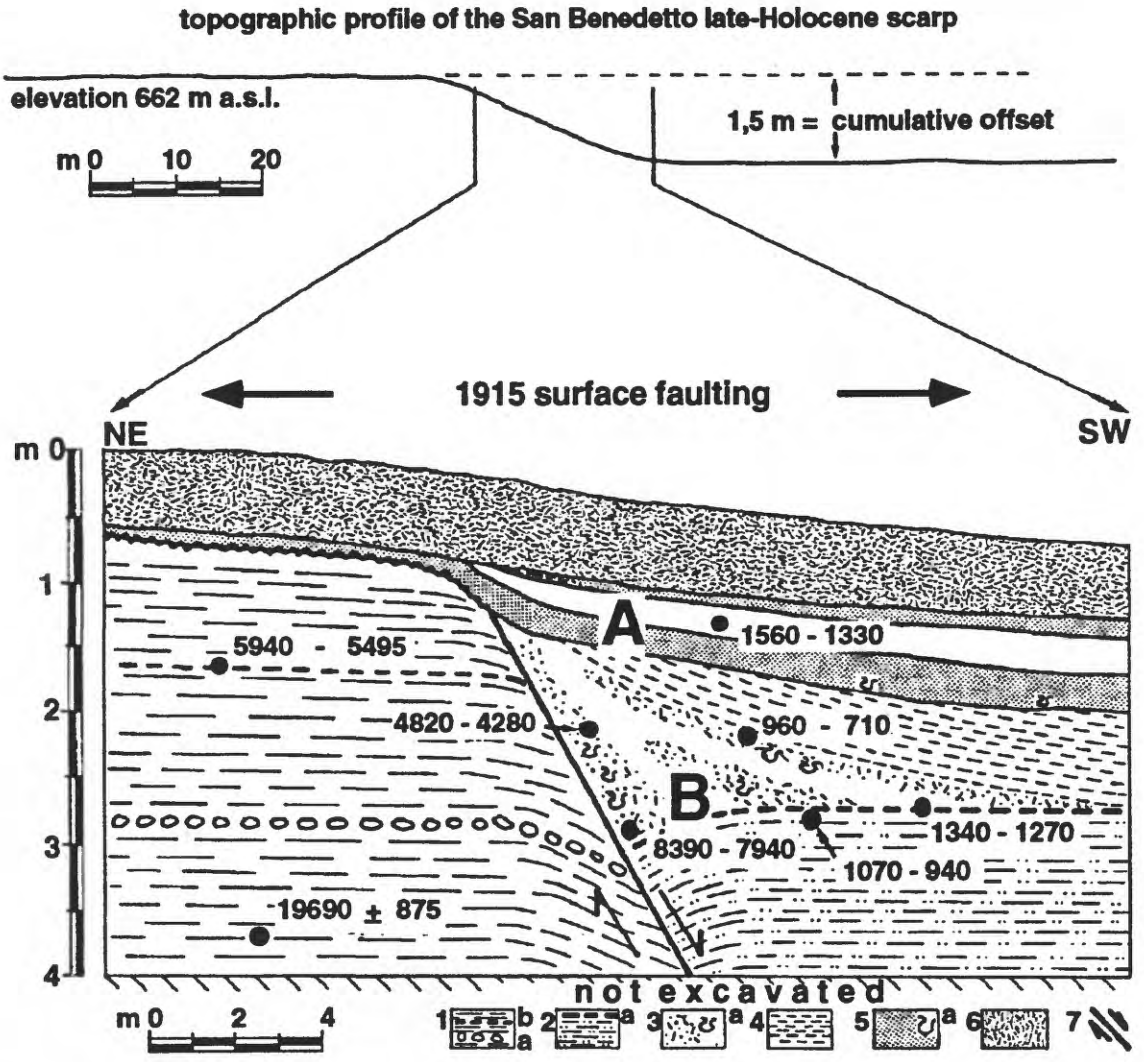

FIGURE 1. Synthetic sketch the data collected in the S. Benedetto trenches. Legend: 1) Unit 1, a=gravel, b=peat; 2) Unit 2, a=peat; 3) Unit 3, a=Roman pottery, Sigillata Italica type; 4) Unit 4; 5) Unit 5, a=late Medieval (?) pottery; 6) Plow zone; 7) Normal fault; ●) Calendar and radiocarbon ages, yr B.P. (Geochron Lab.). Capital letters show the approximate location of the evidence for pre-1915 surface faulting events.

the nearby Apennine and Calabrian structures, there is no historical evidence for large (I > VII MCS, or about M > 5) earthquakes in the Pollino area (Fig. 2).

We conducted airphoto interpretation and reconnaissance field survey along the Pollino Fault Zone that is the major Quaternary structure of the area. We recognized previously unmapped late Pleistocene to Holocene fault scarps at several sites along the fault segment between Masseria Marzano and Civita. This segment runs for a length of about 18 km at the base of the WNW trending Pollino range-front ("a" in Fig. 2). At the eastern boundary of this segment, we also found scarps of the same age along the N-S trending Civita Fault ("b" in Fig. 2).

In particular, some scarps displace (vertical offset 1.0 to 2.0 m) the surface of an active alluvial fan. Other scarps can be traced at the contact between bedrock and slope deposits at the base of a steep mountain front. The geomorphic setting strongly suggests that they are related to surface faulting events with a predominant normal component.

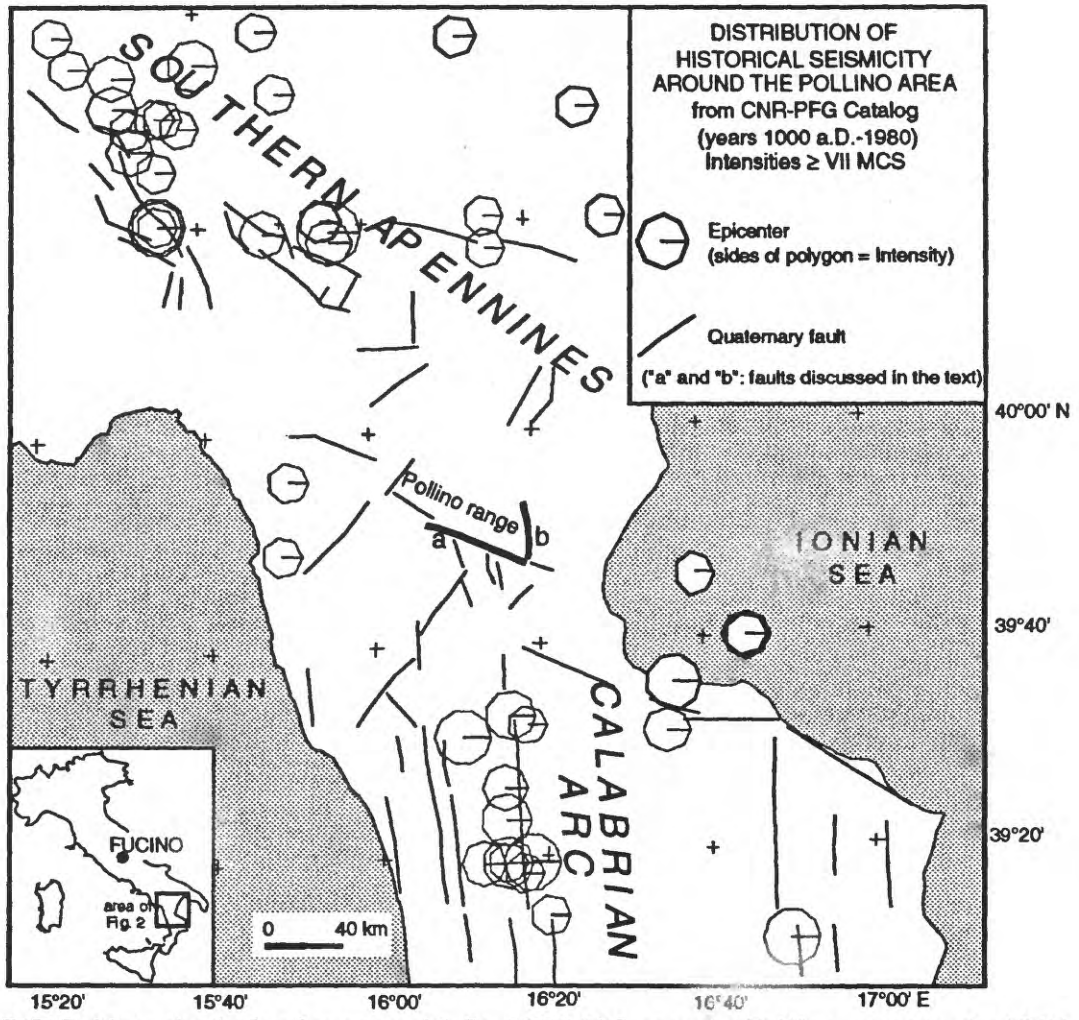

FIGURE 2: Note the lack of events with I > VII MCS near the Pollino range in the PFG Catalogue, while the faults marked with "a" and "b" show evidence of Holocene surface faulting. The inset map indicates the location of the Fucino and Pollino areas.

Based on the range-front morphology and field observations, we associate this evidence of Holocene surface faulting at least to the entire length of the Masseria Marzano - Civita segment ("a" in Fig. 2). Comparison with surface faulting events in the Apennines and abroad indicates that a similar rupture length should be related to M 6.5 to 7 earthquakes.

In order to characterize these earthquakes in terms of age, magnitude, and return period, this summer we investigate some of the Holocene scarps via exploratory trenches. Our preliminary results will be presented at the USGS-ICL Workshop. The evidence of Holocene surface faulting event(s) along the Pollino Fault Zone strongly suggests that the maximum potential earthquake for the Pollino region is anyway much larger than that indicated by the available historical data.

The Fucino and Pollino examples clearly show that the exceptionally long historical catalogue in Italy is still inadequate for assessing the seismic hazard associated with many tectonic structures. However, at present similar results are available only for a few structures in the Central Apennines, for the Irpinia earthquake fault in the Southern Apennines, and for the Belice area in Sicily (some of these results are described in the volume "Perspectives in Paleoseismology", AEG Special Publication n. 5, in press). This emphasizes the need for systematic paleoseismological analyses to improve the seismic hazard reduction in Italy.

"Geological, Geomorphological and Geophysical evidence for Paleoseismic events in Western Puerto Rico".

Juan-Carlos Moya, Department of Geology, University of Colorado at Boulder. Campus Box 250, Boulder, Co. 80309-0250
William R. McCann. Earth Scientific Consultants, Box 5217 College Station, Mayagüez P.R., 00681.

Tectonic activity forming the Puerto Rico metamorphic igneous complex massif culminated in the Eocene. During that time and during the next 20 million years (Ma), two major fault systems, the Great Northern and Southern Puerto Rico fault zones transpressively displaced rocks left-laterally (Briggs, 1968; Seiders et al. 1972). Since that time, tectonic activity has continued, but at a much reduced rate, as evidenced by the lack of recent volcanic activity and the presence of gently tilted limestones of Oligocene to Miocene age covering the older rocks and faults (Monroe, 1980). The Oligocene-Miocene rocks are rarely faulted in the north, but highly faulted and more strongly tilted in the south. The major faults, clearly visible today in the morphology of the island, extend to the submarine areas to the northwest and southeast.

Presently, Puerto Rico lies along the moderately complex, obliquely convergent boundary between the North American and the Caribbean Plates. Relative plate movement in the area is just south of west if one considers movement of the North American Plate relative to a fixed Caribbean Plate. The rate of plate movement is not yet determined to better than a factor of two; estimates range between 37 mm/yr and about 20 mm/yr. The island, and the platform on which it lies, is one of a series of narrow, linear blocks (platelets) absorbing the convergent shearing stress between the larger plates. More specifically, geophysical data demonstrate that most of the island of Puerto Rico lies on the Puerto Rico Platelet. Four tectonically active areas bound the Puerto Rico Platelet: the Puerto Rico Trench, the Anegada Trough, the Muertos Trough, and the Mona Passage and the Western Puerto Rico Seismic Zone.

Focal mechanism of earthquakes in the Puerto Rico Trench indicate west-southeast directed convergence. A southerly dipping seismic zone found beneath the island indicates that subduction has occurred for at least the last few million years. Byrne et al.(1985) in a study of a strong earthquake ($6.7M_S$) in the Muertos Trough have demonstrated that active underthrusting occurs beneath the southern part of the Hispaniola and that the subducted slab (of the Caribbean Plate) is actively deforming. As the features found on the inner wall of the Muertos Trough south of Hispaniola are similar in form to those near Puerto Rico, we surmise that subduction observed south of Hispaniola may also occur near Puerto Rico.

The presence of active faults in the southwestern Puerto Rico has been suggested for some time (Asencio, 1980; Soto et al., 1986; McCann et al., 1987; Joyce et al., 1987a,b; Larue, 1989; McCann, 1989). Soto et al.(1986) reports the discovery of Quaternary alluvium cut by a recently active fault in the southern coastal plain. Joyce et al.(1987b) noted the basin and range form of

the topography of the western area and suggested that it is related to a similar extensional process. Larue (1989) speculates that active faulting exists along nearly all of the western coast of Puerto Rico. Asencio (1980), McCann et al. (1987) and McCann (1989) relate the seismic activity of Western Puerto Rico to the existence of microplates thereby using a plate tectonic interpretation to explain the neotectonics of the area.

Examination of geomorphic features in the western Puerto Rico Seismic Zone demonstrates the existence of truncated spurs, and anomalous drainage patterns. Road cuts and other outcrops present clear evidence of ancient liquefaction and earthquake related displacement events. As this evidence was found in a region of presumably low rates of deformation (mm/yr) and extremely high rainfall (up to 100 inches per year) and high rates of soil erosion, its discovery has been very fortunate. In the nearly shallow marine areas other evidence of recent seismic events has been found. The young age (<8,000 years) of the deformed and displaced sediments, coral reefs and geomorphic features, deposited since the last rise in sea level, demonstrate the recency of the movements.

Mayagüez is a mayor coastal city in mountainous western Puerto Rico. Mayagüez lies in the western Puerto Rico seismic zone and near the Great Southern Puerto Rico Fault Zone (GSPRFZ). The most important discovery of paleoseismicity in Puerto Rico comes from this area. Along the southern margin of the GSPRFZ lies a NW trending, isolated ridge, called the Cordillera de Sabana Alta. Some 19 kilometers to the south of Mayagüez, on Route 100 (kilometer 3.0) along the southern flank of the Cordillera lies a faulted section of outcrop. The Cordillera is composed primarily of Serpentinite and a volcanoclastic unit known as the Yauco Mudstone. Fortunately, covering these basal units across much of the ridge is a thin veneer of Quaternary Tertiary Sands (*QTs*) allowing us to identify recent tectonic movements. This unit has been defined by alternating bands of friable sands and pale pink to pale yellow in color, with stains of reddish-orange to orange-brown color and quartz grains suspended in a clayey matrix of kaolinite, hematite and goethite. Schwartz and Mattson (1967) assigned this unit an age of Pleistocene (?) and is principally found on the tops of ridges or hills. The sediments that compose this unit correspond to alluvial or terrace deposits. The elevation of those terraces fall into two distinct levels: one at 50 the other at 70-80 meters. According to Kaye (1959) the height of the deposits on Cordillera de Sabana Alta could correspond to a high stand of the sea some 500,000 years b.p. (Yarmouth). As all attempts to date this material using thermoluminiscence have failed, we can only say that given the stratigraphy and the geomorphology of the zone and the above presented arguments, the unit *QTs* is of probable Quaternary age.

The outcrop at Route 100 is a road cut displaying faulted rocks in both cuts. The outcrop is composed of the Cretaceous age Yauco formation covered by QTs. Detailed observation of the outcrops show numeroous vertical displacements in the Yauco Formation and less clear deformation of *QTs* because of its ductile response. The most clear offset is one of 1.3 meters, total offset is about double that. Near the road cut lies another cut displaying only QTs. The lack of the more rigid Yauco formation makes difficult the identification of faulting, however, evidence of liquefaction is clear. In this outcrop one sees chaotic structure, and subvertical fractures filled with clastic material from the same unit.

The features observed at the roadcut on route 100 are observed to trend WNW. The area immediately offshore (about two kilometers to the west) also displays evidence of displacements of the seafloor. Importantly these features are seen to cut reflectors in seismic reflection records in the shallow platform area near the coast. Those reflectors represent sediments laid down since the platforms was flooded by the last rise in sea level about 8,000 years ago. The deformed reflectors in the 3.5 Khz records spatially match with offsets observed in multichannel records exhibiting deeper reflectors. Coral reefs formed during the last 8,000 years have been cut and displaced by the fault activity. We conclude that Late Quaternary and Holocene earthquakes have been common in Western Puerto Rico. The last big earthquake occurred 30 kilometers to the northwest of the zone in 1918 with a Magnitude of 7.5 (Reid and Taber, 1919).

Finally, the most recent fault in the GSPRFZ to have moved is the Cordillera Fault. That fault trends WNW and ends just few kilometers to the east of the city. The western end of the fault lies near the surface trace of a planar seismic zone dipping steeply to the SSW. Near the western end of the Cordillera Fault there is a marked changes in geology, to the south lies a major serpentinite body, and to the north various volcanic units of early Tertiary age. The mapped trace of the fault lies less than 200 meters from a major anomalous drainage pattern in western Puerto Rico. The Quebrada La Palma runs nearly linearly for several kilometers, and the drainage arriving from its south side is dominated by trellis rather than the more common dendritic pattern. Nearby are a set of truncated spurs. To date no clear evidence of paleoseismicity has been observed, but we continue to inviestigate this possibility.

Paleoseismology of Blind Thrusts through Analysis of their Fault-Related Folds

K. J. Mueller and J. Suppe, Department of Geological and Geophysical Sciences,
Princeton University, Princeton, New Jersey 08544

Recent earthquakes in California, including the M 6.8 Northridge (1994), M 6.0 Whittier Narrows (1987) and M 6.5 Coalinga (1983) events, demonstrate the destructive nature of earthquakes on blind-thrust faults. Blind-thrust faults include both low-angle thrust ramps and flats and high-angle reverse faults below drape folds, that do not cut the Earth's surface. Because the paleoseismic history of faults which rupture the surface are typically assessed by trenching across the fault trace, blind thrusts require other methods of investigation to determine their seismic risk. Blind-thrust faults do, however, have surface expression in the form of overlying fault-related folds that grow or uplift coseismically during large earthquakes. Fault-related folds are a direct result of slip across bends in underlying thrust faults. Syntectonic or growth sediments that are deposited at the surface during active slip on underlying blind thrusts develop distinctive fold geometries. A characteristic feature of these folds includes narrowing upward kink-bands in the syntectonic section, termed growth triangles, that record the rate of fold growth and fault slip. The recent development of quantitative theories that relate folding and faulting, the occurrence of well monitored blind fault earthquakes and our study of syntectonic sediments deformed by trench scale folds allow us to assess the seismic hazards and past slip behaviour of blind-thrust faults.

Analysis of deep structure in the Los Angeles Basin using seismic reflection data has determined the geometry and long-term slip history of active blind thrust faults and their related folds (Shaw, 1993). Comparison of active axial surfaces with pre-urbanization aerial photos and topographic maps indicate that surface deformation is localized along narrow zones. These narrow zones of deformation, or kink-bands, record recent folding events, or earthquakes on the causative blind thrusts. Earlier recognition of this surface deformation prompted an extensive trenching study on the northeastern margin of the Baldwin Hills. This systematic search for high-angle faulting across the narrow zone of surface deformation uncovered dateable Holocene stratigraphy, but no surface rupture associated with high-angle faults (Figure 1). Trench logs completed for this work indicate that dated Holocene peats are deformed by trench-scale folds, defining a syntectonic growth triangle. Two cycles of Holocene stratal onlap against paleo-kink bands indicate two folding events; at 4200 ybp and 2200 ybp. These kink bands are about 1.5 and 2.0 meters wide, indicating slip events on the causative blind thrust fault of similar amounts (Figure 2A). An older, undated kink-band displays about 3.5 meters of slip. The periodicity of the folding events and their magnitude broadly correspond with the calculated long-term slip rate on the causative blind thrust, and the predicted magnitude and recurrence interval of earthquakes expected to occur along it (Shaw, 1993).

Study of other fault-related folds developed above blind thrusts in California illustrates the remarkable paleoseismic record contained in syntectonic sediments which onlap their flanks. Wheeler Ridge, an active anticline in the northernmost Transverse Ranges is a fault-bend fold developed above a well constrained wedge structure at depth (Figure 2B). The relatively shallow, small displacement thrusts which comprise the wedge structure are linked with the major, north-vergent White Wolf thrust at depth. Syntectonic sediments have been continuously deposited across an active axial surface at the base of the fold and are subsequently carried up its front limb during paleo-folding events, forming a growth triangle. The most recently uplifted parts of Wheeler Ridge have not been significntly eroded. This, and the shallow depth of the blind thrusts comprising the wedge tip (eg.< 2 kilometers) contribute to the remarkable record of paleo-folding events present there.

Evidence for paleofolding events is preserved as an array of sharply defined, small-scale anticlines spaced 2-4 meters apart on the upper surface of the growth triangle. Each micro-anticline, which lie parallel to Wheeler Ridge, records the former postions of the active axial surface, now at the base of the rangefront. The trench-scale folds are not eroded at the recently uplifted base of the structure; they appear progressively more eroded on the older, higher parts of the front limb, in accordance with the overall kinematic development of Wheeler Ridge. Fold-growth events documented by the small-scale anticlines is predicted to be equivalent to slip on the blind thrusts forming the wedge-tip at depth, based on fault-related fold theory. The 30+ kilometer extent of the fold front, and the 2-4 meter fault displacements predicted from the size of related trench-scale anticlines suggest that paleo-folding events may be associated with blind thrust earthquakes of destructive magnitudes.

The regularly spaced nature of the numerous trench-scale anticlines preserved on the front limb of Wheeler Ridge suggest that earthquakes on the causative blind thrust(s) are broadly characteristic in nature. The lateral extent of successive trench-scale anticlines is expressed as tear faults, visible as a series of unevenly-spaced fault scarps of varied height preserved on the easternmost plunge panel. We interpret these tear faults to represent the former positions of the lateral temination of the underlying blind thrust.

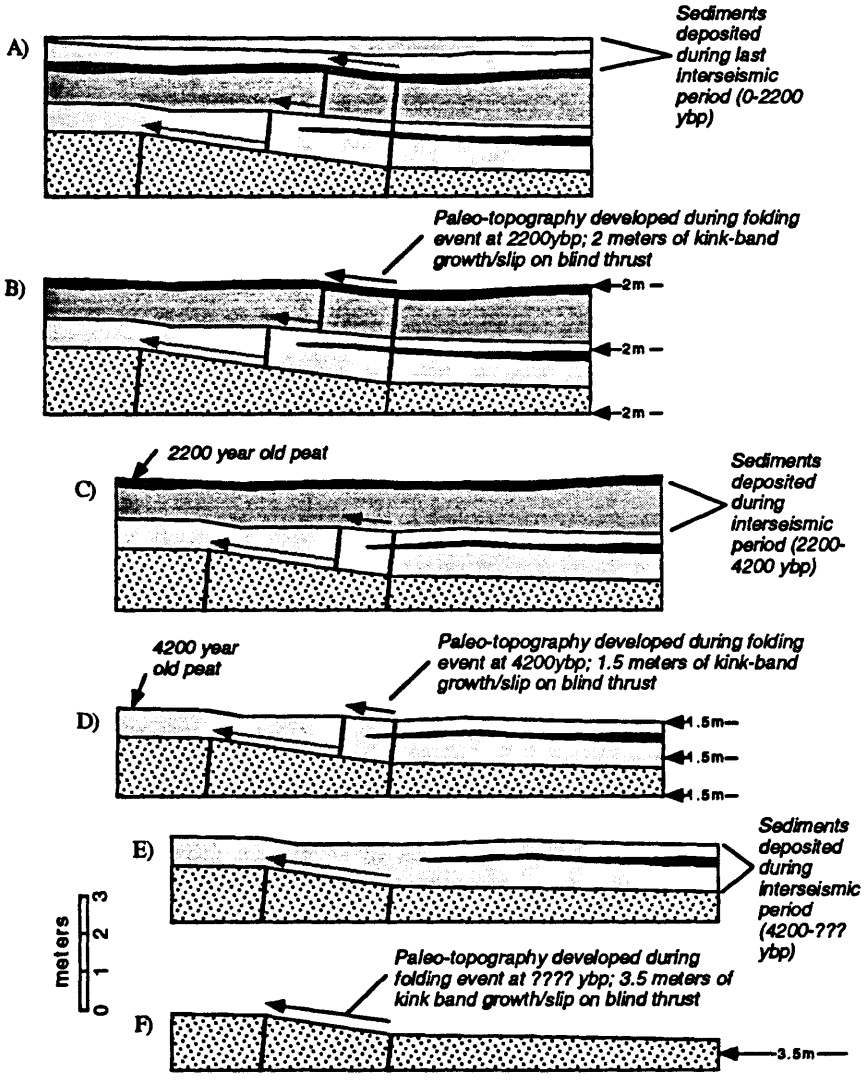

Figure 1. Portion of a trench log excavated across an active synclinal axial surface in the eastern Baldwin Hills, LA basin. 1A is a portion of the trench log as it now appears. Note th stepped nature of inactive axial surfaces in the Holocene sediments. 1B depicts kink-band topography developed at ca. 2200 ybp from a paleo-folding event. This surface feature is present in adjacent areas of lower sedimentation rate as a linear, low angle rise in regional topography. 1C depicts the trench with the latest folding event unfolded, or retrodeformed. 1D illustrates the topography of the site at about 4400 ybp, after an earlier folding event. Frames 1E and 1F depict sedimention and an earlier, undated folding event. Data provided by Moran and Associates, Tustin, California,

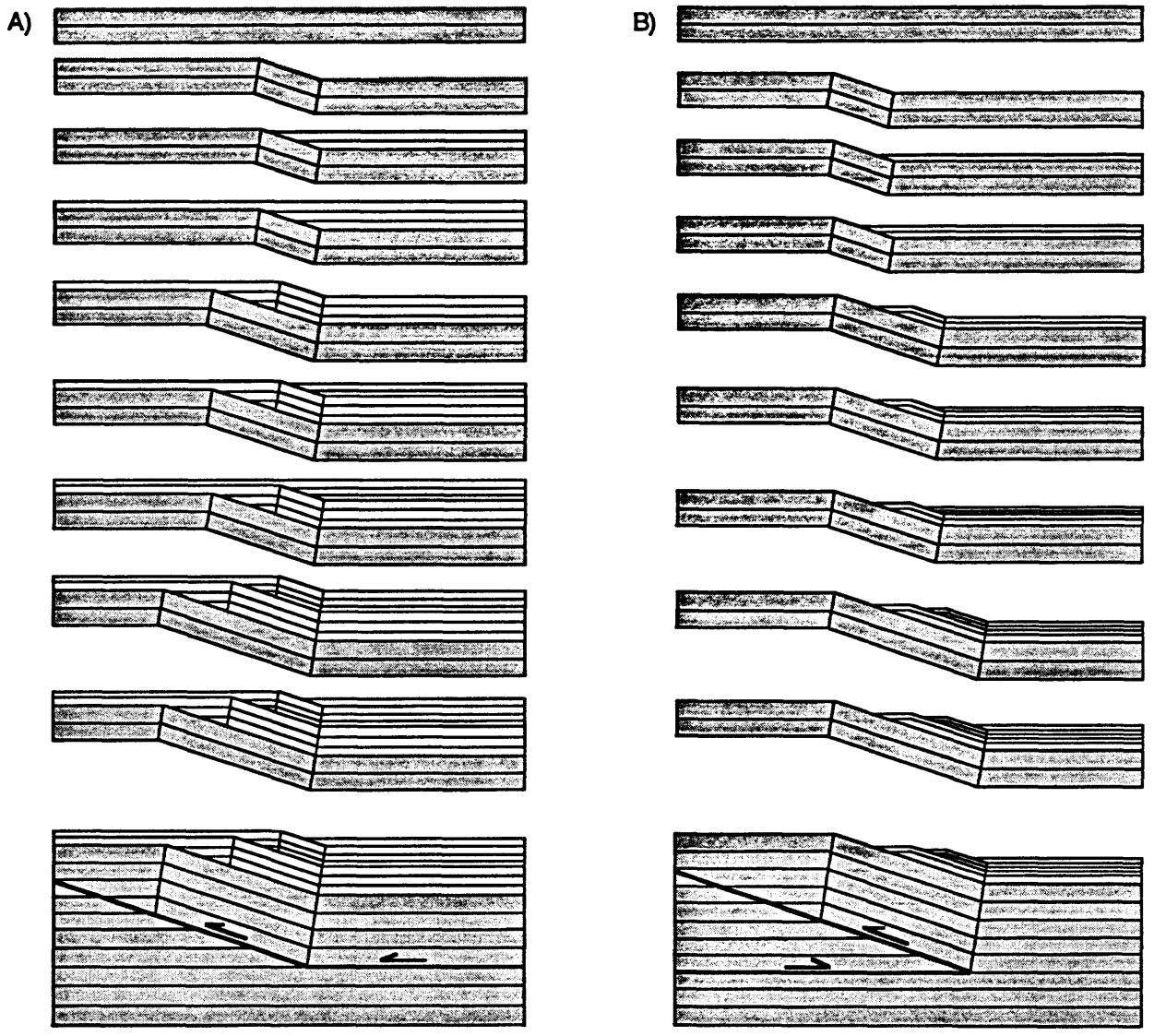

Figure 2. Models of trench-scale stratigraphic packages which onlap against kink-bands developed above blind thust faults. Stippled areas denote pre-growth strata; unpatterned units denote syntectonic growth strata. Note the constant thickness of pre-growth units and the variable thickness of syntectonic units. Active axial surfaces are pinned to bends in faults at depth. Figure 2A illustrates paleofolding events at an active, synclinal axial surface developed at the base of a thrust ramp. Sedimentation here is more rapid than uplift. Slip on the underlying thrust fault produces kink-bands, whose width corrresponds to fault slip on causative faults. Fold growth for each event is the distance between trench-scale, anticlinal axial surfaces in the syntectonic strata. Figure 2A illustrates a growth triangle documented in trenches in the eastern Baldwin Hills, LA basin. Figure 2B defines paleofolding events at an active, synclinal axial surface above a wedge tip exposured on the front limb of Wheeler Ridge anticline. Note the topographic expression of the fold limb, developed in an area where burial is less rapid than thrust derived uplift. In 2B the active synclinal axial surface migrates through the strata fixed in front of the wedge tip. The active synclinal axial surface in Figure 2A remains fixed with time.

Paleoseismological Behavior of Sea Floor Active Faults in Beppu Bay, Kyushu, Japan

Takashi Nakata, Department of Geography, Hiroshima University
Higashi-Hiroshima 724, Japan
Kunihiko Shimazaki, Earthquake Research Institute, University of Tokyo
Tokyo 113, Japan
Noboru Chida, Department of Geography, Oita University, Oita 870-11, Japan
Makoto Okamura, Department of Geology, Kochi University, Kochi 780, Japan
Takashi Miyatake, Earthquake Research Institute, University of Tokyo
Tokyo 113, Japan
Toshio Nakamura, Dating and Material Research Center, Nagoya University
Nagoya 464-01, Japan

On shallow sea floor, if sedimentation rate much exceeds slip rate of active faults, history of seismic activities is well preserved in sub-bottom layers as cumulatively faulted structures. Time-predictable model (Shimazaki and Nakata,1980) and characteristic earthquake model (Schwarz and Coppersmith,1984) are widely accepted models for long-term earthquake prediction proposed by paleoseismological studies. We tested these two models on sea floor active faults in Beppu Bay where the sedimentation rate of late Holocene layers is estimated about 2mm per year against slip rates of the active faults around 0.6mm per year.

Seismic profiling in the western part of Beppu bay delineates a cluster of WNW - ESE parallel-running active faults of normal dip-slip beneath the 40 - 60m sea floor . It is easy to estimate amounts of cumulative fault displacements from distinct acoustic layers in the profile.

We collected samples by piston coring on the both sides of Toyooka-oki fault, for radiocarbon AMS dating in order to correlate faulted layers. In general, dated layers on one side of the fault are not correlated to those on the other side. We correlated faulted layers based on a sedimentation curve on the upthrown side of the fault. As a result, we restored timing and displacement of the past events as 2250, 3600, 4500 and 5900y.B.P., and 130, 70, 60 and 100cm respectively. The time-displacement diagram we restored shows a regularity consistent with the time-predictable model, that is, the larger is a slip, the longer is the subsequent time interval till the next event.

In order to understand slip distribution along the length of the faults, we set profile lines roughly 250m apart almost perpendicular to strike of the faults. Variation of slip along the length of the fault is that the larger is the previous slip, the larger is the subsequent slip among the successive events. This corresponds to the characteristic earthquake model, but size of each event varies with time, and it is an important difference between our observation and this model.

A POTENTIAL RECORD OF TSUNAMIS GENERATED BY GREAT EARTHQUAKES ALONG THE SOUTHERN CASCADIA SUBDUCTION ZONE

Alan R. Nelson, Branch of Earthquake and Landslide Hazards,
U.S. Geological Survey, MS 966, Box 25046, Denver, CO 80225;
Harvey M. Kelsey, Dept. of Geology, Humboldt State University, Arcata, CA 95521;
Eileen Hemphill-Haley, Branch of Pacific Marine Geology, U.S. Geological Survey
at Dept. of Geological Sciences, University of Oregon, Eugene, OR 97403; and
Robert C. Witter, Dept. of Geological Sciences, University of Oregon, Eugene, OR 97403

The magnitude and recurrence times of past great earthquakes along the Cascadia continental margin are important issues in seismic hazard assessment in the U.S. Pacific Northwest. Some argue that the most recent subduction-zone earthquake had a magnitude of 9 (e.g., plate-boundary rupture >500 km long), smilar to the 1964 earthquake in Alaska, and that such an event is typical of the Cascadia subduction zone. Others, citing analogies with historic earthquakes in other suduction zones, suggest that a segmented margin with more frequent magnitude 8 earthquakes (e.g., 100-to-300-km-long ruptures) is more plausible. Recurrence times are also uncertain, with some scientists arguing for average repeat times for M>8 earthquakes of 300 years, and others pointing out that evidence for more than two great earthquakes in the past few thousand years is not widely documented. High-precision ^{14}C dating of trees killed by sudden subsidence at four coastal sites do not rule out an earthquake rupture that may have extended from central Washington to Humboldt Bay, California, about A.D. 1680-1720. A more recent study of correlative buried soils, which are dated with the means of eight marsh-plant AMS ^{14}C ages, does not rule out synchronous subsidence at seven sites along 440 km of the Oregon and Washington coast. Such ages are consistent with either a magnitude 9 earthquake or a series of magnitude 8 earthquakes after A.D. 1650.

The question of whether or not the most recent subduction-zone earthquake was a giant earthquake of magnitude 9, as well as the magnitude and recurrence of earlier earthquakes, is difficult to address because so little paleoseismological work has been completed in the southern half of the Cascadia zone. Precisely dated trees in Humboldt Bay are 530 km south of the nearest other site with dated trees. The only site with precisely dated marsh plants in central and southern Oregon is on the Coquille River, 260 km north of Humboldt Bay. Most paleoseismicity studies along the Cascadia margin have focused on the extensive marshes in northern Oregon, southern Washington, or in the Humboldt Bay region. Such marshes are not found along the steep, rocky coast of the southern part of the subduction zone. Furthermore, the paleoseismic record in the southern Cascadia forearc is probably more complex than the record farther north because the active fold and thrust belt extends on land in this region—coseismic uplift or subsidence of coastal sites in the belt may or may not be synchronous with great earthquakes on the plate boundary.

To deal with the question of the magnitude of the most recent great earthquake and to begin to decipher the complex paleoseismic record of southern Oregon we are taking a new approach—one that emphasizes field mapping and precise dating of tsunami deposits and accompanying land-level changes in adjacent but *contrasting* environmental settings. Unlike earlier work in more northerly marshes, we will collect independent types of evidence of great earthquakes in both brackish-water estuaries and nearby freshwater coastal lakes. An important aspect of the tsunami investigation will be estimating the inundation level (a crude measure of tsunami magnitude) of the most recent and possibily earlier tsunamis. Through detailed stratigraphic and laboratory studies we hope to answer the following questions:

- Did the tsunami generated by the most recent great earthquake in southern Washington and northern Oregon also strike the southern Oregon coast?

- How large was this earthquake; in other words, how far south in Oregon did coseismic land-level changes extend and what was the inundation level of its attendant tsunami?
- How can deposits from local or regional tsunamis be distinguished from the deposits of large storms or floods in southern Oregon?
- Did locally generated tsunamis accompany older great earthquakes in southern Oregon?
- Were the older tsunamis as large as the most recent one?
- Did parts of the coast abruptly rise or fall during any of these earthquakes?
- What is the relation of the timing of older earthquakes to those inferred from the tidal-marsh records of northern Oregon, southern Washington, and the Humboldt Bay region?

Results from the initial lake-coring phase of the project suggest tsunami deposits from repeated great earthquakes may be preserved in low-lying lakes along the southern Oregon coast. From a platform suspended between two canoes, we collected 2-to-6-m-long cores from two or three sites in each of four coastal lakes between Cape Blanco and the Coquille River using a Livingston piston corer. Several small rivers that cross this coastal plain flow into lakes at their downstream ends where sandy barriers block their mouths. We selected lakes with different water-level elevations, surface areas, barrier heights, distances from the coast, and drainage basin sizes along a 40-km segment of coast to see how these factors affect the recoverable sediment record. Most cores could be pushed 2.5-3.0 m into lake sediment before bottoming in unconsolidated medium to coarse sand. These sites were on the oceanward side of the lake, yet far enough from lake-shore dunes to minimize the deposition of wind-blown sand.

The stratigraphy in three of the four lakes (Floras, Croft and Bradley Lakes) consisted of silty clay and clayey gyttja interrupted by sandy intervals. In all lakes, lacustrine sediment apparently overlies dune sand (2-4-ka) that predates the rise of the lakes to their current levels. Sediment in the two deeper lakes (Floras Lake and Bradley Lake) consisted of well-laminated silty clay and clayey gyttja; some of these laminae may be varves. Water at these core sites is deep enough (10 m) that bottom waters do not turn over seasonally. The anoxic bottom water apparently prevented bioturbation, which would disturb sediment laminae.

In most cores, the sandy intervals that may be tsunami deposits are capped by woody debris consisting of detrital leaves, conifer needles, fragments of herbaceous and woody plant roots, and sticks. AMS ^{14}C ages on some of the most fragile materials (those least likely to be reworked), such as the deciduous tree leaves in cores from Bradley and Floras Lakes, provide ages for the times of sand deposition in each core. The five ages obtained so far suggest unusual events of sand deposition at about 0.3 ka, 1.0 ka, and 1.6 ka (e.g., Fig. 1). The youngest and oldest times of sand deposition match the ages of the two most widespread buried marsh soils farther north in Oregon that have been inferred to record regional coastal subsidence during great earthquakes.

The two Bradley Lake cores (B and C on Fig. 1) show three periods of sand deposition, which correlate between cores. Angular clasts of well-laminated lacustrine clay are enclosed in the middle sand, indicating that flow velocities were fast enough to erode the lake bottom prior to sand deposition. Core B did not penetrate totally through the third (deepest) sand, but the complete recovery of this interval in the more distal core (C) shows it was deposited during four sediment pulses. Each pulse consists of medium sand fining upward to very fine sand or silty sand. The period between pulses was apparently too short for silt to settle out of the water column and form laminae before the next pulse occurred. Preliminary diatom analysis shows that core C sediments are dominated by freshwater diatoms, but that there was an incursion of rare but well preserved planktonic marine diatoms just above the sand at 84 cm. The occurences of these delicate planktonic species in samples overwhelmingly dominated by lake species suggests the diatoms were washed into the lake. If a tsunami carried the sand into the lake, it must have reached an elevation of at least 10 m (Fig. 1).

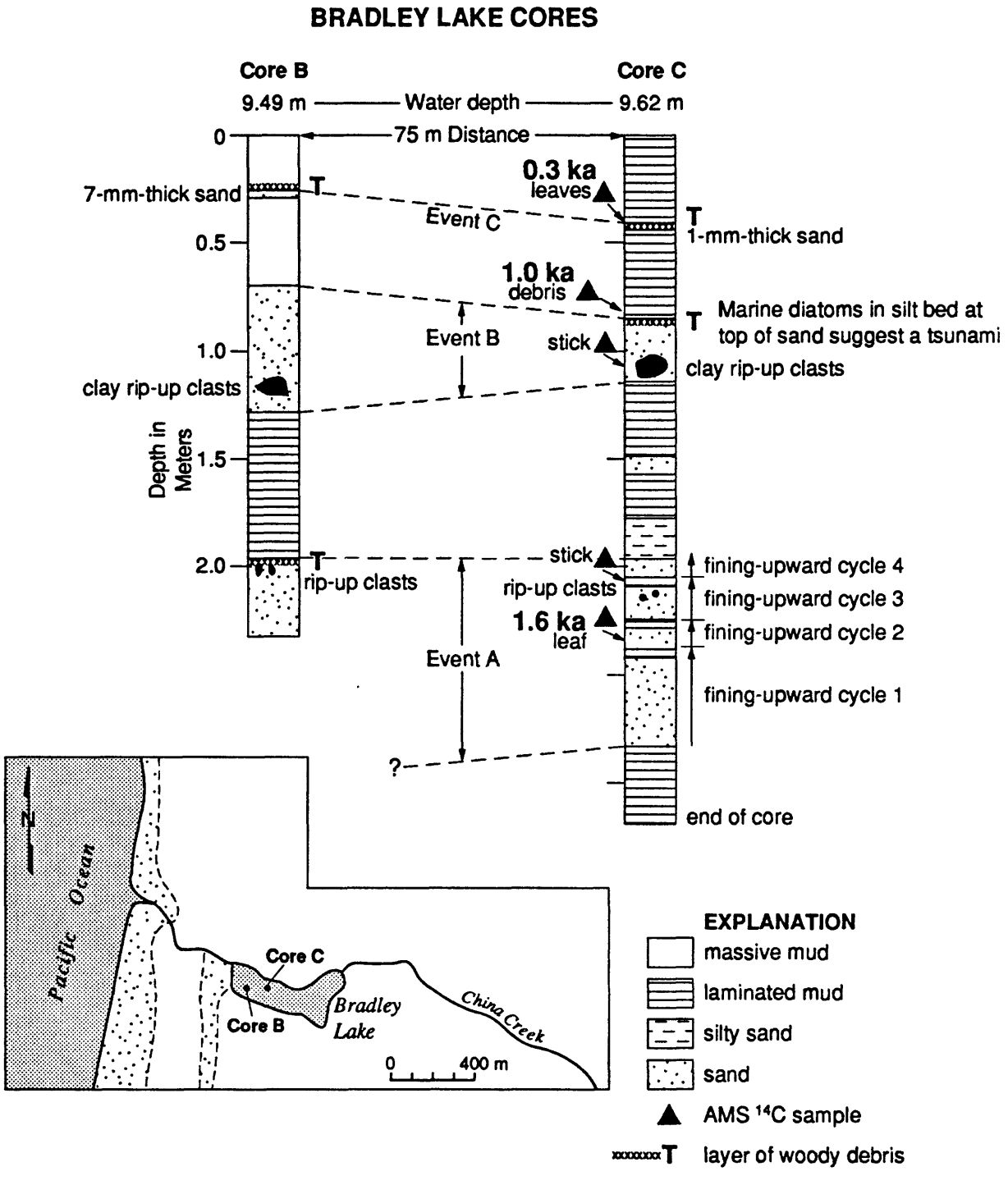

Figure 1. Simplified stratigraphy in two cores from Bradley Lake showing AMS ^{14}C ages and correlation of three sand beds labeled events A, B, and C. The elevation of Bradley Lake is 6 m and the dune that forms the west edge of the lake is about 4 m high. A tsunami capable of depositing sand in the lake would probably have had a runup elevation of at least 10-12 m.

Recognition of Paleoearthquakes within Southern Tien Shan Mountains by Studying of Slope Disturbances

A.A.Nikonov, Joint Institute of Physics of the Earth, RAS,
Moscow, Russia

Occurence of surface ruptures (faults) due to strong earhquakes is commonly rare case within many seismically active regions in comparison with other surficial effects of the earthquakes. So, for mountain regions studying of paleoevents by earthquake-related gravitational deformations is a very important task of paleoseismology.

Solution of this problem in our practice is based upon two main principles: (1) - combined study of relief and deposits in selected areas; (2) - independent (at first) and combined (afterwards) use of some of comparatively precise methods for dating of relief disturbances and associated deposits, such as ^{14}C, lichenometric and archeological techniques.

These principles and techniques were being developed and supplied for such a very seismically active region as southern Tien Shan is. In the region there are two types of areas - epicentral areas of two well-known great earthquakes of the XXth cent., I = 9 -10, and other areas without known previously strong earthquake sources. The former ones have been studied as test areas to learn peculiarities and pattern of earthquake-produced slope disturbances. The latter ones were the objects for recognition of paleoearthquakes by geomorphic and geological traces.

Detailed regional investigations have revealed a number of signs of paleoearthquakes in both of the areas. Their intensities are determined to be not less than I = 8 up to I = 10 in terms of MSK-64 scale. Clustering of old seismic-like slope disturbances in space and time enable us to bound some epicentral areas of paleoearthquakes. Part of them are in good coincidence with known epicentral areas of the XXth cent., but others are singled out to be located rather far from them.

Age determinations of studied deformations by ^{14}C and lichenometric methods led to the conclusion about the recurrence of strong earthquakes within the same epicentral areas during past 5 Kyr. Recurrence intervals of strong earthquakes for the studied areas turned out to vary from 200 to 1200 years.

Seismic archaeology: Using human prehistory to date paleoearthquakes and assess deformation rates of active fault zones

J.S. Noller, W.R. Lettis, and G.D. Simpson, William Lettis & Associates, 1000 Broadway, Suite 612, Oakland, CA 94607

The melding of traditional paleoseismic and archaeologic methods provides a new means to estimate the age of paleoearthquakes and rates of deformation of active seismogenic structures. Our seismic archaeology investigations focus on strike-slip faults belonging to the northern San Andreas Fault System: the northern San Andreas fault at Fort Ross and the northern San Gregorio fault zone at Seal Cove. Archaeological sites of appropriate ages are common in northern coastal California and locally they overlie active faults. We have developed and used this new approach to assess Holocene activity, style of deformation, rate of slip, event stratigraphy, and slip per event. The application of this approach requires the closely coordinated efforts of both a paleoseismologist and an archaeologist.

Native Americans lived on faults just as modern-day Californians do, and their habitation sites and structures were offset by surface-rupturing earthquakes as occurs with modern structures. Archaeological sites provide a wealth of artifacts (fossils) that can provide correlative and relative age estimates for lithologic units. Different types of archaeological features can be used to define piercing points across a fault (Figure 1). These include the outer site margin, margins of components or units (e.g., shell-rich zone) within the site, structures such as a meeting house, and geometric features such as the lip of a roasting pit.

Our estimates of paleoearthquake age, earthquake recurrence, slip rate, and slip per event at Fort Ross are compatible with "traditional" paleoseismic studies of offset fluvial deposits at other sites on the northern San Andreas fault. At the Archae Camp site, the main habitation site is located east of the single 1906 fault trace through this area. Events are recognized by disrupted anthropogenic and scarp-derived deposits. Slip-rate estimates are based on the distance a piercing line of known age is offset along the fault. In this case, we define two piercing lines on the basis of age and assemblage of artifacts. Along the northwestern margin of the Archae Camp site we documented the location and age of artifact concentration (locus) bisected by the fault. For example, using the centroid of this locus, which is offset by 26 m and is 1,200 to 1,400 years old, we preliminarily estimate a late Holocene slip rate of 19 to 22 mm yr^{-1}. In trench excavations at this site we recognize six surface-rupturing events that occurred during the past 2,500 to 3,000 years. On the basis of these estimates we calculate an average earthquake recurrence interval of 300 to 350 years, and an average slip per event of 4 to 5 m.

Our investigations at Seal Cove, where a lack of a traditional paleoseismic site precludes a traditional study, provide the first estimate of event timing and well-constrained Holocene slip rate for the San Gregorio fault. Here our archaeologic and geologic excavations cross two parallel strands of the fault. The western strand bisects an archaeological site (shell and lithic midden), whereas the eastern strand lies east of the site boundary and bisects a pond. The last two events on the western trace occurred during the occupation of this site. Using a closely spaced array of shallow auger borings,

we defined an 12 to 18 m right-lateral offset in the northern margin of the site. On the basis of archaeological artifacts (numeric age estimates are pending) the median site age is about 4,000 years old. Assuming the margin of this site corresponds to this age, we preliminarily estimate a Holocene slip rate of about 3 to 4 mm yr^{-1} on the western strand.

Seismic archaeology investigations also have limitations. These include alternative explanations of irregular site boundaries, uncertainties in estimating ages of features within a site, and the political issues of excavating an archaeological site.

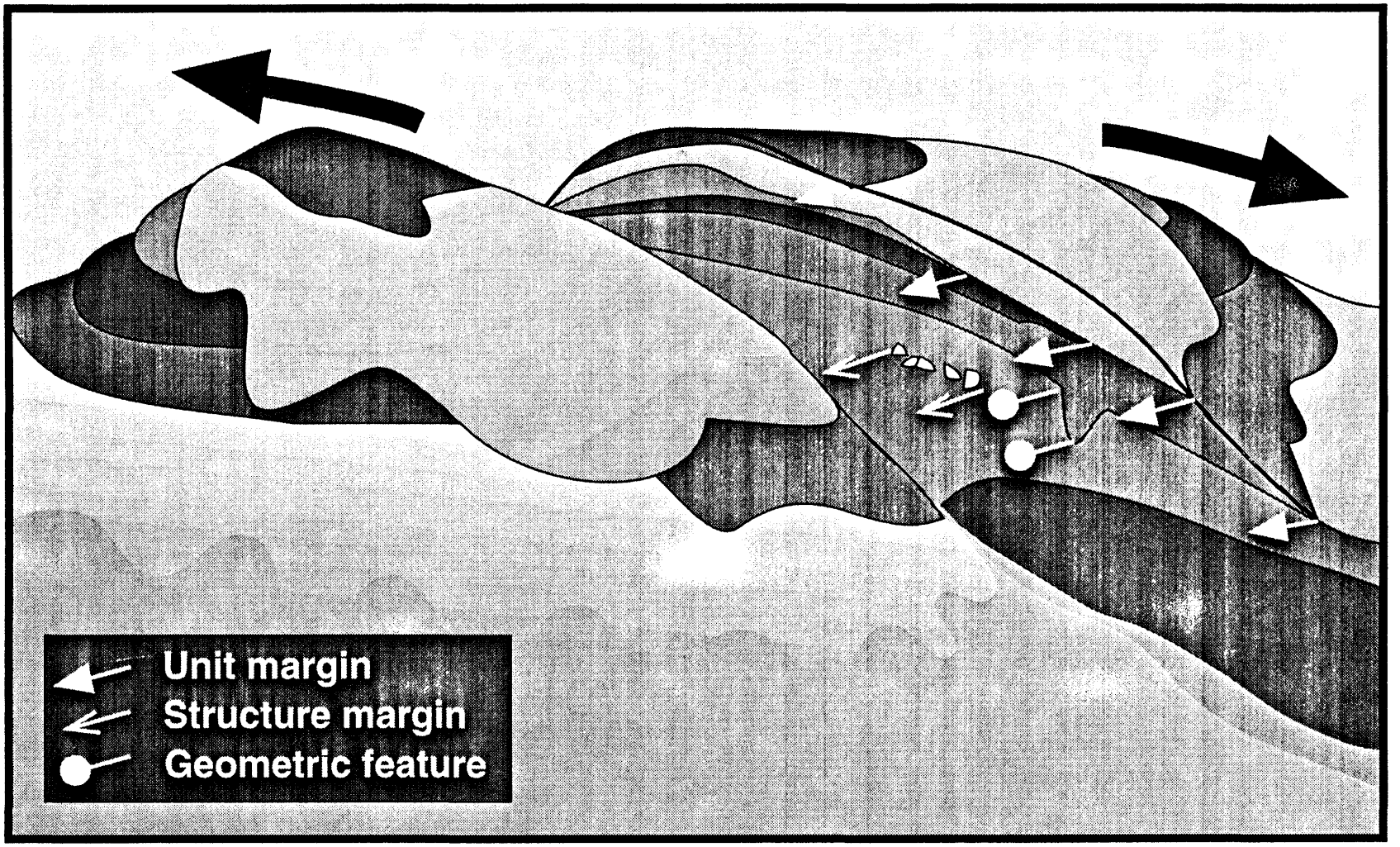

Figure 1. Fault offset of a typical coastal California midden reveals three types of piercing points. Piercing points are defined by the margins of components or units, margins of structures such as hearths, and geometric features such as lip or base of roasting pits.

Paleoliquefaction Effects as Indicators of Strong Prehistoric Earthquakes

S.F. Obermeier, U.S. Geological Survey, Mail Stop 922, Reston, Virginia, 22092

Paleoliquefaction studies are particularly useful to engineers and planners because of the relatively strong shaking required to develop features such as dikes and sills. The threshold is an acceleration of about 0.1 g even in highly susceptible sediments. Worldwide historical data show that the minimum magnitude generally is on the order of 5.5 or higher.

Paleoliquefaction studies are being conducted extensively in the United States because of the short historical record, because of the absence of surface faults in many regions, and because effects of liquefaction sometimes can be used to estimate the magnitude of prehistoric earthquakes. Within the past 10 years, paleoliquefaction studies have shown that very strong Holocene earthquakes (M probably $\approx$7.5) have struck repeatedly in the eastern and central United States, and that a great (M$\approx$8) earthquake struck the coast of Washington State about 300 years ago.

Huge geographic regions in the United States are amenable to paleoliquefaction studies. The best study regions are where there are thick deposits of granular sediments (preferably greater than several meters in thickness) with a thin capping sediment (2 to 6 m in thickness) and a shallow groundwater table (< several meters). Where the ground water table has remained shallow since deposition, sediments can retain a high susceptibility to liquefaction for more than 10,000 years. Clean sands are the most susceptible to liquefaction, but silty very fine sands and gravelly sands (<40 to 50 percent gravel) are also quite susceptible in many field situations.

Field searches for paleoliquefaction effects often can be made very efficiently by using a boat to search the banks of actively eroding streams. Manmade ditches and trenches are sometime used. Ground-penetrating radar is an approach with much promise.

An estimate of prehistoric magnitude can be made where the regional pattern of dikes can be determined for a specific earthquake. Ages of dikes often can be tightly constrained where there was venting to the surface. Techniques for bracketing the ages of dikes make use of stratigraphic relations, radiocarbon ages, and archeological and pedological data.

The regional pattern involves mainly determining maximum dike widths at many widely scattered sites. For the same geologic setting, the largest (widest) dikes occur where shaking has been strongest. These largest features generally have formed by lateral spreading of the ground. Observations of dike density, in terms of number of dikes per unit of outcrop, can also be useful. Dike density, however, is subject to more uncertainties than maximum dike width. Dike density, for example, is highly sensitive to cap thickness, whereas lateral spreading is not.

A number of independent engineering-seismologic procedures can be used to estimate the prehistoric magnitude. Both the dike widths and their regional development can be used to estimate

minimum magnitudes (see for example, Youd and Bartlett, 1992, Empirical Analysis of Horizontal Ground Displacement Generated by Liquefaction-Induced Lateral Spreads: Technical Report NCEER-92-0021, State University of New York at Buffalo; see also Obermeier et al., 1993, Liquefaction Evidence for One or More Strong Holocene Earthquakes in the Wabash Valley of Southern Indiana and Illinois, with a Preliminary Estimate of Magnitude: U.S. Geological Survey Professional Paper 1536.) Seed's procedure can be used to estimate peak accelerations; this procedure is not dependent on locating most distal liquefaction effects. Comparing back-calculated peak accelerations at many widely scattered sites with estimates from seismological models permits assessment of the magnitude of prehistoric earthquakes. (Seed's procedure is described in the article by Seed et al., 1983, Evaluation of Liquefaction Potential using Field Performace Data: American Society of Civil Engineers, Journal of Geotechnical Engineering, v.#109; adjustment of accelerations using Seed's procedure, in terms of probability, can be done by using curves given by Liao et al., 1988, Regression Models for Evaluating Liquefaction Probability: American Society of Civil Engineers, Journal of Geotechnical Engineering, v.#114.)

Surface Faulting on the North Anatolian Fault in These two Millennia

Koji Okumura and Toshikazu Yoshioka
Geological Survey of Japan, 1-1-3 Higashi, Tsukuba, Ibaraki 305, Japan
Ismail Kusçu, MTA General Directorate, Ankara, Turkey

The North Anatolian fault is an important laboratory for substantial segmentation of a strike-slip fault. The series of faulting events during 1939-1967 is one of the most striking observed example of fault segmentation on land. About 850 km of the strand faulted in 3 gigantic (1939, 1943, and 1944) and 3 fairly large (1942, 1957 and 1967) earthquakes with westward epicentral migration (figure 1). Comparison of this series of earthquakes with previous ones should be a key to understand the behavior of strike-slip faults in time and space. However, geologic information on the past activity of the fault has been very limited until late 1980s when detailed survey of recent ruptures including exploratory trenches is introduced to Turkey. At the same time, historic documents were so sparse that only a few events of 1668 A.D. (Ambraseys and Finkel, 1988) and of 1784 A.D. (Barka, 1992) and a few periods of higher activity (Ambraseys, 1975) have been inferred.

Turkey-Japan joint research on the paleoseismology of the North Anatolian fault began in 1989 and has investigated three segments of 1939, 1944, and 1784? [There has been no surface faulting in this century according to Barka(1992).]. Now for the first time, it is being possible to compare time-series of surface faulting events on different segments.

In a trench east of Gerede (40°49'23"N, 32°20'27"E) on the 1944 (Bolu-Gerede) surface fault, we recognized 8 earthquake events since around 30 B.C. Average recurrence interval is estimated to be between 200 and 300 years (figure 2). On the 1784? surface fault, a trench east of Erzincan (39°36'21"N, 39°51'23"E) showed 5 events during these about 1000 years. According to 30 radiocarbon dates, the estimate of the average recurrence interval is between 200 to 250 years. On the 1939 (Erzincan) surface fault, a trench was opened near Susehri (40°02'46"N, 38°33'44"E) in 1993. We recognized two events in the trench and now dating is under way.

Comparing the result from 1944 fault with that from 1784? fault, the timing and the recurrence interval of faulting events in these two segments are probably not the same. This may mean that the westward migration in this century is just a coincidence, or that each segment has different rupture history. Another possible explanation is that in 1784? trench occurence of fairly large earthquakes like 1942, 1951 are recorded in addition to the gigantic ones, while the Gerede trench showed only the gigantic ones. Higher resolution in time will be the key to answer such question.

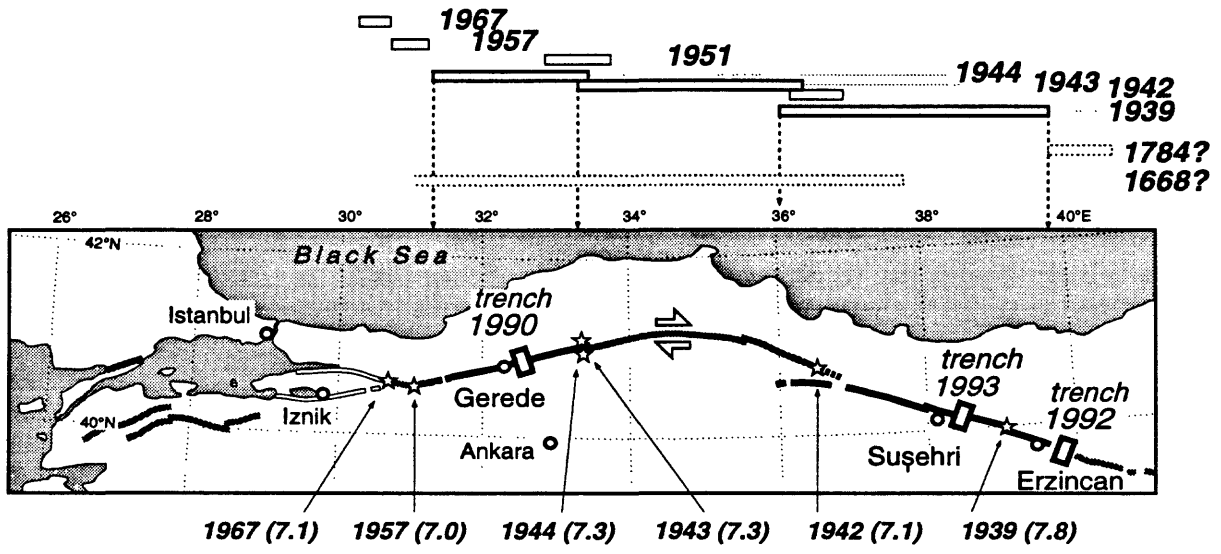

Figure 1. Segmentation and epicentral migration of the North Anatolian fault with the localities of exploratory trenches. Surface faults and epicenters are after Ambraseys (1988).

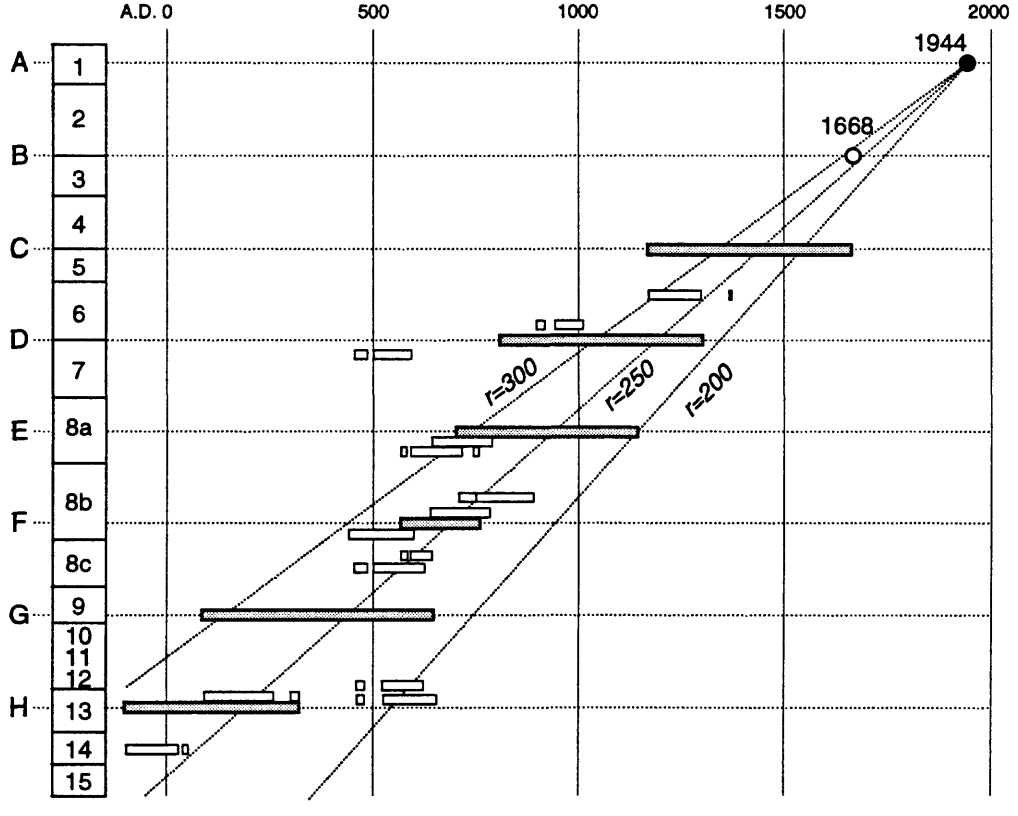

Figure 2. Time-series of surface faulting events on the 1944 (Bolu-Gerede) segement.
open bar: dendrocorrected radiocarbon age, shaded bar: possible age range of an event.

Preliminary interpretations of temporal surface-faulting patterns on the southern Lost River fault zone, northeastern Basin and Range Province, USA

Susan S. Olig, Andrew E. Gorton, Jacqueline D. Bott, and Ivan G. Wong, Woodward-Clyde Federal Services, 500 12th St., Suite 100, Oakland, CA 94607-4014
Peter L. K. Knuepfer, Department of Geological Sciences, Binghamton University, Binghamton, NY 13902-6000
Steven L. Forman, Byrd Polar Research Center, Ohio State University, 1090 Carmack Rd. Columbus, Ohio 43210-1002
Richard P. Smith, EG&G Idaho, Inc., Idaho National Engineering Laboratory, P.O. Box 1625, Idaho Falls, ID 83415

The timing of surface-faulting events on the southern Lost River fault zone (LRFZ) provides some additional key insights into understanding patterns of fault behavior in the northeastern Basin and Range Province and how it may relate to volcanic activity in the eastern Snake River Plain (ESRP). Evidence for temporal clustering of surface-faulting events in southeastern Idaho has been identified along the central segments of the LRFZ and along the central and southern segments of the Lemhi fault zone (see Hemphill-Haley et al., this volume; and, Knuepfer, this volume), but generally little is known about the timing of individual events on the Pass Creek and Arco segments of the southern LRFZ. In addition, the timing of events on the southern LRFZ is relevant to how fault activity may relate to volcanic activity in the adjacent ESRP, and whether temporal clustering of surface faulting events is related to volcanic activity. Many workers have noted that spatial and temporal patterns of earthquakes and faulting in the region may be influenced, or possibly even controlled by, passage of the Yellowstone hot spot and formation of the ESRP. This is partially based on observations of a parabolic belt of more-recent and higher rates of late Quaternary fault activity that surrounds the track of the hot spot. However, what little was previously known about activity on the Pass Creek segment suggested it did not fit the regional pattern as faulting appeared anomalously old and rates of activity anomalously slow compared to what might be expected from regional patterns.

Trench exposures across faulted pre-Bull Lake and Bull Lake age ($\approx$90 to 200 ka) alluvial fans provide a nearly complete and unusually long record of faulting history along the Pass Creek and Arco segments of the southern LRFZ. Our preliminary interpretation of these exposures suggests that the Arco segment is characterized by tight temporal clustering of events with an order of magnitude difference between intervals within clusters (on the order of thousands of years) and intervals between clusters (at least a couple tens of thousand of years). This pattern is also supported by our reinterpretation of Malde's trench exposure a few kilometers to the north (see Knuepfer, this volume). In contrast, although we may see evidence for temporal clustering on the Pass creek segment, the pattern of activity appears more variable, particularly for intervals within clusters, and the evidence is more indirect. We also found evidence suggesting that the most recent activity along the Pass Creek segment is younger than previously believed and estimated slip rates for the Pass Creek segment are comparable to, or higher than, those for the Arco segment. This suggests that activity on the Pass Creek segment is not anomalously slow or old compared to patterns of activity for other faults in the region, as previously believed.

At the Arco Peak trench site along the Arco segment, we found direct stratigraphic evidence for 4 similar-sized events, and a possible additional smaller event, within the past

70,000 to 150,000 years. Differences in the relative development of soil horizons on a series of stacked, fault-scarp-derived colluvial wedges, suggests the following temporal pattern: a long interval of no surface faulting (the first intercluster period), followed by two to three faulting events closely spaced in time (first cluster of events), followed by another long interval of no faulting (second intercluster period), and then two more events closely spaced in time (second cluster of events). Total net vertical tectonic displacement for these events is 5½ ±¼ m, measured on a Bull Lake age alluvial fan surface. Based on the geomorphic position and degree of soil development, including carbonate-rind thickness, we estimate the fan deposits are probably 90 to 150 ka. A small remnant of loess capping the fan deposits is preserved near the main fault. This loess predates all of the surface-faulting events and could be as young as 70 ka (thermoluminescence ages are pending). This loess, along with the degree of soil development on it and the alluvial fan deposits that directly underlie the first event colluvial wedge, indicates a longer interval (at least tens of thousands of years) between the time of alluvial gravel deposition and the first faulting event, establishing the first intercluster period. Shortly after this event, at least one and possibly two events occurred. Based on the lack of soil development on stacked colluvial wedges, and indirectly on the colluvial wedge geometry, the(se) interval(s) between these events is(are) probably less than a few thousand years. This sequence of two to three events defines the first cluster of events. A relatively better developed soil horizon on the antepenultimate event colluvial wedge is the basis for the second intercluster period, (thermoluminescence analyses of samples from this horizon are pending). Finally, a weakly developed soil horizon on the penultimate event colluvial wedge is directly under the most-recent event colluvial wedge and suggests the most-recent and penultimate events were closely spaced in time and form the second cluster of events (thermoluminescence ages for the most-recent event colluvial wedge are also pending).

Our trenches at the Jaggles Canyon site along the Pass Creek segment exposed three different west-dipping fault zones with direct stratigraphic evidence for five to six surface-faulting events, and indirect evidence for as many as eight events in the past 150,000 to 200,000 years. The minimum surface offset of pre-Bull Lake to Bull Lake age alluvial fan deposits across all three fault zones is 13 ±1 m. Along the easternmost fault, at least two, and probably three, fault-scarp derived colluvial wedges overlie an alluvial wedge which we interpret to also be associated with a fault-scarp forming event. We base this interpretation on the shape of the alluvial wedge deposit and its relation to the fault zone, the orientation of bedding and depositional fabric, and the nature of upper and lower contacts. Indirect stratigraphic and pedologic evidence for as many as three additional older events consists of angular disconformities between buried soil horizons developed on the Pre-Bull Lake to Bull Lake age fan deposits, overlying silty gravels, and colluviated loess exposed west of the fault zone. One of these events may correlate with the second faulting event that occurred on the two westernmost faults. We found direct stratigraphic evidence for two faulting events on the two westernmost faults. The first of these events predates any soil development on the Pre-Bull Lake to Bull Lake age fan deposits and is the oldest event we found evidence for at the Jaggles Canyon trench site. Geomorphic, stratigraphic, and pedologic relations indicate that faulting near Jaggles Canyon has stepped to the northeast (toward the range) through time. If this stepping over of faulting activity closer to the range front and the bedrock-alluvium contact is prevalent elsewhere along the Pass Creek segment, it may partially explain why scarps on alluvium are generally not well-preserved along this segment, although further detailed mapping is needed to test this hypothesis. The lack of fault scarps is somewhat surprising given that we

believe the most recent event could be early Pinedale in age and we estimate comparable or higher slip rates for the Pass Creek segment than the Arco segment, which has prominent fault scarps on Pinedale age ($\approx$40 to 15 ka) alluvium.

LATE QUATERNARY COSEISMIC EVENTS ON THE HUON PENINSULA, PAPUA NEW GUINEA, DEDUCED FROM CORAL TERRACES

Yoko Ota (Senshu University, Kawasaki, Japan) and John Chappell (Australian National University, Canberra, Australia)

A flight of coral terraces, up to *ca.* 1000 m above sea level, are well preserved on the northern coast of the Huon Peninsula, Papua New Guinea, and record the sea level and tectonic history since *ca.* 300 ka on this tectonically active coast, that is located near the boundary between the Western Pacific and Australian plates. The uplift rate since the last interglacial maximum (oxygen isotope stage 5e) ranges from 0.7 m/ka, at the northwest end of the terraced coast, up to 3.5 m/ka towards the southeast end (Chappell, 1974). Holocene and late Pleistocene coseismic uplifts are recorded in these coral terrace sequences.

The study area covers about 50 km of coast. Holocene coral terraces, up to 25 m above sea level, are subdivided into a maximum of seven levels, four to five at most sites. The highest Holocene terrace is the reef crest built during the culmination of the post glacial sea level rise at *ca.* 6-6.6 ka BP. The lower terraces are regressive terraces, which record successive intermittent uplift events, probably caused by great earthquakes (Ota *et al.*, 1993). Along the southern coast of the study area, uplift events dating from *ca.* 5.4 ka, 3.9-3.5 ka, 2.9-2.5 ka, 1.9-1.6 ka, 1.5-1.3 ka, and 0.9-0.8 ka are identified. The timing of each uplift event differs locally, implying that there are at least three tectonic subregions on this coast.

Similar small regressive terraces are found from the detailed profiles of late Pleistocene terraces. For example, in the southernmost part of the study area, 9 extra steps occur between transgressive terrace IIIa upper (*ca.* 53 ka) and terrace II (*ca.* 33 ka), and at least 5 steps between terrace II and terrace I(*ca.* 6.5 ka). Thus, we infer that repeated meter-scale uplift events have occurred at least since *ca.* 53 ka ago. The apparent interval of about 2-5 ka, is longer than the interval between Holocene coseismic uplift events, probably because some coseismic uplift features were eroded.

Such meter-scale uplifts with longer recurrence intervals (ka-scale interval) suggest a different or more complex earthquake deformation cycle from that inferred for the centimeter-scale coseismic uplift associated with the 1992 May earthquake (M=7.3) (Pandolfi *et al.*, 1994). Such small events with shorter recurrence intervals are apparently not preserved geomorphologically as regressive terraces.

QUATERNARY PALEOSEISMOLOGY AND NEOGENE TECTONICS AT YUCCA MOUNTAIN, NEVADA

S. K. Pezzopane, US Geological Survey, Yucca Mountain Project, Denver, Colorado 80225
C. M. Menges, US Geological Survey, Yucca Mountain Project, Las Vegas, Nevada 89109
J. W. Whitney, US Geological Survey, Yucca Mountain Project, Denver, Colorado 80225

Yucca Mountain is a dissected Miocene volcanic plateau on the western boundary of the Nevada Test Site in the central southern Basin and Range Province. The US Congress designated Yucca Mountain to be characterized for the potential long-term storage of the nation's high-level radioactive waste. Our efforts are aimed at providing the geologic and paleoseismic data necessary to characterize the Quaternary fault activity and Neogene tectonics for use in a probabilistic seismic hazard analysis. In addition to providing input for the hazard assessments, the observations and results of ongoing site characterization are increasing our understanding of the spatial and temporal characteristics of Quaternary faults in regions where strain rates are uncommonly low and earthquake activity is infrequent, but apparently continuous over hundreds of thousands of years. The datasets provide insight into fault segmentation and earthquake recurrence models, particularly for low-strain-rate faults, which are rarely studied, and have implications for kinematic and tectonic models of Basin and Range faults and for seismic hazards in regions of the western US that are faulted, but seismically quiescent. For extensional magmatic regions like the Basin and Range, the data may help researchers formulate alternative tectonic models that couple volcanic and seismic processes. Vigorous efforts to date different materials with a variety of techniques should provide insight into the merits of each and ultimately produce an improved chronology of Quaternary deposits and paleoclimate in the region. This abstract introduces many of these issues as they relate to the focus of our work. The paleoseismic and tectonic character of Quaternary faults near Yucca Mountain are discussed in order from closest to farthest from the potential repository.

The faults closest to Yucca Mountain are most important to vibratory ground-motion hazards and critical to fault displacement hazards. Within ~10 km of the repository, roughly 8 of the 14 mapped faults have experience repeated surface-rupturing Quaternary earthquakes. These faults are characterized by lengths shorter than ~20 km, slip rates ranging from 0.001 to 0.05 mm/yr, and average earthquake recurrence intervals of 20,000 to 100,000 years. Most of the Quaternary fault movement has been on the five or six principal normal faults, which all strike approximately north, dip moderately to steeply west, and are commonly spaced only a few km apart. The faults split the mountain into a series of north-striking, gently east-dipping structural blocks, the tops of which form slender parallel ridges and plateaus. Many smaller faults cut across the larger blocks, commonly at oblique angles to the strikes of the major block-bounding normal faults.

One of the smaller intra-block faults within the potential repository block is the Ghost Dance fault, which, based on available data, is a late Neogene structure. The fault lacks a youthful geomorphic expression, and no displacement of late Quaternary alluvium is apparent in trenches across the fault trace. In the central part of the mountain, the fault is expressed best for a length of ~3 km, although it is not unreasonable to project the fault north and south along strike, to connect with adjacent fault splays, for a total length of ~7 km. Although the maximum fault length is proportional to a M 6 to 6.5 event, it is questionable whether the fault extends to seismogenic depths, given its close proximity to more prominent Quaternary faults. Similarly, four, northwest-striking, right-slip faults are mapped within relatively long, narrow, washes northeast of Yucca Mountain. Exposures of the right-slip structures are rare, geomorphic expression is poor, and available paleoseismic data indicate the faults have not been active during Quaternary time. Although these smaller intra-block faults lack evidence of Quaternary activity, it has been difficult to demonstrate conclusively that the faults are not active because older Quaternary deposits are commonly not preserved over the fault traces. Like the Ghost Dance fault, it is unlikely that the right-slip faults act as seismogenic structures by themselves because most are less than ~5 km in

length and are structurally contained within the longer and more pervasive block-bounding normal faults.

Because of their Quaternary activity, potential rupture lengths, and close proximity to Yucca Mountain, three normal faults that play a leading role in the hazard assessment are the Solitario Canyon, Paintbrush Canyon, and the Bow Ridge faults. The Solitario Canyon fault is situated along the western flank of Yucca Mountain, less than one kilometer west of the potential underground repository. The Neogene fault movement is responsible for the topographic expression of Yucca Mountain's crest. The fault is 18 to 20 km in length, along which the southern part splays into two, possibly three, principal traces. At least 12 trenches expose the fault; the best of these display evidence for at least five Quaternary faulting events. Fissures in the fault zone contain tephra that have been correlated to Pleistocene eruptions at volcanic centers nearby. Preliminary paleoseismic evaluations of deposits younger than ~200 ka indicate fault slip rates of 0.01 to 0.02 mm/yr and average earthquake recurrence intervals of 40,000 to 50,000 years.

The Bow Ridge and Paintbrush Canyon faults are about four kilometers east of Yucca Mountain and dip west beneath the repository block. The Bow Ridge fault is probably synthetic to the Paintbrush because it is located only ~2 km from the much longer Paintbrush Canyon fault, merging with it at the southern end, and has only one-third to one-half the cumulative vertical separation of bedrock. However, the Bow Ridge fault is particularly important in the hazard assessment because tunnels that connect the potential underground repository to the surface must cross the fault. Three of five trenches across the Bow Ridge fault show evidence for four to five paleoseismic events, each vertically displacing middle and late Pleistocene deposits as much as 25 cm. The faulting events have produced cumulative offsets of about one-half meter in deposits of middle Pleistocene age, consistent with slip rates of 0.001 to 0.002 mm/yr. Preliminary ages of events indicate average earthquake recurrence intervals of 30,000 to 100,000 years, values which are similar, within dating uncertainties, to those developed for the Paintbrush Canyon fault. Although preliminary ages of certain events do not match well on the two faults, the low slip rates for the Bow Ridge as compared to the Paintbrush reflect smaller single-event displacements rather than a longer average earthquake recurrence interval, probably because it is synthetic to the Paintbrush.

The Paintbrush Canyon fault is spectacularly exposed in gullies incised into a sand ramp on the west flank of Busted Butte. The natural exposures are roughly 25 m deep and more than twice as wide. On the gully walls, several wedge-shaped colluvial packages of reworked sand are exposed at various intervals on the downslope side of the fault traces. They reveal evidence for at least six, and possibly eight, surface-rupturing earthquakes on this segment of the Paintbrush fault since eruption of the Bishop ash (~750 ka), which is preserved at two sites near the base of the section. Displacements for each event are commonly less than 1 m along three main fault traces that form a zone ~30 m wide. Two stone lines and four buried soils are displaced various amounts. The oldest soil, which is ~650 to 700 ka in age and is separated vertically ~5 m, indicates slip rates between 0.005 and 0.01 mm/yr. These rates may double, given the uncertainties in ages of middle to late Pleistocene sediments exposed in the upper section. Sites along this sand ramp may be landmark examples of the longest continuous record of paleoseismic events on low-strain-rate Quaternary faults in the western US.

The Stagecoach Road fault lies at the southern end of Yucca Mountain, less than 2 km south of the southern ends of both the Paintbrush Canyon and Solitario Canyon fault zones. Exposures in three trenches across the Stagecoach Road fault provide evidence for four events in late Pleistocene time; each separates middle and late Pleistocene deposits about one-half meter. Uranium-series and thermoluminescence dating, in addition to correlations of tephra with local volcanic eruptions, provide relatively concordant ages for soils and deposits in the trench. The age and cumulative 2- to 3-m separation of middle Pleistocene deposits indicate slip rates between 0.02

and 0.04 mm/yr, the fastest slip rate of the local faults. This fault shows some of the shortest average recurrence intervals in the region, with the youngest three events each separated by ~15,000 to 30,000 years. The Stagecoach Road fault may rupture sympathetically with both the Solitario and Paintbrush Canyon faults because the Stagecoach can be projected along the strike to connect with either fault. The limited geochronologic data, which are sparse for older (early and middle Pleistocene) deposits, do not warrant an assessment of local fault interactions at this time.

Less than 4 km west of the potential repository block are the Windy Wash and Fatigue Wash faults. These two normal faults strike north, dip west, are ~15 to 20 km in length, and at the widest point are separated in map view by about 1 km. The Fatigue Wash is probably a synthetic splay of the Windy Wash fault because the Fatigue merges with the longer Windy Wash fault at its northern and southern ends, and the Fatigue has only 10 to 20 percent of Windy Wash's cumulative vertical separation of bedrock. A 3.7 Ma basalt flow is vertically displaced ~110 m by the Windy Wash fault, which defines a longer-term slip rate of ~0.03 mm/yr. At this time, the only evidence of a Holocene rupture (<10 cm) on faults within 25 km of Yucca Mountain is from the Windy Wash fault. West of Windy Wash about 2 km, one or more Quaternary faults are located in Crater Flat. The paleoseismic and tectonic characteristics of the Windy Wash, Fatigue Wash, and Crater Flat faults are similar to the other local faults already described; they are spaced roughly parallel, but only a few km apart, and in trench exposures they show repeated paleo-earthquakes in middle and late Pleistocene time.

Some workers postulate that faults at Yucca Mountain lie above and are related kinematically to a subhorizontal detachment fault, whereas others consider the faults to be high-angle, relatively planar to seismogenic depths, and loosely coupled spatially and temporally. Yet, some faults, which are adjacent and can reasonably be inferred to be structurally connected, show markedly different temporal behavior, given the available timing data and their analytical uncertainties. In addition, preliminary data indicate that earthquake recurrence intervals on some faults vary by factors of 3 to 5, which some workers interpret as reflecting temporally-clustered earthquakes. Yet, the temporal variations combined with evidence for a broad range of single-event displacements may indicate a more exponential earthquake distribution. On the other hand, these variations may reflect differential partitioning of slip, wherein net slip at depth is partitioned nearer the surface among one or more neighboring faults. At Yucca Mountain, models of earthquake occurrence and fault segmentation are in the early stages of development.

Especially important to the paleoseismic fault characterization are the precision of Quaternary dating techniques and their application to fault-related deposits and paleosols in desert environments. Most of the deposits at Yucca Mountain have been dated using U-series disequilibrium, U-trend, or thermoluminescence techniques. Charcoal is practically nonexistent, and few other techniques are applicable to the early and middle Pleistocene age range of commonplace eolian deposits and petrocalcic soils. At this time, however, these methods are not precise enough to confidently discriminate among various paleoevents on different faults. The common occurrence of tephra preserved in fissures and fault-related deposits exposed in trenches will be useful to correlate events from fault to fault. In some cases this correlation may provide more confident age limits than can analytical techniques.

The common occurrence of tephra preserved almost exclusively in fissures and cracks along several faults near Yucca Mountain may reflect a spatial and temporal coupling of volcanic and seismic processes. Although there have been two or three Pleistocene tephra eruptions in the vicinity, it is unclear which tephra may be involved with faulting, and whether volcanic eruptions trigger fault movements or vice versa. Alternative tectonic models must be envisioned if fault slips are coupled to local volcanic eruptions. This idea has implications for earthquake models in magmatic regions, particularly in light of the observation that the M_W 7.6 Landers, California, earthquake increased seismicity at several sites of geothermal activity or recent volcanism in the western US, including Yucca Mountain.

Historical earthquakes and morpho-structural analysis: the example of south-central Italy.

L. Piccardi, CNR-Centro di Studio di Geologia dell'Appennino e delle Catene Perimediterranee, Via La Pira 4, Firenze, Italy.
P. Tapponnier, Institut de Physique du Globe, Labo. de Tectonique Mecanique de la Lithosphere, 4 Place Jussieu, Paris, France.
M. Boccaletti, Dipartimento di Scienze della Terra, Università degli Studi di Firenze, Via La Pira 4, Firenze, Italy.

This study covers a large sector of the Apenninic chain (from 40°N to 43°N) a region of high seismic activity, as shown by recent and historical earthquakes. This area represent a very interesting background for historical seismicity's studies, either for the data richness, or because the correlation between earthquake and active faults has been very difficult so far.

Using geological and morpho-structural analysis, we realized a map of the active faults of the region, while carrying out a reexamination of historical seismicity. Historical data were used here not only for the definition of macroseismic fields for some of the most important earthquakes, but have also been analysed compared to the structural analysis.

In this work we present some of the first results of a study on the active tectonics in central and southern Apennines, underlying the role of the historical seismology analysis. One of the main result is the possibility to obtain a datation of episodes of historical surface faulting, well documented in our area at least for the last two destructive seismic events that hit the region, the Fucino earthquake of 15.01.1915 (Mo=6,8) and the Irpinia earthquake of 23.11.1980 (Mo=6,9).

A Tectonic Paroxysm in the Eastern Mediterranean during Historical Times

P.A. Pirazzoli, Laboratoire de Géographie Physique, CNRS-URA 141, 1 Place A. Briand, 92190 Meudon Bellevue, France
J. Laborel, Lab. Biologie Marine et Ecologie du Benthos, Univ. Aix-Marseille II, Luminy, Case 901, 13288 Marseille Cedex 9, France
S.C. Stiros, Institute of Geology and Mineral Exploration, 70 Messoghion St.,11527 Athens, Greece.

Evidence of vertically-displaced Holocene shorelines is frequent along many coasts in the Eastern Mediterranean. Submerged shorelines are generally difficult to date, but elevated ones often bear well-preserved datable bioconstructions which may be used to measure relative sea-level changes and estimate uplift dates.

In this paper, after a discussion of some criteria which enable coastal indicators of rapid (coseismic) vertical movement to be identified, coastal sectors which have shown evidence of Holocene coseismic uplifts in Greece and the Eastern Mediterranean are reviewed. It appears that most of these uplifts took place during a short, paroxysmic period (called the Early Byzantine tectonic paroxysm: EBTP) datable between the middle of the 4th and the middle of the 6th century A.D. The areas uplifted at that time include at least Cephalonia and Zante in the Ionian Islands, Lechaion and the Perachora Peninsula in the Gulf of Corinth, the Pelion coast of Thessaly, Antikythira and all the western part of Crete, a coastal sector near Alanya in southern Turkey, and the entire Levant coast, from Hatay (Turkey) to Syria and the Lebanon (stars in the figure, adapted from McKenzie, J.R. Astron. Soc., 30, 1972). The extent of the EBTP uplift was generally between 0.5 m and 1.0 m, but reached a maximum of about 9 m in southwestern Crete.

In several areas (Zante, Pelion coast, Antikythira, western Crete, Alanya), the EBTP uplifted shoreline is the only evidence of Holocene emergence. In other areas, however, a similar uplift

movement occurred earlier in the Holocene (Levant coast), or more recently (Cephalonia). Evidence of preseismic subsidence movements having preceded the EBTP uplift has been reported from at least Thessaly, Antikythira and Crete; in the latter two islands, preparation of the EBTP uplift consisted in a series of about ten coseismic small subsidence movements, each of decimetric order, which occurred in the preceding 3000 years. No evidence was observed of postseismic vertical displacements.

These series of coseismic vertical displacements occurring during a relatively short period of time over a distance of more than 1500 km are exceptional in the regional geological record. They are tentatively ascribed to anomalous tectonic stress created by an occasional acceleration in the subduction thrust of the Ionian crust beneath the Hellenic arc, from Cephalonia to central Crete, and to consequent relative movements and readjustments between various lithosphere blocks situated near the boundaries of the various tectonic plates which border the Eastern Mediterranean.

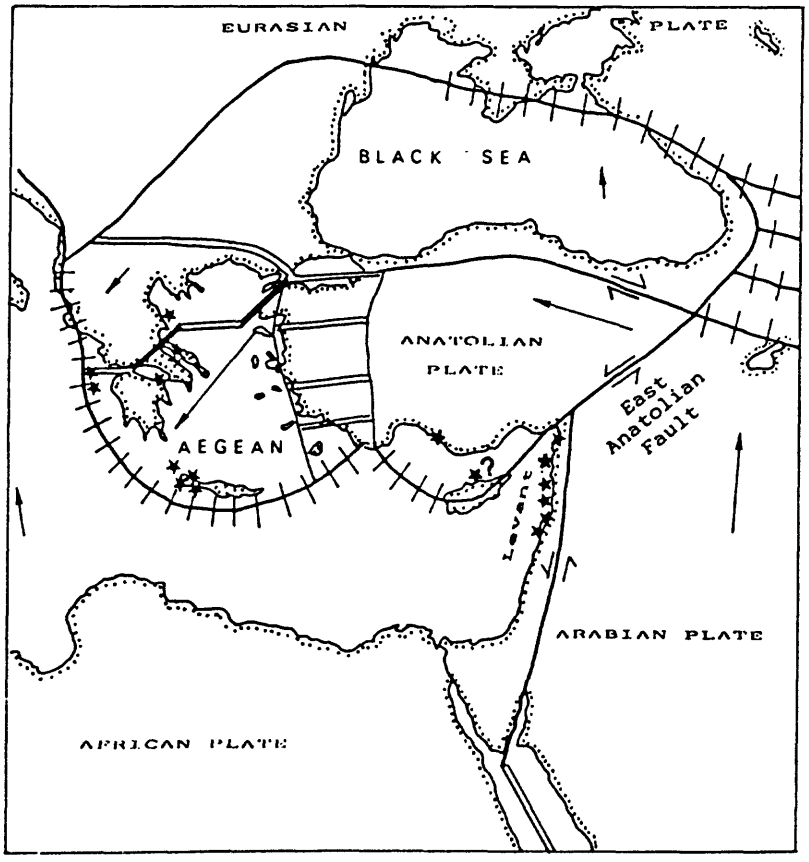

Paleoseismic evidence for "Yo-Yo" tectonics above the eastern Aleutian subduction zone: coseismic uplift alternating with even larger interseismic submergence

George Plafker, U.S. Geological Survey, Menlo Park, CA 94025
Meyer Rubin, U.S. Geological Survey, Reston, VA 22092

The Copper River delta stratigraphic sequence near the eastern end of the Aleutian subduction zone records repeated coseismic uplift events separated by long periods of even larger interseismic submergence. The most recent uplift of about 2 m during the March 27, 1964 Alaska earthquake (9.2 Mw) resulted in abrupt conversion of intertidal mud flats into subaerial fresh-water peat marshes in a belt as much as 4 km wide (Plafker, 1969).

The delta stratigraphy records at least seven, and possibly eight, pre-1964 sudden uplifts that are best interpreted as coseismic events (Plafker and others, 1992). Each event was followed by gradual interseismic subsidence and marine transgression. As a consequence, the upper 11.5 m of the stratigraphic sequence consists of multiple beds of fresh-water peat 10–30 cm thick with sharp basal contacts that grade upward into beds of varved(?) intertidal silt to 2.3 m thick that contain marine diatoms and the rooted remains of salt-tolerant sedge (fig. 1).

Each peat and silt pair is interpreted to reflect a complete earthquake cycle consisting of an abrupt coseismic uplift above the highest tide level during which fresh-water peat formed, followed by gradual resubmergence and burial beneath intertidal sediment ("yo-yo tectonics"). The combined thickness of the peat and silt layers between the last four pre-1964 events for which the best data are available require a minimum of 1 m of coseismic uplift. This suggests that the causative tectonic earthquakes were large and probably comparable in mechanism to the 1964 event.

The three youngest pre-1964 coseismic events are dated from limiting ^{14}C ages at and immediately below the base of the corresponding peat layers at about 790–675, 1400–1270, and 2350–2000 calibrated years bp (fig. 2). The ages of as many as 5 deeper peat layers that may also represent coseismic events are poorly constrained by ^{14}C dates; 4 dated samples from the deepest peat layer yield a tentative age of 5600–5300 calendar years bp (fig. 2). Repeat times for the three most recent earthquakes that have uplifted the delta area are 730±55, 645±120, and 800±140 years; repeat times for the ~5600-year stratigraphic record average 700 or 800 years depending on whether 7 or 8 pre-1964 uplift events are preserved.

^{14}C dating of plant fossils in the intertidal silt indicates average interseismic submergence rates as high as 4.4 mm/yr with annual(?) silt varves that indicate accumulation rates of about 7 mm/yr. Net submergence averages ~2 mm/yr for the ~5,600 years during which 11.5 m of silt and peat accumulated. Assuming an average 1.5 mm/yr eustatic sea level rise and an average 1.5 m coseismic uplift for each of 8 events, the combined tectonic and isostatic interseismic subsidence of the delta is ~2.6 mm/yr.

Tide gage data at Cordova just west of the Copper River delta show linear submergence of about 9.7±0.5 mm/yr since the 1964 earthquake (Savage and Plafker, 1991). At this high rate, only about 200 years are required to recover all of the 1964 coseismic uplift and the combined submergence below sea level and silt accumulation on the delta would be as much as 5–6 m for a recurrence interval of 700-800 years. However, both the long-term average interseismic submergence rate of ~4.1, together with the requirement that the sediment surface remains within a few meters of sea level so that it can become subaerial during coseismic uplift, suggest that the present high submergence rate recorded by the Cordova tide gage since the earthquake must decrease with time.

REFERENCES CITED

Plafker, George, 1969, Tectonics of the March 27, 1964, Alaska Earthquake: U.S. Geological Survey Professional Paper 543-I, 2 pl., 74 p.

Plafker, George, Lajoie, K.R., and Rubin, Meyer, 1992, Determining recurrence intervals of great subduction zone earthquakes in southern Alaska by radiocarbon dating: *in* Taylor, R.E., Long, Austin, and Kra, R.S., eds., Radiocarbon After Four Decades: An Interdisciplinary Perspective, New York, Springer-Verlag, p. 436–453.

Savage, J.C., and Plafker George, 1991, Tide-gage measurements of uplift along the south coast of Alaska: Journal of Geophysical Research, v. 96, no. B3, p. 4325–4335.

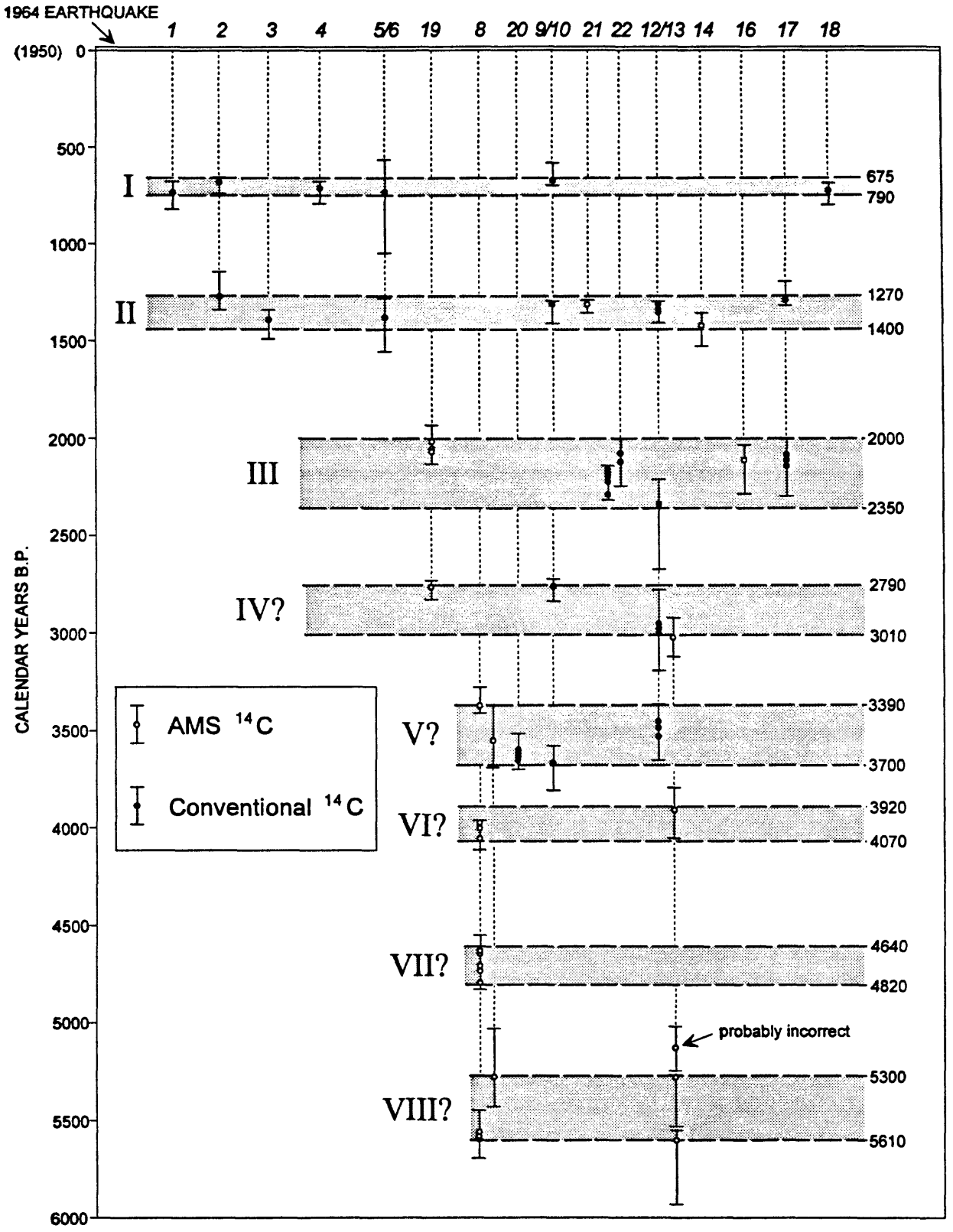

Figure 2. Inferred pre-1964 coseismic uplift events at the Copper River delta and their most probable calendar age ranges based on ^{14}C ages of samples that bracket these events. Numerals above the upper gray band indicate measured sections and auger holes shown in figure 1. Open and filled circles represent the intersection of the sample radiocarbon age with he calendar age calibration curve; attached bars indicate the maximum error limits at 1σ confidence level. Gray bands bracket the most likely age ranges for the pre-1964 paleoseismic events (Roman numerals I–VIII).

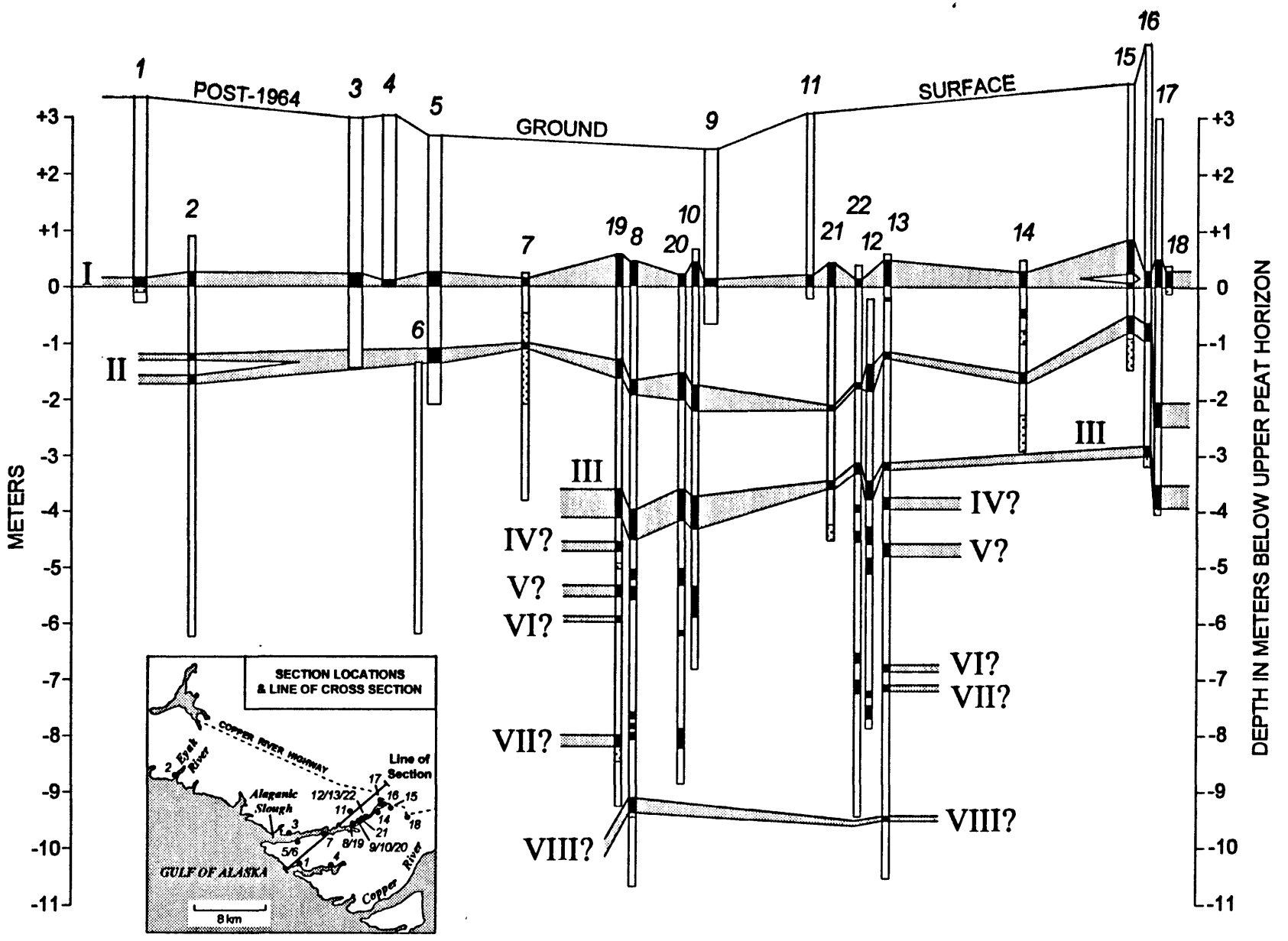

Figure 1. Stratigraphy of interbedded subaerial peat (black), intertidal silt (white), and sand (dotted) in measured sections and auger holes on the Copper River delta. Numbered holes and sections correspond to localities shown on index map. Sections referenced to base of upper peat layer; correlation of peat layers is based on stratigraphic position and ^{14}C age. The abrupt change from intertidal silt to subaerial peat is interpreted as due to coseismic uplift during paleoseismic events (Roman numerals I–VIII) comparable in mechanism to the 1964 Alaska earthquake.

Timing and Size of the Most Recent Earthquake Along the Central Septentrional Fault, Dominican Republic

Carol S. Prentice, U. S. Geological Survey, Branch of Earthquake Geology and Geophysics, 345 Middlefield Rd., MS 977, Menlo Park, CA 94025
Paul Mann, University of Texas Institute for Geophysics, 8701 MoPac Expressway, Austin, TX 78759-8397
G. Burr, NSF Accelerator Facility, University of Arizona, Tucson, AZ 85721
L. R. Peña, Facultad de Ingeniería, Universidad Catolica Madre y Maestra, Santiago, Dominican Republic

The Septentrional fault zone (SFZ) is the major strike-slip fault separating the North American and Caribbean plates in northern Hispaniola (Fig. 1). In many locations the active plate-boundary faults are either offshore or crop out in pre-Quaternary rocks that do not preserve a record of recent activity. However, in Hispaniola, the SFZ traverses the densely populated Cibao Valley of the Dominican Republic (Fig. 2). In this area the fault forms a prominent scarp in alluvium and provides a unique opportunity to study the Quaternary behavior of the SFZ and to quantify the seismic hazard it represents to Hispaniola and neighboring Puerto Rico. Excavations at two sites in the Cibao Valley (Fig. 2) revealed faulted and folded Holocene deposits that provide evidence for the timing and size of the most recent ground-rupturing earthquake along the central SFZ.

Trench 91-2 (Fig. 3) (Prentice et al., 1993) shows faults that displace unit 80 and terminate in unit 70, and several fault fissures filled by unit 70 material. In addition, units 70 and 80 are folded into a broad anticline; units 65A, B, C, and D were deposited on the flanks of this anticline and pinch out over the crest. Younger units are not faulted. These relations indicate the occurrence of a ground-rupturing earthquake while unit 70 formed the ground surface. Radiocarbon analyses of 32 samples collected from these sediments show that this earthquake occurred before 1260 AD (Fig. 4).

This earthquake is also recorded in the sediments of trench 93-2 (Fig. 5). Evidence for this event includes the folding of units 70 and below, and the presence of a sand-blow deposit indicating paleoliquefaction. Radiocarbon dates on charcoal samples from this excavation (Fig. 6) confirm that this is the same earthquake as seen in trench 91-2 , and that this earthquake occurred between AD 1150-1230, about 760-840 years ago, giving us both upper and lower bounds on the age of the most recent ground-rupturing event along the central Septentrional fault. In addition, we used 3-dimensional excavation techniques to determine the amount of offset of a buried channel deposit near trench 93-2. Analysis of these data shows that the AD 1150-1230 earthquake was accompanied by about 5 m of left-lateral offset and about 2 m of vertical displacement at this site (Fig. 7). This shows that the AD 1150-1230 earthquake was large, $\geq$ M7.5.

Because no slip-rate data are available for the Septentrional fault, we used an assumed minimum slip rate of 5 mm/yr (based on published plate-boundary slip-rate estimates that range from 12±3 to 37±5 mm/yr) to calculate that energy equivalent to about 4m of slip may have accumulated in the 800±40 years since the last ground-breaking earthquake observed in our excavations (Prentice et al., 1993). The absence of ground rupture in more than 760 years suggests a high earthquake potential for the Puerto Rico-Hispaniola segment of the plate boundary, if the slip rate is > 5 mm/yr. Slip-rate and additional paleoseismic data are needed to more quantitatively assess the seismic potential of this fault zone.

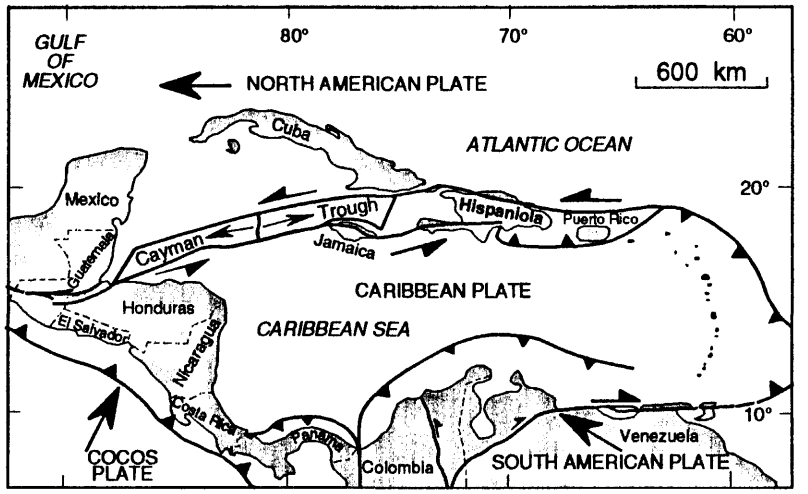

Figure 1: Map showing tectonic setting of Hispaniola. Large arrows indicate plate motion relative to a fixed Caribbean plate.

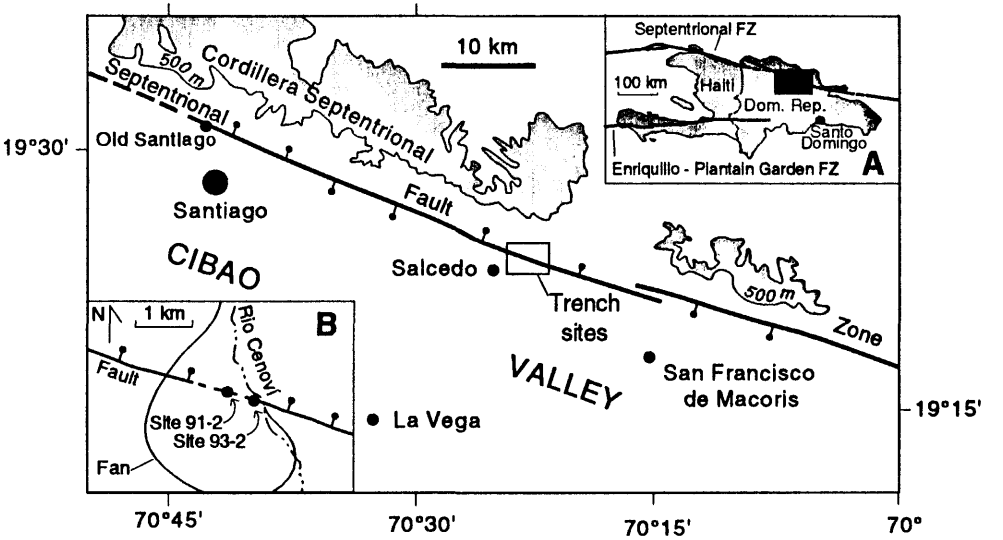

Figure 2: Map showing locations of trench sites along the central Septentrional fault in Hispaniola. Inset A shows location of study area (black rectangle). Area of trench sites (white rectangle) shown in inset B.

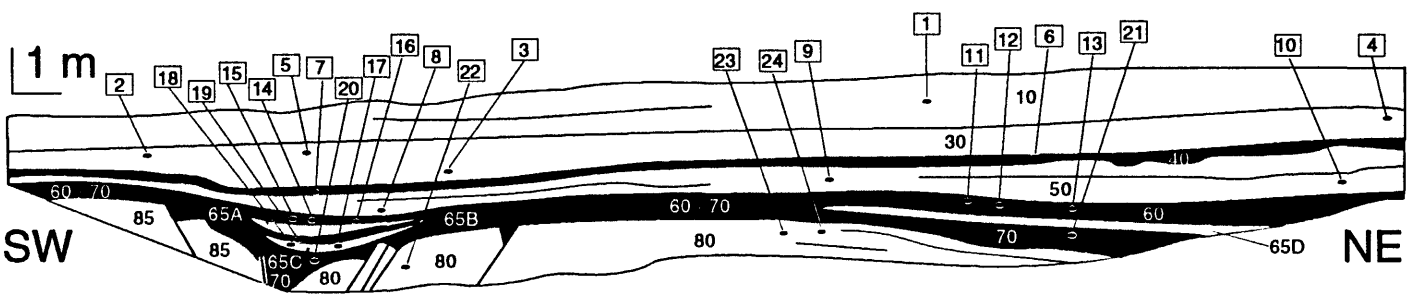

Figure 3: Log of trench at site 91-2. Black horizons are organic-rich silty clay units. Numbered points represent radiocarbon samples. An earthquake caused faulting and folding when unit 70 formed the ground surface. Upper horizons are not faulted.

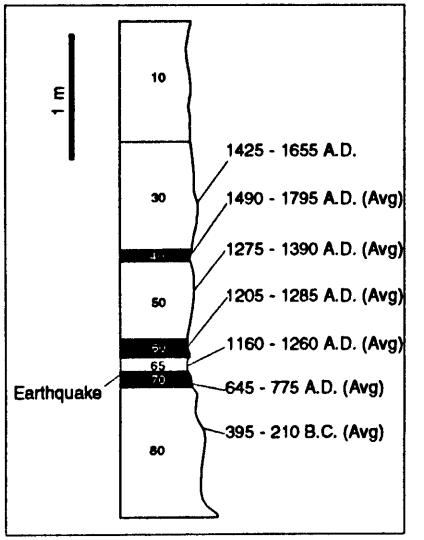

Figure 4: Stratigraphic column summarizing results of radiocarbon analysis of samples collected from trench 91-2, and showing relation of dated units to earthquake horizon. Dates are dendrochronologically-calibrated weighted-mean averages (2σ). Earthquake occurred between AD 640-1260.

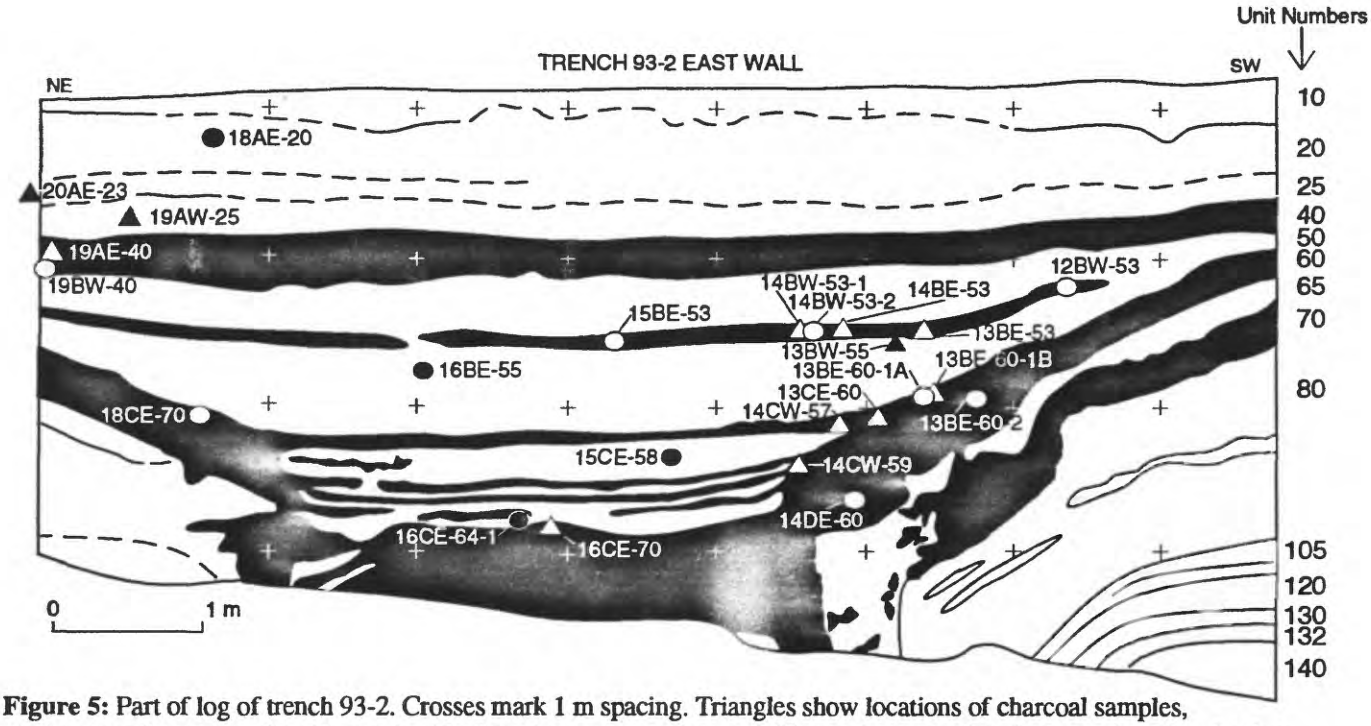

Figure 5: Part of log of trench 93-2. Crosses mark 1 m spacing. Triangles show locations of charcoal samples, circles show locations of shell samples. Earthquake occurred when unit 70 was the ground surface, causing liquefaction of unit 65 and tilting of horizons 70-140. Higher units are unfaulted and fill in depression created by syncline.

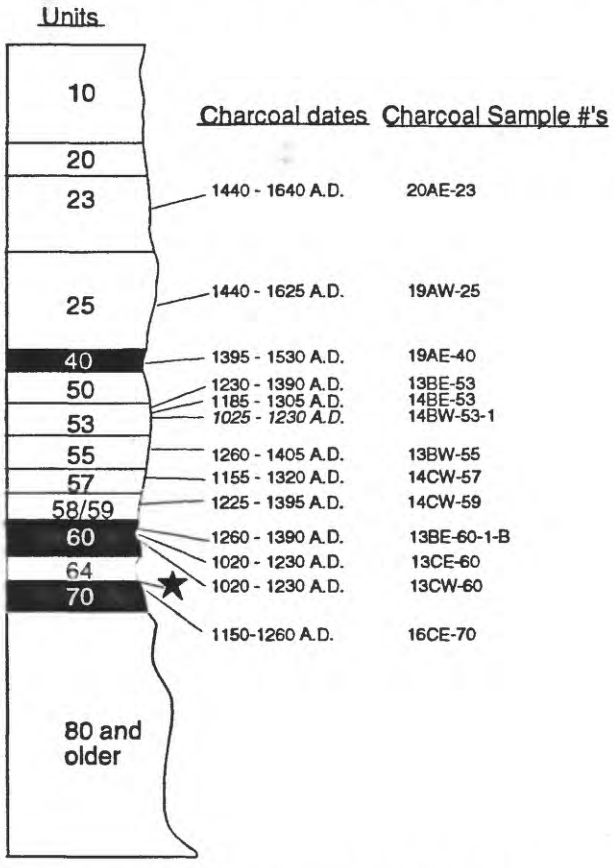

Figure 6: Stratigraphic column showing dendrochronologically calibrated radiocarbon dates (2σ) of samples collected from trench 93-2 and showing relation of dated units to earthquake horizon (star). Radiocarbon dates indicate this earthquake occurred between AD 1150-1230. This is consistent with the results from trench 91-2.

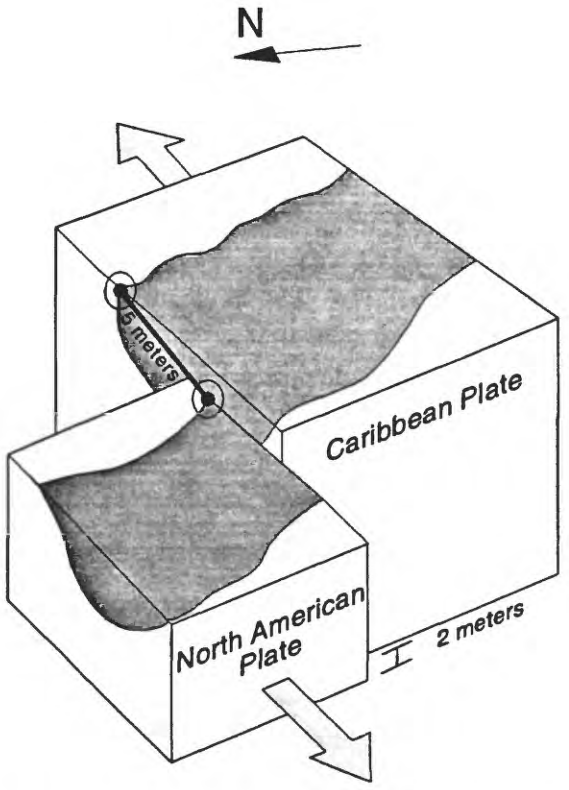

Figure 7: Schematic block diagram showing offset of buried Holocene channel deposit (shaded) excavated using 3-D techniques to determine horizontal and vertical offset of approximately 2 and 5 meters, respectively. This offset occurred as a result of the earthquake of AD 1150-1230, indicating this was a large (M7.5) event.

CLUSTERED ANCIENT EARTHQUAKES IN THE IMPERIAL VALLEY, SOUTHERN CALIFORNIA, PRESERVED IN COEVAL LACUSTRINE STRATA

T.K. ROCKWELL, Dept. of Geological Sciences, San Diego State Univ., San Diego, CA 92182
K. SIEH, Seismological Lab., California Institute of Technology, Pasadena, CA 91125.

Flow of the Colorado River into the Salton Trough of southern California and northern Baja California has resulted in the periodic filling of freshwater Lake Cahuilla to about 13 m elevation. Detailed study of the shoreline stratigraphy of this prehistoric lake demonstrates that it has filled at least five times during the past 1200 years, with partial or complete desiccation between the highstands. High-precision ^{14}C dates for peat and detrital charcoal buried by transgressive shoreline deposits indicate fillings about A.D. 1660 and 1680 (two highstands with partial desiccation), A.D. 1450, A.D. 1360, and A.D. 885. A lower lacustrine highstand of 9.5 m probably occurred between the A.D. 1360 and 1450 lakes, although some ambiguities remain.

The shorelines of ancient Lake Cahuilla cross many of the major faults of the southern San Andreas system, including the San Andreas fault, the Superstition Hills, Superstition Mountain, and Coyote Creek strands of the San Jacinto fault zone, and the Imperial fault. The regionally extensive strata of these lakes thus enables more confident ordering of late Holocene seismic events on these faults than would be possible from radiocarbon analysis alone. In this region, such constraints are critical to assessing the long-term regional behavior of faults in terms of current concepts of earthquake clustering, loading of faults and triggering of earthquakes due to adjacent ruptures, and the behavior of faults over multiple earthquake cycles.

Based on existing data from the San Andreas, Superstition Mountain, and Imperial faults, which all cut strata of Lake Cahuilla, and the south-central San Jacinto fault, which is constrained by high-precision ^{14}C dates on peats at Hog Lake, it appears that large earthquakes on individual fault segments have not been periodic, but rather have clustered. Furthermore, clustering of earthquakes on the faults of the region probably has occurred.

Clustering has occurred on at least the Superstition Mountain and San Andreas faults. The Superstition Mountain fault ruptured three times between A.D. 885 and 1440, but no surface ruptures have occurred in the past 550 years. The average return time for large earthquakes has therefore varied between about 250 years for the first interval to over 500 years for the second. Similarly, three or four large surface ruptures occurred on the San Andreas fault between about A.D. 1290 and 1680 (R.I. ~150-200 years), but there have been no seismic ruptures in the past 300 years. The Imperial fault has broken at least twice this century (1940 and 1979) leading some to assume a short recurrence interval for that fault. Trenching across the Imperial fault at the International Border, however, has demonstrated that there were no surface ruptures between 1940 and about A.D. 1680. This argues for a long average recurrence interval. These data indicate that knowledge of many recurrence cycles is required to determine either the average return time or the slip rate for a fault. Thus, previous slip rate estimates for faults utilizing recurrence data averaged over only a few cycles may substantially misconstrue the average rate.

Close timing between earthquakes on different faults is also apparent in our data. Several of the faults appear to have sustained rupture during the periods A.D. 1200-1350, A.D. 1450-1500, and A.D. 1680-1750. These data suggest that large ($M \geq 7$) earthquakes in the Imperial Valley region occur in temporal clusters. They also indicate that the Imperial Valley region appears overdue for at least one large earthquake.

Long Recurrence Interval for the Emerson Fault: Implications for Characteristic Earthquakes, Slip Rates and Probabilistic Seismic Hazard Calculations

C. Rubin, Department of Geology, Central Washington University, Ellensburg, Washington 98926
K. Sieh, Seismological Laboratory, California Institute of Technology, Pasadena, California 91125

The last two ruptures of the northern Emerson fault prior to the 1992 M_w7.3 Landers earthquake occurred about 9,000 years ago and between 14,800 and 24,100 ^{14}C years ago. Thus, during the Holocene epoch, large earthquakes produced by the Emerson fault appear to have been about forty times less frequent than they have been along the San Andreas fault, nearby. The great interval of dormancy on the Emerson fault divided into its dextral slip during the 1992 earthquake yields a Holocene slip rate of less than a millimeter/yr. Thus, at least one of the other five major fault zones of the Eastern California Shear Zone (ECSZ) would have to slip much more rapidly than the Emerson fault, in order to accommodate the geodetically determined rate of about 7 mm/yr across the entire ECSZ.

In an excavation, we exposed datable sediments and soils broken by the Emerson fault, near the southern end of its 1992 rupture. AMS radiocarbon ages from charcoal in playa sediments indicate that the last slip event prior to 1992 occurred about 9,000 years ago. Because the playa sediments lap onto an older scarp, similar in height to the 1992 scarp, this penultimate rupture was similar in size to the 1992 rupture, at least at this site. Our exposure also revealed clear evidence of at least one older major rupture, between two pedogenic carbonate horizons. The date of this earthquke is ostensibly between the radiocarbon ages of the two carbonate layers, 14,800 and 24,100 ^{14}C years ago. The actual bracketing ages for this rupture may, however, be somewhat older, because of the mean residence time for the pedogenic carbonate and calibration of the radiocarbon ages to calendric dates. A dormant period of 6,000 to 15,000 years separates this event (or events) from the event of about 9,000 years ago. The dates of the last two prehistoric ruptures of the northern Emerson fault are slightly older than or the same as those determined by Hecker and others for the nearby Homestead Valley fault.

Dextral slip at the playa site was about 2 meters in 1992. A few kilometers farther north, however, dextral slip was about 6 meters. Thus the average slip rate for the Emerson fault during the past 9,000 years is 0.2 mm/yr at the playa, but may be as high as 0.7 mm/yr at the 1992 maximum, farther north. This is only 1/10 to 1/30 of the geodetic rate of 7 mm/yr of slip across the six major faults of the ECSZ. Therefore, at least one other fault within the ECSZ must be slipping at a much faster average rate. The Calico fault, which has the largest cumulative geological offset, may be the best candidate.

If we had known of the great contrast between the period of dormancy of the Emerson and the San Andreas faults prior to 1992, we would have calculated a much higher probability for an event on the San Andreas than the Emerson fault. This irony demonstrates the critical importance of incorporating the dates of the past several earthquakes in calculations of realistic probabilities.

Tsunami Heights in the Pacific Northwest from Cascadia Subduction Earthquakes

Kenji Satake, Dept. of Geological Sciences, Univ. of Michigan, Ann Arbor, MI
Joanne Bourgeois, Dept. of Geological Sciences, Univ. of Washington, Seattle, WA
Mary Ann Reinhart, GeoEngineers, Redmond, WA

1. Introduction

The earthquake potential in the Pacific Northwest has been argued for the last decade (e.g., Heaton and Kanamori, 1984). Although there is no instrumental record of subduction-zone earthquakes except for the recent Petrolia earthquake in April '92 (Oppenheimer et al., 1993), much geological evidence of paleo-earthquakes has been presented (e.g., Atwater, 1987; 1992; Adams, 1990; Clarke and Carver, 1992), and there seems to be a general consensus that the last one occurred about 300 years ago. However, the size and spatial extent of this event has not been determined; was it a single M~9 event that ruptured the entire Cascadia Zone or a series of smaller (M~8) events rupturing smaller segments? Earthquakes with M~9 and M~8 have significantly different slip amounts on the fault; hence the recurrence time would be also different.

We made numerical computations of crustal deformation and tsunamis from hypothetical earthquakes in order to compare with paleo-seismological data and to estimate the time-space distribution of the subduction earthquakes in Cascadia. In this paper, we present the computed tsunami heights along the Pacific coast, and make comparison with paleo-tsunami data in Willapa Bay and Grays Harbor in southern Washington.

2. Tsunami Heights along the Pacific Northwest

We consider four different earthquakes. The case M9 represents a single earthquake rupturing almost the entire Cascadia Subduction Zone, in a way similar to the 1960 Chilean earthquake (slip is 24 m). The cases M8 represent smaller (M~8) earthquakes that rupture smaller segments of the Cascadia Subduction Zone. The case M8 CA is for a segment south of the Blanco Fracture Zone and corresponds to the Gorda plate. The case M8 OR is for a segment offshore Oregon, from off Cape Blanco to off the Columbia River mouth. The Case M8 WA is for a segment offshore Washington, from the Columbia River mouth to near off Vancouver Island. The slip amount for the M~8 events is assumed to be 8 m, which has a recurrence interval of 200 to 270 years.

Figure shows the crustal deformation and tsunami heights along the coast calculated from the four scenario earthquakes. Depending on the fault width, more precisely if the fault extends below the coastline, the coast may be uplifted or subsided. In the above four cases, the northern California coast near Cape Mendocino and the Oregon coast near Cape Blanco are uplifted and other places are subsided, which is consistent with geological observations (e.g, Atwater, 1992). The maximum subsidence is nearly 2 m for the M~8 events and nearly 6 m for the M~9 event.

Generation and propagation of tsunamis are numerically computed using the above crustal deformation as the initial conditions. Finite-difference computations of non-linear shallow water equations are made with a grid size of 1 minute (about 1.6 km). Tsunami heights along the coast are affected by coseismic crustal deformation; the tsunami inundation would be more significant if the coast is coseismically subsided rather than uplifted. Figure shows the double (peak-to-trough) amplitude of tsunamis, which is independent of datum (i.e., not affected by coseismic deformation). To a first order approximation, the plotted heights are similar to run-up heights; detailed run-up calculations would provide more accurate estimations. The tsunami heights from the M9 event are more than 10 m along the Pacific coast of Northern California, Oregon and Washington, whereas an M8 event would cause about 5 m tsunamis in coastal areas facing to the source.

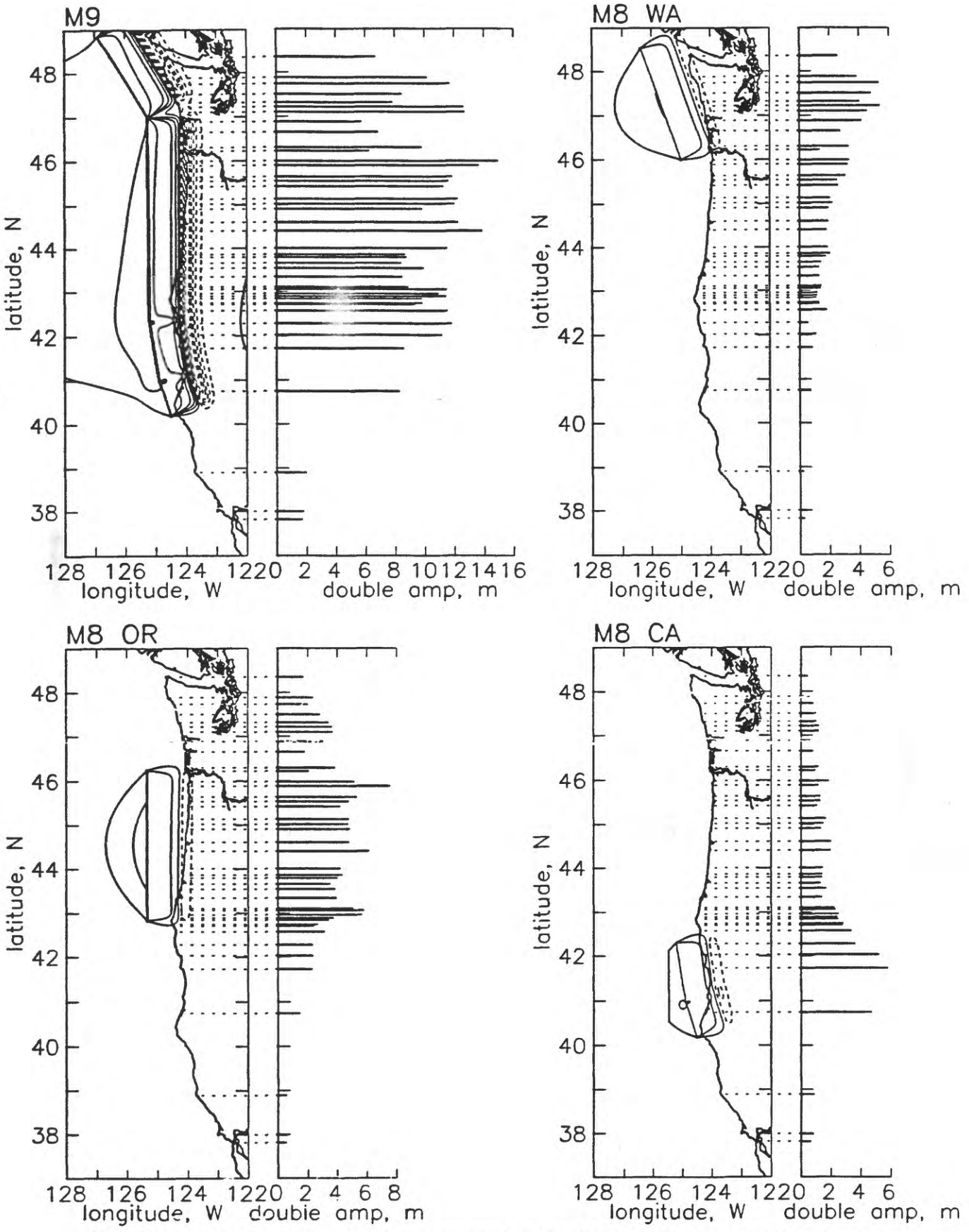

Figure. Crustal deformation and tsunami amplitudes along the Pacific coast from four scenario earthquakes (M9, M8 WA, M8 OR and M8 CA). The contour interval for ground deformation is 1m (solid curves are uplift and dashed are subsidence).

3. Willapa Bay and Grays Harbor

Geological data of paleo-tsunamis in coastal and estuarine sediments in southwest Washington from the 300-year-old event have been studied by Reinhart and Bourgeois (1989) and Reinhart (1991). Based on detailed mapping of the postulated tsunami sand layer in Willapa Bay and Grays Harbor, and on sediment transport analysis of the sand in Willapa Bay (in particular, the Niawiakum River), they calculated paleo-tsunami "run-up" at the Niawiakum of 1-2 m above the marsh surface. Comparable numbers are appropriate for, e.g., the Johns River in Grays Harbor, where the 300-year-old sand has a similar expression.

Our computations show that at least three tsunami waves would arrive at Niawiakum River, after the area is coseismically subsided but before the inundation due to the subsidence is completed. For the case M9, the coseismic subsidence is more than 5 m and the tsunami amplitudes are 2~3 m; for the case M8 WA, the subsidence is 1.7 m and the tsunami amplitudes are 1.2~1.4 m. For the other two cases, the coseismic subsidence is negligibly small and the tsunami amplitudes are less than 40 cm for the case M8 OR and less than 20 cm for the case M8 CA. The comparison with the geological data indicates that the tsunami source was at least M~8 earthquake offshore Washington. An earthquake from off California cannot explain the observed tsunamis.

Similar comparisons of geological data and numerical computation at different sites would make it possible to estimate the spatial extent of the paleo-earthquakes in the Cascadia subduction zone.

References

Adams, J., Paleoseismicity of the Cascadia subduction zone: evidence from turbidites off the Oregon-Washington margin, *Tectonics, 9*, 569-583, 1990.

Atwater, B.F., Evidence for great Holocene earthquakes along the outer coast of Washington state, *Science, 236*, 942-944, 1987.

Atwater, B.F., Geologic evidence for earthquakes during the past 2000 years along the Copalis River, southern coastal Washington, *J. Geophys. Res., 97*, 1901-1919, 1992.

Clarke, S.H., and G.A. Carver, Late Holocene tectonics and paleoseismicity, southern Cascadia subduction zone, *Science, 255*, 188-192, 1992.

Heaton, T.H., and H. Kanamori, Seismic potential associated with subduction in the northwestern United States, *Bull. Seism. Soc. Am., 74*, 933-941, 1984.

Oppenheimer, D., G. Beroza, G. Carver, L. Denglar, J. Eaton, L. Gee, F. Gonzalez, A. Jayko, W.H. Li, M. Lisowski, M. Magee, G. Marshall, M. Murray, R.McPherson, B. Romanowicz, K. Satake, R. Simpson, P. Somerville, R. Stein, and D. Valentine, The cape Mendocino earthquake sequence of April, 1992, *Science,, 261*, 433-438, 1993.

Reinhart, M.A., Sedimentological analysis of postulated tsunami-generated deposits from Cascadia great-subduction earthquakes along southern coastal Washington. M.S. paper, Univ. of Washington, 90pp., 1991.

Reinhart, M.A. and Bourgeois, J., Tsunami favored over storm or seiche for sand deposit overlying buried Holocene peat, Willapa Bay, WA, *Eos, 70*, 1331, 1989.

The Pitman Canyon Paleoseismic Record Will Test San Andreas Fault Segmentation

Gordon G. Seitz, Ray J. Weldon II, Glenn P. Biasi, 1272 Department of Geological Sciences, University of Oregon, Eugene, Oregon 97403-1272

Introduction

Pitman Canyon is the only paleoseismic site (Seitz and Weldon, 1994) on the San Bernardino Mountains segment (WGCEP, 1988) of the San Andreas Fault. The site is located along the southwest flank of the San Bernardino Mountains, 10 km northwest of San Bernardino (Fig. 1). The two longest paleoseismic records on the San Andreas Fault are located on the Mojave segment (WGCEP, 1988), 26 and 48 km to the northwest of Pitman Canyon near Wrightwood (Fumal et al., 1993; Weldon, 1991) and at Pallett Creek (Sieh, 1978; 1984; Sieh et al., 1989), respectively. Exceptional site stratigraphy has allowed the recognition of at least 12 events at each of these sites. The only San Andreas Fault paleoseismic site located to the south is 130 km southeast on the Coachella Valley segment near Indio (Sieh, 1986), where 4 events were recognized between A.D. 1000 and A D. 1700.

Inherent in a useful segmentation concept is that the segment boundaries are approximately stationary for at least several seismic cycles, thus they should be recognizable by a correlation of adjacent well resolved paleoseismic records. The Pitman Canyon site, located on the San Bernardino Mountains segment, adjacent to the best resolved paleoseismic records on the adjacent Mojave segment, is particularly well situated to assess fault segmentation of the San Andreas Fault. The distance of about 25 km between each of these sites appears to be on the same order as the minimum rupture length continuation expected from empirical ground rupture displacements on mature faults for the estimated +2 m slip per event (Wells and Coppersmith, 1993). Additionally the site location near the northwestern terminus of the San Jacinto Fault, will help define the slip partitioning, and possible temporal event interaction of the San Jacinto and San Andreas Faults.

The Pitman Canyon Paleoseismic Site

At Pitman Canyon a greater than 6 m thick section of interbedded debris flow gravels, fluvial sands, and peats has been deposited during at least the past 1400 y, and is cut by the fault. Six trench excavations reveal that the fault zone consists of en-échelon left-stepping breaks on the order of 10 m in length, which trend more northerly than the scarp. The clastic units have distinct morphologies which include debris flow lobes, levees, and fluvial channels that commonly cross the fault at high angles. Abundant datable peat layers are located throughout the section and currently twelve conventional ^{14}C age determinations give age control.

Preliminary interpretations, based on detailed surficial mapping and trench exposures (Fig. 2), reveal 8 events and ~3.5 m of right lateral slip for each of the past two events. While lateral offsets on earlier events are not yet fully resolved, facies mismatches suggest that they are similarly large. Event horizons were recognized by consistent upward termination of faults, often with fissure fills, folding, and an incremental down-section increase in vertical separation.

The event (Fig. 3) and sedimentary layer dates were quantitatively refined by applying newly developed Baysian techniques (Biasi and Weldon, 1994a; 1994b) which fully utilize the knowledge of sample growth order and thickness to achieve maximum dating constraint. These techniques achieve significant variance reductions in the resultant event dates by including the assertion that overlying layers are younger and inferring the minimum amount of time necessary to accumulate a given thickness of peat (Fig. 4).

Discussion

Considering the occurrence of 7 events preceding the last inferred event in 1812 results in an average recurrence of 142 y. Although estimates of the timing of individual events have considerable variance, the average recurrence estimate is more robust, and compares reasonably with the +6 event record average recurrence estimates at Pallett Creek and Wrightwood of about 135 y. Concluding that ~7.5 m and ~15.5 m of lateral slip was the result of the last 2 and 4 events, respectively, results in slip rates of about 30 mm/yr. This is in reasonable agreement with the best constrained Holocene slip rate of 24.5± 3.5 mm/yr determined at Cajon Creek (Weldon

and Sieh, 1985) about 4 km to the northwest. Applying this Holocene slip rate to the elapsed time since the inferred last event in 1812 results in an accumulated slip potential of 4.4 ± 0.6m, which is about the estimated slip per event.

Commonly paleoseismic events from different sites along a fault are assumed to correlate when the event dating uncertainties overlap, however, such overlap only allows the determination of a correlation possibility. Because of this difficulty in correlating events, a non-correlation i.e. site exclusive event date distributions may be more significant since they can be used to define the extent of past ground ruptures. A comparison of the Pitman Canyon event record to the Wrightwood record (Biasi and Weldon, 1994b) shows that within the dating uncertainties, the records are compatible with the exception of the 1857 ground rupture, which apparently did not extend south beyond Cajon Creek (Weldon and Sieh, 1985). This absence of significant non-correlation of event dates suggests that the Wrightwood/Pitman Canyon fault segments behave as or more similar than the Wrightwood/Pallett Creek segments, located on different and identical segments (as defined by WGCEP, 1988), respectively. The fact that only 3 or 4 of the most recent 6 Wrightwood events correlate to Pallett Creek (Biasi and Weldon, in prep.), as compared to the correlation of 5 of the most recent 6 Wrightwood events to Pitman Canyon events, suggests that the ground rupture locations are more variable than a strict segmentation model may imply. Although the current event dating resolution at Pitman Canyon limits the confidence of event correlations, the addition of this site record to the well-resolved Pallett Creek and Wrightwood records presents new possibilities of achieving an unprecedented understanding of the past fault behavior.

References cited

Biasi, G., and R.J. Weldon II, 1994a, Quantitative refinement of C-14 distributions: Quaternary Res., 41, 1-18.

Biasi, G., and R.J. Weldon II, 1994b, Quantitative approaches to event dating and constraint, ICL-USGS workshop abstract.

Fumal, T.E., Pezzopane, S.K., Weldon, R.J., and Schwartz, D.P., 1993, A 100 year recurrence interval for the San Andreas Fault at Wrightwood, California: Science, 259, 199-203.

Seitz, G. and R.J. Weldon II, 1994, The paleoseismology of the southern San Andreas Fault at Pitman Canyon, San Bernardino, California. Geol. Soc. Amer., Cordilleran Sec. Guidebook, Geol. Investigations of an Active Margin, ed. McGill, S.F.,and T.M. Ross.

Sieh, K.E., 1978, Prehistoric large earthquakes produced by slip on the San Andreas fault at Pallett Creek, California: J. Geophys. Res., 83, 3907-3939.

Sieh, K.E., 1984, Lateral offsets and revised dates of large earthquakes at Pallett Creek, California: J. Geophys. Res., 89, 7641-7670.

Sieh, K.E., 1986, Slip rate across the San Andreas and prehistoric earthquakes at Indio, California: Eos Transactions, American Geophysical Union, 67, 1200.

Sieh, K.E., Stuiver, M., Brillinger, D., 1989, A more precise chronology of earthquakes produced by the San Andreas fault in Southern California: J. Geophys. Res., 94, 603-623.

Stuiver, M. and Reimer, P., 1993, Extended C14 data base and revised CALIB 3.0 C14 age calibration program: Radiocarbon, 35, 215-230.

Weldon, R.J.II, and K.E. Sieh, 1985, Holocene rate of slip and tentative recurrence interval for large earthquakes on the San Andreas fault, Cajon Pass, southern California: Geol. Soc. Amer. Bul., v. 96, no. 6, p.793-812.

Weldon, R.J., 1986, The late Cenozoic geology of Cajon Pass: Implications for tectonics and sedimentation along the San Andreas fault, Ph.D. thesis, 400 pp., Calif. Inst. of Tech.

Weldon, R.J., 1991, Active tectonic studies in the United States, 1987-1990, Tectonophysics, 890-906.

Wells, D.L., K.J. Coppersmith, 1993, Updated empirical relationships among magnitude, rupture length, rupture area, and surface displacement, Geomatrix report, submitted to Bulletin of the Seismological Society of America.

WGCEP, 1988, Probabilities of large earthquakes occurring in California on the San Andreas fault, U.S.Geological Survey Open-File Report 88-398.

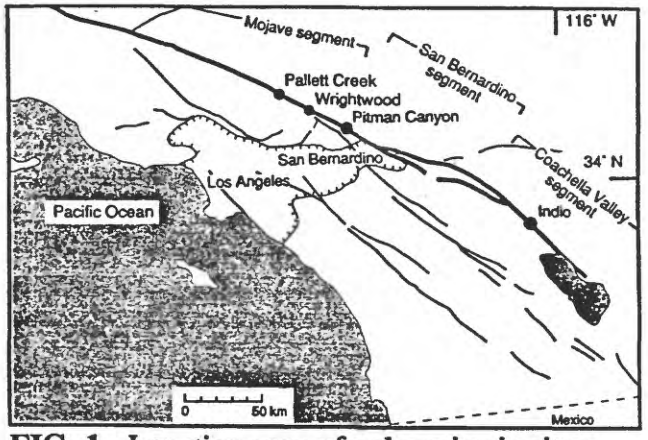

FIG. 1 Location map of paleoseismic sites along the southern San Andreas Fault (heavy line). The lighter lines show other faults in the region. The densely populated area is indicated by hatchures. Segment boundaries are shown as defined by WGCEP (1988).

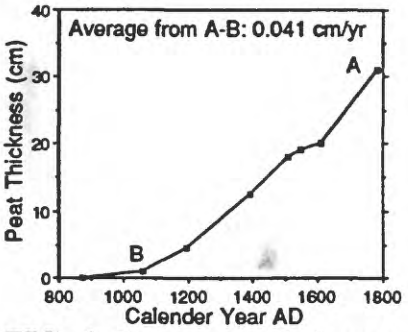

FIG. 4 Peat accumulation curve for the average thickness of peat layers at Pitman Canyon. For the event date refinement we used local higher less constraining rates than the average rate. For comparison note the average rates at Wrightwood: 0.057 cm/yr and Pallett Creek: 0.054 cm/yr (Biasi and Weldon, 1994a).

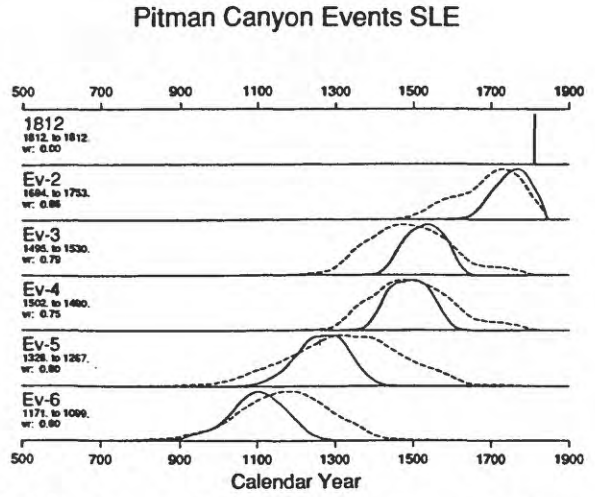

FIG. 3 Pitman Canyon event date distributions calculated from bounding prior dendrochronologically calibrated (Stuiver and Reimer, 1993) ^{14}C date distributions alone (dashed), fully constrained distributions (solid) include: stratigraphic ordering, sedimentation between layers, and sediment partitioning at the event horizon as constraints. Prior to posterior best estimate and variance reduction (vr) shown. The best event estimates of the Wrightwood record are: 1857, 1812, 1693, 1587, 1452, 1192 (Biasi and Weldon, 1994b).

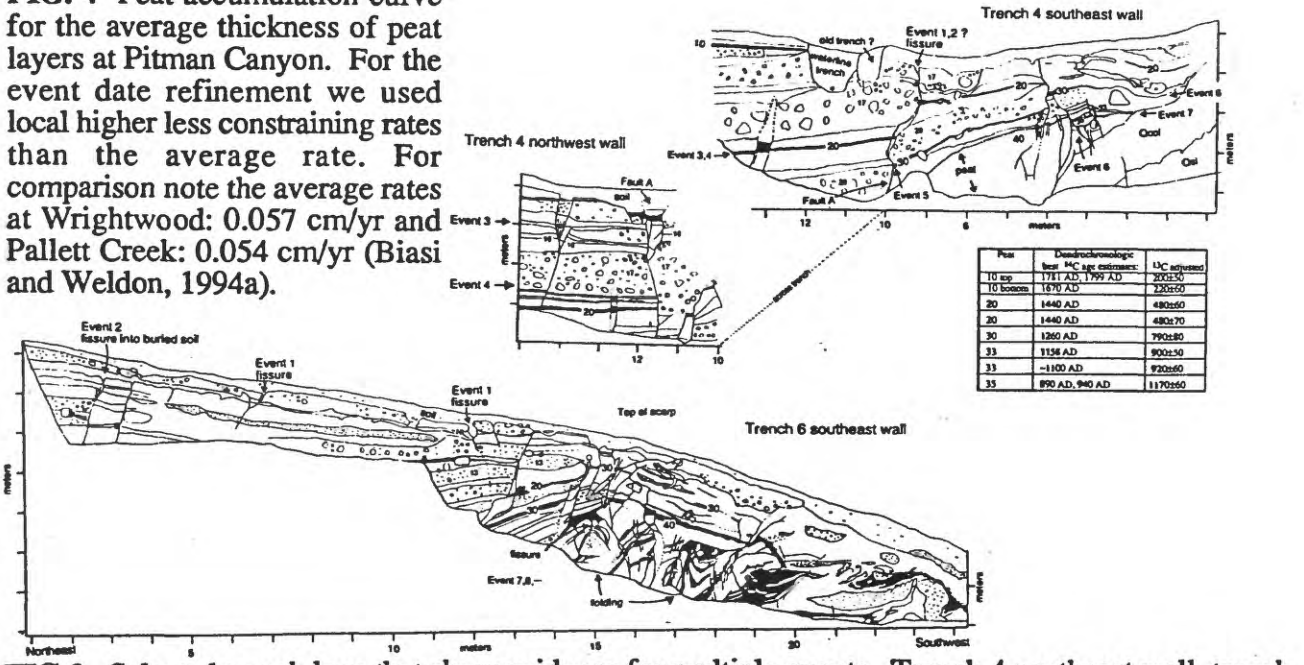

FIG.2 Selected trench logs that show evidence for multiple events. Trench 4 southeast wall, trench 4 northwest wall, and trench 6 southeast wall. The stratigraphic section consists of interbedded debris flows (outlined clasts), fluvial sands (unmarked), and peat layers (black unless indicated).

Fault-controlled offset of the ocean floor

Kunihiko Shimazaki, Earthquake Research Institute,
University of Tokyo, 1-1-1 Yayoi, Bunkyo-ku, Tokyo, 113 Japan

Modification of faulting-controlled land forms of the ocean floor can be represented by a simple formula slightly modified from that proposed by Hanks et al. in 1984 for subaerial land forms by adding a correction term. The term added represents an effect of sedimentation, whose rate is usually assumed to be constant in space. However, a simple mathematical manipulation leads to a conclusion that the land form itself is unaffected by sedimentation. This contradicts with a naive intuition. We tend to assume that a vertical offset of the ocean floor caused by faulting would soon be buried when the sedimentation rate is high. And also we tend to suppose that a feature of vertical offset shows a recent occurrence of earthquake where the sedimentation rate is high. According to the formula the most effective factor is the bathymetry, especially the slope of the ocean floor.

The formula is useful to estimate an occurrence time of a sudden vertical offset of the ocean floor, i. e. an earthquake. Where the amount of the offset is large but the sedimentation rate is low, the transient behavior after the earthquake can be well preserved in the sedimentation sequence. The western segment of the Central Beppu Bay fault appears to have experienced a locally large vertical offset amounting to 10m. The sedimentation rate is as small as 2-3mm/y. The applicability of the formula is tested by comparing layers of sediments on the both sides of the fault by using seismic profiling records and samples obtained by piston coring. The last offset event is preliminary dated about 2,000 years ago.

Stream Channel Offset and Abandonment and a 200-year Average Recurrence Interval of Earthquakes on the San Andreas Fault at Phelan Creeks, Carrizo Plain, California

John D. Sims, U.S. Geological Survey, National Center 905, Reston VA 22092

The Carrizo Plain segment of the San Andreas fault is noteworthy as an area that clearly displays offset, diverted, and abandoned channels. The channels result from the interaction of strike-slip fault processes, and the geomorphic processes of erosion, transport, and deposition. This interaction produces periodically abandoned channels accompanied by the incision of new channels across the San Andreas fault. Geomorphic features such as scarps, offset stream channels, grabens, and pressure ridges mark the surface trace of the fault. Excavations reveal offset sedimentary and stratigraphic features, evidence of individual earthquake events, and features related to the process of tectonically-induced stream abandonment. The offset channels consist of three elements; a pair of offset modern streams and two abandoned paleochannel groups: a partly infilled channel of intermediate age (paleochannel H), and a pair of mostly infilled, older abandoned coeval channels (paleochannels L and M). Thalwegs of the modern stream channels are offset 17.4 ± 1.6 m and 15.8 ± 0.6 m respectively. Excavations in the alluvium-filled younger abandoned paleochannel reveal that it is offset 101.9 ± 1.4 m from the smaller and 152 m from the larger of the modern channels.

The model developed here is applied to a pair of intermittant streams with a small to moderate-sized drainage basin in an arid to semiarid climate such as that of Phelan Creek, a site at which the pair of intermittant streams has been recurrently offset throughout most of Holocene time (see figure). This model is a new paradigm for neotectonic investigations seeking detailed paleoseismological histories from alluvial paleochannel deposits. It further demonstrates the usefulness of commonly available fluvial channel deposits in contrast to the rarer but more frequently studied ponded deposits. At the Phelan site, the southern channel, Big Phelan Creek, is larger than the northern stream, Little Phelan Creek. Northward extension of Big Phelan Creek west of the fault eventually results in the capture of the northern channel. Additional discharge contributed by the newly captured channel may aid in rejuvenation of the channel below their confluence and may cause erosion of the older deposits in the channel. Rejuvenation at this stage is largely dependent on storms because the size of the smaller drainage basin is about one-quarter that of the larger basin.

The major control on deposition at Phelan Creeks is lengthening of the stream channel along the fault after each surface rupture event. Fault movement develops a low-slope along-fault segment of the stream. Deposition occurs largely in this segment because of reduced slope and from the reduced stream-flow rate required to turn from the initial fault-normal segment to the along fault segment. The channel again turns sharply at the end of the along-fault segment to the downstream fault-normal fault-normal segment. Deposition begins in the upstream bend area as a response to decreased current velocity as the stream rounds the upstream bend to the along-fault channel segment. Each lengthening episode forces the along-fault segment to readjust to its slope and a new depositional cycle is initiated.

The paleochannel deposits at the Phelan Creeks site span a period of about 7000 years and record depositional responses to channel deformation over that period. The younger paleochannel deposits at Phelan Creeks contain abundant charcoal and record five major earthquakes over the last 1150 years. We also tentatively identify a sixth event. The recurrence interval of the last five earthquakes ranges from about 150 to about 300 years. Surface displacement in each of the last two events was about 7½ meters. Charcoal is less abundant in paleochannel deposits older than about 1,150 years. Thus, we are unable to determine an equally detailed history of recurrent offset of Phelan Creeks by the San Andreas fault for the period from ~1,100 to ~7,000 BP. The effects of earlier recurrent offset of the channels of Little and Big Phelan Creeks is recorded in the two abandoned paleochannel sequences. The modern channels illustrate the effects of recurrent movement along the fault after only two earthquakes. Recurrent offset of Big and Little Phelan Creeks results in lengthening of their along-fault channel-segments. After about 45 m of offset the western reach of Big Phelan Creek captures Little Phelan Creek. The signature of this capture may be seen in the sequence of deposits in the along-fault channel segment.

Four sedimentologically distinct phases of alluviation record the recurrent offset of this abandoned paleochannel. Alluviation within the paleochannel occurred as a response to its increased length and decreased slope along the fault during recurrent offset. Characteristically the vertical component of fault slip is small. We hypothesize that unconformity-bounded sedimentary units represent phases of alluviation associated with increased offset of the stream channels along the fault and thus constrain the times of earthquakes. The older abandoned paleochannel contains three phases of alluviation and two phases of colluvium accumulation, and the younger abandoned paleochannel contains four phases of alluviation. Earlier phases of alluviation represent longer periods of time than later ones because the earlier ones are representative of cut-and-fill conditions so that accumulation was low. Later phases of alluviation in the younger paleochannel represent depositional phases associated with individual earthquakes. Alluvial fill in the older abandoned paleochannels at the northwest end of the study site records their separation from their headwaters by recurrent strike-slip movement on the San Andreas fault over the past 7,000 years. The pair of older abandoned channels is offset 238 m ± 1.5 m from the pair of modern channels. This yields a Holocene slip rate of ~34 mm/yr.

The last six events at Phelan Creeks are dated, in the AD/BC convention at 1857, ~1505, 1361 ± 38, 1236 ± 15, 1003 ± 20, and tentatively 838 ± 35. The 1505 event is not directly dated at Phelan Creeks although physical evidence for it is present. I use the date of the event from the Bidart site 5 km southeast of Phelan Creeks. The 1361 event is dated by the abandonment of paleochannel H and probably postdates the earthquake. The date of event R, 1346 ± 17, at Pallet Creek may be more accurate. The remaining dates for earthquakes at this site derived from multiple radiocarbon dates applied to the interpretation of depositional sequences using the tectono-sedimentological model presented above.

EPHEMERAL CHANNEL RESPONSE TO RECCURENT OFFSET--SCHEMATIC MODEL

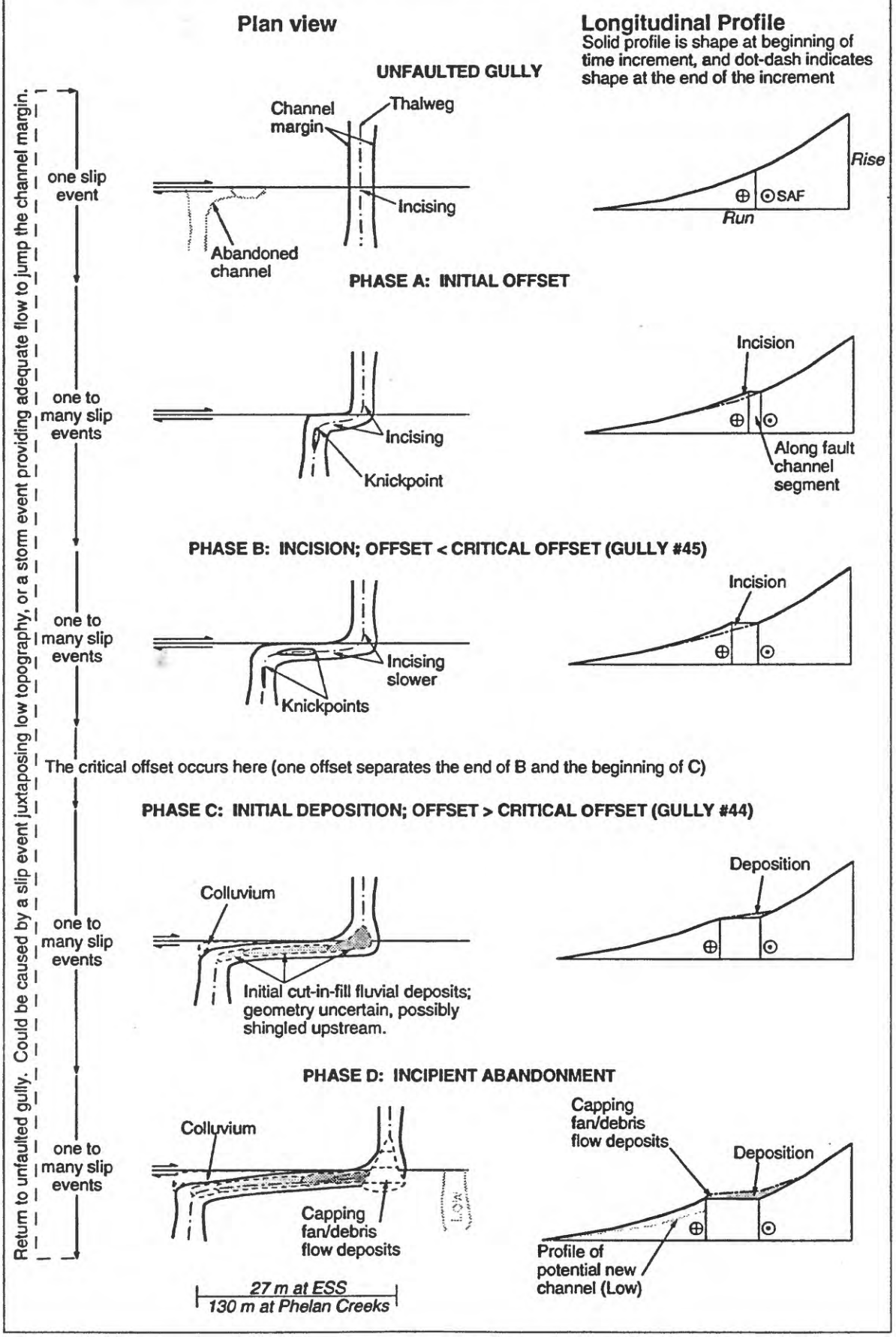

Complications in Making Evaluations within the Basin and Range Province, Western United States

D. Burton Slemmons, 2905 Autumn Haze Lane, Las Vegas NV 89117

Several factors contribute to the difficulty of making paleoseismic assessments of surface faults in the Basin and Range Province-Intermountain Seismic Belt. Study of the eleven historic earthquakes that had extensive surface faulting indicate the following difficulties in assessing paleoseismic events:

Difficulties in correlating events between faults in zones with complex rupture patterns: Complex patterns are present in most fault zones of $M_w > 6.75$ earthquakes and appear to be normal for the province.

Difficulties in using fault segmentation models: Most earthquakes of $M_w > 6.75$ rupture more than one fault segment, and simple models that use only one segment may underestimate potential earthquakes.

Difficulties evaluating temporal clustering of activity: Abrupt changes in the rates of activity by temporal clustering, or spatial shifting of the location of active zones make it hard to assess recurrence intervals and fault slip rates. About 50 percent of the highest magnitude historical earthquakes have different modern, Holocene, or late Quaternary slip rates than for longer periods.

Difficulties in the assessment of the influence of strike-slip faulting related to the San Andreas fault system in the western Basin and Range Province: This problem is especially important in the southern Walker Lane where strike-slip faults extend northward from the San Andreas into an extensional province.

Other difficulties are of more limited scope, or are not fully assessed:

Strain partitioning: Zones of oblique-slip deformation may partition strain into sub-parallel faults that have different styles of deformation. Assessing seismic hazards in zones with possible partitioning may be restricted to faulting in Owens Valley, Panamint Valley-Saline Valley, and Death Valley-Fish Lake Valley.

Detection of concealed active faults: The detection of active faults that underlie shallow detachments or blind faults require the evaluation of more subtle, non brittle failure. Accordingly, the assessments may require geomorphological studies of monoclinal warps, tilted alluvial fans and tilted range fronts, or the use of special geophysical methods, such as seismic reflection profiling.

Reactivation of Paleocene or earlier thrust faults during a Cenozoic extensional regime, or activation of Tertiary low angle faults: This relatively new consideration has been studied in only a few parts of the province, and some of the results are still controversial.

Paleoseismology in Extensional Volcanic Terrains

R.P. Smith and S.M. Jackson, Idaho National Engineering Laboratory, EG&G Idaho, Inc., P.O.Box 1625, Mail Stop 2107, Idaho Falls, Idaho 83415
W.R. Hackett, WRH Associates, 1524 Juniper Drive, Pocatello, Idaho 83204

In volcanic regions worldwide, linear belts of eruptive fissures, tensile fissures, normal faults, flexural monoclines, and graben are developed within volcanic rift zones. These volcano-extensional features are sometimes interpreted as structures associated with major tectonic faults, but, they are the surface expression of dikes intruded in the shallow subsurface beneath volcanic rift zones (Figure 1). Such misinterpretations can lead to invalid and overly conservative assessments of their seismic hazards. We present criteria for recognition of volcano-extensional structures, discuss the implications of the dike-intrusion process for paleoseismic assessments, and suggest suitable approaches to paleoseismic analyses in volcano-extensional terrains using the eastern Snake River Plain (ESRP), Idaho as an example.

Structures formed by deformation above shallow dikes in volcanic rift zones can be distinguished from those related to major tectonic faults using several criteria. Commonly the extensional deformation features are developed cogenetically in volcanic deposits. Tensile fissures with little or no vertical displacement are predominant. Fissures, faults, and monoclines typically occur within broad zones, not narrow belts near a main fault zone, reflecting their origin by repeated injection of dikes beneath volcanic rift zones (Figure 1). Fissure swarms, normal faults, and monoclines are commonly symmetrically distributed about a central eruptive fissure, sometimes forming a graben. The vertical displacement of faults and monoclines changes rapidly along strike, and may vary by several meters within distances of 10 to 20 meters.

The mechanism of dike intrusion and the nature of co-intrusive seismicity have important implications for the paleoseismic analyses of extensional volcanic terrains, especially for the estimation of earthquake recurrence and maximum magnitude. Fault scarps with ten-meter vertical displacements may occur in volcanic bedrock, but reflect the cumulative effects of many decimeter-scale displacement events. Such scarps commonly represent several volcano-intrusive episodes, each with multiple dike intrusions which are usually separated by 10^2 to 10^5 years. Thus, colluvial wedges containing records of single large earthquakes are not formed.

Small to moderate size earthquakes are associated with volcano-extensional structures because their rupture dimensions are constrained by the dike-related fault geometry and mechanism of formation. Dike-induced normal faults do not transect the entire thickness of the seismogenic crust, but extend slightly deeper than the dike tops. Because co-intrusive surface deformation occurs when dikes ascend within 2 to 4 km of the surface, the down-dip extent of associated faults and fissures can safely be assumed as less than 5 km (Figure 1). Estimated maximum magnitudes of about 5.5 are typical, given the small fracture-surface areas. Such estimates are extremely conservative because slip typically does not occur instantaneously across an entire fault surface, but gradually (about 0.5 m/s) traverses the shallow subsurface as a migrating swarm of low-magnitude earthquakes around and above the propagating dike. Maximum magnitudes of paleoseismic events in volcanic rift zones without historical seismicity can be estimated by analogy with observed earthquake magnitudes in active volcanic rift zones such as those in Iceland and Hawaii. Maximum magnitudes associated purely with dike intrusion are about 4.0-5.0. Magnitudes greater than 5.0 usually involve some component of tectonic deformation. As exhibited by contemporary transform faulting in Iceland and gravity-driven thrust faulting in Hawaii, dike intrusion episodes may trigger tectonic earthquakes. Demonstration of such triggered earthquakes in the paleoseismic record will require the development of more precise age control than is now possible.

The relationship of volcano-extensional structures to subsurface dike swarms and their formation in cogenetic volcanic rocks, typically lavas, makes them difficult to analyze with

conventional paleoseismologic field methods. We suggest that the geochronology of the associated lavas and volcaniclastic materials be used to estimate recurrence, rather than conventional approaches requiring the presence of fault scarps and colluvial wedges. Promising methods include radiocarbon dates from charred vegetation, the use of *in situ* cosmogenic radionuclides to date the exposure times of volcanic rock surfaces, and thermoluminescence dating of fine quartzose substrates, heated beneath lava flows. In all cases, the volcanic recurrence data must be interpreted as representing recurring periods of co-intrusive seismicity, not the recurrence of individual earthquakes as are typically used for estimating slip rates.

Volcano-extensional features in the ESRP volcanic rift zones, have been suggested to be extensions of tectonic normal faults (Figure 2). Such interpretations lead to conservative and inappropriate assessments for seismic design at the Idaho National Engineering Laboratory (INEL). Development and application of the concepts described above have led to more reasonable estimates of maximum magnitude and earthquake recurrence. Normal fault and fissure dimensions within the volcanic rift zones have been used to estimate a maximum moment-magnitude 5.5 earthquake for an episode of rift-zone volcanism. Detailed investigations of volcanic rift zone chronology suggest annual probabilities of about $2x10^{-5}$ for the area of the INEL.

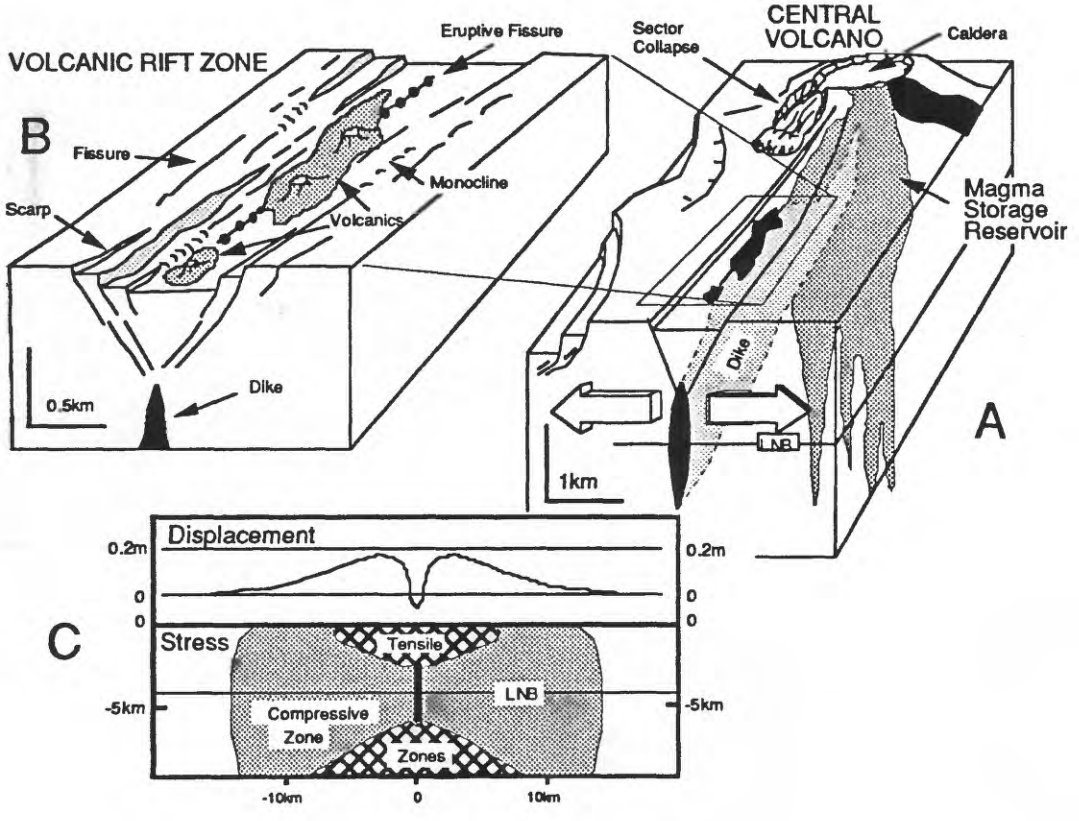

Figure 1. Schematic diagrams, summarizing the configurations of extensional structures in volcanic terrains and their relationship to magmatic processes: [A] Brittle deformation associated with upper crustal magmatism (LNB = level of neutral buoyancy); [B] Dike-induced structures along a volcanic rift zone; [C] Results of numerical elastic deformation model of dike intrusion (Rubin, 1992) are comparable to observed brittle deformation features of [B]. Upper part of the diagram shows a vertical displacement profile above a dike of 1 meter thickness, extending from 1 to 6 km depth. Lower part of the diagram shows the compressive and extensional zones that develop around a dike as a result of magma pressure.

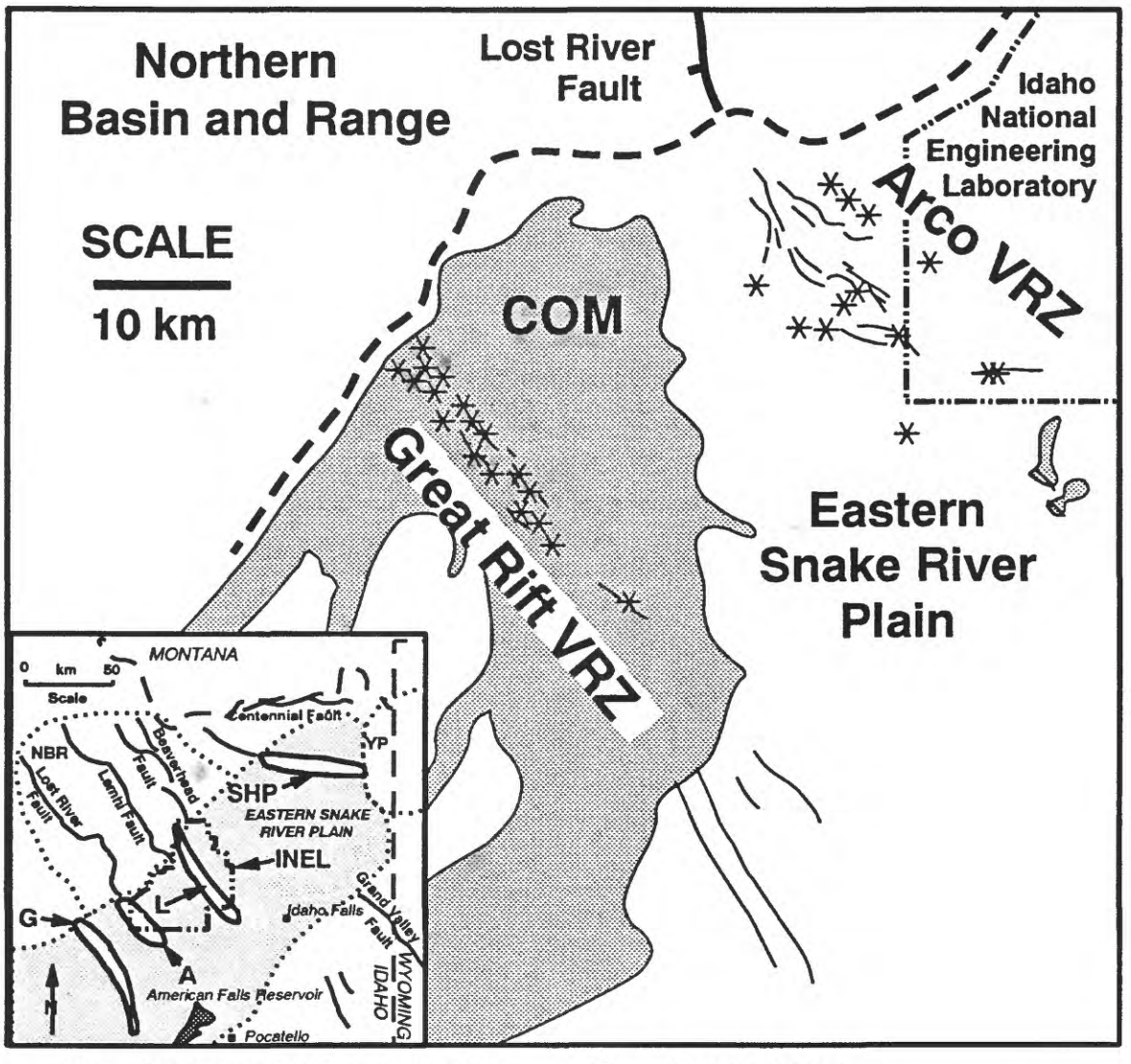

Figure 2. Map of the eastern Snake River Plain (ESRP) showing volcanic rift zone structures within the volcanic province and Basin-and-Range normal faults adjacent to the Plain. Both provinces are experiencing NE-SW directed crustal extension. The Basin-and-Range extension occurs by normal faulting with associated large-magnitude earthquakes. The ESRP extends by repeated intrusion of northwest-trending vertical dikes in volcanic rift zones. Estimated numbers and thicknesses of dikes in the upper crust beneath the ESRP are comparable to estimated total extension in the normal-faulting province.

Palaeoseismological investigations on anthropogenic constructions, and implications for the earthquake recurrence intervals.

S.C. Stiros, Institute of Geology and Mineral Exploration (IGME)
70, Mesoghion St., Athens 11527, Greece

The palaeoseismic research usually focusses on deformation of elements of the physical environment, while the traces of ancient earthquakes on anthropogenic constructions and human life are ignored. Yet, the branch of palaeoseismology focussing on these last three fields is very important for certain regions, East Mediterranean for instance: Numerous strong earthquakes have affected human life and history in this region, destroying buildings and sites, influencing the building style and leading to the development of genuine and sophisticated anti-seismic construction techniques. Earthquakes have also controlled the inhabitation pattern of certain areas, at least for some periods, while their impact in the social, cultural and civic life was probably very important: the effects of the earthquakes were mixed with myths and cultures; in one case, a human sacrifice, assumed to be an ultimate, though unsuccessful, antiseismic protection technique was discovered. Signs of some of these earthquakes can be traced in archaeological remains, and provide excellent and inexpensive palaeoseismic information.

In the last years archaeological data, both from literature and unpublished works have been studied as a potential source of palaeoseismic information, and a methodology for the identification and documentation of the necessary information, as well as an archaeoseismic database have been developed. The information obtained is sometimes confirmed or completed from written data, and is either direct or indirect: Direct information comes from inscriptions in tombs of earthquake victims, or from inscriptions acknowledging the post-seismic reconstruction of sites and public buildings, usually naming a donator, an emperor, or a governor.

Indirect information is deduced from observations of remains of earthquake victims, ancient remains offset by seismic faulting, characteristic structural damage (for example, "detachments" along horizontal discontinuities of structural elements) and characteristic pattern of fallen structural elements of ancient constructions (for example, oriented fallen structural members, or drums of columns lying as slices of salami), as well as cases where an earthquake appears as the only possible and reasonable explanation for a destruction.

An advantage of the archaeological palaeoseismology is that provides information not only for permanent deformations of certain elements of the physical environment, but of vibrations as well, functioning as a "palaeoseismogram" recording practically local shocks; this is due to the fact that the ancient constructions (with the exception of tall, slender buildings like minarets, columns and towers) were practically influenced by short period waves only.

Some workers assume that from the examination of ancient remains information on the parametres of ancient earthquakes (intensity, magnitude, epicentre, causative faults, etc) can be obtained. We are of the opinion, however, that the study of anthropogenic

constructions is extremely important for the estimation of recurrence intervals of major shocks in a certain area, (or better of the lapse time since the last major shock), though their source faults cannot be determined. A characteristic example is the contrast in the surviving traditional buildings in Heracleion, Rethymnon and Chania, the major towns of central and west Crete: before their reconstruction in the last decades, no traditional buildings more than two and three-stroreys high existed in Heracleion and Rethymnon, respectively, while the core of the old town of Chania is composed by 500-yr old, four to five storey buildings or remains of buildings. The larger recurrence intervals of destructive shocks in Chania (possibly 1500 years) relative to those in Heracleion (about 200 years) may explain the contrast in their building pattern. At Rethymnon, in the middle of the distance between the other two towns, earthquakes rather remote selectively prevent constructions of a certain height from preservation. Historical data reveal that while anti-seismic construction styles were known, they were not in use, because there was obviously no reason for that. But after a destructive shock, the whole towns were rebuilt on the base of the antiseismic techniques known for centuries, and suffered little from subsequent strong earthquakes. This is the case of Smyrna (Izmir), for instance, the building style of which was drastically changed after the 1688 earthquake without any significant change in the socio-economic and political context. Thus, it is reasonable to conclude that the 1688 earthquake marked the end of a certain period of seismic quiescence in the Smyrni area, during which people, oblivious of the seismic threat, adopted a weaker structural style. The same situtation can be observed in Constantinople (Istanbul) as well: The monuments of the city suffered from strong shocks untill approximately the 14th century, but subsequently, no strong earthquakes affected the area and weaker structural styles were adopted and are successfully still in use. In other cases, the continuous threat of earthquakes was responsible for a conservative architectural style that has not been affected by changes in the social, political and economic context of the society. Another advantage of the archaeoseismic methodology is the dating, based mainly on stylistic archaeological and architectural techniques (variations of the style of pottery objects and other artifacts, etc), which provide a relative dating; the latter is combined with historical information, and can be accurate up to within a few years or decades.

Earthquake Surface Ruptures: Quantitative Analysis and Paleoseismological Implications

A.L.Strom, Hydroproject Institute, Geophysical Department, Moscow, Russia
A.A.Nikonov, Joint Institute of Physics of the Earth, RAS, Moscow, Russia

To get more reliable estimations of paleoearthquake magnitudes from the surface rupture parameters the world-wide data on earthquakes accompanied by surface faulting have been collected and analysed.

In elaboration of studies performed by Tocher (1958), Iida (1965), Chinnery (1969), Solonenko (1973), Slemmons (1982), Bonilla et al. (1984), Khromovskikh (1989) and others, one of the present authors compiled the catalogue of seismic ruptures which comprises empirical data of more than 250 earthquakes all over the World. About 200 events have got instrumentally determinated magnitudes. Two data sets are presented, namely on earthquakes themselves (date, location, magnitude [M_S], focal mechanism) and on associated surface ruptures (total length [L], maxima vertical and lateral displacement values [D_{max}], maxima net displacement (when data available)). Besides for surface ruptures of 60 earthqakes investigated in more details average weighted displacement values [D_{av}] were calculated.

On the base of the data collected the relationships of $D_{max} \sim L$, $D_{max} \sim M_S$, $D_{av} \sim D_{max}$ are being analysed. The peculiarity of the utilized approach consists in the analysis of not only the regressions of above-mentioned parameters but also of the enveloping curves corresponding to the limited measured displacements [D_{lim}] versus rupture length and earthquake magnitude. It was found out that, while L and M_S increase, maxima measured single-event displacements increase consequently, although nonlinearly, up to the limited values of 12 - 14 m. The greatest offsets (> 10 m) accompanied large ($M_S \geq 8.0$) earthquakes with strike-slip focal mechanisms.

The calculated average weighted displacement values make up, on an average, about 1/3 of maxima measured ones.

On the ground of the analysis performed it seems to be expedient in the course of paleoseismological investigations: (1) - to check out whether do $D_{max} \sim L$ relationship for a fault, assumed to be the paleoearthquake rupture, corresponds to that, typical of modern earthquake surface ruptures; (2) - to estimate minimal possible magnitude of paleo-earthquake on the basis of D_{lim} versus M_S graphs, especially when magnitude of the studied paleo-earthquake is expected to be less than 6.5 or more than 8.0; (3) - to examine the correspondence of the displacement measured at a separate individual outcrop (for example in a trench) to the real maximum displacement along the studied paleorupture, to get more accurate magnitude estimation.

Paleoseismological Studies in South Carolina

P. Talwani, Department of Geological Sciences, University of South Carolina, Columbia, South Carolina

The discovery in 1983 of a sand blow associated with the 1886 Charleston earthquake demonstrated that indirect evidence of large earthquakes can be preserved in soft sediments in the South Carolina Coastal Plain (SCCP).

In-depth investigations by USGS, EBASCO Services and the University of South Carolina, over the last decade has led to the discovery of over one hundred sand blows associated with 1886 and earlier earthquakes. By obtaining C-14 dates of the entrapped organic material (roots, pieces of wood, leaves, bark, charcoal, peat, etc.) it has been possible to establish dates of prehistoric earthquakes. Cross cutting relationships between host material and intruding sands have been used to bracket dates of paleoearthquakes. Roots growing into sand blows, sand blows cutting roots, pieces of wood, leaves, bark found in sand blows have been used to obtain minimum, maximum and contemporary ages of the paleoearthquakes. Embedded pieces of charcoal also provide maximum ages.

Within the accuracy of the C-14 dates, six episodes of prehistoric earthquakes could be identified in the South Carolina Coastal Plain. These occurred about 600, 1200, 1800, 2350, 3200, 5150 and 5150+ years before present. The sand blows were located in three general regions along the SCCP around Charleston and about 100 km NE near Georgetown and about 100 km to the south near Bluffton. These were identified as the Charleston, northern and southern areas.

Since liquefaction of sediments can occur at large distances from the hypocenter, we established the following criteria to identify the source of the paleoearthquake from the observations above. The frequency and dimensions of the sand blows were found to decrease as we went away from the source. So, for sand blows associated with a particular date, the seismic source was taken to be near the location of the largest and greatest number of sand blows. In two cases, sand blows of a particular date were only found in a particular area. Seventeen sand blows associated with the 1800 event were found at five locations in the northern area and at one location about 20 km east of the Charleston source zone. The 1800 event was identified as being associated with the northern seismic zone. Similarly the 600 and 2350 YBP events were identified as being associated

with the southern seismic zone. The other events were identified with the Charleston seismic zone. The event dated 3200 YBP was found to be most widely preserved in sand blows in all three regions and was judged to be the largest.

The results are summarized in Figure 1. They show that paleoseismological investigations cannot only establish dates of prehistoric earthquakes but also identify their sources.

APPROXIMATE TIME OF EVENT (YBP)	Southern Sites	Charleston	Northern Sites
108	2(2)	Many	Reports
600	5(7)	1(1)	1(1)
1200	3(3)	1(5)	1(4)
1800	-	-	5(17)
2200	2(3)	-	-
3200	1(3)	4(11)	-
5150	1(2)	2(4)	1(1)
>5150		1(1)	(>4500)

FIGURE 1: Six episodes of prehistoric earthquakes identified in the South Carolina Coastal Plain. Number sequences (e.g., 5(7))indicate number of events and number of sand blows found.

Geomorphic Clues to Paleoseismicity
Examples From the Eastern Ventura Basin
Los Angeles County, California

Jerome A. Treiman
California Division of Mines and Geology
107 S.Broadway, Rm.1065
Los Angeles, CA 90012

Most paleoseismic studies have dealt with *surface* faulting from past events, however recent earthquakes (Loma Prieta, Whittier, Northridge) have shown us that non-surface rupturing events may be more common than previously considered. The study of features that directly reflect regional (rather than local) surface deformation has promise for providing data that are source specific. This is in contrast to shaking phenomena (such as liquefaction, lurching and landsliding) that tell us only that there was a seismic event within the region. Geomorphic indications of seismicity on two fault zones in the eastern Ventura basin (see Figure 1) are described below.

The 17 January 1994 Northridge earthquake produced no primary surface rupture that has been identified. Bedding-plane slip that occurred during the Northridge earthquake has been mapped in close proximity to a pre-existing closed depression which has been identified on the north slope of the Santa Susana Mountains, approximately 20km north of the epicenter (Treiman, 1994). Slip occurred along at least five bedding planes exposed in building pads and cut slopes of a residential development west of Interstate 5. Displacement was consistently northeast side up (up to 19cm measured) and lateral separations varied from 4cm right-lateral to 7cm left-lateral. The zone of rupture was about 250m long with additional ground fracturing occurring for another 350m (Figure 1). This zone of faulting and fracturing is considered to be the result of flexural slip within the north limb of the Pico anticline, which underlies the northern Santa Susana Mountains. A naturally occurring closed depression, about 70m long and 40m wide, is aligned with and northwest of the zone of faulting, but within the more extensive zone of fracturing. This depression and others in the region are believed to record flexural slip from prior Northridge-type events.

A previous study (Treiman, 1983) also addressed near-field geomorphic indications of fault displacement in the Santa Clarita area. The San Gabriel fault zone is a major structure in southern California which was, and perhaps still is, directly related to the San Andreas fault system. Holocene faulting has been documented on a portion of this fault zone near Santa Clarita (Cotton,1985).

Previous work in the Santa Clarita area (Dort, 1948; Winterer and Durham, 1962; Treiman, 1987) has identified one principal late-Pleistocene geomorphic surface southwest of the San Gabriel fault zone and as many as seven surfaces (fluvial terraces) localized northeast of the fault zone. These seven terraces merge upstream, away from the fault, into just two or three terraces. The youngest three or four terraces are present only in the vicinity of the fault and appear to be Holocene in age. This is suggestive of episodic uplift adjacent to and northeast of the fault zone. Information further supporting local deformation is the lower gradient of the upper terrace levels, as noted by Winterer and Durham (1962), which may be a result of backtilting of these older surfaces.

There is also independent evidence, southwest of the fault zone, of several deformational episodes (Treiman, 1983). Progressive deflections have occurred in the direction of headward erosion of several ephemeral streams dissecting the alluvial surface southwest of the San Gabriel fault zone. Five distinct progressively younger sets of stream headings separated by 15 to 35 degrees each (average azimuth) suggest that a minimum of four movements on the San Gabriel fault zone have tilted the late-Pleistocene alluvial surface.

REFERENCES

Cotton, W.R., 1985, Holocene behavior of the San Gabriel fault, Saugus/Castaic area, Los Angeles county, California: Final Technical Report to the U.S. Geological Survey, Contract No. 14-08-0001-21950, June, 1985.

Dort, Wakefield, Jr., 1948, The geology of a portion of eastern Ventura basin, California: unpublished M.S. thesis, California Institute of Technology, 100p.

Treiman, J.A., 1983, (abstract) Geomorphic evidence for recurrent late Quaternary movement on the San Gabriel fault, Saugus, California: Abstracts and Program, Association of Engineering Geologists 26th Annual Meeting, October 2-7, 1983, San Diego, California, p.96.

Treiman, J.A., 1987, Geologic map of the SE/4 Newhall quadrangle: California Division of Mines and Geology, unpublished mapping for Los Angeles County Engineers, 1"=800'.

Treiman, J.A., 1994, (abstract), Bedding-plane slip associated with the 17 January 1994 Northridge earthquake: Seismological Society of America, 89th Annual Meeting, Program for Northridge Abstracts, abstract 34.

Winterer, E.L., and Durham, D.L., 1962, Geology of southeastern Ventura basin: U.S. Geological Survey Professional Paper 334-H, p.275-366.

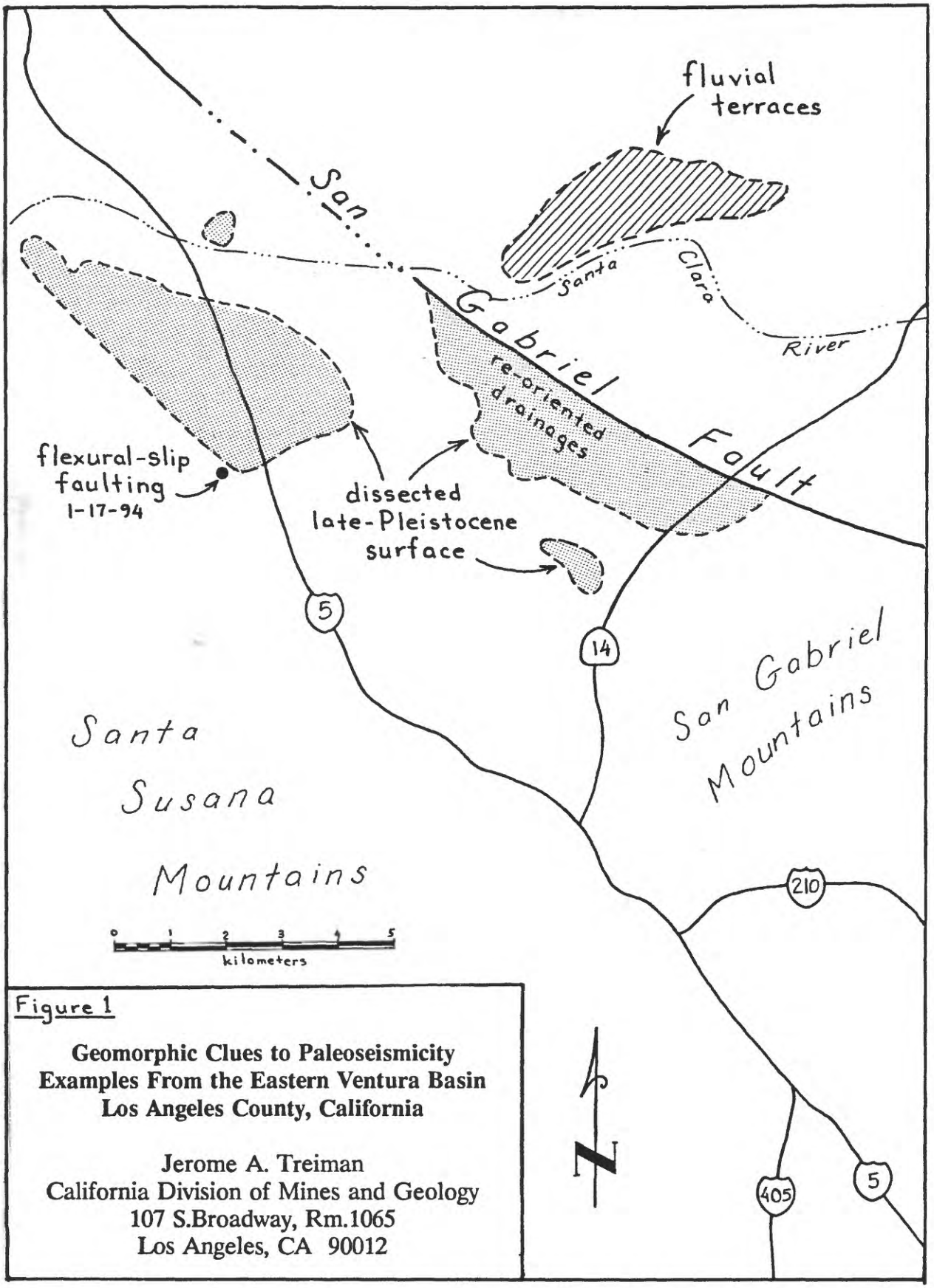

Figure 1

Geomorphic Clues to Paleoseismicity
Examples From the Eastern Ventura Basin
Los Angeles County, California

Jerome A. Treiman
California Division of Mines and Geology
107 S.Broadway, Rm.1065
Los Angeles, CA 90012

SEGMENTATION AND HISTORY OF HOLOCENE SURFACE FAULTING ON THE MEDIAN TECTONIC LINE, SOUTHWEST JAPAN

Hiroyuki Tsutsumi, Department of Geosciences, Oregon State University, Corvallis, OR 97331
e-mail: tsutsumh@ucs.orst.edu
Atsumasa Okada, Institute of Geophysics, Kyoto University, Kyoto 606-01, Japan
e-mail: okada@stardust.kugi.kyoto-u.ac.jp

ABSTRACT

The Median Tectonic Line active fault system (MTL) is an arc-parallel, right-lateral strike-slip fault related to the oblique subduction of the Philippine Sea plate beneath the Eurasian plate along the Nankai trough, southwest Japan. The 300-km-long fault has one of the highest late Quaternary slip rates (5-10 mm/yr) in onshore Japan but was considered to be unruptured at least in the past 1,000 years. We identified 12 segments in the MTL, separated by geometric discontinuities, such as en échelon steps, bends, and gaps in the surface trace. A chronology of latest Holocene surface faulting on the MTL was constructed through trenching and geomorphic mapping, as well as acoustic profiling and piston coring of the submarine extension of the fault zone. The MTL does not rupture along its entire length in a single earthquake, but instead consists of multiple "earthquake segments" that rupture independently of one another. The recurrence interval and surficial offset for ground-rupturing earthquakes on the MTL are 1,000-3,000 years and 5-8 m, respectively. The relatively long recurrence interval and large surficial offset per earthquake suggest large seismic moment release during surface-rupturing earthquakes on the MTL, as commonly observed for Japanese moderate to large intraplate earthquakes. Because the most likely surface rupture lengths calculated from empirical relations between surface displacement and rupture length are considerably larger than individual segments, large earthquakes on the MTL probably rupture multiple geometrically-defined segments. Trenching shows that part of the MTL ruptured most recently after the 16th century A.D. with at least 6.9 ± 0.7 m of slip along the main fault trace. The correlation of this event to a historical earthquake is not straightforward and is currently in debate. Among the historical earthquakes catalogued in Usami [1987], only the 1596 Keicho-Kinki earthquake is accompanied by a historical document suggestive of slip along the MTL in the past 500 years. This document records coseismic uplift of a village immediately north of the MTL, which is consistent with down-to-the-south Quaternary scarps on the MTL closest to the village. The credibility of this historical document, however, has been disputed by some Japanese historians. The resolution of this debate awaits identification of geologic evidence of the uplift, as well as further investigation of historical documents regarding the earthquake.

Recognizing and Dating Prehistoric Earthquake-Induced Liquefaction Features in the New Madrid Seismic Zone, Central United States

M.P. Tuttle, Department of Geology, University of Maryland, College Park, MD
E.S. Schweig, U.S.G.S. and CERI, University of Memphis, Memphis, TN

As part of an ongoing study, we have recognized and estimated the ages of numerous prehistoric liquefaction features in the southern part of the New Madrid seismic zone (NMSZ). The NMSZ is the source of the great earthquakes of 1811 and 1812 which induce intense and widespread liquefaction (Fig. 1; Fuller, 1912; Obermeier, 1989). As seen on aerial photographs and reported in other field studies, liquefaction features are abundant in the region. Liquefaction features have been used in the northern part of the region to identify prehistoric earthquakes and to estimate a 400 to 1,100 yr recurrence interval for large events (Russ, 1982; Saucier, 1991; Vaughn, 1991; Kelson et al., 1992).

Recognizing prehistoric liquefaction features in the southern part of the zone has been more problematic. Previous studies found no definitive evidence of paleoliquefaction features in this area despite reconnaissance of many kilometers of drainage ditches (Wesnousky and Leffler, 1992; Rodbell and Schweig, 1993). We have been able to recognize prehistoric liquefaction features where others have not by taking an interdisciplinary approach, combining archaeology, geology, and pedology, and conducting detailed site investigations, involving careful examination of structural and stratigraphical relations and pedological characteristics of liquefaction features.

Estimates of the ages of prehistoric liquefaction features are based on radiocarbon dating of organic samples collected from horizons that pre- and post-date the liquefaction features and on stratigraphic relations between Native American cultural horizons containing artifacts and the liquefaction features. With additional study, soil properties may provide another means of dating liquefaction features in the region. Liquefaction features whose ages are well-constrained by other means provide the opportunity to study the development of soil characteristics with time. Once soil development time scales have been established, then soil properties can be used to estimate the age of liquefaction features.

The age clustering of liquefaction features suggests two large earthquakes occurred during the thousand year period preceding the great earthquakes of 1811 and 1812. One of the prehistoric events occurred about A.D. 900 and the other event occurred about A.D. 1500. These results are consistent with the findings of paleoseismological studies in the northern part of the zone and support a short (400 to 1,100 yr) recurrence interval for large earthquakes in the NMSZ. With additional study, we hope to define the magnitude of these prehistoric events and to date earlier earthquakes for which we now have only limited information.

References Cited

Fuller, M.L., 1912, The New Madrid earthquake: U.S. Geological Survey Bulletin, v. 494, 119 p.

Kelson, K.I., VanArdsdale, R.B., Simpson, G.D., and Lettis, W.R., 1992, Assessment of the style and timing of late Holocene surficial deformation along Reelfoot scarp, Lake County, Tennessee: Seismological Research Letters, v. 63, n. 3, p. 349-356.

Obermeier, S.F., 1989, The New Madrid Earthquakes: An engineering-geologic interpretation of relict liquefaction features: U.S. Geological Survey Professional Paper 1336-B, p. 114.

Rodbell, D.T., and Schweig, E.S., III, 1993, The record of seismically-induced liquefaction on late Quaternary terraces in northwestern Tennessee: Bulletin of Seismological Society of America, v. 83, p. 269-278.

Russ, D.P., 1982, Style and significance of surface deformation in the vicinity of New Madrid, Missouri *in* McKeown, F.A. and Pakiser, L.C., eds., Investigations of the New Madrid, Missouri, earthquake region: U.S. Geological Survey Professional Paper 1236, p. 94-114.

Saucier, R.T., 1991, Geoarchaeological evidence of strong prehistoric earthquakes in the New Madrid (Missouri) seismic zone: Geology, v. 19, p. 296-298.

Vaughn, J.D., 1991, Evidence for multiple generations of seismically induced liquefaction features in the Western Lowlands, southeast Missouri: Seismological Society of America, Program with Abstracts, p. 67.

Wesnousky, S.G., and Leffler, L., 1992, The repeat time of the 1811 and 1812 New Madrid earthquakes: A geological perspective: Bulletin of the Seismological Society of America, v. 84, n. 4, p. 1756-1785.

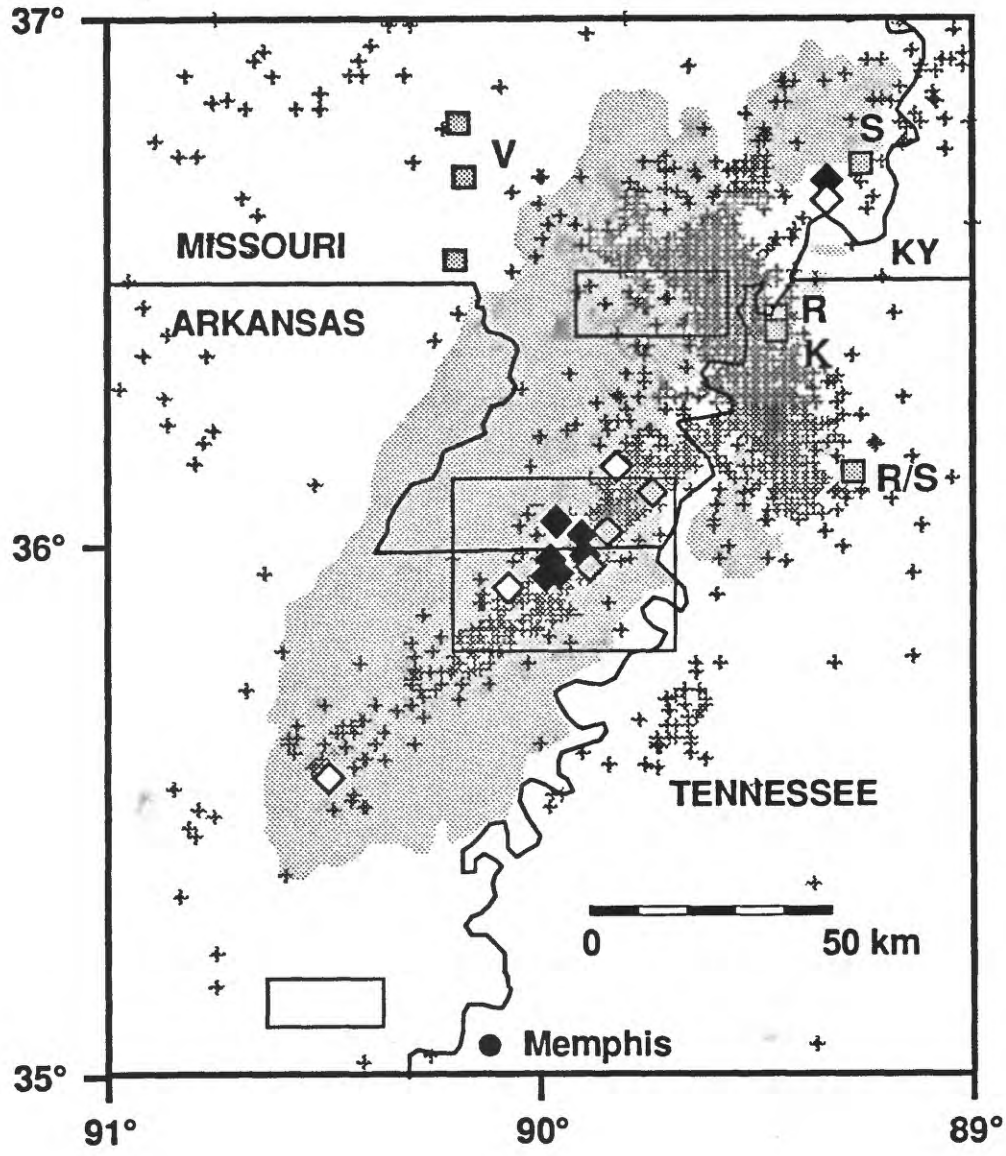

Figure 1. Map of the New Madrid seismic zone. Area where > 1% of the ground surface is covered by sand blow deposits shown by gray shading (Obermeier, 1989) and locations of recent (1974-1991) seismicity shown by crosses. Sites of other paleoseismological studies denoted by gray squares and labeled R=Russ (1982), K=Kelson et al. (1992), R/S=sites of Rodbell and Schweig (1993), S=Saucier (1991), and V=Vaughn (1991). Study areas of Wesnousky and Leffler (1992) outlined by black boxes. Sites where paleoliquefaction features found denoted by black diamonds; sites of probable paleoliquefaction features indicated by gray diamonds; white diamonds denote sites where investigations are scheduled in the fall of 1994.

Active vs. seismogenic faulting in the Santa Cruz Mts.: can field observations alone tell the difference?

Gianluca Valensise, Istituto Nazionale di Geofisica, Roma, Italy
(temporarily at: C.F. Richter Lab, U.C. Santa Cruz, Santa Cruz, CA 95064)

The issue of active vs. seismogenic faulting has taken on special importance in California during the past few years following a series of large blind thrust and reverse faulting earthquakes, such as the 1983 Coalinga, the 1987 Whittier Narrows, the 1989 Loma Prieta, the 1992 Cape Mendocino, and the 1994 Northridge events, all of which were generated by previously unrecognized faults. A large blind fault is usually accompanied by surface-breaking faults affecting the crustal volume directly above it. For instance,the Loma Prieta, Cape Mendocino and Northridge earthquakes all occurred in areas where many surface-breaking faults had been known for decades. Most of these faults had already been labeled as "active" prior to the earthquake on the grounds that they displace late Pleistocene deposits, and some even moved during the large earthquake on the nearby blind fault. For the largest of them, finally, the quality of "being active" was straightforwardly translated into an earthquake potential, the extent of which was normally calculated based on the only measurable feature, the length. In retrospect, this procedure was indeed an ill-posed one as it failed to identify the potential of the hierarchically highest fault, i.e., the fault that actually generated the large earthquake. Nevertheless the question remains: do these surface-breaking faults still hold a significant seismogenic potential, or are they simply passive participants in a bigger scale process driven by the underlying blind fault? And could this be ascertained prior to the large earthquake using traditional geologic or geodetic tools?

The Loma Prieta fault in the southern San Francisco Bay Area and the region around it make perhaps the best possible example to address this issue. The figure shows the region around the Loma Prieta fault and the location of the San Andreas and other major reverse or oblique surface-breaking faults. Aside from the San Andreas, that ruptured through this area in 1906, most of these faults have been assigned a significant potential by studies completed both before and after 1989 [e.g., *Kovach and Beroza*, 1993, and references therein]. The identification and exact location of the Loma Prieta fault and the calculation of its focal mechanism have been largely based on modeling of elevation changes measured along a series of first order leveling routes [*Marshall et al.*, 1991]. The figure also shows an interpretation for the correspondence between significant (>±2 cm) jumps in the distribution of residuals with respect to the elevation changes predicted by *Marshall et al.*'s model, and the location of the sites where the leveling routes cross the main faults of the area. The interpretation suggests that all of these faults slipped passively in 1989 in a direction consistent with their geologic slip vector, a fact that had already been pointed out for the Sargent fault [*Stein et al.*, 1991] and directly observed in the field along the Monte Vista and Berrocal fault zones [*Haugerud and Ellen* , 1990]. Assuming that this phenomenon is repeated for every subsequent Loma Prieta-type earthquake, and that such earthquakes recur every ≈600 years [*Valensise and Ward*, 1991], this process alone is able to account for 0.05-0.15 mm/yr of dip-slip along some of these faults. In addition, pre-1989 leveling work (reported in *Marshall et al.* [1991]) shows continuous vertical deformation at fault crossings, particularly across the southern section of the Sargent fault, which had already been shown to slip in a right lateral sense at 2-3 mm/yr. The local geologic record confirms that motion on these faults is extremely youthful and also that they are largely responsible for the creation of the highest topography of the range, which occurs in a 10 km-wide band between the Zayante and the Sargent-Berrocal faults.

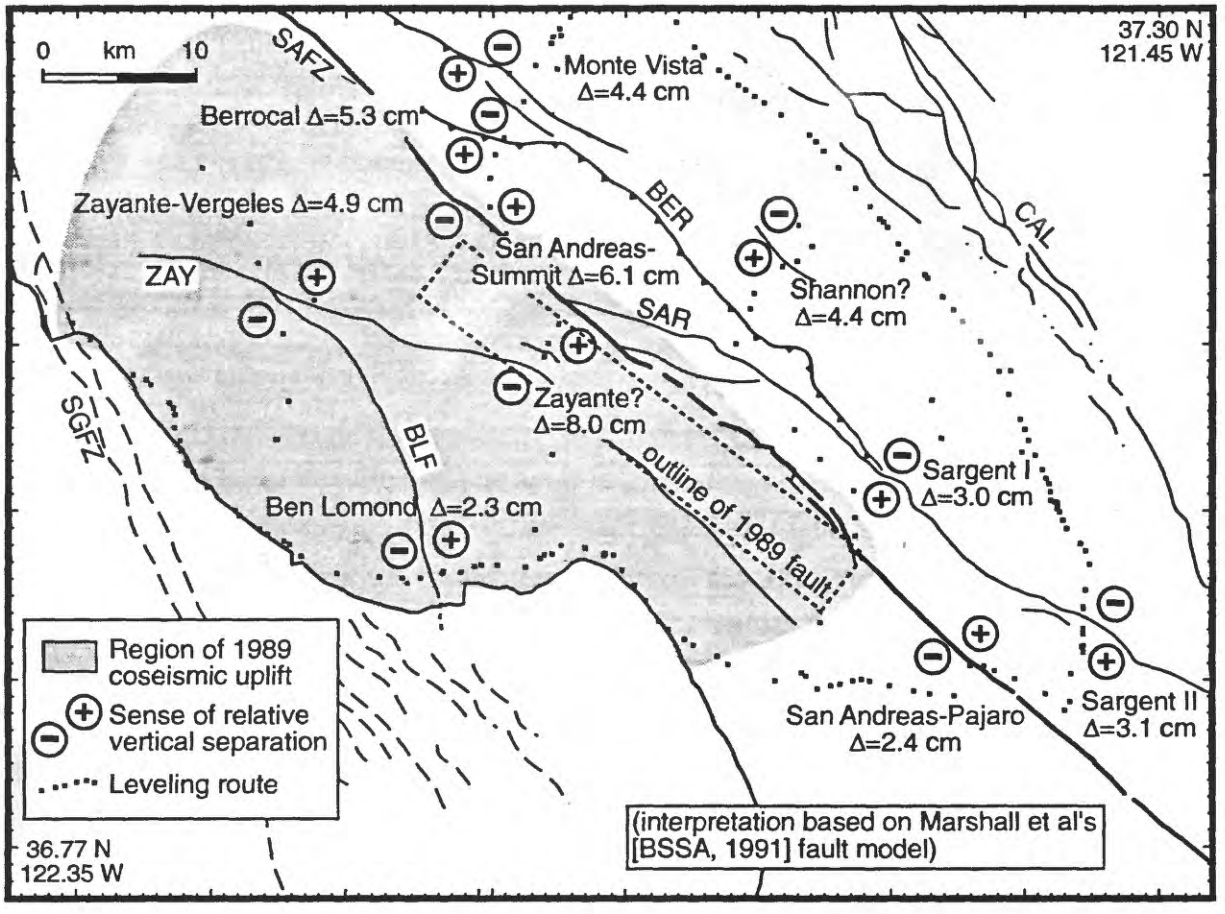

Although there is plenty of evidence that the surface-breaking faults of the Santa Cruz Mts. are *active* in a full geologic sense, we do not believe any of them bears a large independent seismogenic potential. Our contention is based on three main lines of geologic evidence:

Rates of deformation. Individual rates of late Pleistocene activity of these faults are rather low and represent only a fraction of the ≈1.0 mm/yr contraction across the Loma Prieta fault predicted by *Valensise and Ward* [1991] and expected based on simple plate tectonics arguments. In addition, geodetic evidence shows that this activity includes transient slip events associated with motion on the Loma Prieta fault (and possibly San Andreas?) and continuous deformation accompanied by limited background seismicity. For instance, a large fraction of the 0.2 mm/yr slip rate estimated by *Coppersmith* [1979] for the Zayante fault could be accounted for by passive motion following Loma Prieta-type events, leaving virtually no room for genuine, dynamic-faulting dislocation events.

Geometry and size. The location and geometry of some of these faults (for instance the Sargent fault and the southern portion of the Zayante fault) suggests that they are either rooted into the San Andreas at depths shallower than 5 km, or truncated by the Loma Prieta fault. Considering that the Loma Prieta rupture was confined to below 5 km depth, motion on overlying shallow reverse faults could simply help the uppermost portion of the crust to keep up with deformation at depth. Alternatively, one could regard the blind nature of the Loma Prieta fault as due to the weakness of the uppermost 5 km of the crust due to presence of these faults, all of which have been shown to predate the onset of modern compression across the plate margin (≈3.0 Ma) [*McLaughlin*, 1990] and the inception of the Loma Prieta fault itself [*Valensise*, 1992].

Hierarchy of faults based on their associated strain field. Every active fault contributes to determining the cumulative geologic strain field with a signal having a wavelength that is a function of its geometry and width (measured downdip), and a spatial distribution that is a function of its length and of the orientation of the slip vector. Ideally, one should be able to deconvolve the cumulative signal recorded in the geology and isolate the components that correspond to the largest faults. Based on a systematic analysis of the post-Miocene geologic record of the Pacific side of the Santa Cruz Mts., *Valensise* [1992] has shown that only the Loma Prieta and San Andreas faults leave a signal that is compatible in wavelength with that produced by a fault that extends to seismogenic depth, and that deformation associated with the other known faults is very localize and thus indicative of a shallow source. In addition, *Bürgmann et al.* [1994] have modeled an even larger scale tectonic signal
related to post-1906 relaxation along the San Andreas fault proper. This process would contribute to explain the uplift of the Santa Cruz Mts. (and the subsidence of the southern Bay Area and of the Pajaro Plain) and the progressive exhumation of preexistng faults without invoking the action of other large seismogenic sources.

The observations and interpretations presented suggest that in many cases the seismogenic potential can not be regarded merely as a function of the visibility of a fault, of its ability to produce extreme deformation at the surface, or of the amount of topography associated with it. Although the Santa Cruz Mts. offer a remarkably complete set of observations on how tectonic deformation is accommodated in the upper crust, our conclusions may apply to other seismogenic areas in California and elsewhere.

References

Bürgmann, R., R. Arrowsmith, T. Dumitru, and R. McLaughlin (1994). Rise and fall of the southern Santa Cruz Mountains, California, from fission tracks, geomorphology, and geodesy, *J. Geophys. Res.*, in press.

Coppersmith, K. (1979). Activity assessment of the Zayante-Vergeles fault, central San Andreas fault system, California, Ph.D. thesis, University of California, Santa Cruz, 216 p.

Haugerud, R. A., and S. D. Ellen (1990). Coseismic ground deformation along the northeast margin of the Santa Cruz Mountains, U.S. Geol. Surv. Open File Rep. 90-274, 32-37.

Kovach, R. L., and G. C. Beroza (1993). Seismic potential from reverse faulting on the San Francisco peninsula, *Bull. Seism. Soc. Am.*, **83**, 597-602.

Marshall, G.A., R. S. Stein, and W. Thathcher (1991). Faulting geometry and slip from co-seismic elevation changes; the 18 October, 1989, Loma Prieta, California, earthquake: Seismological Society of America Bulletin, **81**, 1,660-1,693.

McLaughlin, R.J. (1990). Sargent fault zone at Loma Prieta. U.S. Geol. Surv. Open File Rep. 90-274,19-22.

Stein, R., G. Valensise, and G. Marshall (1991). Catching a shutter-ridge shuddering, poster presented at the *Conference on the Seismotectonic Significance of the Loma Prieta Earthquake*, Asilomar (California)12-15 May 1991.

Valensise, G., and S. N. Ward (1991). Long-term uplift of the Santa Cruz coastline in response to repeated earthquakes along the San Andreas fault, *Bull. Seism. Soc. Am.*, **81**, 1,694-1,704.

Valensise, G. (1992). Geologic assessment of the relative contribution of strike-slip faulting, reverse-slip faulting and bulk squeezing in the creation of the Central Santa Cruz Mountains, California, *U.S. Geological Survey Prof. Pap.*, special volume on the Loma Prieta Earthquake, in press.

Apparent non-clustering of surface-rupture earthquakes in the past 1000 years in the Wellington region, New Zealand

R.J. Van Dissen & K.R. Berryman
Institute of Geological & Nuclear Sciences
PO Box 30-368, Lower Hutt, New Zealand

The Wellington region is cut by five major right-lateral strike-slip faults: Wairarapa, Wellington, Ohariu, Shepherds Gully/Pukerua, and Wairau faults. These faults have average recurrence intervals of metre-scale surface rupture that range from ca. 500 years to 5000 years. The cross-strike distance between these faults at the ground surface is 5-25 km, which is often less than the thickness of the seismogenic crust, estimated to range between 15-30 km. Only the Wairarapa fault has ruptured in historic time. The geologic record on the other faults provides information regarding the timing, and size of past surface-rupture earthquakes. A summary of paleoseismic data available for each of the faults is presented below, from east to west.

Along the ca. 110 km long portion of the Wairarapa fault that ruptured in 1855, single-event displacements of approximately 12 m, and a dextral slip-rate of 10-12 mm/yr are estimated from offset stream channels, alluvial terraces, and other geomorphic features. Trenching studies suggest that past surface rupture events occurred at approximately 5500, 4200, 2700, and $\leq$1620 yr BP.

Rupture of the southern portion of the Wellington fault - the Wellington-Hutt Valley segment - is one of the most serious natural hazard scenarios in all of New Zealand. This segment has a dextral slip-rate of 6.0-7.6 mm/yr, and at one site, single-event displacements of 3.2-4.7 m have been measured. The combined results from seven trenches indicates that the two most recent surface-rupture events on this segment occurred at 300-450 yr BP and 670-830 yr BP.

The Ohariu fault extends for ca. 70 km from the Wellington south coast to north of Waikanae. The fault has a dextral slip-rate of 1-2 mm/yr, and single-event displacements appear to be in the order of 3-5 m. The most recent surface-rupture event on the portion of the fault north of Porirua - the Kakaho section - occurred at or slightly before 970-1080 yr BP, based on dates from the base of peat deposits ponded by an uphill-facing fault scarp. Trenching studies on the portion of the fault south of Porirua - the Porirua section - indicate that the most resent surface-rupture occurred at $\leq$1160 yr BP. If the most resent rupture of the Ohariu fault involved both the Kakaho and Porirua sections, then the timing of this rupture is 970-1160 yr BP.

The surface trace of the Shepherds Gully fault and Pukerua fault is generally poorly preserved, suggesting a low overall rate of movement, in the order of $\leq$1 mm/yr, and an appreciable elapsed time since the last surface-rupture event. Horizontal displacements of 3-4 m, probably representing a single-event displacement, have been documented.

No data are available regarding the recent movement history of the offshore portion of the Wairau fault closest to Wellington, apart from the probable location of its trace. However, onland in the South Island, approximately 100 km southwest from Wellington, the fault has a dextral slip-rate of 3-5 mm/yr, and single-event increments of horizontal displacement of 5-7 m.

Paleoseismological studies of the strike-slip faults in the Wellington region have allowed the compilation of a rather complete record of surface-rupture events over the past 1000 years. Within this time period, there has been one surface faulting event on the

Wairarapa fault, two on the Wellington fault, one, possibly two, on the Ohariu fault, and none on the Shepherds Gully/Pukerua faults. Within the bounds of uncertainty determined by ^{14}C dates, there does not appear to be a temporal clustering of surface rupture event on adjacent faults. The 1855 Wairarapa earthquake does not appear to have triggered rupture on any other fault in the region. The most recent surface-faulting event on the Wellington fault does not coincide with rupture of any other onland fault, and, if the Ohariu fault represents a single earthquake source, at least 140 years separates the timing of the second most recent rupture on the Wellington fault and the most recent rupture of the Ohariu fault.

The above statement regarding the apparent non-clustering of surface-rupture earthquakes in the Wellington region applies only to the onland strike-slip faults. There are other possible seismogenic sources in the region, and thus important issues remain to be addressed regarding the history of large earthquakes in the Wellington region. 1) The Wellington region is underlain by a northwest-dipping subduction thrust between the Pacific plate and the overriding Australian plate. The seismogenic potential, and earthquake recurrence interval of this portion of the subduction zone is not known. 2) The timing of rupture events on the offshore portion of the Wairau fault are not known. 3) The Ohariu fault is assumed to represent a single earthquake source; however, the data do not discount the possibility that rupture of the Porirua or Kakaho section is closely spaced in time with, or triggered by, rupture of the other section. 4) Paleoseismic data are not available for the section of the Wellington fault in the Tararua Ranges to the north of Wellington.

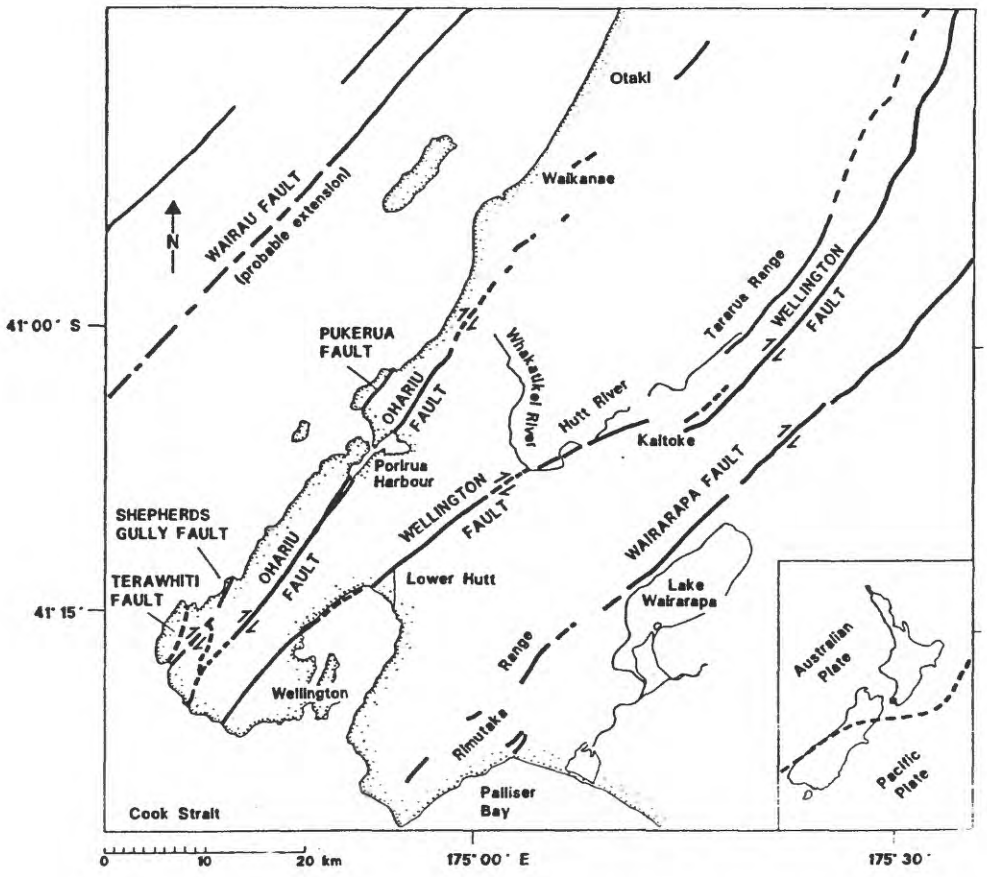

Figure. Active strike-slip faults in the Wellington region.

Research on paleosismology by large combinative trench across the piedmont fault of Mt. Daqingshan, Inner Mongolia

Weimin Wu and Li Ke
Institute of Crustal Dynamics, SSB, Beijing 100085, P.R.China

In order to make researches on the stable criteria of paleoearthquake events, the great earthquakes recurrence interval and average slip rate of typical normal fault zones, a large combinative trench has been excavated recently across the piedmont fault of Mt. Daqingshan, Inner Mongolia.

The piedmont fault of Mt. Daqingshan, with a total length of 200 km and general strikes of E-W,is the north boundary fault of the eastern part of Hetao basin in Inner Mongolia. The data collected by geological mapping (scale 1:50000) along the fault have shown that the fault is an active normal fault of the late Quaternary, and its average Holocene slip rate estimated from the height of fault scarps on Holocene deposits are 0.5~1.7mm/a at five different segments of the fault. The large combinative trench is seated at Meidai—Touzhu segment which has the maximum Holocene slip rate of all segments on the fault zone. It is composed of two parallel large trenches (trench No.1 and No.2) with 25 —30m in length, 4m in width and 5— 9m in depth. The distance between the two trenches is 15m. A normal fault with steep dip angle and some localized deposits as colluvial wedge and triangluar filling wedge which related to paleoearthquake events are exposed in both trenches.

Four events can identified in the large combinative trench (Fig. 1).The first event formed colluvial wedge A; the second event formed triangluar filling wedge B; the third event formed triangluar filling wedge C and colluvial wedge D;the last event formed triangluar filling wedge E. From the ^{14}C and TL age data of the strata in the trench, we can infer that the first event occurred before 10790±750 a B.P., the second one later than 9123 ±256 a B.P., but before 7286±150 a B.P., the third one later than 7286±150 a B.P., but before 5505±10 a B.P., and the fourth event later than 2115± 105 a B.P..

The total verticaly displacement of the fault determined by comparing

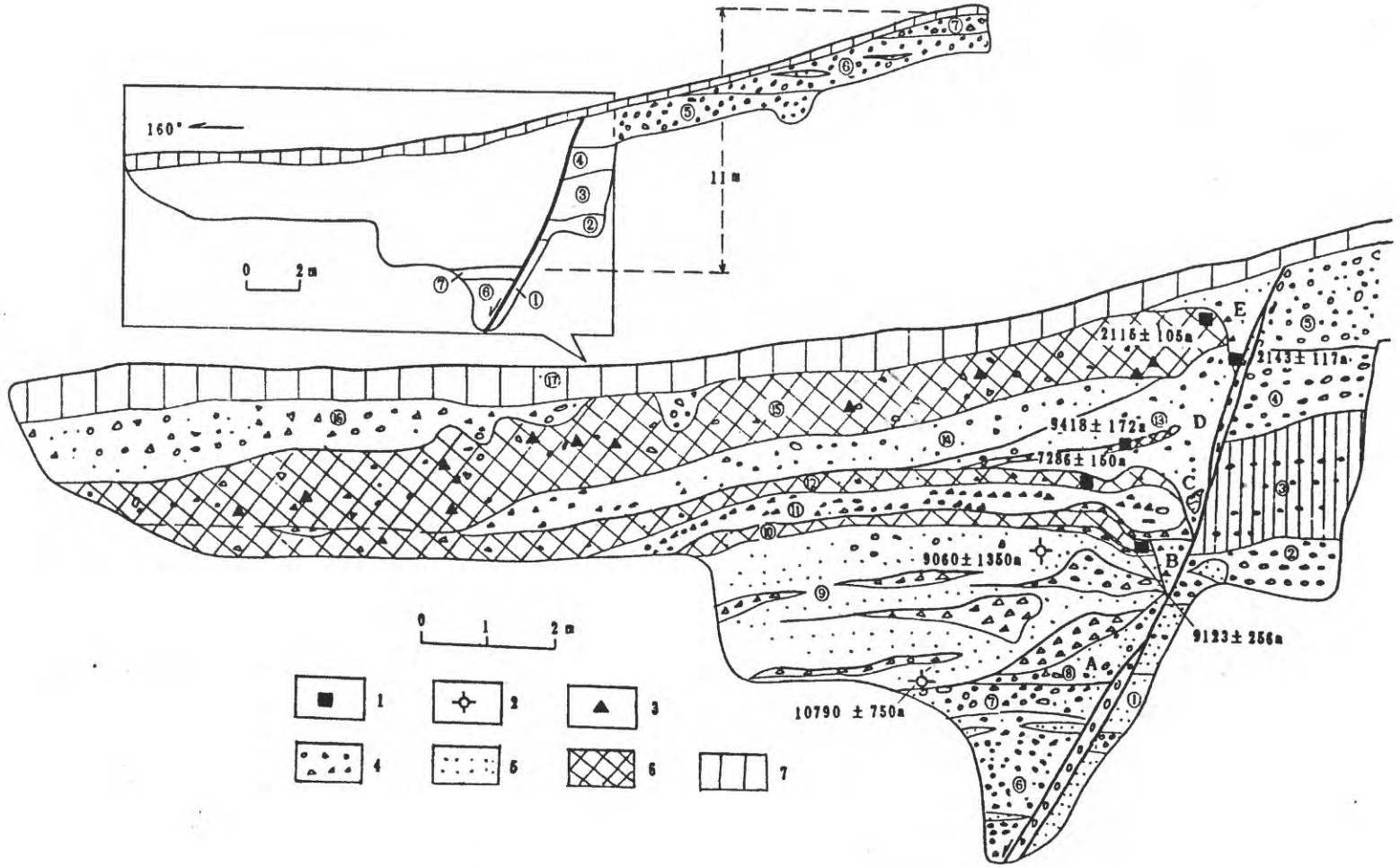

Fig.1 Sketch of the western wall of trench No.1

1. Location of ^{14}C samptes; 2. Location of TL samples; 3. Pottery chip; 4. Gravels; 5. Yellow sand; 6. Black soil; 7. Yellow surface soil; A, D — colluvial wedge; B, C, E — triangluar filling wedge

the strata on both side of the fault in the trench is 11m(Fig.1). Based on the age dating of the strata, an average Holocene slip rate of 1.02mm/a can be calculated for the fault. This result approximates the value of 1.13mm/a which estimated from the height of fault scarp in the trench site.

The recurrence interval of great earthquakes of Meidai —Touzhu segment estimated from the paleoevents in this large combinative trench is approximately 2000～5000 years in Holocene. Another result estimated form slip rates in Holocene is about 3500 years.

Using the Shallow Marine Record to Detect the Geometry and Recurrence Behavior of Active Faults

Patrick L. Williams, Earth Sciences Division, Lawrence Berkeley Laboratory, Berkeley, CA, 94720; 510/486-7156, plw@geo.lbl.gov
Lynn Ingram, Department of Geology and Geophysics, University of California, Berkeley, CA 94720

Recent technical developments have enabled the routine high resolution study of active faults in the shallow marine environment. The combination of seismic imaging targeting the Holocene sedimentary record, and stratigraphic data from cores, provides a powerful tool for the discovery and interpretation of patterns of Holocene fault activity. New tools for high resolution data acquisition and processing include compact and reliable digital recording systems, highly precise real-time satellite navigation, and the transfer of conventional seismic data processing tools to the processing of shallow high resolution data. An additional significant development is the introduction of a distinctive receiver geometry, manufactured by Japanese and Canadian companies, to field data acquisition in the US. This instrumentation is capable of recording subsurface images with a lower but comparable resolution to that available in trench observation. These marine data are superior in resolution to high resolution geophysical data recorded on land. Theoretically, resolution with this equipment should be about 2.5 cm, but practical resolution is on the order of 5 to 10 cm. In many marine environments, sharp images are obtainable throughout the shallow subsurface (depths of 0 to 25 m). With these data, detailed interpretation of sedimentation and the subsurface structure of faulting is possible.

Challenges for acquisition and interpretation of seismic reflection data from the shallow marine environment include the masking, attenuation and scattering of seismic energy by various kinds of environmental noise, shallow gas pockets, and coarse lithologies. Interpretation can be difficult where submerged objects, out-of-line obstructions, and seismic multiples complicate the seismic records. Gas pockets can produce bright reflectivity in otherwise unreflective horizons. Most difficulties with marine high resolution data are identical to those encountered in conventional seismic reflection data, and can be similarly dealt with. Criteria can be developed for evaluation of candidate structural features interpreted from high resolution marine data. A partial list of criteria for interpretation of structure includes: 1) reproducibility of results from image to image along the interpreted fault; 2) consistency of map pattern of structure; 3) evidence of sequential growth of interpreted structure; 4) independence from likely sedimentary complexities (e.g., ripples, berms, foresets, channel-fills, scours, banks, bars); 5) consistency with structure imaged deeper in the section; 6) independence from multiples and other misleading seismic attributes.

A Very High Resolution (VHR) profiling instrument was operated across the Pinole and Rodgers Creek faults in San Pablo Bay, California. This VHR instrument produces a source pulse containing energy at frequencies ranging from 3 to 10 kHz. Unique to this VHR system, return energy is captured with a separate hull-mounted, laterally-shielded receiver. The fidelity of this equipment proved to be superb in soft sediment areas with low bottom roughness. The maximum sediment penetration achieved with the VHR system is 25 m in San Francisco Bay; in San Pablo Bay most VHR records penetrate about 12 m. Holocene deposits are on the order of 10-15 m thick in the San Francisco estuary, and the geological record of Holocene fault displacements is thus largely recoverable with VHR studies.

VHR acoustic imaging in San Pablo Bay estuary reveals the detailed spatial and temporal patterns of Recent seismogenic deformation. Growth features produced by multiple vertical fault offsets are imaged in Holocene strata (Figure 1), and demonstrate that the Pinole fault, formerly believed inactive, produced two major earthquakes during a 1800-year-interval ca. 800 and 2600 radiocarbon years before present. Ages are obtained from direct dating of plant and shell

material from cores. The Pinole fault ruptures thus appears to have an average recurrence interval of ca. 900 years, and a latest detected event about 800 years ago. The Pinole recurrence rate is a factor-of-five smaller than that of the associated Hayward and Rodgers Creek faults. VHR data indicate that the Rodgers Creek and Pinole faults are attached beneath San Pablo Bay, extending the known length of these faults by 15 and 11 kilometers, respectively. Connection of the Pinole and Rodgers Creek faults greatly increases the area across which slip is transferred between the Hayward and Rodgers Creek fault systems. This significantly increases the maximum credible magnitude of ruptures produced by the Rodgers Creek fault and extends the Hayward-Rodgers Creek fault step into the northern Berkeley Hills, indicating that the step-over begins much farther south than previously recognized, and also suggesting that the Hayward fault loses slip to the Rodgers Creek across the entire width of San Pablo Bay. VHR geophysical data have proven to be a powerful aid in study of active structures and tectonic hazards in the northern San Francisco Bay area.

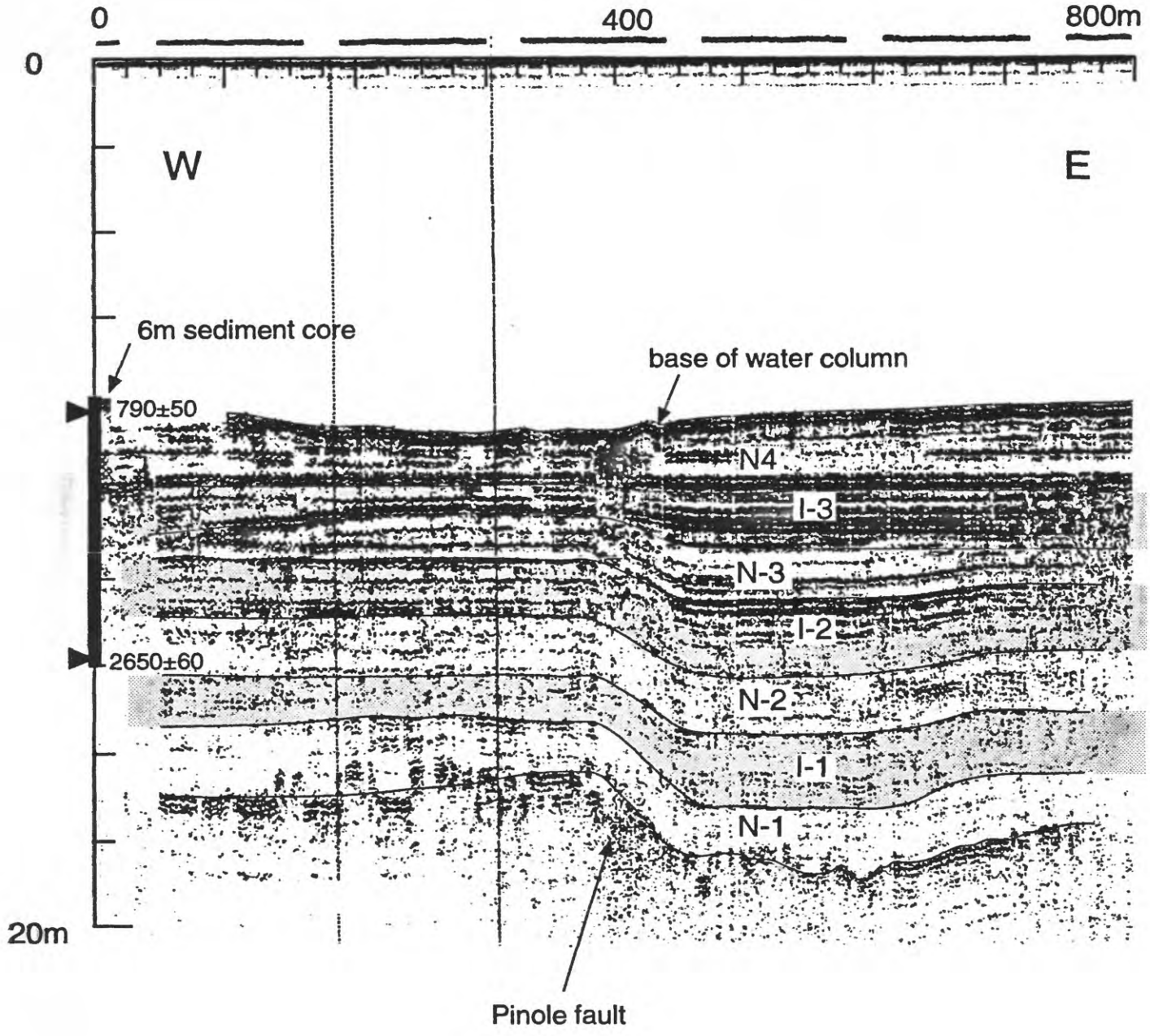

Figure 1. VHR image across the Pinole fault, San Pablo Bay California. The infill of bay silt across the fault plane (units labeled I-1, I-2 and I-3) records paleo-earthquakes. The lower portions of the labeled sediment packages were deposited immediately after three Pinole fault quakes. After the infill is complete, beds of uniform thickness are deposited across the fault, these "normal" layers are labled N-1, N-2 and N-3. Radiocarbon ages of 2650±60 and 790±50 bound events represented by I-2 and I-3, indicating a maximum recurrence interval of 930 radiocarbon years for these events.

Preliminary Results of Paleoseismic Studies of the Concord Fault at Galindo Creek, Concord, California

Christopher J. Wills, California Division of Mines and Geology,
185 Berry St., Ste. 3600, San Francisco, California
David L. Snyder, Rogers/Pacific, Inc., 396 Civic Dr., Pleasant Hill, California
Glenn Borchardt, Soil Tectonics, P.O. Box 5335, Berkeley, California

The Concord fault is a well-known right-lateral strand of the San Andreas fault system in the San Francisco Bay area. It is well expressed through the center of the City of Concord by scarps, small hills, a sag pond and a groundwater barrier (Wills and Hart, 1992). Evidence for creep was mapped by Sharp (1973) and a 3 mm/yr creep rate has been measured by Galehouse (1992). Numerous trenches have been excavated to locate the fault for development. We have recently completed the first trenches excavated to determine the activity of the fault.

We chose a site where Galindo Creek crosses the fault at a high angle and sand and gravel deposits were reported from previous construction excavations. The natural stream channel had a sharp, right-lateral offset before it was replaced with a concrete-lined channel in 1984. The natural channel upstream of the fault is incised into Pliocene bedrock and its location probably has not varied greatly over time. It seemed likely that older, offset channels of Galindo Creek could be located downstream of the fault, and if datable materials could be found, a slip rate could be calculated.

The site is also one of the few undeveloped parcels in central Concord. Despite some disturbance of the site, including the concrete channel constructed to carry Galindo Creek across the site, a 60 inch diameter storm drain, and an unknown amount of grading, we anticipated that undisturbed Pleistocene and Holocene deposits could be found.

In June 1994, we excavated seven trenches north of Galindo Creek. Three of the trenches crossed the fault approximately perpendicularly and four were approximately parallel to it.

The three fault-crossing trenches encountered Plio-Pleistocene siltstone bedrock, overlain by Pleistocene alluvium on the east side of the fault. The age of the bedrock is constrained by a fossil upper jaw, possibly of the late Pliocene-Pleistocene camel *Camelops*, recovered from trench T-1. Age of the alluvium is estimated based on soil development. On the west side of the fault, channels filled with Holocene alluvium are cut into Pleistocene alluvium.

At the fault, apparent soil-filled fissures may record prehistoric earthquakes. The youngest of these features dips steeply to the west and contains cobbly colluvium, similar to the material on the current ground surface. Other similar features, several of which also widen upwards, underlie the first. If each of these features represent prehistoric

earthquakes, up to eight events may be recorded in trench T-1 and more may be recorded in trench T-7. Several of these features may represent dismembered portions of alluvial stratigraphy bounded by shear surfaces, rather than fissure fills. Any true "fissure fill", however, would represent the first evidence of significant ground-rupturing earthquakes on the Concord fault.

Two fault-parallel and two fault-crossing trenches encountered portions of a Holocene-age channel. It appears to be approximately the same size and orientation as the current Galindo Creek channel. This channel projects to the fault approximately 30 to 60 meters from its upstream equivalent. C-14 dating of charcoal recovered from this channel will allow us to calculate a slip rate.

Thirty meters offset during the last 10,000 years could be due to creep. The possibility of a higher slip rate and the evidence for ground-rupturing earthquakes suggest that the Concord fault may be a significant source of major earthquakes.

The site at Galindo Creek shows great promise for further studies to refine the slip rate and earthquake history on the Concord fault. Additional, possibly younger channel deposits may exist south of our current trenches. We would also like to refine the location of channels on the upstream side of the fault. With further work, an accurate assessment of the contribution of the Concord fault to the earthquake hazards of the San Francisco Bay area may be possible.

References

Galehouse, J.S., 1992, Creep rates and creep characteristics of Eastern San Francisco Bay Area faults: 1979-1992, *in* Borchardt, Glenn, and others, eds., Proceedings of the Second Conference on Earthquake Hazards in the Eastern San Francisco Bay Area: California Department of Conservation, Division of Mines and Geology Special Publication 113, p. 45-53.

Sharp, R.V., 1973, Map showing recent tectonic movement on the Concord fault, Contra Costa and Solano Counties, California: U.S. Geological Survey Miscellaneous Field Studies Map MF-505, scale 1:24,000.

Wills, C.J., and Hart, E.W., 1992, Progress in understanding the Concord fault through site specific studies, *in* Borchardt, Glenn, and others, eds., Proceedings of the Second Conference on Earthquake Hazards in the Eastern San Francisco Bay Area: California Department of Conservation, Division of Mines and Geology Special Publication 113, p. 311-317.

RESEARCH ON NONLINEAR CHARACTERISTICS OF PALEOSEISMICITY IN CHINA

Xiwei XU and Qidong DENG
Institute of Geology, State Seismological Bureau, Beijing 100029, China

Abstract

Our analysis of the pattern, concentration and rates of activity on late Quaternary faults leads us to suggest a natural division of China and surrounding areas into tectonic provinces that are based on modern plate-tectonic models. Seven tectonic provinces of active faulting have been defined in China. These tectonic provinces are Qinghai-Tibetan (QTTP) and Xinjiang (XTP) in the western China, Dongbei (DTP), Huabei (North China, HBTP) and Huanan (HNTP) in the eastern China, and Taiwan (TTP) and Nanhai (NTP) in the southeastern China. These provinces have remarkable differences in mechanical properties of active faults, kinematic behavior of fault blocks, seismicity, and seismotectonics. Slip rates of active faults and strain rates of interplate deformation are highest in the QTTP and gradually decrease outwards in the surrounding tectonic province (XTP, HBTP, DTP and HNTP). Horizontal slip rates of major active faults in the QTTP reach 6-15 mm/yr. The Tibetan Plateau is subjected to EW extension at a rate of 12-13 mm/yr. To the north, major active faults in the XTP have horizontal slip rates of as much as 3.0-6.3 mm/yr and vertical (reverse) slip rates of 0.5-2.0 mm/yr. Here the crustal is subjected to NNE-SSW compression at a rate of 6 mm/yr. In the eastern part of China, NNE-trending faults in the HBTP have been actively deforming at horizontal rates of 1.3-5.7 mm/yr and ENE-trending normal faults at vertical rates of 0.3-2.8 mm/yr, causing a NNW-SSE extension and ENE-WSW compression of the crust of the HBTP. This neotectonic framework suggests that the Quaternary geodynamics in China mainly comes from the interaction of the Indian and Eurasian plates along the Himalayan frontal thrust fault. The interation of the western Pacific and Eurasian plates also plays an important role in neotectonics of the eastern China. But their affection is especially restricted to the TTP, southeastern coasts of the HNTP and eastern part of the DTP.

Paleoearthquake recurrence intervals in the tectonic provinces of China reflect unique seismogenic properties that are related to their position relative to the converging Indian and Eurasian plates. The average recurrence intervals are less than 2,000 yrs to as little as 500-800 yrs on some active faults in the QTTP, whereas recurrence intervals are 2,000-4,500 yrs

in the XTP and longer than 2,000 yrs to as much as 7,300 yrs in the HBTP. From this point of view, it seems to be reasonable to infer that the geodynamics of large earthquakes in China comes mainly from the collision of the Indian and Eurasian plates. The average recurrence intervals are closely related to the degree of late Quaternary faulting in the tectonic provinces, but no simple linear relationship exists between slip rate and recurrence interval. Slip rate is only one of the main factors affecting fault behavior and occurrence of large earthquakes.

Case studies of major active faults in China from both historic seismicity and paleoseismic data show that there are spatial and temporal patterns to paleoseismic activity, besides spatial heterogeneity of late Quaternary faulting and seismicity. These nonlinear temporal characteristics within a seismicly active period can be graphically fitted with the logarithm curve N=a+logb T. This curve indicates that during the early part of an active period, large-earthquake recurrence intervals are nearly equal, which corresponds to the characteristic-earthquake model described by R=(S-C)/D. In the late part of an active period, the interval between neighboring earthquakes becomes shorter as one comes closer to the present—this relationship corresponds to earthquake clustering within a short period. Therefore, we can infer from the Holocene paleoseismic data that the major active faults in the HBTP discussed above are now in the early part of active periods and that large earthquakes will tend to occur at or near the average recurrence intervals of each fault. Conversely, seismicly active periods on the Xiaojiang and Xianshuihe fault zones in the QTTP seem to be finished; they are now either in a seismicly quiet period or just in the early phase of a new active period. By comparison, the Zemuhe fault is near the end of an active period: large earthquakes should occur at shorter intervals than they have on average during the Holocene.

Experimental results also show that changes in mechanical conditions, geometrical structures and environments and rock materials in and around active faults are the main factors that cause large earthquakes to occur. Our explanations of the nonlinear characteristics of paleoseismicity are summarized in view of these factors.

Boundary Behavior And Paleoearthquake Pattern Along Strike-Slip Fault Systems In Central Japan

Xiwei XU* and Nobuyuki YONEKURA
Department of Geography, Graduate School of Science, University of Tokyo, Japan

Abstract

The Nobi, Atera, Kita-Izu and Atotsugawa fault systems as well as Itoigawa-Shizuoka tectonic line are five major strike-slip faults in central Japan. Segment boundaries of the Atera and Atotsugawa fault systems can effectively stop or slow down the coseismic rupture propagating. The segments themselves behave independently in seismicity. Their paleoearthquake sequence y (scattered points) versus occurrence time x (in yrs before 1950 AD) can be graphically fitted by straight line: y=a+bx, where a and b are two constants. Then, the average recurrence intervals (ARI) on segments can be described by the slope (b) of the fitted lines: ARI=1/b. This paleoseismic pattern corresponds to the characteristic earthquake model. The paleoseismic pattern is quite different when the segment boundaries of the Nobi and Kita-Izu fault systems and Itoigawa-Shizuoka tectonic line begin to break and fail to work. Their seismotectonics migrates from internal structures within segments to boundaries. The broken processes of the boundaries are always accompanied by several great earthquakes at a shortening interval as one is close to the present. Thus, the whole paleoearthquake sequence y (scattered points) versus occurrence time x (in yrs before 1950 AD) can be graphically fitted by Logarithmic curve: y=a+bLog(x), where a and b are two constants. When x is less than a certain value t, the recurrence interval becomes obviously shortening, which corresponding to the broken process of the segment boundaries and earthquake clustering model. When x is larger than the value t, the recurrence intervals are approximately equal to each other, which corresponding to the characteristic earthquake model on the segment. Deviations of paleoearthquakes from the fitted line or curve demonstrate the irregularity of paleoseismology. They may be resulted from differences in seismotectonics. We can use these two paleoseismic patterns to evaluate future seismic risk of strike-slip faults through careful checking of their segmentation, boundary behavior and paleoseismicity.

* Permanent address and correspondence to: Xiwei Xu, Institute of Geology, State Seismological Bureau, Beijing 100029, Peoples' Republic of China.

Reconstruction of fault behavior and paleoseismicity in the onshore plate convergence zone, central Japan

Haruo Yamazaki, Dept. Geography, Faculty of Science,
Tokyo Metropolitan Univ.
1-1 Minami-Ohsawa, Hachioji, Tokyo, 192-03 JAPAN

A geologically constrained model of the fault behavior and paleoseismicity at the northern tip of Izu-Bonin arc is described.

In the last stage of Early Pleistocene, the buoyant Izu block on the Philippine Sea plate collided with Honshu of Japanese Islands on the Eurasian plate. The event resulted in the onshore plate boundary connecting the Suruga and Sagami troughs along the northern border of Izu Peninsula, central Japan (Fig.1). The deformed Quaternary and active faults with high slip-rate along the border region indicate that the plate convergence has successively continued in the onshore plate boundary even after the Izu collision (Fig.2).

Although earthquakes larger than magnitude 7.5 have repeatedly occurred along subduction zones off the Japanese Islands, the onshore plate boundary has historically no record of destructive earthquake or crustal deformation including the surface fault-break except the Taisho- Kanto earthquake of 1923.

The integrated Quaternary information at the Ashigara Plain-Oiso Hills region located in the northwestern extension of the Sagami trough provides the clue to reveal the features of paleoseismicity and fault activity in the onshore plate convergent zone. The northwest striking Kozu-Matsuda fault divides the Quaternary sedimentary basin into subsiding Ashigara Plain in the southwest and uplifting Oiso Hills in the northeast at the vertical slip rate of 3.6 mm/yr.

The Ashigara Plain shows 0.65 mm/yr of mean subsiding rate through the Late Pleistocene to Holocene. A low curious terrace indicating the recent crustal uplift, however, occurs in the coastal region of the plain. The Oiso Hills consists mainly of deformed and uplifted Quaternary. Three marine terraces formed in the Holocene show that the hills have intermittently uplifted at the mean rate of 3 mm/yr since 6,300 years ago.

The coseismic crustal movement of the 1923 Taisho-Kanto earthquake, that epicenter is recently assumed to be beneath the Oiso Hills, results in the 1 to 2m of uplift in the coastal regions of the Ashigara Plain and Oiso Hills. No obvious uplifted platform was formed along the coast. On the other hand, the Kozu-Matsuda fault locked the slip during the event and did not show any surface break along its whole trace.

Assuming that the above tectonic features have resulted from the coseismic events occurred in the onshore plate boundary, the author proposes an earthquake recurrence model that can interpret well the origin of geological evidences (Fig.3). This model assumes that the two types of coseismic

deformation overlap each other on the Ashigara Plain-Oiso Hills region. One is the coastal uplift resulted in the Taisho-type earthquake at a recurrence interval of about 1,000 years, the other is the break of Kozu-Matsuda fault associated with a huge earthquake (Oiso-type earthquake) at an interval of about 3,000 years. Coseismic displacement of the Kozu-Matsuda fault may reach as much as 10m vertically. At the event, the Oiso Hills upheaves drastically and the Ashigara Plain subsides to exceed the amount of uplifts accumulated by some Taisho-type earthquakes in one Oiso-type cycle.

Although the magnitude of Oiso-type earthquake may be larger than M8 estimating from the large displacement of the fault, the length of Kozu-Matsuda fault is too short to cause such a huge earthquake referring to the empirical relationship between the earthquake magnitude and the length of fault break. This fact suggests that the Kozu-Matsuda fault is not the source of Oiso-type earthquake but one of the imbricated thrusts branching off a megathrust on the plate subduction surface beneath the Oiso Hills and Tanzawa Mts. to the north.

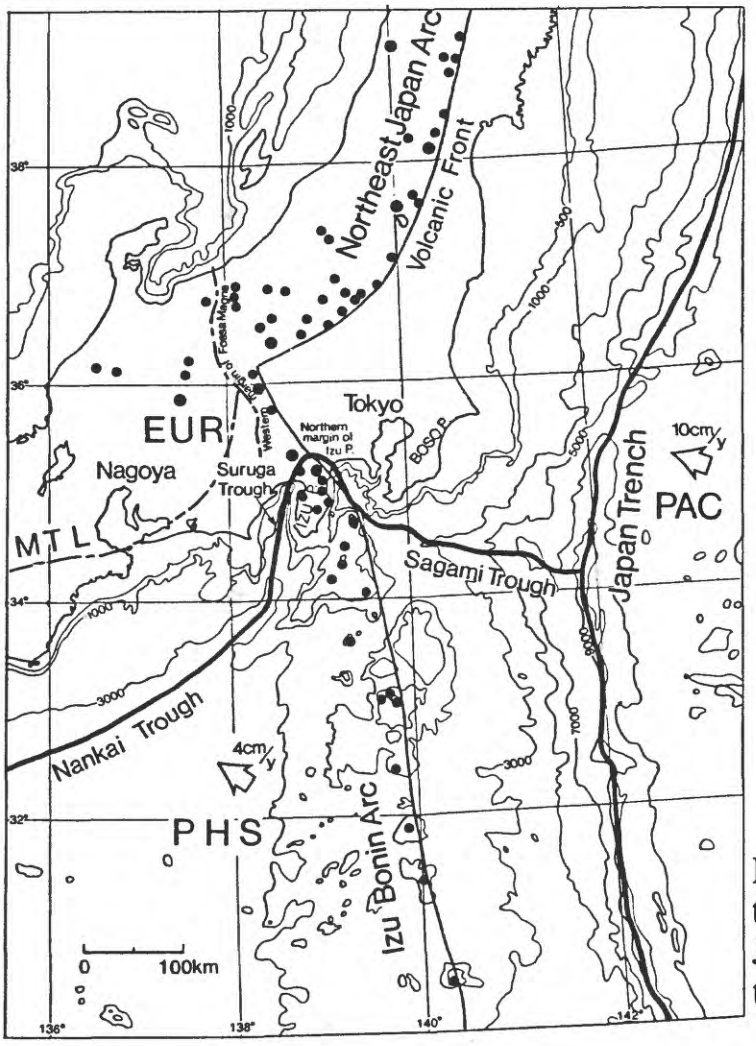

Fig.1. Setting of the plate tectonics around the central Japan. Filled circles indicate the Quaternary volcanoes.

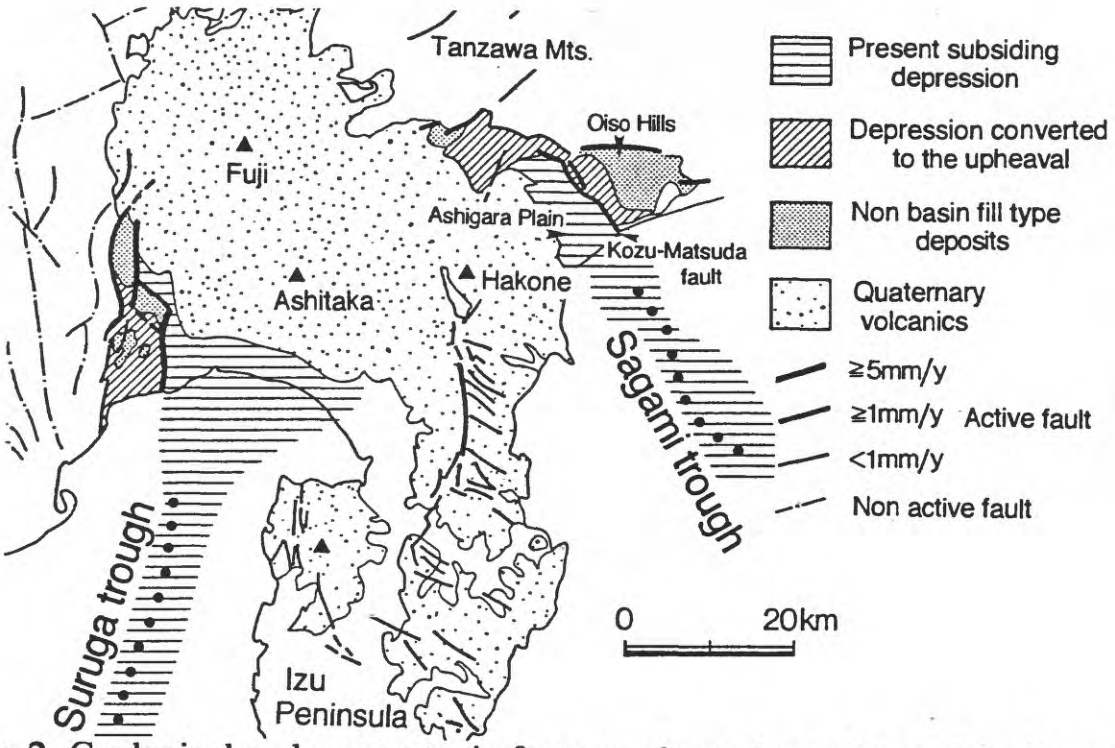

Fig.2. Geological and neo-tectonic features along the onshore plate boundary at the northern tip of the Izu-Bonin arc.

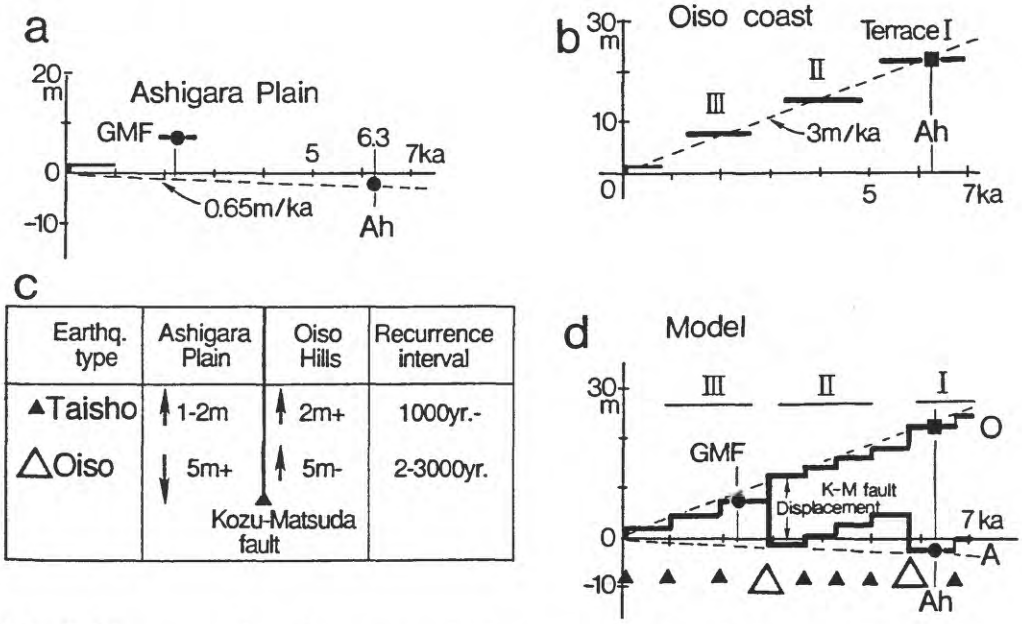

Fig.3. Model interpreting the tectonic features in the Ashigara Plain-Oiso Hills region. a: Tectonic features of the Ashigara Plain. b: Tectonic features of the Oiso Hills. c: Crustal movements on the Ashigara Plain and Oiso Hills caused by the Oiso-type and Taisho-type earthquakes. d: Model showing the paleoseismicity, coseismic movement and its long-term accumulation in the Ashigara Plain and Oiso Hills.

Historical Paleoseismology

Robert S. Yeats, Dept. of Geosciences, Oregon State University, Corvallis, OR 97331-5506, USA

I compiled a table of 295 historical earthquakes with surface rupture as part of a forthcoming textbook in earthquake geology. The table includes date, M, latitude and longitude, name of earthquake and of the fault that ruptured, nature of rupture (e.g., normal, oblique reverse-left slip, etc.), length and strike of rupture, maximum vertical and horizontal displacement, and references. The table highlights a flaw in the assumption that the historical written record, more than 2000 years long in some regions, is a reliable guide to correlating earthquakes with mapped faults.

Blaming an earthquake on a specific fault long after the fact is controversial, especially prior to 1800 A.D., when contemporary observers had no concept of faulting, active or otherwise. Scarps reported at the time, such as those formed during the 1783 Calabria, Italy, earthquakes and described by Dolomieu in 1784 may refer to headwall scarps of landslides. Pleistocene strata are faulted against basement where Dolomieu described a scarp, but there is no clear evidence of surface rupture in 1783. The surface rupture of the 1861 M 7.0 Egion, Greece, earthquake, was the first to be mapped by a scientist (J. Schmidt in 1875), but some workers consider these scarps to be landslide-related.

Elongate zones of high intensity along a known active fault, such as the 1202 A.D. M 7.3 earthquake on the Dead Sea transform fault, have not been confirmed independently in the field as surface ruptures, and descriptions by contemporary observers is equivocal. Trenching on faults that ruptured the surface in the 1980 M 6.9 Irpinia, Italy, earthquake showed that these faults did not rupture during the 1694 A.D. earthquake with an even larger meizoseismal zone centered on the same region. On the other hand, the 1759 A.D. M 7.4 Bekaa Valley earthquake on the Dead Sea transform produced surface rupture on the Yammouneh fault, based on contemporary accounts.

Despite these problems, historical paleoseismology (HP), the establishment of lengths and displacements of ruptures on specific active faults due to historical earthquakes, can offer important insights to earthquake hazard. HP began with Lawson et al. (1908) with a description of rupture on the Hayward fault in 1868. Assignment of the 1812 San Juan Capistrano earthquake to the San Andreas fault based on trenching and tree-ring dating is a triumph

of HP, but there is still disagreement on rupture length. Ideally, a historical event centered on a known fault can be confirmed by trenching and site-specific geomorphology, as at Pallett Creek and Carrizo Plain, California, but establishing rupture length requires many trenches. Also, consider a Landers scenario, where an earthquake ruptured several faults. This has produced controversy in assigning the 1596 A.D. Keicho, Japan, earthquake to rupture on part of the Median Tectonic Line as well as other faults in the Kinki district to the NE.

Sharpness of geomorphic expression was used to map the rupture length of the 1645 M 8 and 1796 M 7.2 earthquakes on the Philippine fault and to tie the destruction of Sparta in 464 B.C. to a nearby normal fault at the base of Mt. Taygetos. Sharp vegetation-free zones at range fronts clearly mark the 1915 earthquakes at Pleasant Valley, Nevada, USA, and Avezzano, Italy, where they are called nastri di faglia or fault ribbons. But other nastri di faglia in Italy and Greece, such as the Tre Monti scarps near Avezzano, cannot be correlated to historical earthquakes despite 2000 years of record keeping.

A complicating factor is controversy in recognition of surface rupture in recent earthquakes examined by trained scientists, as illustrated for the 1989 M 7.1 Loma Prieta, California, earthquake and the 1992 M 6.8 Erzincan, Turkey, earthquake. In these earthquakes, tectonic features were discovered, but are they primary, connecting directly to the mainshock rupture plane, or are they secondary (bending moment or flexural-slip faults on near-surface folds, as at 1980 El Asnam), or triggered ruptures on faults, as for the surface rupture north of the Willow Creek Hills accompanying the 1983 Borah Peak, Idaho, earthquake. The 1979 Imperial Valley earthquake triggered up to 10 mm dextral slip on a 39-km section of the San Andreas fault more than 90 km away from the Imperial fault that was the seismogenic source.

Very short surface ruptures, such as those reported for the 1934 M 6.3 Excelsior Mountain, Nevada, the 1957 M 6.5 Velestino, Greece, and the 1966 M 6.2 Kremasta, Greece, earthquakes, should be viewed skeptically. Blind-thrust earthquakes such as the 1905 Kangra, India, earthquake and the 1994 Northridge, California, earthquake would have been hard to recognize in pre-modern times because there is no surface rupture, and contemporary observers would have had to recognize subtle evidence of uplift or subsidence.

Japan and China, both with long historical records, have done the most work in HP, but the USA is working actively on 19th-century Bay Area faults, the San Jacinto, Elsinore, and southern San

Andreas faults, and earthquakes in the supposedly-stable eastern part of the country. In New Zealand, the 1855 M 8.2 earthquake was successfully tied to the West Wairarapa fault, but the 1848 earthquake in eastern Marlborough could not be assigned to the Awatere fault, despite considerable effort. Israel, Turkey, Italy, Greece, and Iran have a rich HP record. Future work in HP requires collaboration among geologists (tectonic geomorphology, trenching, Holocene coastal uplifts and subsiding marshes, tsunami deposits, liquefaction deposits), geophysicists (interpretation of intensities from historical accounts), and historians (acquisition, translation and analysis of historical documents).

Workshop participants are invited to visit my poster and add earthquakes I have missed or take potshots at earthquakes I have incorrectly correlated to surface ruptures.